Organisation for Economic Co-operation and Development

ENV/CBC/MONO(2021)1/ANN4

Unclassified English - Or. English

4 February 2021

ENVIRONMENT DIRECTORATE
CHEMICALS AND BIOTECHNOLOGY COMMITTEE

Cancels & replaces the same document of 3 February 2021

Annex 4. CASE STUDIES TO THE GUIDANCE DOCUMENT ON THE CHARACTERISATION, VALIDATION AND REPORTING OF PBK MODELS FOR REGULATORY PURPOSES

Series on Testing and Assessment
No. 331

JT03470956

This document, as well as any data and map included herein, are without prejudice to the status of or sovereignty over any territory, to the delimitation of international frontiers and boundaries and to the name of any territory, city or area.

OECD Environment, Health and Safety Publications
Series on Testing and Assessment no. 331

Annex 4. CASE STUDIES TO THE GUIDANCE DOCUMENT ON THE CHARACTERISATION, VALIDATION AND REPORTING OF PBK MODELS FOR REGULATORY PURPOSES

INTER-ORGANIZATION PROGRAMME FOR THE SOUND MANAGEMENT OF CHEMICALS

A cooperative agreement among FAO, ILO, UNDP, UNEP, UNIDO, UNITAR, WHO, World Bank and OECD

Environment Directorate

ORGANISATION FOR ECONOMIC COOPERATION AND DEVELOPMENT

Paris 2021

About the OECD

The Organisation for Economic Co-operation and Development (OECD) is an intergovernmental organisation in which representatives of 36 industrialised countries in North and South America, Europe and the Asia and Pacific region, as well as the European Commission, meet to co-ordinate and harmonise policies, discuss issues of mutual concern, and work together to respond to international problems. Most of the OECD's work is carried out by more than 200 specialised committees and working groups composed of member country delegates. Observers from several countries with special status at the OECD, and from interested international organisations, attend many of the OECD's workshops and other meetings. Committees and working groups are served by the OECD Secretariat, located in Paris, France, which is organised into directorates and divisions.

The Environment, Health and Safety Division publishes free-of-charge documents in twelve different series: **Testing and Assessment**; **Good Laboratory Practice and Compliance Monitoring**; **Pesticides**; **Biocides**; **Risk Management**; **Harmonisation of Regulatory Oversight in Biotechnology**; **Safety of Novel Foods and Feeds; Chemical Accidents; Pollutant Release and Transfer Registers; Emission Scenario Documents; Safety of Manufactured Nanomaterials;** and **Adverse Outcome Pathways.** More information about the Environment, Health and Safety Programme and EHS publications is available on the OECD's World Wide Web site (www.oecd.org/chemicalsafety/).

This publication was developed in the IOMC context. The contents do not necessarily reflect the views or stated policies of individual IOMC Participating Organizations.

The Inter-Organisation Programme for the Sound Management of Chemicals (IOMC) was established in 1995 following recommendations made by the 1992 UN Conference on Environment and Development to strengthen co-operation and increase international co-ordination in the field of chemical safety. The Participating Organisations are FAO, ILO, UNDP, UNEP, UNIDO, UNITAR, WHO, World Bank and OECD. The purpose of the IOMC is to promote co-ordination of the policies and activities pursued by the Participating Organisations, jointly or separately, to achieve the sound management of chemicals in relation to human health and the environment.

This publication is available electronically, at no charge.

Also published in the Series on Testing and Assessment: link

For this and many other Environment, Health and Safety publications, consult the OECD's World Wide Web site (www.oecd.org/chemicalsafety/)

or contact:

OECD Environment Directorate,
Environment, Health and Safety Division
2 rue André-Pascal
75775 Paris Cedex 16
France

Fax: (33-1) 44 30 61 80

E-mail: ehscont@oecd.org

© OECD 2021
Applications for permission to reproduce or translate all or part of this material should be made to: Head of Publications Service, RIGHTS@oecd.org, OECD, 2 rue André-Pascal, 75775 Paris Cedex 16, France
OECD Environment, Health and Safety Publications

Table of Contents

Case Study I

Generic PBK model for farm animal species: Cattle (*Bos taurus*), Swine (*Sus scrofa*), Sheep (*Ovis aries*) and Chicken (*Gallus gallus domesticus*)

Part I. PBK model reporting template

A. Name of model

Generic PBK model for farm animal species: cattle (*Bos taurus*), swine (*Sus scrofa*), sheep (*Ovis aries*) and chicken (*Gallus gallus domesticus*)

B. Contact details

(1) Leonie Lautz, (1) Jan Hendriks, (1) Ad Ragas, (2) Carlo Nebbia, (3) Jean Lou CM Dorne

1) Radboud University, Nijmegen, Netherlands; 2) University of Turin; 3) European Food Safety Authority, Parma, Italy

C. Summary of model characterisation, development, validation, and potential applicability

Animal risk assessment of chemicals for the protection of various animal species as well as food safety is a key regulatory and scientific research field which is undergoing constant development in modelling approaches and efforts to further harmonise with human and environmental risk assessment. A recent review highlighted available PBK models for various farm animal species and identified the need to further develop generic models for these species (Lautz et al., 2019a). Here, generic PBK models for the species cattle (*Bos taurus)*, swine (*Sus scrofa domesticus)*, sheep (*Ovis aries*) and chicken (*Gallus gallus domesticus*) have been developed in the open source freeware R. For each species, the PBK model has been implemented for regulated compounds and environmental contaminants to predict the concentration in a range of body compartments and organs (blood, liver, kidney etc), milk (sheep and cattle) and eggs (chicken). Global sensitivity analyses have been performed using the function "soboljansen" in the "sensitivity" package to identify parameters which have the most impact on the model's output. Predictions for tissue concentrations and milk for two chemicals in cattle, swine and sheep and 6 chemicals for chicken were compared to experimental data and were accurate with 71% of the predictions within a 3-fold factor. It is acknowledged that the performance of these generic PBK models in farm animals with regards to the accuracy of tissue and milk concentration predictions for different chemicals still needs improvement before full confidence can be built towards their use in routine regulatory risk assessment. Further work is needed to reduce uncertainties and to fill in data gaps in the regulatory framework of pesticides and other substances such as feed additives and contaminants. For future applications, species-specific and chemical-specific kinetic data should be provided by the user for PBK modeling purposes.

D. Model characterisation (modelling workflow)

Step 1 – Scope and purpose of the model (problem formulation)

Animal risk assessment of chemicals for the protection of various animal species as well as food safety is a key regulatory and scientific research field which is undergoing constant development in modelling approaches and efforts to further harmonise with human and environmental risk assessment.

Step 2 – Model conceptualisation (model structure, mathematical representation)

The generic models are described below in Figure I1, physiological data, R codes and case studies are available in references (Lautz et al., 2019b,c; 2020a,b,c,d). The model includes eleven compartments (arterial and venous blood, gastrointestinal tract (gut lumen, gut tissue), liver, heart, brain, adipose tissue, kidney, muscle, lung, bone). Milk is included as twelfth compartment for cattle and sheep, while this compartment is replaced by eggs in chicken All the organs/tissues are modelled as well mixed compartments with a blood flow-limited distribution. The venous blood that flows out gastrointestinal tract collects in the portal vein and enters the liver. The model equations and parameter abbreviations are provided in the supporting information of the manuscripts (Lautz et al., 2020b, c).

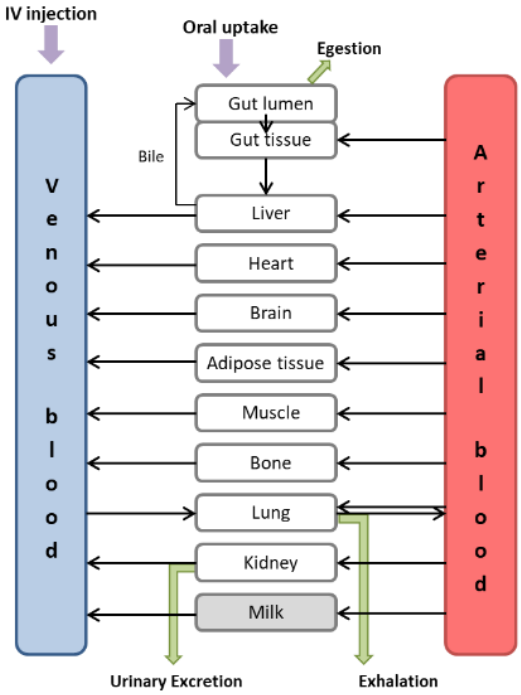

Figure I1. Schematic description of the PBK model developed for cattle, sheep, and swine. Uptake and excretion sites are presented in the purple and green, respectively. In chicken the milk compartment is replaced by an egg compartment.

Step 3 – Model parameterisation (parameter estimation and analysis)

An extensive literature search was performed to collect physiological parameters and their inter-individual variability (mean, coefficient of variation, sample size) for four farm animal species: cattle (*Bos taurus*), swine (*Sus scrofa*), and sheep (*Ovis aries*) and chicken (*Gallus gallus domesticus*). These physiological parameters were estimated based on the results of extensive literature searches described in Lautz et al., (2019b; 2020a,c,d). Relative tissue volumes and blood flows were mostly assessed using data on mature animals.

Step 4 – Computer implementation (solving the equations)

Model was developed using R software (version 3.3.3). The physiological input parameters and R codes for the PBK models and its application to the four farm animal species are also available on the EFSA knowledge junction (see Lautz et al., 2019 b,c , Lautz et al., 2020d in references) with a Creative Common Attribution 4.0 license. Physiological input parameters are available on the EFSA knowledge junction under the DOI 10.5281/zenodo.3433224 with a Creative Common Attribute 4.0 license and published elsewhere (Lautz et al., 2019).

Abbreviations and units used in PBK model equations.

Physiological parameters	Symbol	Unit
Body mass	BM (t)	kg
Organ volume	V_i	L
Cardiac output	Q_{tot}	L/min
Organ blood flow	Q_i	L/min
Milk production	Q_{milk}	L/min
Exhalation	Q_{exhale}	L/min
Concentration in organ *i*	C_i (t)	mg/kg
Chemical specific parameters		
Absorption rate constant	k_a	min^{-1}
Hepatic clearance	$Cl_{hepatic}$	L/min/kg
Renal clearance	Cl_{renal}	L/min/kg
Tissue *i*: blood partition coefficient	P_i	-
Maximal metabolic velocity	V_{max}	mg/min/L liver
Michaelis constant	K_m	mg/L

Differential equations describing the rate of change of chemical mass in each compartment

Tissue compartment	Equation
Gut lumen	$\frac{dM_{lumen}}{dt} = Q_{food} * (C_{food} - C_{faeces}) + f_1 \left(\frac{V_{max} * C_{liver}}{K_m + C_{liver}} * V_{liver} \right)$
Gut tissue	$\frac{dM_{gut}}{dt} = Q_{gut} * \left(C_{art} - \frac{C_{gut}}{P_{gut}} \right) + k_a * M_{lumen}$

Liver Metabolism Clearance	$\frac{dM_{liver}}{dt} = Q_{liver} * \left(C_{art} - \frac{C_{liver}}{P_{liver}}\right) - \frac{V_{max} * C_{liver}}{K_m + C_{liver}} * V_{liver} + Q_{gut} * \left(\frac{C_{gut}}{P_{gut}}\right) - Q_{gut} * \left(\frac{C_{liver}}{P_{liver}}\right)$ $\frac{dM_{liver}}{dt} = Q_{liver} * \left(C_{art} - \frac{C_{liver}}{P_{liver}}\right) - \left(C_{liver} * Cl_{hepatic}\right) + Q_{gut} * \left(\frac{C_{gut}}{P_{gut}}\right) - Q_{gut} * \left(\frac{C_{liver}}{P_{liver}}\right)$
Heart, Brain, Bone, Adipose tissue, Muscle, Lung	$\frac{dM_{tissue}}{dt} = Q_t * \left(C_{art} - \frac{C_t}{P_t}\right)$
Kidney	$\frac{dM_{kidney}}{dt} = Q_{kidney} * \left(C_{art} - \frac{C_{kidney}}{P_{kidney}}\right) - \left(C_{kidney} * Cl_{renal}\right)$
Venous blood	$\frac{dM_{ven}}{dt} = \sum_{T}^{not\ liver+gut} Q_t * \left(\frac{C_t}{P_t}\right) + \left(Q_{gut} + Q_{liver}\right) * \left(\frac{C_{liver}}{P_{liver}}\right) - Q_{tot} * C_{ven}$
Arterial blood	$\frac{dM_{art}}{dt} = Q_{tot} * C_{ven} * \left(\frac{Q_{tot}}{Q_{tot} + Q_{exhale} * P_{air}}\right) - Q_{tot} * C_{art}$
Milk	$\frac{dM_{mgland}}{dt} = Q_{mgland} * \left(C_{art} - \frac{C_{mgalnd}}{P_{milk}}\right) - Q_{milk} * C_{mgland}$
Egg	$\frac{dM_{reprod}}{dt} = Q_{reprod} * \left(C_{art} - \frac{C_{reprod}}{P_{egg}}\right) - Q_{egg} * C_{reprod}$

Step 5 – Model Performance

Validation of the model: comparison of predicted blood and tissues concentrations with measured data- Due to the extremely limited availability of experimental data for partition coefficients, the partitioning behaviour of a chemical in the included species was estimated using a QSAR model based on several tissue constituents (e.g. polar and non-polar lipids, water, and proteins) and the octanol/water partition coefficient. The PBK model was evaluated through comparing model predictions of tissue concentrations with experimental data measured in farm animal species and available from the literature for melamine, oxytetracycline, deltamethrin, fipronil, monensin, salinomycin, and sanguinarine (Figure I2 & I3).

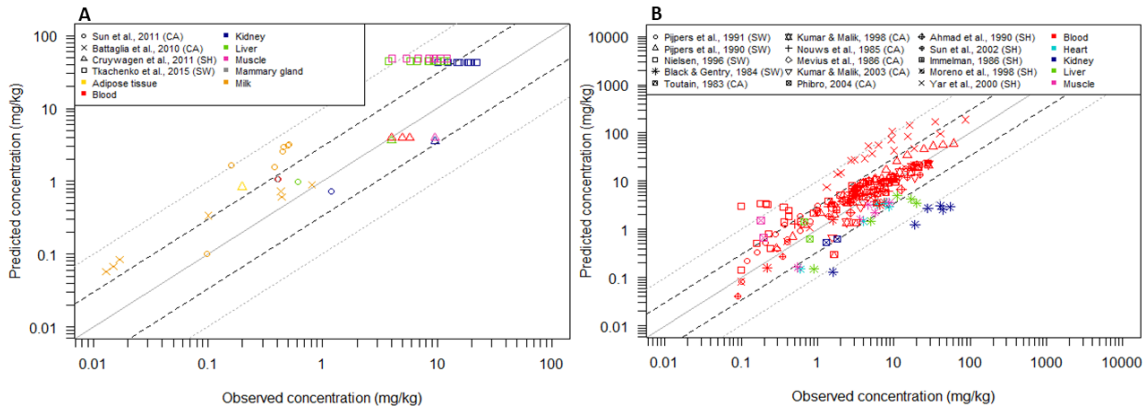

Figure I2. Comparison between concentrations measured in various organs of cattle (CA), sheep (SH), and swine (SW) and PBK model predictions for A) melamine and B) oxytetracycline. Dotted lines represent the 3-fold and 10-fold changes. Organs, species, and references of experimental datasets are indicated in legend: colours and shapes represent organs and studies, respectively.

For melamine, a data gap for melamine was identified with regards to absorption rate in the digestive tract of ruminants. However, differences between exposure and excreted concentrations in ruminants suggest that the absorption of melamine is higher than 75%. In monogastric animals, such as swine, the absorption of melamine is nearly 100% and unchanged melamine is detected in urine only. Since absorption rates for melamine in the included species were not available in literature, melamine absorption rates were extrapolated from chicken, leading to uncertainty in the PBK model inputs for this parameter with still reliable predictions in cattle and sheep. Overall, literature data on melamine in various tissues of the included species were very limited, so the quality of the included papers is of high relevance for the reliability of the model performance. Milk concentrations were overpredicted by the model in most cases when only about 2% of ingested melamine has been reported to be excreted in milk. For oxytetracycline, a veterinary antibiotic administered orally and intravenously, absorption is only partial in the swine' intestine and was not characterised in adult ruminants, i.e. cattle and sheep, and may vary compared to monogastric species. For other substances, such differences in absorption between monogastric and ruminants already have been observed. Oxytetracycline undergoes no metabolism and is excreted in urine unchanged. Overall, measured blood concentrations were often available in literature, whereas tissue concentrations were scarce for more than one time point. For oxytetracycline, model predictions were reliable compared to observed data.

Global Sensitivity analyses were performed using the variance-based Sobol method (Saltelli et al., 2008; Sobol et al., 2007). First order and total Sobol' sensitivity indices were estimated for a polar compound oxytetracycline (cattle, swine, and sheep) and melamine and deltamethrin in chicken. Sensitivity was assessed at three time points for the concentration in blood and kidney. Parameter values and exposure scenario characteristics are described in detail in the supplementary material of Lautz et al. (2019d,e, 2020c). Global sensitivity analysis of the PBK models for cattle, sheep, and swine with oxytetracycline shows that body weight (BW), cardiac output (CO) and renal blood flow (fCO_kidney) were the main contributors to the overall variance of the model output (Figure I4). However, the relative contribution of each of those varied between cattle, sheep and swine. During the absorption phase, the model output for the blood concentration was impacted by the intestinal blood flow (fCO_intestine) as well as distribution of the chemical

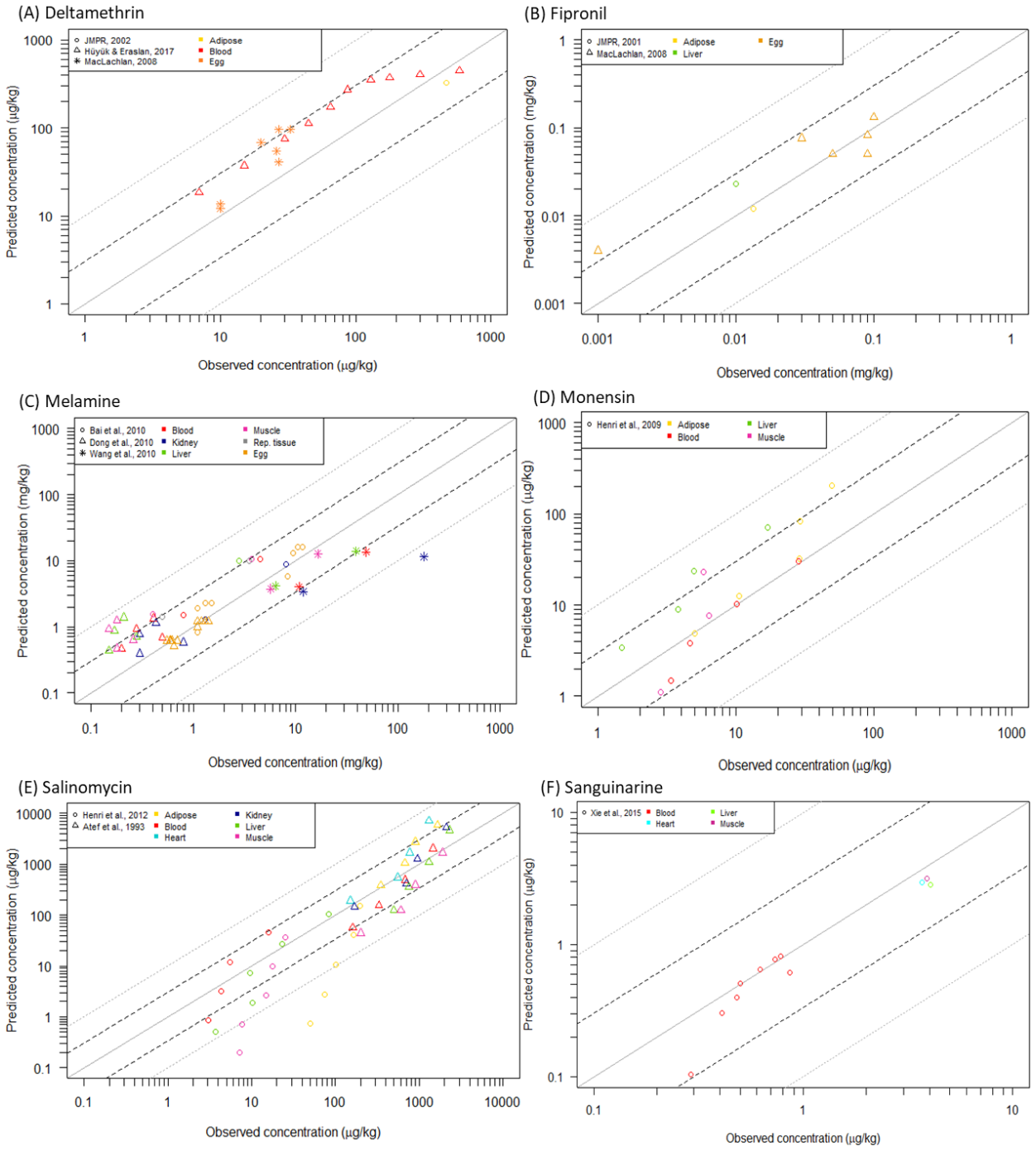

Figure I3. Comparison between quantities measured in chicken and PBK model predictions for six chemicals in various organs. Dotted lines represent the 3-fold and 10-fold changes. Organs, species, and references of experimental datasets are indicated in legend: colours and shapes represent organs and studies, respectively (Lautz et al., 2020c).

towards other organs such as muscle and adipose tissue (fBW_adipose, fCO_muscle). In the elimination phase, renal blood flow was the most sensitive parameter and had a strong influence on model outputs. The results of the global sensitivity analysis for model outputs with regards to kidney concentrations were similar to that for blood concentrations. In chicken, BW and CO were also parameters that contributed most to the variation of the model outcome, as well as intestinal blood flow (fCO_intestine) during the absorption phase (Figure I5). In the elimination phase renal blood flow (fCO_kidney) was the most sensitive parameter for melamine. For the lipophilic compound deltamethrin the neutral fraction of the tissue (nl), the adipose tissues relative volume (fBW_adipose), blood flow to the adipose tissue (fCO_adipose) and the lipid content of the tissues contributed the most to the overall variance and predictions of internal concentrations.

For melamine, a data gap for melamine was identified with regards to absorption rate in the digestive tract of ruminants. However, differences between exposure and excreted concentrations in ruminants suggest that the absorption of melamine is higher than 75%. In monogastric animals, such as swine, the absorption of melamine is nearly 100% and unchanged melamine is detected in urine only. Since absorption rates for melamine in the included species were not available in literature, melamine absorption rates were extrapolated from chicken, leading to uncertainty in the PBK model inputs for this parameter with still reliable predictions in cattle and sheep. Overall, literature data on melamine in various tissues of the included species were very limited, so the quality of the included papers is of high relevance for the reliability of the model performance. Milk concentrations were overpredicted by the model in most cases when only about 2% of ingested melamine has been reported to be excreted in milk. For oxytetracycline, a veterinary antibiotic administered orally and intravenously, absorption is only partial in the swine' intestine and was not characterised in adult ruminants, i.e. cattle and sheep, and may vary compared to monogastric species. For other substances, such differences in absorption between monogastric and ruminants already have been observed. Oxytetracycline undergoes no metabolism and is excreted in urine unchanged. Overall, measured blood concentrations were often available in literature, whereas tissue concentrations were scarce for more than one time point. For oxytetracycline, model predictions were reliable compared to observed data.

Global Sensitivity analyses were performed using the variance-based Sobol method (Saltelli et al., 2008; Sobol et al., 2007). First order and total Sobol' sensitivity indices were estimated for a polar compound oxytetracycline (cattle, swine, and sheep) and melamine and deltamethrin in chicken. Sensitivity was assessed at three time points for the concentration in blood and kidney. Parameter values and exposure scenario characteristics are described in detail in the supplementary material of Lautz et al. (2019d,e, 2020c). Global sensitivity analysis of the PBK models for cattle, sheep, and swine with oxytetracycline shows that body weight (BW), cardiac output (CO) and renal blood flow (fCO_kidney) were the main contributors to the overall variance of the model output (Figure I4). However, the relative contribution of each of those varied between cattle, sheep and swine. During the absorption phase, the model output for the blood concentration was impacted by the intestinal blood flow (fCO_intestine) as well as distribution of the chemical towards other organs such as muscle and adipose tissue (fBW_adipose, fCO_muscle). In the elimination phase, renal blood flow was the most sensitive parameter and had a strong influence on model outputs. The results of the global sensitivity analysis for model outputs with regards to kidney concentrations were similar to that for blood concentrations. In chicken, BW and CO were also parameters that contributed most to the variation of the model outcome, as well as intestinal blood flow (fCO_intestine) during the absorption

phase (Figure I5). In the elimination phase renal blood flow (fCO_kidney) was the most sensitive parameter for melamine. For the lipophilic compound deltamethrin the neutral fraction of the tissue (nl), the adipose tissues relative volume (fBW_adipose), blood flow to the adipose tissue (fCO_adipose) and the lipid content of the tissues contributed the most to the overall variance and predictions of internal concentrations.

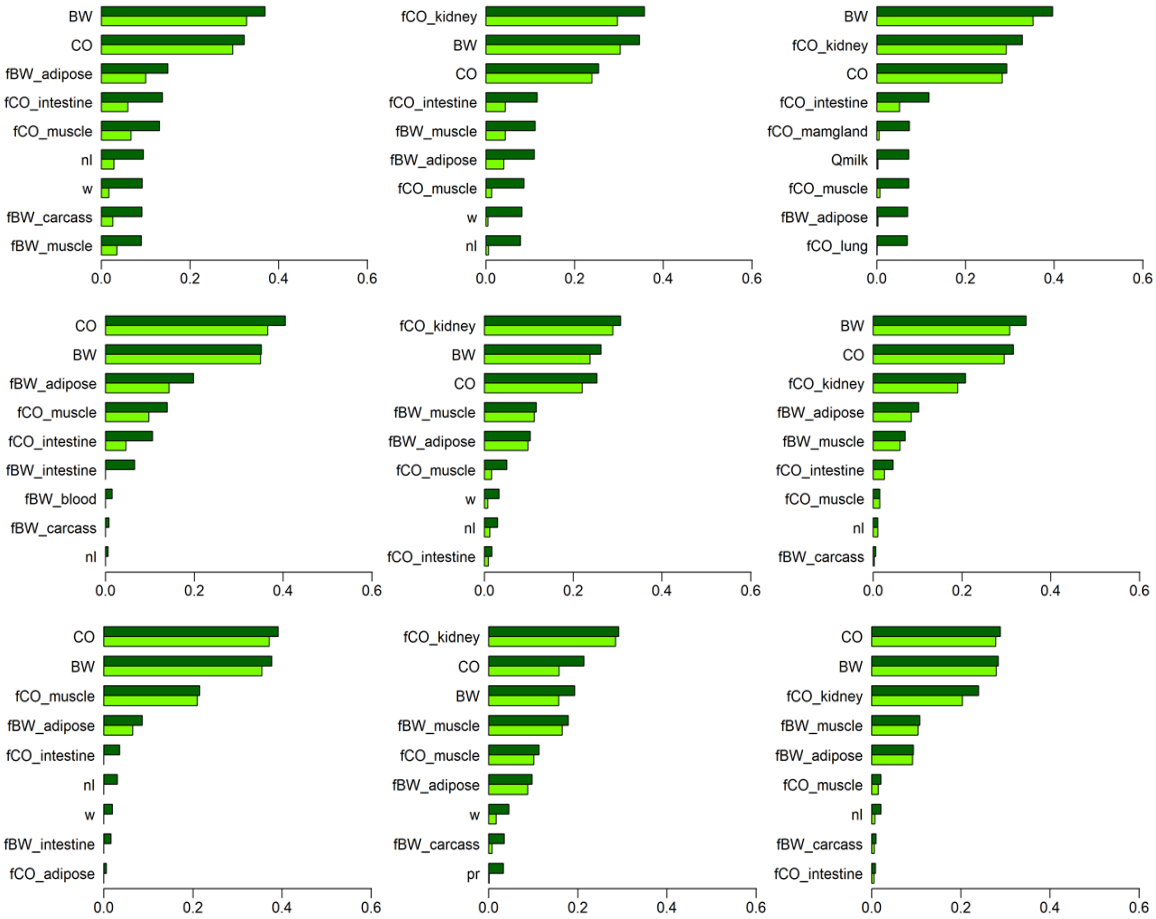

Figure I4. Sensitivity analysis of the cattle (upper panels), sheep (middle panels) and swine (lower panels) PBK model applied to oxytetracycline. Sobol's sensitivity indices were estimated for the blood concentration in the three species at three time points (from left to right): 1.25, 9.5, and 24 hours for cattle, 0.5, 6.5, and 21 hours for sheep; 0.5, 5, and 21 hours for swine. Estimation of the Sobol' total sensitivity indices (TI) are presented in dark green and estimation of the Sobol' first-order indices (FOI) in light green. The nine most influencing parameters according to the total sensitivity indices are shown.

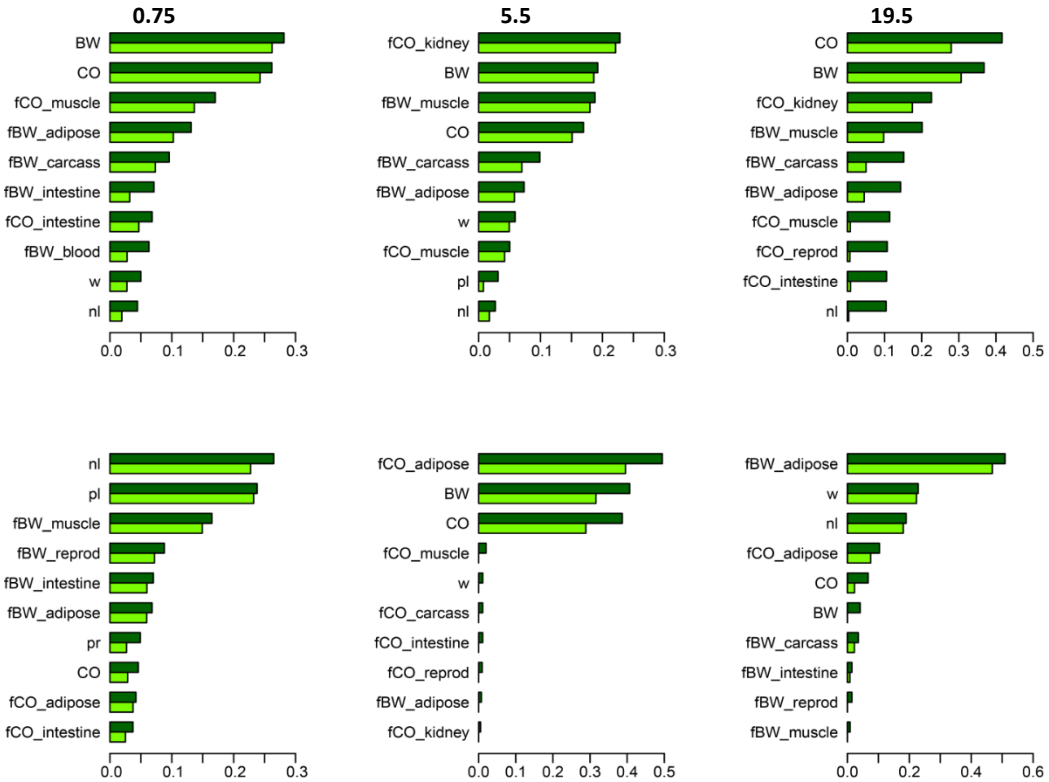

Figure I5. Sensitivity analysis of the chicken PBK model applied to melamine (upper panel) and deltamethrin (lower panel). Sobol' sensitivity analysis indices were estimated for the blood concentrations at three time points: 0.75, 5.5, and 19.5 hours. Sobol's total indices (TI) are presented in dark green and Sobol's first-order indices (FOI) in light green. Parameters were ordered according to the TI. The eleven most influencing parameters according to the total sensitivity indices are shown. BW: body weight, CO: cardiac output, fCO_tissue: fraction cardiac output of a specific tissue; fBW_tissue: fraction body weight of a specific tissue; tissue constituents neutral lipids (nl), polar lipds (pl), proteins (pr) and water (w) (Lautz et al., 2020c).

Step 6 – Model Documentation

The current generic PBK models have been published in the peer-reviewed literature (Lautz et al., 2020a, b, c) (see reference below).

E. Identification of uncertainties

Model structure

Metabolism, excretion and ingestion routes, which are chemical-specific, were the main sources of uncertainty in model structure.

Input parameters

Basic data on farm animal physiology (including blood flow, chemical uptake) were still not fully available for the included species and should be measured to improve the mechanistic aspects of the PBK models. Values for all the sheep physiological parameters were available, in contrast to cattle and swine for which interspecies extrapolations were performed. The uncertainty due to species extrapolation has not been quantified, but the global sensitivity analysis highlighted the parameters for which extrapolation may critically

affect model outputs. However, the lack of data relative to the tissue constituents in farm animal species limits the level of complexity of the QSAR models that can be used to predict partition coefficients.

Model output

Predictions of tissues concentrations for two chemicals were compared to experimental data and were accurate with 71% of predictions within a 3-fold factor. At the tissue or organ level, 58-84% of the predictions in blood, kidney, and muscle were within 3-FC, whereas 67% of the predicted concentrations in liver were between 3-FC to 10-FC. From an inter-species perspective, the model predictions showed relatively low variability with 82%, 76%, and 63% of predictions within a 3-FC for cattle, sheep, and swine respectively. Model predictions exceeded 10-FC in only 3% of cases in sheep and cattle and 9% in swine. In chicken, predictions of tissues concentrations for six chemicals were compared to experimental data and were accurate with 71% of predictions within a 3-fold factor. At the tissue or organ level, 57-97% of the predictions were within 3-FC, whereas 33-35% of the predicted concentrations in adipose tissue, liver and muscle were between 3-FC and 10-FC.

Other uncertainties (e.g. model developed for different substance and/or purpose)

None to report

Overall evaluation of uncertainties: Overall, the model accuracy did not depend on the species to a large extent with PBK model predictions in From an inter-species perspective, the model accuracy did not depend on the species to a large extend with PBK model prediction within a 3-fold change of 82%, 76%, 71%, and 63% for cattle, sheep, chicken, and swine respectively. Model predictions exceeded 10-FC in only 3% of cases in sheep and cattle and 9% in swine. However, literature data on chemical data in various tissues of the included species were very limited, so the quality of the included papers is of high relevance for the reliability of the model performance (Lautz et al., 2019d, 2020c).

F. Model implementation details

- software (version no): The code was written and executed in in R. 3.3.3
- availability of code: Yes, code is accessible via the peer reviewed publication.
- software verification / qualification: was done by peer reviewed publication.

G. Peer engagement (input/review)

Done by publishing the model in peer-reviewed journals, see references

H. Parameter tables

Physiological data and their inter-individual variability estimated based on the results of extensive literature searches are available for download in Excel (Lautz, 2019c, 2020d) [DOI: 10.5281/zenodo.3433224] and related manuscript (Lautz et al., 2019e, 2020c).

Strategy for reducing overall uncertainty

1. Peer-reviewed literature providing tissue residues, milk residues, and egg residues for a range of regulated compounds (pesticides, feed additives) and anthropogenic or naturally-occurring contaminants (e.g. persistent organic pollutants, mycotoxins) are still relatively scarce. Extensive literature searches and data collection from pre-market dossiers should be performed to develop kinetic databases to further explore the predictability of the models for a larger group of compounds.
2. The PBK models for cattle, sheep, and swine are validated for chemicals which are excreted only via the kidney, while the chicken model includes metabolism. Chemicals which may undergo transport and phase I and/or Phase II metabolism are not included in the model case studies. Integration of the *in vitro* metabolism, kinetic data and generic enzymes activities can provide the basis to further develop quantitative *in vitro* to *in vivo* extrapolation models, which can be implemented in PBK models for animal risk assessment and ultimately limit *in vivo* testing in farm animal species. More case studies would need to be conducted on chemicals of relevance to animal risk assessment in the three animal species.

I. References and background information

Lautz, LS, Oldenkamp, R, Dorne, JL, Ragas, AMJ, 2019a. Physiologically based kinetic models for farm animals: Critical review of published models and future perspectives for their use in chemical risk assessment. Toxicology in Vitro, 60: 61-70.

Lautz, LS, Hoeks, S, Oldenkamp, R. 2019b. Development of generic physiologically based kinetic models for three farm animal species, cattle, sheep, and swine. DOI: 10.5281/zenodo.3432796.

Lautz, LS. 2019c. Physiological parameters for three farm animal species (cattle, sheep, and swine) as the basis for the development of generic physiologically based kinetic models. DOI: 10.5281/zenodo.3433224.

Lautz, LS, Hoeks, S, Oldenkamp, R, Hendriks, AJ, Dorne, JL, Ragas, AMJ. 2020a. Generic physiologically based kinetic modelling for farm animals: Part II. Predicting tissue concentrations of chemicals in swine, cattle, and sheep. Toxicology Letters. 318:50-56.

Lautz, LS, Dorne, JL, Oldenkamp, R, Hendriks, AJ, Ragas, AMJ. 2020b. Generic physiologically based kinetic modelling for farm animals: Part I. Data collection of physiological parameters in swine, cattle and sheep. Toxicology Letters. Toxicology Letters 319:95-101.

Lautz LS, Nebbia C, Hoeks, Oldenkamp R, Hendriks AJ, Ragas A M J, Dorne J L C M (2020c) An Open Source Physiologically Based Kinetic Model for the Chicken (Gallus Gallus Domesticus): Calibration and Validation for the Prediction Residues in Tissues and Eggs. Environ Int. 136:105488. doi: 10.1016/j.envint.2020.105488.

Lautz,LS; Oldenkamp, R; Hendriks, AJ; Ragas, AMJ; Dorne, JLCM, (2020d) Open source physiological data and physiological-based kinetic model code for the chicken (Gallus gallus domesticus). DOI:10.5281/zenodo.3603114.

PBK model code

Model was developed using R software (version 3.3.3). The full data collection and R codes of the PBK models for cattle, swine, sheep and chicken including case studies are described in Lautz et al. and are available for download (Lautz et al, 2019a,b,c; Lautz et al, 2020d) on EFSA knowledge junction under the Creative Commons attribution 4.0 international.

PBK model input for cattle, sheep and swine

```
### Model PBK (cattle, sheep, swine) generic ###
# 01/2019
# L.S. Lautz, S. Hoeks, R. Oldenkamp
#==================================#
# probabilistic                    #
# multi-compartment model for      #
# farm animal species              #
#==================================#

#source functions
source('singlechemical_dmdt.R')

#Loading physiology data
fBW <- read.csv("data_fBW_animals.csv",stringsAsFactors = FALSE)      #organ fractions, incl distribution parameters
fCO <- read.csv("data_fCO_animals.csv",stringsAsFactors = FALSE)      #blood flow fractions, incl distribution parameters
rates <- read.csv("data_rates_animals.csv",stringsAsFactors = FALSE)  #physiological rates
fPC <- read.csv("data_pc_tissue.csv",stringsAsFactors = FALSE)        #tissue composition

#Loading TK data
TK <- read.csv("data_TK.csv",stringsAsFactors=FALSE)                  #toxicokinetic parameters

#Loading physicochemical data
chem <- read.csv("data_chem.csv", stringsAsFactors = FALSE)      #physicochemical parameters

# Inputs ----
  #Defining the exposure scenario
    species <- "species"          #cattle_d/cattle_b/sheep/swine
    chemical <- "chemical"        #add chemical name

    regime <- "bolus"             #exposure regime (bolus)
    route <- "route"              #exposure route (oral/iv)
    E_dose <- 0                   #exposure dose (mg/kgbw)
    E_start <- 0                  #start of exposure phase (h)
    E_end <- 24                   #end of exposure phase (h)
    E_int <- 24                   #interval between doses (h)

  #Simulation parameters
    A_type <- "single"            #type of probabilistic analysis ("single" or "VA")
    chem_fix <- TRUE              #fixing the chemical and TK parameters or not (TRUE/FALSE)
    n_sim  <- 1000                #number of iterations
    n_out  <- 9                   #number of compartments to output (blood, total body)
    t_start <- 0                  #start of simulation (h)
    t_end <- 24                   #end of simulation (h)
    t_A <- c(seq(0.025,0.225,by=0.025),seq(0.25,24,by=0.25)) #time points (h), only relevant when chem_fix=TRUE

#=============================================================================================
#Setup single animal simulation-----

if(A_type=="single"){
    Names_fix <- c("BW",
                   paste("fBW",colnames(fBW[2+3*c(1:19)]),sep="_"),
                   "CO",
                   paste("fCO",colnames(fCO[2+3*c(1:19)]),sep="_"),
                   colnames(rates[2+3*c(0:4)]),
                   colnames(fPC[2:57]),
                   "nl","pl","pr","w",
                   colnames(TK[3:8]),
                   colnames(chem[2:5]))
    NP_fix <- length(Names_fix) #number of fixed parameters

    fix_in <- cbind(fBW[fBW$species==species,"BW"],

fBW[fBW$species==species,colnames(fBW)%in%substr(Names_fix[grep('fBW',Names_fix)],start=5,stop=nchar(Names_fix[grep('fBW',Names_f
ix)]))],
                    fCO[fCO$species==species,"CO"],

fCO[fCO$species==species,colnames(fCO)%in%substr(Names_fix[grep('fCO',Names_fix)],start=5,stop=nchar(Names_fix[grep('fCO',Names_f
ix)]))],
                    rates[rates$species==species,colnames(rates)%in%Names_fix],
                    fPC[fPC$species==species,colnames(fPC)%in%Names_fix],
                    data.frame(nl=1,pl=1,pr=1,w=1),
                    TK[TK$species==species&TK$chemical==chemical,colnames(TK)%in%Names_fix],
                    chem[chem$chemical==chemical,colnames(chem)%in%Names_fix])
    colnames(fix_in) <- Names_fix

    par_in <- fix_in
}

#=============================================================================================
```

```
    #Setup probabilistic simulations----

    if(A_type=="VA") {
        #variability analysis with fixed chemical and toxicokinetic parameters
        Names_var <- c("BW",
                       paste("fBW",colnames(fBW[2+3*c(1:19)]),sep="_"),
                       "CO",
                       paste("fCO",colnames(fCO[2+3*c(1:19)]),sep="_"),
                       colnames(rates[2+3*c(0:4)]))

        #initial list with mean + sd values of all varying parameters
        Means <- cbind(fBW[fBW$species==species,2+3*c(0:19)],
                       fCO[fCO$species==species,2+3*c(0:19)],
                       rates[rates$species==species,2+3*c(0:4)])
        SDs <- cbind(fBW[fBW$species==species,3+3*c(0:19)],
                     fCO[fCO$species==species,3+3*c(0:19)],
                     rates[rates$species==species,3+3*c(0:4)])
        Distributions <- cbind(fBW[fBW$species==species,4+3*c(0:19)],
                               fCO[fCO$species==species,4+3*c(0:19)],
                               rates[rates$species==species,4+3*c(0:4)])
        colnames(Means) = colnames(SDs) = colnames(Distributions) = Names_var
        Names_var_not <- colnames(SDs[which(is.na(SDs))])

        Means <- Means[!(colnames(Means)%in%Names_var_not)] #exclude all parameters without SD
        SDs <- SDs[!(colnames(SDs)%in%Names_var_not)] #exclude all parameters without SD
        Distributions <- Distributions[!(colnames(Distributions)%in%Names_var_not)] #exclude all parameters without SD

        Names_var <- colnames(SDs)
        NP_var <- length(Names_var) #number of varying parameters

        #list with names of all fixed parameters (including 'varying parameters' that are 0 or NA)
        Names_fix <- c(colnames(fPC[2:57]),
                       "nl","pl","pr","w",
                       colnames(TK[3:8]),
                       colnames(chem[2:5]),
                       Names_var_not)
        NP_fix <- length(Names_fix) #number of fixed parameters

        fix_in <- cbind(fPC[fPC$species==species,colnames(fPC)%in%Names_fix],
                        data.frame(nl=1,pl=1,pr=1,w=1),
                        TK[TK$species==species&TK$chemical==chemical,colnames(TK)%in%Names_fix],
                        chem[chem$chemical==chemical,colnames(chem)%in%Names_fix],

fBW[fBW$species==species,colnames(fBW)%in%substr(Names_fix[grep('fBW',Names_fix)],start=5,stop=nchar(Names_fix[grep('fBW',Names_f
ix)]))],

fCO[fCO$species==species,colnames(fCO)%in%substr(Names_fix[grep('fCO',Names_fix)],start=5,stop=nchar(Names_fix[grep('fCO',Names_f
ix)]))],
                        rates[rates$species==species,colnames(rates)%in%Names_fix])
        colnames(fix_in) <- Names_fix

        #create data frames with random samples
        X1 <- matrix(NA, nrow = n_sim, ncol = NP_var)
        colnames(X1) <- Names_var
        X1 <- as.data.frame(X1)
        SARes <- X1

        for(i in 1:NP_var){
          if (Distributions[i] == "N") {
            SARes[,i] <- rnorm(n_sim, mean = Means[,i], sd = SDs[,i])
          } else if (Distributions[i] == "B") {
            alpha <- ((1 - Means[,i]) / SDs[,i]^2 - 1 / Means[,i]) * Means[,i] ^ 2
            beta <- alpha * (1 / Means[,i] - 1)
            SARes[,i] <- rbeta(n_sim, shape1 = alpha, shape2 = beta)
          } else if (Distributions[i] == "LN") {
            CV <- SDs[,i]/Means[,i]
            mlog <- log(Means[,i]/sqrt(1+CV^2)) #mean of log values
            slog <- sqrt(log(1+CV^2)) #sd of log values
            SARes [,i] <- rlnorm(n_sim, meanlog = mlog, sdlog = slog)
          }
        }

        var_in <- SARes
        par_in <- cbind(var_in,fix_in)
        write.csv(par_in,"par_in.csv",row.names = FALSE)

    }

    #============================================================================
    #Model application-----
    #setup table model results
      SimRes <- matrix(NA, nrow = nrow(par_in), ncol = n_out*length(t_A))
      colnames(SimRes) <- c(paste("blood_t",t_A,sep=""), paste("fat_t",t_A,sep=""),paste("liver_t", t_A, sep=""),
                            paste("kidney_t",t_A,sep=""), paste("muscle_t",t_A,sep=""),paste("heart_t", t_A, sep=""),
                            paste("brain_t",t_A,sep=""), paste("carcass_t",t_A,sep=""),paste("lung_t", t_A, sep=""))

    #Input model function
      for (j in 1:nrow(par_in)) {
        print(paste0("Running loop: ", j))
        print(paste("Current time: ", Sys.time()))

        SimRes[j,] <- multi_tool(
          par_in = par_in[j,], #input data frame
          species = species, regime = regime, route = route, E_dose = E_dose, E_start = E_start, E_end = E_end, E_int = E_int,
```

```
          n_out = n_out, t_start = t_start, t_end = t_end, t_A = t_A, chem_fix = chem_fix)
      }

    write.csv(SimRes,"results.csv",row.names = FALSE)
```

PBK model function with integrated QSAR for tissue:blood partition coefficients

```
    ### Model PBK (cattle, sheep, swine) generic ###
    # 01/2019
    # R. Oldenkamp, S. Hoeks, L.S. Lautz
    #==================================#
    # probabilistic                    #
    # multi-compartment model function  #
    # for farm animal species          #
    #==================================#
    dMdt <- function(i, M, C, h, physnames,
                     Qin, Qout, CO, PC, OW,
                     E_bolus, E_cont, E_iv, kgastric,
                     Qbolus, Qingest, Qiv, Qexhale,
                     kabs, Vmax, Km, Cl, fbile, fbact, Qmilk) {
      #input via food
      dMfood <- E_bolus[i] * Qbolus + E_cont[i] * Qingest
      #input via iv
      dMiv <- E_iv[i] * Qiv
      #absorption over intestinal wall
      dMabs <- M[physnames=="lumen"] * kabs
      #delivery via arterial blood
      dMart <- Qin * C[physnames=="art"]
      dMart[physnames=="art"] <- -sum(dMart)
      #delivery to venous blood and passage through portal vein
      dMven <- Qout * (C / PC)
      dMart[physnames=="liver"] <- dMart[physnames=="liver"] - dMven[physnames=="intestine"]
      dMven[physnames=="liver"]   <-   dMven[physnames=="liver"]   +   Qout[physnames=="intestine"]   *   (C[physnames=="liver"]   /
PC[physnames=="liver"])
      dMven[physnames=="ven"] <- -sum(dMven[physnames!="intestine"])
      #metabolism an enterohepatic circulation and retransformation
      dMmet <- ifelse(!is.na(Vmax)&!is.na(Km),(Vmax*(C/PC))/(Km+(C/PC))*OW,0)
      dMmet[physnames=="liver"] <- ifelse(!is.na(Cl[physnames=="liver"]),Cl[physnames=="liver"]*C[physnames=="liver"])
      dMmet[physnames=="lumen"] <- -dMmet[physnames=="liver"] * fbile * fbact
      dMmet[physnames=="metab"] <- -dMmet[physnames=="liver"] - dMmet[physnames=="lumen"]
      #transport over lung and exhalation
      dMexh <- -CO * C
      dMexh[physnames!="ven"] <- 0
      dMexh[physnames=="art"] <- -dMexh[physnames=="ven"] * (CO / (CO + Qexhale * PC[physnames=="air"]))
      dMexh[physnames=="air"]   <-   -dMexh[physnames=="ven"]   *   ((Qexhale   *   PC[physnames=="air"])/(CO   +   Qexhale   *
PC[physnames=="air"]))
      #excretion to urine, milk, feces
      dMexc <- M[physnames=="lumen"] * kgastric
      dMexc[physnames=="kidney"] <- C[physnames=="kidney"] * Cl[physnames=="kidney"]
      dMexc[physnames=="mamgland"] <- C[physnames=="mamgland"] * Qmilk[physnames=="mamgland"]
      dMexc[physnames=="urine"] <- -dMexc[physnames=="kidney"]
      dMexc[physnames=="milk"] <- -dMexc[physnames=="mamgland"]

      dMdt <- dMfood + dMiv + (dMabs + dMart + dMven + dMmet + dMexh + dMexc) * (h / 60)

      M <- M + dMdt
      C <- ifelse(OW==0,0,M/OW)

      return(list(M=M,C=C))
    }

    #Function to run model
    multi_tool <- function(par_in, species, regime, route, E_dose, E_start, E_end, E_int, n_out, t_start, t_end, t_A, chem_fix) {

      #Physicochemical properties ----
      MW <- par_in$MW
      Kow <- par_in$Kow #Kow
      S <- (0.001*par_in$S) / MW  #solubility
      Temp <- 298       #Temperature 298 K = 25 degC
      R <- 8.314        #Gas constant (J/mol/K)
      Pv <- par_in$Pv #vapor pressure

      #General physiology ----
      BW <- par_in$BW            #bodyweight (kg)
      CO <- par_in$CO         #cardiac output (L/min)

      Qexhale <- (0.499 * (BW^0.81))      #Ventilation mammalian (L/min)

      #one matrix per relevant phys parameter (in right order)
      comp <- colnames(par_in[grep('fBW',colnames(par_in))])
      comp <- comp[order(comp)]
      physnames <- c(substr(comp,start=5,stop=nchar(comp)),"ven","art","lumen","milk","urine","air","feces","metab","feed","iv")

      #Organ weights
      fBW <- c(t(par_in[comp]),rep(0,11))
      fBW[physnames=="ven"] <-  2/3 * fBW[physnames=="blood"]
      fBW[physnames=="art"] <-  1/3 * fBW[physnames=="blood"]
      fBW <- fBW[physnames!="blood"]
      OW <- BW*fBW/sum(fBW) #organ volums (L), based on normalized weight fractions and overall assumed density of 1 L/kg
```

```
      #Blood flows Q
      comp <- gsub('fBW','fCO',comp)
      fCO <- c(t(par_in[comp]),rep(0,11))
      fCO <- (fCO[physnames!="blood"])
      Qin <- fCO*CO/sum(fCO) #blood flows (L/min), normalized to CO
      Qout <- -Qin

      #Tissue-blood partitioning
      comp                                                                                                                  <-
c(colnames(par_in[grep('_nl',colnames(par_in))]),colnames(par_in[grep('_pl',colnames(par_in))]),colnames(par_in[grep('_pr',colnam
es(par_in))]),colnames(par_in[grep('_w',colnames(par_in))]))
      comp <- comp[order(comp)]

      PCcomp <- comp[c(-grep('exp_',comp),-grep('int_',comp))] #all tissue composition -names
      fPC_old <- c(t(par_in[PCcomp])) #'old fractions'
      fPC_new <- fPC_old*c(par_in$nl,par_in$pl,par_in$pr,par_in$w) #new fractions

        #normalisation to mean sum
        sumold <- rep(tapply(fPC_old,rep(seq(length(fPC_old)/4),each=4),sum),each=4)
        sumnew <- rep(tapply(fPC_new,rep(seq(length(fPC_old)/4),each=4),sum),each=4)
        fPC_new <- fPC_new*(sumold/sumnew)

      PCexps <- comp[grep('exp_',comp)]
      fPC_exp <- c(t(par_in[PCexps]))   #all QSAR exponents
      PCints <- comp[grep('int_',comp)]
      fPC_int <- c(t(par_in[PCints]))   #all QSAR intercepts

      tissnames <- c(substr(PCcomp[grep('_nl',PCcomp)],start=1,stop=nchar(PCcomp[grep('_nl',PCcomp)])-3))
      PC1 <- fPC_int*fPC_new*Kow^fPC_exp
      PC1 <- tapply(fPC_int*fPC_new*Kow^fPC_exp,rep(seq(length(PC1)/4),each=4),sum) #partitioning coefficients tissue-water
      PC <- rep(PC1[tissnames=="blood"],length(physnames))
      PC[match(tissnames,physnames)] <- PC1
      PC[physnames=="air"] <- (Pv/S)/(R*Temp)
      PC[is.na(PC)] <- PC[physnames=="blood"]
      PC <- PC/PC[physnames=="blood"]
      PC <- PC[physnames!="blood"]

      #Rates and flows (not chemical-dependent)
      physnames <- physnames[physnames!="blood"]
      Qingest <- rep(0,length(physnames))
      Qiv <- rep(0,length(physnames))
      Qbolus <- rep(0,length(physnames))
      kgastric <- rep(0,length(physnames))
      Qmilk <- rep(0,length(physnames))
      fbile <- par_in$fbile #fraction of metabolites reentering lumen with bile (-)

      Qingest[physnames=="lumen"] <- par_in$Qingest / (24*60) #ingestion rate kgfeed/min
      Qingest[physnames=="feed"] <- -par_in$Qingest / (24*60)
      Qiv[physnames=="ven"] <- 1
      Qiv[physnames=="iv"] <- -1
      Qbolus[physnames=="lumen"] <- 1
      Qbolus[physnames=="feed"] <- -1
      kgastric[physnames=="feces"] <- par_in$kgastric
      kgastric[physnames=="lumen"] <- -par_in$kgastric           #gastric emptying rate constant (1/min)
      Qmilk[physnames=="mamgland"&Qin!=0] <- -par_in$Qmilk       #milk production rate (L/min)

      #TK parameters
      kabs <- rep(0,length(physnames))
      Vmax <- rep(NA,length(physnames))
      Km <- rep(NA,length(physnames))
      Cl <- rep(0,length(physnames))

      fbact <- par_in$fbact
      kabs[physnames=="intestine"] <- par_in$kabs
      kabs[physnames=="lumen"] <- -par_in$kabs
      Vmax[physnames=="liver"] <- -par_in$Vmax_tot
      Km[physnames=="liver"] <- par_in$Km_tot
      Cl[physnames=="liver"] <- -par_in$Cl_hepatic * BW
      Cl[physnames=="kidney"] <- -par_in$Cl_renal * BW


      #Time vector for exposure ----
      h <- 3                                        #stepsize in seconds
      t <- seq(3600*t_start,3600*t_end,by=h)        #vector with timepoints (seconds)
      E_iv <- rep(0,times=length(t))
      E_bolus <- rep(0,times=length(t))
      E_cont <- rep(0,times=length(t))

      if (route=="oral" & regime == "bolus") {
        E_bolus[t>=E_start*3600 & t<3600*E_end & t%%(3600*E_int)==0] <- (E_dose/MW)*BW
      } else if (route=="oral" & regime == "continuous") {
        E_cont[t>=E_start*3600 & t<3600*E_end] <- ((E_dose/MW)/par_in$Qingest)*BW #mmol/kgfeed
      } else {
        E_iv[t==E_start*3600] <- (E_dose/MW)*BW
      }

      M <- rep(0,length(physnames)) #mass per compartment (mmol)
      C <- rep(0,length(physnames)) #concentration per compartment (mmol/L)

    #Create output sheet ----
      if (chem_fix) {
        results <- matrix(NA,nrow=1,ncol=n_out*length(t_A))
        colnames(results) <- c(paste("blood_t",t_A,sep=""), paste("fat_t",t_A,sep=""),paste("liver_t", t_A, sep=""),
                               paste("kidney_t",t_A,sep=""), paste("muscle_t",t_A,sep=""),paste("heart_t", t_A, sep=""),
```

```
                              paste("brain_t",t_A,sep=""), paste("carcass_t",t_A,sep=""),paste("lung_t", t_A, sep=""))
      } else {
        results <- matrix(0,nrow=1,ncol=3)
        colnames(results) <- c("Cmax","tmax","AUC_24h")
      }

    #Model simulation ----
      for (i in 1:length(t)) {
        output <- dMdt(i=i, M=M, C=C, h=h, physnames=physnames, Qin=Qin, Qout=Qout, CO=CO,
                       PC=PC, OW=OW, E_bolus=E_bolus, E_cont=E_cont, E_iv=E_iv, kgastric=kgastric,
                       Qbolus=Qbolus, Qingest=Qingest, Qiv=Qiv, Qexhale=Qexhale, kabs=kabs, Vmax=Vmax,
                       Km=Km, Cl=Cl, fbile=fbile, fbact=fbact, Qmilk=Qmilk)

        M <- output$M
        C <- output$C

    #Write to results for t_A
    if (chem_fix & any(t[i]==round(t_A*3600))) {
        results[,paste("blood_t",t[i]/3600,sep="")] <- C[physnames=="ven"] * MW
        results[,paste("fat_t",t[i]/3600,sep="")] <- C[physnames=="adipose"]* MW
        results[,paste("liver_t",t[i]/3600,sep="")] <- C[physnames=="liver"] * MW
        results[,paste("kidney_t",t[i]/3600,sep="")] <- C[physnames=="kidney"] * MW
        results[,paste("muscle_t",t[i]/3600,sep="")] <- C[physnames=="muscle"] * MW
        results[,paste("heart_t",t[i]/3600,sep="")] <- C[physnames=="heart"] * MW
        results[,paste("brain_t",t[i]/3600,sep="")] <- C[physnames=="brain"] * MW
        results[,paste("carcass_t",t[i]/3600,sep="")] <- C[physnames=="carcass"] * MW
        results[,paste("lung_t",t[i]/3600,sep="")] <- C[physnames=="lung"] * MW

      } else if (!chem_fix) {
        results[,"tmax"] <- ifelse(C[physnames=="ven"]>results[,"Cmax"],t[i]/3600,results[,"tmax"])
        results[,"Cmax"] <- ifelse(C[physnames=="ven"]>results[,"Cmax"],C[physnames=="ven"],results[,"Cmax"])
        results[,"AUC_24h"] <- results[,"AUC_24h"] + C[physnames=="ven"]
      }
    }

      return(results)
}
```

Part II Checklist for model evaluation

PBK Model Evaluation Checklist	Checklist assessment	Comments
Name of the PBK model (as in the reporting template)	Generic PBK model for farm animal species	
Model developer and contact details	(1) Leonie Lautz, (1) Jan Hendriks, (1) Ad Ragas, (2) Jean Lou Dorne 1) Radboud University, Nijmegen, Netherlands; 2) European Food Safety Authority, Parma, Italy	
Name of person reviewing and contact details	**A Paini**	
Date of checklist assessment	**10/01/2020**	
A. Context/Implementation		
A.1. Regulatory Purpose		
1. What is the acceptable degree of confidence/uncertainty (e.g. high, medium or low) for the envisaged application (e.g. priority setting, screening, full assessment?)	**high**	
2. Is the degree of confidence/uncertainty in application of the PBK model for the envisaged purpose greater or less than that for other assessment options (e.g. reliance on PBK model and *in vitro* data vs. no experimental data)?	**high**	
A.2. Documentation		
3. Is the model documentation adequate, i.e. does it address the essential content of model reporting template, including the following:	**YES**	
• Clear indication of the chemical, or chemicals, to which the model is applicable?	**YES**	
• Is the model being applied for the same scientific purpose as it was developed, or has it been repurposed somehow?	**YES**	
• Model assumptions?	**YES**	
• Graphical representation of the proposed mode of action, if known?	**NO**	
• Graphical representation of the conceptual model?	**YES**	
• Supporting tabulation for parameters (names, meanings, values, mean and standard deviations, units and sources)?	**YES**	
• Relevance and reliability of model parameters?	**YES**	
• Uncertainty and sensitivity analysis?	**YES**	
• Mathematical equations?	**YES**	
• PBK model code?	**YES**	**Reported in the peer reviewed articles and EFSA**

		Knowledge junction
• Software algorithm to run the PBK model code?	**NR**	**R**
• Qualification of PBK software platform?	**NA**	
A.3 Software Implementation and Verification		
4. Does the model code express the mathematical model?	**YES**	
5. Is the model code devoid of syntactic and mathematical errors?	**YES**	
6. Are the units of input and output parameters correct?	**YES**	
7. Is the chemical mass balance respected at all times?	**YES**	
8. Is the cardiac output equal to the sum of blood flow rates to the tissue compartments?	**YES**	
9. Is the sum total of tissue volumes equal to total body volume?	**YES**	
10. Is the mathematical solver a well-established algorithm?	**YES**	
11. Does the mathematical solver converge on a solution without numerical error?	**YES**	
12. Has the PBK modelling platform been subjected to a verification process (for a different use, for instance, in the pharmaceutical domain)?	**YES**	**Pharmaceutical examples in the publications**
A.4 Peer engagement (input/review)		
13.a Has the model been used previously for a regulatory purpose?	**NO**	
• Is prior peer engagement in the development and review of the model sufficient to support the envisaged application?	**YES**	
• Is additional review required? Peer engagement includes input/review by experts on specific aspects of model development, individual reviews of the model by experts, or collective reviews by peer review panels. Availability of the comments and tracking of revisions to the model in response to peer input contributes to increased confidence in the model for potential application.	**YES**	
B. Assessment of Model Validity		
B.1 Biological Basis (Model Structure and Parameters)		
14. Is the model consistent with known biology?	**YES**	
• Is the biological basis for the model structure provided?	**YES**	
• Is the complexity of the model structure appropriate to address the regulatory application?	**YES**	
• Are assumptions concerning the model structure and parameters clearly stated and justified?	**YES**	
• Is the choice of values for physiological parameters justified?	**YES**	
• Is the choice of methods used to estimate chemical-specific ADME parameters justified?	**YES**	

• Saturable kinetics	**YES**	
B.2 Theoretical Basis of Model Equations		
15. Are the underlying equations based on established theories, .e.g. Michaelis-Menten kinetics, Fick's laws of diffusion?	**YES**	
• In the case of PBK models for particles, does the model take into consideration the properties of particles, e.g. particle size ranges, (poor) solubility, aggregation, partitioning and diffusion/sedimentation behaviour?	**NA**	
B.3. Reliability of input parameters		
16. Has the uncertainty (individual variability, experimental reproducibility and reliability) in the input parameters been characterised?	**YES**	
B.4. Uncertainty and Sensitivity Analysis		
17. Has the impact of uncertainty (individual variability, experimental reproducibility and reliability) in the parameters on the chosen dose metric been estimated?	**YES**	
• Local sensitivity analysis?	**NO**	
• Global sensitivity analysis?	**YES**	
18. Is confidence in influential input parameter estimates (i.e., based on comparison of uncertainty and sensitivity) reasonable (within expected values; similar to those of analogues) in view of the intended application?	**YES**	
B.5. Goodness-of-Fit and Predictivity		
19. For PBK models for which there are sufficient *in vivo* data for the chemical of interest:		
• Suitability as analogue (chemical and biological similarity)?	**NA**	
• Reliable estimation of chosen dose metric for analogue?	**NA**	
• In general is the biological Variability of *in vivo* reference data (from analogue) established?	**NA**	

NA = not applicable, NR = not reported

Part III Overall Evaluation

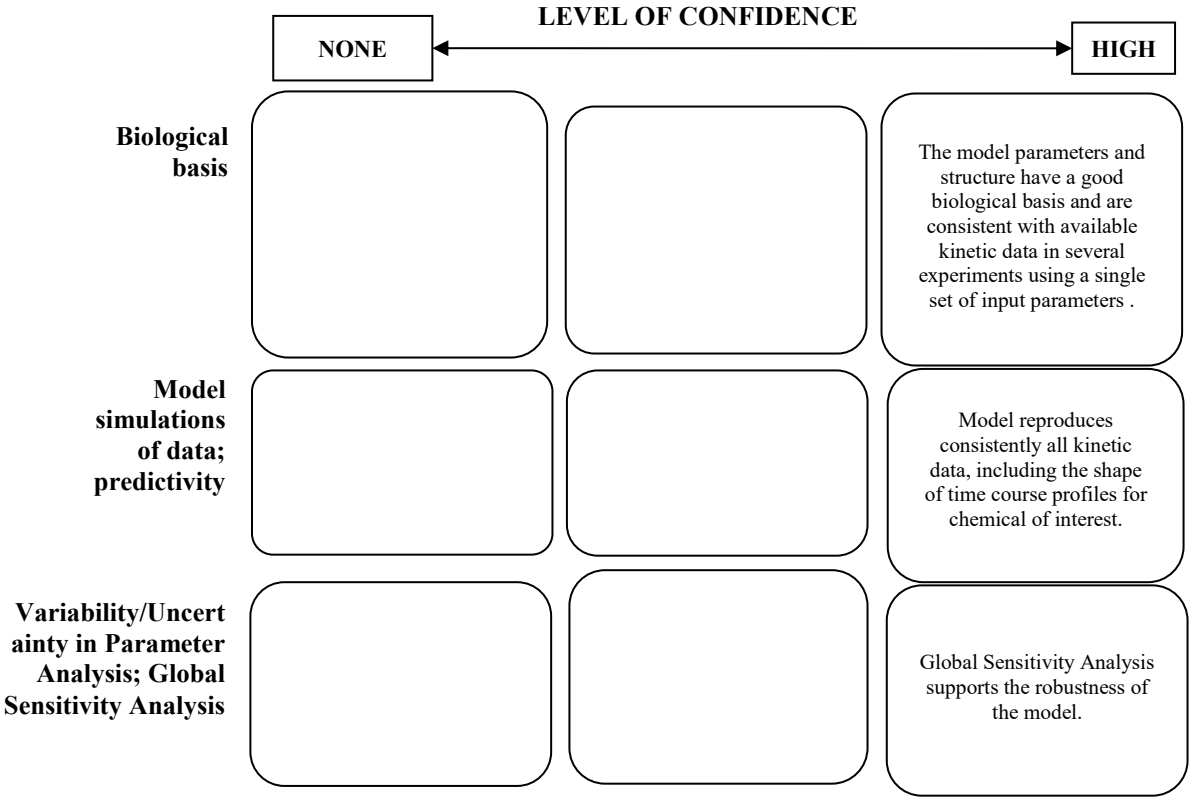

These generic farm animal PBK models reported in the present work were developed to determine residues in tissues of four farm animal species (cattle, sheep, swine and chicken), milk (cattle and sheep) and eggs (chicken) for applications in the feed and food safety areas. The documentation provided is strong and the level of confidence scored is high. The models presented here can be applied in feed and food risk assessment of chemicals with high confidence.

Summary Table

The table below provides a summary evaluation of the model using WHO criteria (WHO, 2010).

Evaluation of the generic PBK chicken model according to WHO criteria (from Lautz et al., 2020c)

Category	Characteristic
Scope and purpose of the model	- Model purpose: generic PBK model - Species: Chicken - Age, life stage(s), sex, exposure window(s): adult, males and females, single and multiple doses - Exposure route(s), and dose metric(s): Oral - Target organs and tissues: whole body, blood, organs and tissues, eggs
Model structure and mathematical description	- Graphical representation of the model available - 12 compartments including eggs - Steady-state and differential calculations - Mass balance equations given
Computer implementation	- Model implemented in R - Model codes and syntax available (DOI to be inserted)
Parameter estimation and analysis	- Anatomical and physiological parameter values from the literature or predicted - Physicochemical and biochemical parameter values from literature or predicted
Model calibration and validation	- Global sensitivity analysis performed - Model calibrated with measured data from 7 compounds - Calibration data adequately reported - Model validation against independent data - Validation data reported (Figures I4 and I5) - Variability analysis of the model predictions: predicted versus experimental data expressed as fold changes
Model documentation	- Peer-reviewed model - Publicly available model

Case Study II

Generic PBK models for four fish species

Part I. PBK model reporting template

A. Name of model

Generic PBK model for four fish species

B. Contact details

(1) Remy Beaudouin, (1) Audrey Grech, (1) Cleo Tebby, (2) Frédéric Bois (2) Nadia Quignot, (3) Jean Lou CM Dorne, (1) Celine Brochot

1) INERIS, Paris, France; 2) CERTARA, Paris, France; 3) European Food Safety Authority, Parma, Italy

C. Summary of model characterisation, development, validation, and potential applicability

Environmental risk assessment of chemicals for the protection of ecosystems integrity is a key regulatory and scientific research field which is undergoing constant development in modelling approaches and efforts to further harmonise with human risk assessment. A recent review highlighted available one-compartment models and PBK models for terrestrial and aquatic organisms and identified the need to further develop generic models for species of environmental relevance (Grech et al., 2017). Here, generic physiologically-based models for four fish species: rainbow trout (Onchorhynchus mykiss), zebrafish (Danio rerio), fathead minnow (Pimephales promelas), and three-spined stickleback (Gasterosteus aculeatus) have been developed in the open source freeware R. For each species, the PB(T)K model has been implemented for nine regulated compounds and environmental contaminants (with log kow from -0.9 to 6.8) to predict whole-body concentrations, assess the overall bio-concentration of each compound as well as the concentration in fish organs. Global sensitivity analyses have been performed using the functions "ODE" in desolve package and "soboljansen" to identify parameters which have the most impact on the models's outputs. Predictions of whole body and tissues concentrations for nine chemicals were compared with experimental data and were accurate with 50% of predictions within a 3-fold factor for six out of nine chemicals and 75% of predictions within a 3-fold factor for three of the most lipophilic compounds. For future applications, fish-specific and chemical-specific kinetic data should be provided by the user for PBK modeling purposes.

D. Model characterisation (modelling workflow)

Step 1 – Scope and purpose of the model (problem formulation)

The scope of these models ranges from priority settings and screening of data poor chemicals for which bioconcentration factors and whole-body concentrations from water exposures to potentially estimate internal dose at the target organ of toxicity. The generic models can also allow full environmental risk assessment of chemicals for regulated

chemicals and contaminants for which data are available including bioconcentration factors, internal dose (concentrations) in the blood, plasma, organs (liver, kidney etc.), kinetic parameters (Cmax, AUC, Clearance, half-life etc..). From such predictions, internal doses can be used as input for deriving points of departure in fish species using benchmark dose modelling on an internal dose basis as well as assess and predict carry over and residues on an internal basis in organs of interest.

Step 2 – Model conceptualisation (model structure, mathematical representation)

The generic models are described below in figure II 1, physiological data, R Codes and case studies are available in references (Grech et al., 2018a,b and Grech et al., 2019). The model comprises twelve compartments (arterial and venous blood, gills, gastrointestinal tract, skin, kidney, fat, liver, gonads, brain, poorly perfused tissues, and richly perfused tissues). All the organs/tissues are modelled as well mixed compartments with a blood flow-limited distribution. The venous blood that flows out of the richly perfused tissues, gastrointestinal tract, and gonads collects in the portal vein and enters the liver. The model equations and parameter abbreviations are provided in the supporting information of the manuscript (Grech et al., 2019).

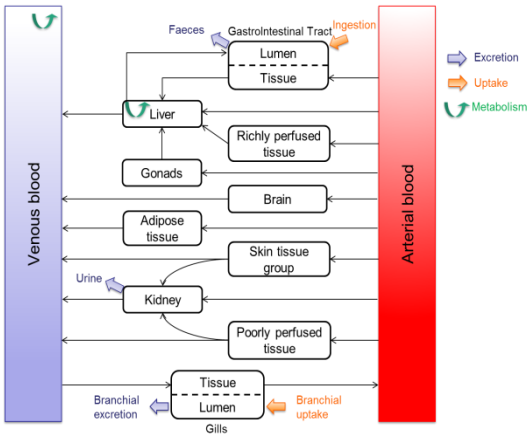

Figure II 1. Schematic description of the generic PBTK model for Rainbow trout, Zebrafish, Fathead minnow, and Stickleback. Uptake, excretion, and metabolism sites are represented in orange, purple, and green, respectively.

Step 3 – Model parameterisation (parameter estimation and analysis)

An extensive literature search was performed to collect physiological parameters and their inter-individual variability (mean, coefficient of variation, sample size) for four fish species: rainbow trout (Onchorhynchus mykiss), zebrafish (Danio rerio), fathead minnow (Pimephales promelas), and three-spined stickleback (Gasterosteus aculeatus). These physiological parameters were estimated based on the results of extensive literature searches and specific experimental data described in Grech et al., (2019). Relative tissue volumes and blood flows were mostly assessed using data on adults (i.e. sexually mature females and males, ignoring sexed juveniles) and were assumed to remain constant during the whole life time.

The QSAR models presented by Bertelsen et al. (1998) and Nichols et al. (2006) were used, as suggested by Pery et al. (2014).

Step 4 – Computer implementation (solving the equations)

Model equations

For clarity in the following equations, the times dependence of the parameter is not indicated.

The rate of change in amount of compound in compartments with no input, elimination, or metabolism, i.e. brain, gonads, richly perfused tissue (RPT), poorly perfused tissue (PPT), adipose tissues, and skin were described by the following differential equation:

$$\frac{dQ_i}{dt} = F_i \times (C_{art} - \frac{C_i}{PC_i}) \text{(Eq. 1)}$$

The PPT is composed of the bones, fins, and white muscle. The RPT is composed of the spleen, heart, pancreas, thyroid glands, adrenals, bone marrow, and red muscle.

Arterial blood

$$\frac{dQ_{art}}{dt} = F_{card} \times (C_{ven} - C_{art}) \quad \text{(Eq. 2)}$$

Gastrointestinal Tract

Absorption by ingestion of contaminated food was modelled in the GIT. The GIT was divided into two sub-compartments (lumen and tissue) includes enterohepatic circulation.

$$\frac{dQ_{lumen\_GIT}}{dt} = Frac_{abs} \times Q_{ingest} - (K_u + Ke_{feces}) \times Q_{lumen_{GIT}} + K_{BG} \times Q_{bile}$$

(Eq. 3)

With Qingest the quantity administered in the GIT, Fracabs the absorption fraction, Ku the diffusion coefficient, Kefeces the faecal excretion, Qbile the biliary quantity, and KBG the transfer rate constant from bile to GIT lumen.

With $\frac{dQfeces}{dt} = Ke_{feces} \times Q_{lumen_{GIT}}$ (Eq. 4)

$$\frac{dQ_{GIT}}{dt} = K_u \times Q_{lumen\_GIT} + F_{GIT} \times (C_{art} - \frac{C_{GIT}}{PC_{GIT}}) \quad \text{(Eq. 5)}$$

Kidney

Part of the venous blood draining the skin and PPT is assumed to flow to the kidney (Nichols et al., 1996; Satchell, 1991; Satchell, 1992; Steffensen and Lomholt, 1992).

$$\frac{dQ_k}{dt} = F_k \times C_{art} + (1 - \alpha_{Fpp}) \times F_{pp} \times \frac{C_{pp}}{PC_{pp}} + (1 - \alpha_{Fs}) \times F_s \times \frac{C_s}{PC_s} - (F_k + (1 - \alpha_{Fpp}) \times F_{pp} + (1 - \alpha_{Fs}) \times F_s) \times \frac{C_k}{PC_k} - \frac{dQurine}{dt} \quad \text{(Eq. 6)}$$

With $\frac{dQurine}{dt} = Ke_{urine} \times Q_k$ (Eq. 7)

Where αFpp is the fraction of venous blood flow distribution of PPT and αFs the fraction of venous blood flow distribution of skin.

Liver

In the liver, chemicals can be eliminated to the bile (Kebile) or metabolised. QMl is the quantity metabolized in liver. Consequently, for the liver, accounting for fish blood circulation and possible metabolism, we have:

$$\frac{dQ_l}{dt} = F_l \times C_{art} + F_{rp} \times \frac{C_{rp}}{PC_{rp}} + F_{git} \times \frac{C_{git}}{PC_{git}} + F_{go} \times \frac{C_{go}}{PC_{go}} - \left(F_l + F_{rp} + F_{git} + F_{go}\right) \times \frac{C_l}{PC_l} - Ke_{bile} \times Q_l - \frac{dQ_{M_l}}{dt} \quad \text{(Eq.8)}$$

Biliary excretion takes place in the liver according to first order kinetics, and bile is excreted in the small intestine lumen:

$$\frac{dQbile}{dt} = Ke_{bile} \times Q_l - (K_{BG} \times Q_{bile}) \quad \text{(Eq. 9)}$$

Metabolism can occur in the liver, at a rate proportional to the concentration in venous blood at liver exit. Depending on data availability, it can be described as a linear or saturable process.

In case of a first-order metabolic rate (linear process), the metabolism was modelled as:

$$\frac{dQ_{M_l}}{dt} = Cl_{hepatic} \times \frac{C_l}{PC_l} \quad \text{(Eq. 10)}$$

Clhepatic being the hepatic clearance (mL/d).

The saturable Michaelis-Menten model uses two parameters: the maximal metabolic rate (V_{max}) and the affinity constant (K_m; substrate concentration at which the reaction rate is half of V_{max}):

$$\frac{dQ_{M_l}}{dt} = \frac{V_{max} \times \frac{C_l}{PC_l}}{K_m + \frac{C_l}{PC_l}} \quad \text{(Eq. 11)}$$

Venous blood

Absorption and excretion are supposed to occur through the gills and take place in venous compartment.

$$\frac{dQ_{ven}}{dt} = F_b \times \frac{C_b}{PC_b} + F_f \times \frac{C_f}{PC_f} + \left(F_l + F_{rp} + F_{go} + F_{GIT}\right) \times \frac{C_l}{PC_l} + \left(F_k + \left(1 - \alpha_{Fpp}\right) \times F_{pp} + (1 - \alpha_{Fs}) \times F_s\right) \times \frac{C_k}{PC_k} + \alpha_{Fpp} \times F_{pp} \times \frac{C_{pp}}{PC_{pp}} + \alpha_{Fs} \times F_s \times \frac{C_s}{PC_s} - F_{card} \times C_{ven} + \frac{dQ_{admin\_gill}}{dt} - \frac{dQ_{M_p}}{dt} - \frac{dQ_{excret\_gill}}{dt} \quad \text{(Eq. 12)}$$

With Qadmin_gill the uptake rate from water into blood, QMp the quantity metabolized in plasma, and Qexcret_gill the quantity excreted through gills.

Qadmin_gill is defined as:

$$\frac{dQ_{admin\_gill}}{dt} = K_x \times C_{water} \quad \text{(Eq. 13)}$$

Kx being the exchange coefficient between blood and water and Cwater the chemical concentration in water (µg/mL).

Kx is defined as (Erickson and McKim, 1990; Nichols et al., 1990):

$$K_x = \min(F_{water}, F_{card} \times PC_{b:w}) \qquad \text{(Eq. 14)}$$

The effective respiratory volume (Fwater, mL/d) is lower than the total gill ventilation volume because not all the inspired water passes through the channels between the perfused lamellae (Randall, 1970). This was described by Erickson and McKim (1990) using the ratio:

$$F_{water} = \frac{VO_2}{OEE \times Cox} \qquad \text{(Eq. 15)}$$

Where VO2 is the oxygen consumption rate (mg O2/d), Cox the afferent dissolved oxygen concentration (mg O2/mL), and OEE the oxygen extraction efficiency (%).

The afferent dissolved oxygen concentration in water depends on the dissolved oxygen saturation (S, %) and the temperature (T, °C):

$$C_{ox} = (-0.24 \times T + 14.04) \times \frac{S}{100} \qquad \text{(Eq. 16)}$$

Erickson and McKim (1990) proposed a value of afferent oxygen concentration around 90% of saturation at 26°C. They proposed that with an afferent oxygen of nearly 100% of saturation, the oxygen extraction efficiency within the lamellar channels varies from 62% to nearly 80%, and proposed 71% as the median value.

Exhalation takes place in the venous compartment and is limited by the unbound fraction in blood (UF) between 0 and 1:

$$\frac{dQ_{excret\_gill}}{dt} = K_x \times \frac{C_{ven} \times UF}{PC_{b:w}} \qquad \text{(Eq. 17)}$$

Metabolism can occur in the plasma according to:

$$\frac{dQ_{Mp}}{dt} = Cl_{plasma} \times C_{ven} \qquad \text{(Eq. 18)}$$

Clplasma being the plasmatic clearance (mL/d).

Water in aquarium condition

$$\frac{dQ_{water}}{dt} = \frac{dQ_{excret}}{dt} - \frac{dQ_{elim\_water}}{dt} - \frac{dQ_{admin\_gill}}{dt} \qquad \text{(Eq. 19)}$$

With Qexcret the total excretion (branchial, urinary and fecal excretion) and Qelim_water the quantity eliminated from water.

$$\frac{dQ_{elim\_water}}{dt} = Ke_{water} \times Q_{water} \qquad \text{(Eq. 20)}$$

With Kewater the chemical elimination from water (degradation or water renewal in the case of a depuration phase).

Abbreviations and units used in PBK model equations.

Physiological parameters	Symbol	unit
Afferent dissolved oxygen concentration	C_{ox} (t)	mg O_2/mL
Blood flow entering in compartment i[a]	F_i (t)	mL/d
Body mass	BM (t)	g
Cardiac output	F_{card} (t)	mL/d/g
Concentration in organ i	C_i (t)	µg/mL
Effective respiratory volume	F_{water} (t)	mL/d
Exchange coefficient between blood and water	K_x (t)	mL/d
Fraction of dissolved oxygen saturation	S	-
Fraction of oxygen extraction efficiency	OEE	-
Fraction of PPT blood flow going to venous	α_{Fpp}	-
Fraction of skin blood flow going to venous	α_{Fs}	-
Quantity in organ i	Q_i (t)	µg
Oxygen consumption rate	VO_2 (t)	mg O_2/d
Volume in organ i	V_i (t)	mL
Chemical specific parameters		
Blood: water partition coefficient	$PC_{b:w}$	-
Absorption diffusion coefficient	K_u	d^{-1}
Excretion rate constants		
Bile	Ke bile	d^{-1}
Feces	Ke feces	d^{-1}
Urine	Ke urine	d^{-1}
Water	Ke water	d^{-1}
Fraction absorbed	$Frac_{abs}$	-
Fraction unbound in blood	UF	-
Hepatic clearance	$Cl_{hepatic}$	mL/d
Maximal metabolic velocity	V_{max}	µg/d/mL liver
Michaelis constant	K_m	µg/mL
Plasma clearance	Cl_{plasma}	mL/d
Tissue i: blood partition coefficient	PC_i	-
Simulation parameters		
Chemical quantity administered in		
GIT	Q_{ingest}	µg
Water	Q_{water}	µg
Transfer rate constant from bile to GIT lumen	K_{BG}	d^{-1}
Temperature	T	°C
Times	-	d

a- Compartments index organs: f = adipose tissue, art = arterial blood, b = brain, git = GIT, go = gonads, k = kidney, l = liver, pp = poorly perfused tissue, rp = richely perfused tissue, s = skin, ven = venous blood, are referenced by the following indices.

Step 5 – Model Performance

Due to the extremely limited availability of experimental data for partition coefficients in aquatic vertebrates, the partitioning behaviour of a chemical in fish was estimated using a QSAR model based on the lipid content of an organism/ tissue and the octanol/water partition coefficient, or, more accurately, on several tissue constituents and compound

properties (e.g. polar and non-polar lipids, water, albumin and the remaining proteins). For species without an existing PBK model such as the stickleback, these parameters were mostly unavailable and there is a high level of uncertainty surrounding QSAR model predictions for partition coefficients in stickleback. For the blood:water partition coefficient, the QSAR models used were based on the octanol/water partition coefficient and often inaccurately predicted the actual partition coefficient compared to the value estimated by fitting the PBTK model to the data. Moreover, this model is limited to nonpolar compounds and as any QSAR approach the obtained equations yield reliable predictions only inside their applicability domains, in particular with respect to the chemical space covered by the model. The PBK model was evaluated through comparing model predictions of tissue concentrations with experimental data measured in fish and available from the literature for atrazine and bisphenol A, chlorpyrifos, ethinylestradiol fipronil, oxytetracycline, permethrin, PCB52,TCDD (d2,3,7,8-Tetrachlorodibenzo-P-dioxin).

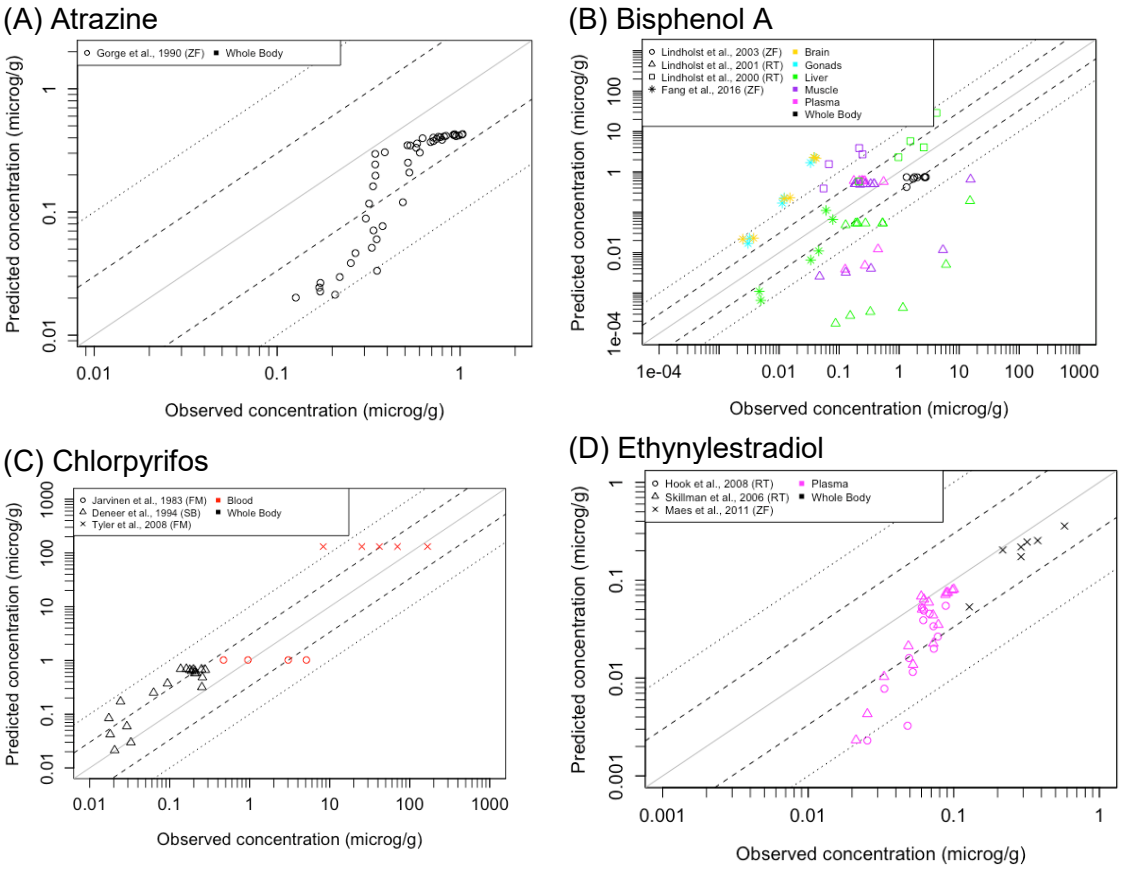

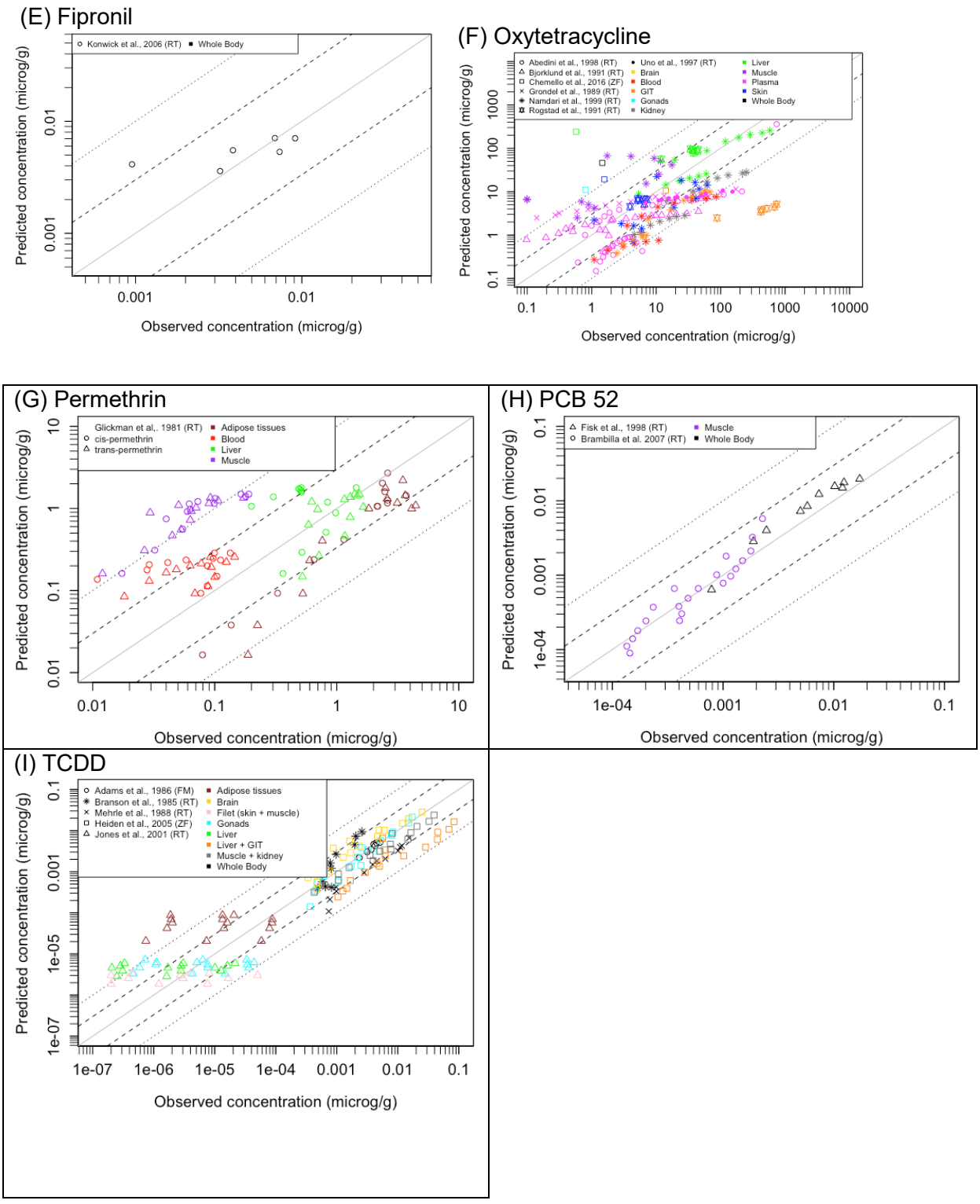

Figure II2. Comparison between the PBTK model predictions for four fish species (Rainbow trout (RT), Zebrafish (ZF), Fathead minnow (FM), and Stickleback (SB)) and measured data for 9 chemicals (microg/g fish) in a range of organs. Dotted lines represent the 3-fold and 10-fold changes.

Organs, species, and references of experimental datasets obtained are indicated in legends: colors and shapes represent organs and studies, respectively (modified from Grech et al., 2018).

A fraction of the venous blood draining the skin and poorly perfused tissues was assumed to flow directly to the kidney, and the remaining blood flow returns to the mixed venous circulation. Both gastro-intestinal (after of food intake) and branchial absorption were modelled. Exchanges with water occur in the gills and are modelled using an exchange coefficient. Chemical exchanges were assumed to be limited either by the effective respiratory volume or by cardiac output. Absorption from contaminated food is modelled in the gastrointestinal tract as a first order process. Chemical binding to plasma proteins was considered by introducing an unbound fraction of the chemical in plasma. Metabolism has been modelled in the liver using either a first order equation, or the Michaelis-Menten equation in case the literature indicated saturable metabolism. Excretion can occur via urine, expired water, and faeces (as unabsorbed fraction or by biliary excretion). Compounds excreted by the gills and urine are released in the water and can be reabsorbed in static water conditions.

Global Sensitivity analyses were performed using the variance-based Sobol method (Saltelli et al., 2008; Sobol et al., 2007). First order and total Sobol' sensitivity indices were estimated for two different chemicals: a highly lipophilic chemical, TCDD, and a polar compound, OTC. For both chemicals, sensitivity was assessed at three time points for the concentration in whole fish, arterial blood, and liver. Parameter values and exposure scenario characteristics are described in detail in the supplementary material of Grech et al. (2019).

The global sensitivity analyses of the trout PBK model using TCDD, as a lipophilic compound, and Oxytetracycline (OTC), as a polar compound, demonstrated that the TK of the two compounds were strongly impacted by the water temperature and the fish growth. Indeed, the parameters driving the growth (parameters with a prefix "DEB_", b_BW_L, f_cst) and the effect of the water temperature (Temperature, TA) are well represented in the fifteen most influential parameters on the three model outputs. As the two case studies consist of an exposure via food, as expected, intestinal absorption rate (Ku) and faecal excretion rate (Ke_feces) have also a strong influence on the outputs monitored.

For TCDD, 5 days after the beginning of the exposure, the physiological parameters of the GIT compartment (sc_GIT, frac_GIT, PC_gi) have high sensitivity indices, whereas after this initial uptake phase, their weights considerably decrease. Surprisingly, for a lipophilic compound the adipose tissues relative volume (sc_fat) and blood flow (frac_fat) have relative low sensitivity indices, although they are in the fifteen most important parameters. In the analysis of OTC, the parameters governing liver concentration and the bile elimination (Ke_bile, sc_liver, PC_l) have a high sensitivity index at the three time points explored.

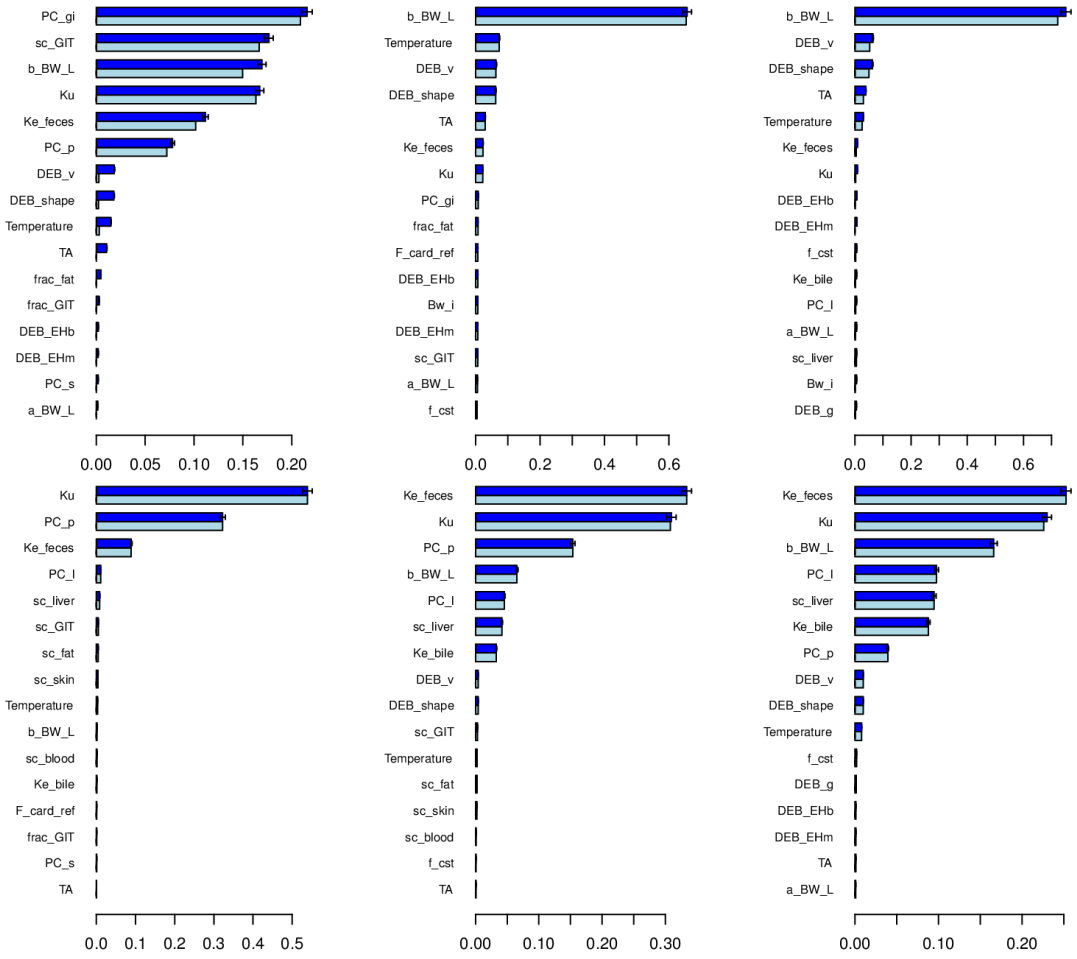

Figure II3: Sensitivity analysis of the trout PBTK model applied to TCCD (upper panels) and OTC (lower panels). The Sobol' sensitivity indices are estimated for the arterial concentration in males at three points in time: 5, 35 and 175 days for the TCCD and 1, 7, and 14 days for the OTC (from left to right). Estimation of the Sobol' total sensitivity indices (TI) are presented in dark blue and estimation of the Sobol' first-order indices (FOI) in light blue. Fifteen most influential parameters according to the total sensitivity indices.

Step 6 – Model Documentation

The current work was published in peer review journals, see reference below.

E. Identification of uncertainties

Model structure

Excretion and ingestion routes, which are chemical-specific, were the main sources of uncertainty in model structure

Input parameters

Basic data on fish physiological processes were still not fully available (excretion routes, blood flow, egg production) for all species and should be measured to improve the mechanistic aspect of fish PBTK models. Values for nearly all the rainbow trout physiological parameters were available, in contrast to the smaller fish species for which interspecies extrapolations were performed. The uncertainty due to species extrapolation has not been quantified, but the global sensitivity analysis highlighted the parameters for which extrapolation may critically affect model outputs. However, the lack of data relative to the tissue constituents in fish limits the level of complexity of the QSAR models that can be used to predict partition coefficients.

Model output

Predictions of whole body and tissues concentrations for nine chemicals were compared with experimental data and were accurate with 50% of predictions within a 3-fold factor for six out of nine chemicals and 75% of predictions within a 3-fold factor for three of the most lipophilic compounds. Within the nine compounds selected, accuracy also varied from one organ to another. On the one hand, adipose tissue and blood were the organs with the most accurate predictions: 49% of the concentrations were within a 3-fold factor. On the other hand, the predictions of brain concentrations were less accurate: 55% of the concentrations were over- or under-predicted by more than a 10-fold factor.

Other uncertainties (e.g. model developed for different substance and/or purpose)

None to report.

Overall evaluation of uncertainties: Uncertainties in the prediction of blood and adipose tissue concentrations for 49% of case studies were within 3-fold of the experimental data which can be considered as a relatively good performance. However, further improvement are still required can be supported with further work. Specifically, predictions of brain concentrations were more uncertain with 55% over- or under-predicted by more than a 10-fold factor. Overall, the model accuracy did not depend on the species to a large extent with PBTK model predictions in rainbow trout, zebrafish, and fathead minnow within 3-fold factor in 57%, 49%, and 65% of cases whereas deviation by more than a 10-fold factor were noted in 16%, 22% and 7% of cases, respectively. The predictions of the PBTK model on stickleback provided accurate predictions for chlorpyrifos (57% of the predictions were within a 3- fold factor and 24% were larger than a 10-fold factor) but were only evaluated on one dataset (Grech et al., 2019). Overall, further characterisation of 1. phase I, phase II metabolism and transporters in fish species 2. relative contributions of gill, urinary and fecal excretion of chemicals, will support the refinement of such PK models in fish species.

F. Model implementation details

- software (version no): The code was written and executed in in R. 3.3.3
- availability of code: Yes, code are accessible via the peer reviewed publication.
- software verification / qualification : was done by peer reviewed publication.

G. Peer engagement (input/review)

Done by publishing the model in peer-reviewed journals, see references

H. Parameter tables

Physiological data and their inter-individual variability estimated based on the results of extensive literature searches and specific experimental data are available for download in Excel (Grech et al., 2018a) DOI: 10.5281/zenodo.1414332

Compound-specific parameters used for the case studies.

Parameter	Unit	Parameter values and references				
		ATR	**BPA**	**CPF**	**EE2**	**FIP**
Log K_{ow}	-	2.61	3.32	4.96	3.67	4.01
Partition coefficient						
blood:water	-	1.26 [a]	2.06	1119	10.64 [l]	203
liver:blood	-	5.35 [a]	1.51	8.56	3 [m]	1.08
gonads:blood	-	1.47 [a]	1.95	17.93	1 [n]	1.35
brain:blood	-	1.94 [a]	1.95	5.95	1 [n]	1.75
fat:blood	-	1.47 [a]	2.55	8.15	23.29	22.6
skin:blood	-	1.47 [a]	1.19	3.75	0.72	0.70
GIT:blood	-	5.47 [a]	1.13	6.03	7.12	6.90
kidney:blood	-	1.47 [a]	4.25	13.54	1.29	1.25
RPT:blood	-	1.47 [a]	1.74	5.52	1.68	1.63
PPT:blood	-	1.18 [a]	1.18	2.04	0.75	0.72
Ku	d^{-1}	-	-	-	0.1 [k]	0.21 [p]
$frac_{abs}$	-	-	-	-	1	1
$Cl_{hepatic}$	mL /d/g liver	0.024 [b]	-	-	0	80 [q]
V_{max}	µg/d/g liver	-	129095.3 [e]	3375.38 [i]	-	-
K_m	µg/mL	-	7.1 [e]	50.31 [i]	-	-
Cl_{plasma}	mL /d/g fish	-	-	-	-	-
Ke urine	d^{-1}	0	0 [f]	0 [j]	0	0
Ke bile	d^{-1}	0.5 [a]	0 [f]	0 [j]	0.239 [k]	0
Ke feces	d^{-1}	0.83 [c]	0.83 [c]	0.83 [c]	0.83 [c]	0.83 [c]
Ke water*	d^{-1}	0	0	0	3.9 [k]	1E12
K_{BG}	d^{-1}	0	1E12	1E12	1E12	0
Ratio blood to plasma	-	1	1.075 [h]	1	0.84 [o]	1
UF	-	0.74 [d]	0.035 [g]	0.05 [j]	0.02 [l]	1

*Study dependent - Data were retrieved from: a- (Gunkel and Streit, 1980), b- (Han et al., 2007; Han et al., 2009), c- (Nichols et al., 2004), d- (Lu et al., 1998), e- (Ohkimoto et al., 2003), f- (Pery et al., 2014), g- (Edginton and Ritter, 2009), h- (Edginton and Ritter, 2009; Shin et al., 2004), i- (Lavado and Schlenk, 2011), j- (Weelling and De Vries, 1992), k- (Schultz et al., 2001), l- (Kim, 2004), m- (Watanabe et al., 2009), n- (Teeguarden and Barton, 2004), o- (Cherkaoui-Rbati et al., 2017), p- (WHO., 2000), q- (Chapleo and Hall, 1992)

Compound-specific parameters used for the case studies (continued).

Parameter	Unit	Parameter values and references			
		OTC	PCB 52	PER	TCDD
Log K_{ow}	-	- 0.9	5.84	6.5	6.8
Partition coefficient					
blood:water	-	0.03	8990	17782.8	30478.94
liver:blood	-	33 [a]	6.60	8.0	9.31
gonads:blood	-	1.5 [a]	8.26	10.0	11.65
brain:blood	-	0.06 [a]	10.7	13.5	15.73
fat:blood	-	0.70 [b]	138	167.5	195.01
skin:blood	-	0.70 [b]	4.25	5.16	6.00
GIT:blood	-	1.40 [b]	42.2	51.2	59.62
kidney:blood	-	3.75 [b]	7.63	9.2	10.76
RPT:blood	-	2.57 [b]	9.93	12.0	14.01
PPT:blood	-	0.70 [b]	4.40	5.3	6.21
Ku	d^{-1}	0.14 [b]	2.4 [h]	-	0.85 [k]
$frac_{abs}$	-	1 [c]	1	-	1
$Cl_{hepatic}$	mL /d/g liver	0	-	300 (trans), 150 (cis) [i]	0
V_{max}	µg/d/g liver	-	42.0 [f]	-	-
K_m	µg/mL	-	204400 [f]	-	-
Cl_{plasma}	mL /d/g fish	-	-	10 (trans), 4 (cis) [i]	-
Ke urine	d^{-1}	0 [b]	0.7 [g]	0	0
Ke bile	d^{-1}	0.7 [a]	1.5 [g]	0	1.5 [k]
Ke feces	d^{-1}	0.83 [d]	0.2 [h]	0.83 [d]	0.83 [d]
Ke water*	d^{-1}	0	36 or 45	0	0
K_{BG}	d^{-1}	0.86 [e]	1	0	1
Ratio blood to plasma	-	1	1	1	1
UF	-	0 [b]	1	0.21 [j]	1

*Study dependent - Data were retrieved from: a- (Black et al., 1991), b- (Law, 1999), c- (Cravedi et al., 1987), d-: (Nichols et al., 2004), e- (Talbot and Higgins, 1983), f- (White et al., 1997), g- (McKim and Heath, 1983), h- (Nichols et al., 2001), i- (Glickman and Lech, 1981), j- (Sethi et al., 2014), k- (Fisk et al., 1997)

Strategy for reducing overall uncertainty (excluding generation of data based on new animal test)

New QSAR models can be developed to refine compound-specific parameterisation such as partition coefficients. The influence of physiological, metabolic and environmental factors on TK in fish species needs to be investigated further as well as their relative contribution to the prediction power of fish PB-TK models for ERA purposes. The quantification of differential elimination via the gills versus urine and feces in fish species needs further investigation. More case studies would need to be conducted on chemicals of relevance to environmental risk assessment in the four fish species.

I. References and background information

Grech A, Brochot C, Dorne JL, Quignot N, Bois FY, Beaudouin R. (2017) Toxicokinetic models and related tools in environmental risk assessment of chemicals. Sci Total Environ. 578:1-15.

Grech, Audrey, Tebby, Cleo, Brochot, Celine, Bois, Frederic, Bado-Nilles, Anne, Dorne, Jean Lou, Guignot, Nadia, Beaudoin, Remi (2018a). Physiological parameters for four fish

species (rainbow trout, zebra fish, fathead minnow and three-spined stickleback) as the basis for the development of generic physiologically-based kinetic models [Data set]. Zenodo. http://doi.org/10.5281/zenodo.1414332.

Grech, Audrey, Tebby, Cleo, Brochot, Celine, Bois, Frederic, Bado-Nilles, Anne, Dorne, Jean Lou, Guignot, Nadia, Beaudoin, Remi (2018a). Development of generic physiologically based kinetic models for four fish species: rainbow trout, zebra fish, fathead minnow and three-spined stickleback. http://doi.org/10.5281/zenodo.1414325.

Grech A, Tebby C, Brochot C, Bois FY, Bado-Nilles A, Dorne JL, Quignot N, Beaudouin R.(2019) Generic physiologically-based toxicokinetic modelling for fish: Integration of environmental factors and species variability. Sci Total Environ. 651(Pt 1):516-531.

Links to other resources

The full data collection and implementation of the models using case studies is described in Grech et al., (2019) and are available for download on EFSA knowledge junction under the Creative Commons attribution 4.0 international:

1. Physiological data and their inter-individual variability estimated based on the results of extensive literature searches and specific experimental data are available for download in Excel (Grech et al., 2018a) DOI: 10.5281/zenodo.1414332

2. R codes for the models (Grech et al., 2018b) DOI: 10.5281/zenodo.1414332

Generic R codes for PB-K modelling for each species and sex with a deterministic model for a single animal, a probabilistic model approach to simulate individual differences of the physiology within a population as well as a partition coefficient Quantitative Structure Activity Relationship (QSAR) models

Parameterisation of models for each males and females of each species separately

The models include new mechanistic approaches to include the effects of growth and temperature in the generic PBK models.

PBK model code

PBK model code in r

R codes for the models (Grech et al., 2018b) DOI: 10.5281/zenodo.1414332

Generic R codes for PB-K modelling for each species and sex with a deterministic model for a single animal, a probabilistic model approach to simulate individual differences of the physiology within a population as well as a partition coefficient Quantitative Structure Activity Relationship (QSAR) models

Parameterisation of models for each males and females of each species separately

The models include new mechanistic approaches to include the effects of growth and temperature in the generic PBK models.

PB(T)K model

```
### Model PBPK (rainbow trout / zebrafish / fathead minnows / stickleback) generic ###
# 10/2017
# A. Grech, C.Tebby, C. Brochot, R. Beaudouin.

##############################
### Variable -(Notation)- Units
```

```
# Quantity  -(Q_x) - microg
# Volumes:   -(V_x) - mL
# Time:   -(t)   - d
# Flows:     -(F_x) - mL/d
# Concentrations: -(C_x) - microg/mL
# Masses:   -(BW)  - g
# Lenght:    -(L)   - mm
# Temperature: -(TC_c)  - Celsius
#  ''     -(TC_k)  - Kelvin
# Density of each tissue is considered equal to 1
################################



# Arrhenius temperatures function
KT <- function(T, TR, TA){ exp ( (TA / TR) - (TA / T) ) }


PBPK.model <- function(t, Initial.Values, Parameters, input.T) {

  with( as.list(c(Initial.Values, Parameters)),{

 # Temperature
 TC_k = input.T(t) + 273.15 # (degree K)
 TC_c = input.T(t)    # (degree C)

 # body weight : DEB growth model anisomorphic
 DEB_v_t   = DEB_v  * KT(T=TC_k , TR=TR_DEB ,TA=TA)  # mm/d
 DEB_Lm = DEB_v / (DEB_KM * DEB_g)    # mm
 DEB_M  = (DEB_EHm / DEB_EHb)^(1/3)      # EHm and EHb = J
 dL  = (DEB_v_t / (3 * (f_cst + DEB_g))) * (f_cst * DEB_M - (L/DEB_Lm))
 BW  = a_BW_L *( (L/10)/DEB_shape ) ^ b_BW_L   # BW = g; a = g/cm;  L = mm --> /10 = cm

 #  volumes (mL)
 V_art = sc_blood  * BW  * frac_art_ven
 V_ven = sc_blood  * BW  - V_art
 V_liver  = sc_liver  * BW
 V_gonads = sc_gonads * BW
 V_brain  = sc_brain  * BW
 V_fat = sc_fat * BW
 V_skin   = sc_skin   * BW
 V_GIT = sc_GIT * BW
 V_kidney = sc_kidney * BW
 V_rp  = sc_rp  * BW
 V_pp  = BW - (V_art + V_ven + V_liver + V_gonads + V_brain + V_fat + V_skin + V_GIT + V_kidney + V_rp)

 V_bal = BW - (V_art + V_ven + V_liver + V_gonads + V_brain + V_fat + V_skin + V_GIT + V_kidney + V_rp + V_pp) # balance

 # Blood flow (mL/d)
 F_card_g = F_card_ref * KT(T=TC_k , TR=TR_Fcard,TA=TA)  * (BW/Bw_Fcard_ref)^(-0.1) # cardiac output = mL/d/g
 F_card   = F_card_g * BW # mL/d

 F_liver  = frac_liver  * F_card
 F_gonads = frac_gonads * F_card
 F_brain  = frac_brain  * F_card
 F_fat = frac_fat * F_card
 F_skin   = frac_skin   * F_card
 F_GIT = frac_GIT * F_card
 F_kidney = frac_kidney * F_card
 F_rp    = frac_rp  * F_card
 F_pp  = F_card - (F_liver + F_gonads + F_brain + F_fat + F_skin + F_GIT + F_kidney + F_rp)

 F_bal = F_card - (F_liver + F_gonads + F_brain + F_fat + F_skin + F_GIT + F_kidney + F_rp + F_pp) # balance

 # Effective respiratory volume (mL/d)
 V_O2_g = V_O2_ref * KT(T=TC_k, TR=TR_VO2,TA=TA)  * (BW/Bw_VO2_ref)^(-0.1) #mg O2/d/g
 V_O2   = V_O2_g * BW   # mg O2/d

 C_O2_water = ((-0.24 * TC_c + 14.04) * Sat )/10^3 # mg O2/mL
 F_water = V_O2/ (O2_EE * C_O2_water)     # mL/d

 Kx   = min (F_water, F_card * PC_blood_water)  # mL/d

 # Concentrations in tissues (microg/g = microg/mL)
 C_art = Q_art / V_art
      C_plasma = C_art / Ratio_blood_plasma
 C_ven = Q_ven / V_ven
 C_liver  = Q_liver  / V_liver
 C_gonads = Q_gonads / V_gonads
 C_brain  = Q_brain  / V_brain
 C_fat = Q_fat / V_fat
 C_skin   = Q_skin   / V_skin
 C_GIT = Q_GIT / V_GIT
 C_kidney = Q_kidney / V_kidney
 C_rp  = Q_rp  / V_rp
 C_pp  = Q_pp  / V_pp
 C_tot = ((Q_art + Q_ven + Q_liver + Q_gonads + Q_brain + Q_fat + Q_skin + Q_GIT + Q_kidney + Q_pp + Q_rp)
    / (V_art + V_ven + V_liver + V_gonads + V_brain + V_fat + V_skin + V_GIT + V_kidney + V_pp + V_rp))

 # concentration in the water : exposure --> microg/g = microg/mL
 C_water    = Q_water / V_water
 dQ_elim_water = Ke_water * Q_water

 # concentration in urine
```

```
dV_urine  = urine_rate * BW
C_urine   = Q_urine  / V_urine

     # Scaling clearence and excretion constant
     if ( !is.na(Vmax)) { Vmax_sc  =  Vmax * V_liver  }
     if ( !is.na(Cl_liver)) { Cl_liver_sc = Cl_liver * V_liver }
rate_plasma_sc = rate_plasma * BW

     # Excretion
dQ_feces  = Q_lumen_GIT * Ke_feces
dQ_excret_gills = Kx * (C_ven * Unbound_fraction / PC_blood_water)
dQ_bile   = (Ke_bile * Q_liver) - (Q_bile * K_BG)
dQ_urine  = Ke_urine * Q_kidney      # initialized by scenario for urine discharge
dQ_urine_cum = Ke_urine * Q_kidney      # not initialized
dQ_excret    = dQ_excret_gills + dQ_urine_cum + dQ_feces


# Quantity absorbed : differentials in microg/d
dQ_admin_gills = Kx * C_water   ###Gills
dQ_lumen_GIT   = ( - Ku * Q_lumen_GIT
       - Q_lumen_GIT * Ke_feces
       + Q_bile * K_BG)  ###GIT
dQ_admin_GIT   = 0

# Metabolism
dQ_met_plasma  = rate_plasma_sc * Q_ven

dQ_met_liver = ifelse ( is.na(Cl_liver),
     ( ( Vmax_sc *(C_liver/PC_liver) )/(Km + C_liver/PC_liver) ),
     ( Cl_liver_sc * C_liver / PC_liver) )

     dQ_met = dQ_met_plasma + dQ_met_liver


# Blood quantity
dQ_art = ( F_card * C_ven - F_fat * C_art - F_rp * C_art - F_pp * C_art
     - F_liver  * C_art - F_kidney * C_art   - F_GIT * C_art
     - F_gonads * C_art  - F_skin   * C_art - F_brain  * C_art )

dQ_ven = (F_brain * C_brain/PC_brain
    + (F_liver + F_rp + F_gonads + F_GIT ) * C_liver/PC_liver
    +  F_fat   * C_fat/PC_fat
    + (F_kidney + ((1 - a_Fpp) * F_pp) + ((1 - a_Fs) * F_skin)) * (C_kidney / PC_kidney)
    + a_Fpp * F_pp  * (C_pp / PC_pp)
    + a_Fs * F_skin * (C_skin / PC_skin)
    - F_card * C_ven
    + dQ_admin_gills - dQ_excret_gills
    - dQ_met_plasma)

# Quantity in tissues
dQ_gonads = F_gonads*(C_art - C_gonads/PC_gonads)
dQ_fat = F_fat   *(C_art - C_fat/PC_fat)
dQ_rp  = F_rp *(C_art - C_rp/PC_rp)
dQ_pp  = F_pp *(C_art - C_pp/PC_pp)
dQ_brain  = F_brain *(C_art - C_brain/PC_brain)
dQ_skin   = F_skin  *(C_art - C_skin/PC_skin)

dQ_liver  =  ( F_liver * C_art
      + F_rp *(C_rp/PC_rp)
      + F_GIT *(C_GIT/PC_GIT)
      + F_gonads*(C_gonads/PC_gonads)
      - ( F_liver + F_rp + F_GIT + F_gonads  ) *(C_liver/PC_liver)
      - (Ke_bile * Q_liver) - dQ_met_liver )

dQ_kidney = ( F_kidney * C_art
     + (1-a_Fpp) * F_pp * (C_pp / PC_pp)
     + (1-a_Fs) * F_skin * (C_skin / PC_skin)
     - (F_kidney + (1-a_Fpp) * F_pp + (1-a_Fs) * F_skin) * (C_kidney / PC_kidney)
     - dQ_urine)

dQ_GIT = ( Ku * Q_lumen_GIT +  F_GIT*(C_art - C_GIT/PC_GIT))

# Chemical kinetic in  aquarium water
dQ_water = (dQ_excret - dQ_elim_water - dQ_admin_gills)


# Mass-balance
Q_Body   = (Q_art + Q_ven + Q_bile + Q_liver + Q_gonads + Q_brain + Q_fat + Q_skin + Q_kidney + Q_GIT + Q_pp + Q_rp)
Q_admin_tot = Q_admin_gills + ivQuantity - Q_lumen_GIT + Q_admin_GIT # amount entering body
Q_elim_tot  = Q_met + Q_excret
Mass_Bal = Q_admin_tot - Q_Body - Q_elim_tot
     Mass_Bal_Sys = (Q_admin_tot - Q_admin_gills) - Q_Body - ( Q_elim_tot - Q_excret) - Q_water - Q_elim_water




list("Q"=c(dQ_water, dL, dV_urine,
     dQ_art,  dQ_ven,
     dQ_brain, dQ_fat,  dQ_GIT,  dQ_lumen_GIT, dQ_gonads,
     dQ_kidney, dQ_liver, dQ_skin, dQ_rp, dQ_pp,
     dQ_admin_gills, dQ_admin_GIT,
     dQ_met_plasma, dQ_met_liver, dQ_met, dQ_elim_water,
     dQ_excret, dQ_feces, dQ_excret_gills, dQ_bile, dQ_urine, dQ_urine_cum), # derivatives
```

```
c( C_water = C_water,
C_art = C_art,    C_ven = C_ven,   C_plasma = C_plasma,
C_brain = C_brain,   C_fat = C_fat,   C_GIT = C_GIT, C_gonads = C_gonads,
C_kidney = C_kidney, C_liver = C_liver,  C_skin = C_skin,
C_rp = C_rp,   C_pp = C_pp, C_urine = C_urine, C_tot = C_tot),

c( V_water = V_water,
V_art = V_art,  V_ven = V_ven,
V_brain = V_brain, V_fat = V_fat, V_GIT = V_GIT,  V_gonads= V_gonads,
V_kidney = V_kidney, V_liver = V_liver, V_skin = V_skin,
V_rp  = V_rp,  V_pp = V_pp),

c(V_bal = V_bal,
  F_bal = F_bal,
  Q_admin_tot = Q_admin_tot,
  Q_elim_tot  = Q_elim_tot,
  Q_Body = Q_Body,
  Mass_Bal = Mass_Bal,
  Mass_Bal_Sys =Mass_Bal_Sys),


"BW"   = BW,
"F_card"  = F_card,
"F_water" = F_water,
"Kx"   = Kx)
}) }
```

Partition coefficient function: QSAR model

```
### Partition coefficient function #####
# 10/2017
# A. Grech, C.Tebby, C. Brochot, R. Beaudouin.
##############################

##############################
### Units:
# Volumes:    mL
# Masses:     g
##############################

PC_qsar_model = function(a_PC  = 0.78,  # PC between blood and water and logKow
       b_PC  = 0.82,  # PC between blood and water and logKow

       e_Bar = 0.05, # Parameter 1 of Nichols et al. 2006

       a_Bar = 0.74, # Parameter 1 of Bertelsen et 1998
       b_Bar = 0.72, # Parameter 2 of Bertelsen et 1998
       c_Bar = 1.00, # Parameter 3 of Bertelsen et 1998

       log_Kow,

       water_liver,  water_gonads, water_brain,
       water_fat, water_skin,   water_GIT,
       water_kidney, water_rp,  water_pp,

       lipids_liver, lipids_gonads, lipids_brain,  lipids_fat,
       lipids_skin,  lipids_GIT, lipids_kidney, lipids_rp,
       lipids_pp,

       PC_bw, PC_l, PC_go, PC_b, PC_f, PC_s, PC_gi, PC_k, PC_r, PC_p   ){


 #================================================
 # (I.) QSAR Model : partition coefficient between blood and water,
 #================================================

 PC_QSAR_blood_water = 10^(a_PC * log_Kow - b_PC)

 PC_blood_water = ifelse (is.null(PC_bw), PC_QSAR_blood_water, PC_bw)

 if( log_Kow > 4.04) {

#================================================
# (I.) QSAR Model
# Nichols, J W.; Schultz, I R.; Fitzsimmons, P N.
# Aquat. Toxicol. 2006, 78, 74-90.
#================================================

#PC = lipidcontent * Kow + 0.05 * nonlipidcontent * Kow + watercontent

# Calcul des PCs # SU
PC_QSAR_liver   = (water_liver   +  lipids_liver  * 10^( log_Kow) +  e_Bar * (1 - lipids_liver  - water_liver ) )/PC_blood_water
PC_QSAR_gonads  = (water_gonads  +  lipids_gonads * 10^( log_Kow) +  e_Bar * (1 - lipids_gonads - water_gonads) )/PC_blood_water
PC_QSAR_brain   = (water_brain   +  lipids_brain  * 10^( log_Kow) +  e_Bar * (1 - lipids_brain  - water_brain)  )/PC_blood_water
PC_QSAR_fat   = (water_fat   +  lipids_fat * 10^( log_Kow) +  e_Bar * (1 - lipids_fat - water_fat )   )/PC_blood_water
PC_QSAR_skin  = (water_skin +  lipids_skin   * 10^( log_Kow) +  e_Bar * (1 - lipids_skin   - water_skin )  )/PC_blood_water
PC_QSAR_GIT   = (water_GIT   +  lipids_GIT * 10^( log_Kow) +  e_Bar * (1 - lipids_GIT - water_GIT )   )/PC_blood_water
PC_QSAR_kidney  = (water_kidney  +  lipids_kidney * 10^( log_Kow) +  e_Bar * (1 - lipids_kidney - water_kidney) )/PC_blood_water
PC_QSAR_rp    = (water_rp   +  lipids_rp  * 10^( log_Kow) +  e_Bar * (1 - lipids_rp  - water_rp ) )/PC_blood_water
PC_QSAR_pp    = (water_pp   +  lipids_pp  * 10^( log_Kow) +  e_Bar * (1 - lipids_pp  - water_pp ) )/PC_blood_water

 } else {

#================================================
# (II.) QSAR Model
# Bertelsen, S. L.; Hoffman, A. D.; Gallinat, C. A.; Elonen, C. M.; Nichols, J. W.
# Environ. Toxicol. Chem. 1998, 17, 1447-1455.
#================================================

# Calcul des PCs # SU

PC_QSAR_liver    = (water_liver   + 10^(a_Bar*log_Kow + b_Bar + c_Bar * log10(lipids_liver )  )) /PC_blood_water
PC_QSAR_gonads   = (water_gonads  + 10^(a_Bar*log_Kow + b_Bar + c_Bar * log10(lipids_gonads)  )) /PC_blood_water
PC_QSAR_brain    = (water_brain   + 10^(a_Bar*log_Kow + b_Bar + c_Bar * log10(lipids_brain)   )) /PC_blood_water
PC_QSAR_fat   = (water_fat  + 10^(a_Bar*log_Kow + b_Bar + c_Bar * log10(lipids_fat)  )) /PC_blood_water
PC_QSAR_skin  = (water_skin + 10^(a_Bar*log_Kow + b_Bar + c_Bar * log10(lipids_skin) )) /PC_blood_water
PC_QSAR_GIT   = (water_GIT  + 10^(a_Bar*log_Kow + b_Bar + c_Bar * log10(lipids_GIT)  )) /PC_blood_water
PC_QSAR_kidney   = (water_kidney  + 10^(a_Bar*log_Kow + b_Bar + c_Bar * log10(lipids_kidney)  )) /PC_blood_water
PC_QSAR_rp    = (water_rp   + 10^(a_Bar*log_Kow + b_Bar + c_Bar * log10(lipids_rp)   )) /PC_blood_water
PC_QSAR_pp    = (water_pp   + 10^(a_Bar*log_Kow + b_Bar + c_Bar * log10(lipids_pp)   )) /PC_blood_water
 }

 #================================================

 PC_liver   = ifelse (is.null(PC_l), PC_QSAR_liver, PC_l)
 PC_gonads  = ifelse (is.null(PC_go), PC_QSAR_gonads, PC_go)
 PC_brain   = ifelse (is.null(PC_b), PC_QSAR_brain, PC_b)
 PC_fat  = ifelse (is.null(PC_f), PC_QSAR_fat, PC_f)
 PC_skin = ifelse (is.null(PC_s), PC_QSAR_skin, PC_s)
```

```
  PC_GIT  = ifelse (is.null(PC_gi), PC_QSAR_GIT, PC_gi)
  PC_kidney  = ifelse (is.null(PC_k), PC_QSAR_kidney, PC_k)
  PC_rp   = ifelse (is.null(PC_r), PC_QSAR_rp, PC_r)
  PC_pp   = ifelse (is.null(PC_p), PC_QSAR_pp, PC_p)

  return(   c("PC_blood_water" = PC_blood_water,  "PC_liver"   = PC_liver,  "PC_gonads"   = PC_gonads,
     "PC_brain"    = PC_brain,  "PC_fat"  = PC_fat ,   "PC_skin"  = PC_skin,
     "PC_GIT"   = PC_GIT, "PC_kidney"   = PC_kidney,
     "PC_rp"    = PC_rp,    "PC_pp"    = PC_pp ))
}
```

Parameterisation for PBTK model male rainbow trout

```
### Parameterisation for PBPK model male rainbow trout #####
# 10/2017
# A. Grech, C.Tebby, C. Brochot, R. Beaudouin.
#
##############################

##############################
### Units:
###
# Quantity    microg
# Volumes:    mL
# Time:    d
# Flows:   mL/d
# Concentrations:   microg/mL
# Vmax:    microg/d/ mL Liver
# Km:      microg/mL
# Masses:     g
# Lenght:     mm
# Temperature:   Celsius
# Ventilation rate: mL/d

# Density of each tissue is considered equal to 1

##############################

library("deSolve")


#================================================
# source("PBTK_model.r")
# source("PBTK_PC_QSAR_function.r")
#================================================


#================================================
# (II.) Model integration
#================================================

PBPK.RT.M = function(
  #================================================
  # (II.1) Parameters
  #================================================

  # Physiological parameters
  Bw_i    = NULL ,  # Body weight initial (g fresh weight)
  Bw_Fcard_ref= 270.1  ,  # Body weight of reference for F_card from
  Bw_VO2_ref = 1000 ,  # Body weight of reference for VO2 from Elliot experiments
  DEB_v   = 0.38 ,  # Energy conductance (mm/d) (DEB model parameter)
  DEB_g   = 0.196   ,  # Energy investment ratio (SU) (DEB model parameter)
  DEB_KM  = 0.027   ,  # Somatic maintenance rate coefficient (1/d) (DEB model parameter)
  DEB_EHm = 452  ,  # Energy at State of maturity at metamorphosis (J)
  DEB_EHb = 52   ,  # Energy at State of maturity at birth (J)
  DEB_shape  = 0.113   ,
  a_BW_L  = 0.0051  ,  # a relation BW(g)=F(L(cm))
  b_BW_L  = 3.3513  ,  # b relation BW(g)=F(L(cm))

  # Environmental condition
  Temperature  = 10   , # c
  TA     = 6930 , # Arrhenius temperature  in Kelvin
  TR_DEB    = 293.65,   # (Kelvin)
  TR_Fcard  = 279.15,   # (Kelvin)
  TR_VO2    = 283.15,   # (Kelvin)
  f_cst  = 1 , # food level 1 = ad-libitum, 0= starvation
  V_water   = 1000 , # Volume of aquarium (mL)

  # Effective respiratory volume & cardiac output
  F_card_ref  = 28.5,  # reference cardiac output (mL/min/g): F_card_ref = mL/min/g --> F_card_ref * (60*24) = mL/d/g
  V_O2_ref = 3.26, # reference oxygen comsuption rate (mg O2/d/g), determined by visual fitting from Elliot, 1969 experiments
  O2_EE    = 0.71, # Oxygen extraction efficiency of 71% proposed by Erickson, 1990
  Sat   = 0.90, # dissolved oxygen saturation of 90% proposed by Erickson, 1990
  frac_art_ven = 1/3, # fraction of arterial blood

  sc_blood  = 0.0527, # volume scaling factor : fraction of BW (%)
  sc_gonads = 0.018 ,
  sc_brain  = 0.0049,
  sc_liver  = 0.0146,
  sc_fat = 0.0797,
```

```
      sc_skin   = 0.10  ,
      sc_GIT = 0.099 ,
      sc_kidney = 0.0076,
      sc_rp  = 0.0257,

      sc_pp  = (1 -  sc_blood - sc_gonads - sc_brain - sc_liver - sc_fat
          -  sc_skin - sc_GIT - sc_kidney -sc_rp),

      frac_gonads =0.0138  ,  # Fraction of arterial blood flow
      frac_brain  =0.018   ,
      frac_liver  =0.0158  ,
      frac_fat =0.0059  ,
      frac_skin   =0.0570  ,
      frac_GIT =0.1759  ,
      frac_kidney =0.0817  ,
      frac_rp  =0.0952  ,

      frac_pp  = (1 - frac_gonads - frac_brain - frac_liver - frac_fat
         - frac_skin - frac_GIT -  frac_kidney - frac_rp),

      # Exposure quantity (microg)
      WaterQuantity  = NULL,
      IngestQuantity = NULL,
      ivQuantity  = NULL,

      # Chemical parameters
      log_Kow  = NULL , #
      Unbound_fraction = 1, # in blood. between 0 and 1. Limits excretion by gills.
      Ratio_blood_plasma = 1, # blood/plasma global equilibrium (hemtocrite, fu, ...)

      # Organs composition
      water_liver = 0.746   , # relative value (%)
      water_brain = 0.75 ,
      water_gonads= 0.66 , #female value
      water_fat   = 0.05 ,
      water_skin  = 0.667   ,
      water_GIT   = 0.582   ,
      water_kidney= 0.789   ,
      water_rp = 0.5293  , # value of zebrafish model
      water_pp = 0.769   , # muscle value


      lipids_liver = 0.045 , # relative value (%)
      lipids_brain = 0.073 ,
      lipids_gonads= 0.0563 , #female value
      lipids_fat   = 0.942 ,
      lipids_skin  = 0.029 ,
      lipids_GIT   = 0.288 ,
      lipids_kidney= 0.052 ,
      lipids_rp = 0.0677 , # value of zebrafish model
      lipids_pp = 0.03  , # muscle value

      PC_bw = NULL,
      PC_l = NULL,
      PC_go = NULL,
      PC_b = NULL,
      PC_f = NULL,
      PC_s = NULL,
      PC_gi = NULL,
      PC_k = NULL,
      PC_r = NULL,
      PC_p = NULL,

      a_Fpp = 0.4, # Fraction of PPT blood going to venous
      a_Fs  = 0.1, # Fraction of skin blood going to venous

      #Oral absorption
      Ku    = 0,   # Diffusion coefficient
      frac_abs = 0,   # Absorption fraction.  /!\ Parametrisation with frac_abs implies Ke_feces null !

      #Metabolism
      Km   = NULL , # microg/ml
      Vmax = NA , # microg/d/mL liver
      Cl_liver   = NA , # mL/d/mL liver
      rate_plasma  = 0, # mg/d/g fish

      #Excretion
      Ke_bile  = 0, # 1/d
      Ke_urine = 0, # 1/d
      Ke_water = 0, # 1/d
      K_BG  = 0, # 1/d chemical rate constant from bile to GIT_lumen # 0 : no bile excretion: accumulation in bilary vesicule #
1E12 : Complete bile excretion in GIT_lumen

      #Feces and urination
      Ke_feces   = 0.83 , # 1/d estiamted from Nichols  et al. 2004
      urine_rate = 1.2e-03*60*24/29.82, # V_burst = 1.2 mL.kg-1 every 29.82 minutes proposed by Curtis 1991 --> 1.2e-03 mL.g BW-1
      urination_interval = NULL  , # 30min proposed by Curtis 1991 --> 30/60/24hr

      # temps
      Times  = NULL,    # days
      Time_end_exposure = max(Times), # days
      period = NULL,    # days between two doses
      frac_renewed = NULL, # fraction of the water of the aquaria renewed
      time_final_dose = NULL,
```

```
      time_first_dose = NULL
    ){


      #================================================
      # (I.) Vectors of parameters
      #================================================

      # Physiological parameters
      parms_physio <- c (# DEB model parameters
     "Bw_i" = Bw_i, "Bw_VO2_ref" = Bw_VO2_ref, "Bw_Fcard_ref" = Bw_Fcard_ref, "DEB_v" = DEB_v, "DEB_g" = DEB_g, "DEB_KM" = DEB_KM,
     "DEB_EHm" = DEB_EHm,  "DEB_EHb" = DEB_EHb,
     "DEB_shape"  = DEB_shape   , "a_BW_L" = a_BW_L  ,  "b_BW_L" = b_BW_L,

     # cardiac ouptut & respiratory parameters
     "F_card_ref" = F_card_ref,  "O2_EE" = O2_EE, "Sat" = Sat, "V_O2_ref" = V_O2_ref,
          "frac_art_ven" = frac_art_ven,

     # relative flux to cardiac ouptut
     "frac_liver" = frac_liver, "frac_gonads"= frac_gonads, "frac_brain"  = frac_brain,
     "frac_fat"   = frac_fat ,   "frac_skin"   = frac_skin,
     "frac_GIT" = frac_GIT , "frac_kidney" = frac_kidney, "frac_rp" = frac_rp,
     "frac_pp" = frac_pp,

     # relative weight to BW
     "sc_GIT" = sc_GIT, "sc_skin"  = sc_skin,   "sc_blood"   = sc_blood,
     "sc_liver"  = sc_liver,  "sc_gonads"= sc_gonads,   "sc_fat"   = sc_fat,
     "sc_brain"  = sc_brain,  "sc_rp" = sc_rp,    "sc_pp" = sc_pp,
     "sc_kidney" = sc_kidney,

     # urination
     "urine_rate" = urine_rate, "urination_interval" = urination_interval
      )

      # Partition coefficients : QSAR model
      parms_PC  = PC_qsar_model(log_Kow =log_Kow, PC_bw = PC_bw,
           water_liver = water_liver  , lipids_liver  = lipids_liver ,   PC_l  = PC_l,
           water_gonads= water_gonads , lipids_gonads = lipids_gonads,   PC_go = PC_go,
           water_brain = water_brain  , lipids_brain  = lipids_brain, PC_b  = PC_b,
           water_fat   = water_fat , lipids_fat = lipids_fat,   PC_f  = PC_f,
           water_skin  = water_skin   , lipids_skin   = lipids_skin,  PC_s  = PC_s,
           water_GIT   = water_GIT , lipids_GIT = lipids_GIT,   PC_gi = PC_gi,
           water_kidney= water_kidney , lipids_kidney = lipids_kidney,   PC_k  = PC_k,
           water_rp = water_rp  , lipids_rp  = lipids_rp,    PC_r  = PC_r,
           water_pp = water_pp  ,  lipids_pp  = lipids_pp,   PC_p  = PC_p)


      # chemical-dependant. Non relevant parameters can be set to NA
      parms_chemical <- c(# Metabolism
     "Cl_liver" = Cl_liver, "rate_plasma" = rate_plasma,
     "Km" = Km, "Vmax" = Vmax,
     "log_Kow" = log_Kow,
     "Unbound_fraction" = Unbound_fraction, "Ratio_blood_plasma" = Ratio_blood_plasma,
     "Ke_bile"= Ke_bile, "Ke_urine" = Ke_urine,  "Ke_water" = Ke_water, "Ke_feces" = Ke_feces, "K_BG" = K_BG,

     # Venous blood flow distribution
     "a_Fpp" = a_Fpp,  "a_Fs"   = a_Fs,


     # Oral absorption
     "Ku" = Ku, "frac_abs" = frac_abs)


      # exposure parameters
      parms_exposure <- c(# environmental parameters
     "TA"=TA, "TR_DEB"=TR_DEB, "TR_Fcard"=TR_Fcard, "TR_VO2"=TR_VO2, "f_cst"= f_cst, "V_water" = V_water,

     # Exposure quantity
     "IngestQuantity" = IngestQuantity,
     "WaterQuantity" = WaterQuantity,
     "ivQuantity" = ivQuantity,

     # Exposure time scenario
     "Time_end_exposure"         =         Time_end_exposure,         "period"=period,         "time_final_dose"=time_final_dose,
"time_first_dose"=time_first_dose)

      Parameters <-c(parms_physio, parms_PC, parms_chemical, parms_exposure)


      #================================================
      #(II.1) Initial values
      #================================================
      L0 = ((Bw_i/ a_BW_L) ^ (1/b_BW_L)) * DEB_shape * 10  # g --> cm Ltotale --> Lstruc --> mm

      Initial.Values <- c("Q_water"= WaterQuantity,
           "L"   = L0,
           "V_urine"= 0,

           "Q_art"  = 0,  "Q_ven"   = ivQuantity,

           "Q_brain"= 0, "Q_fat"=0, "Q_GIT" =0, "Q_lumen_GIT" = (IngestQuantity * frac_abs),
           "Q_gonads"= 0, "Q_kidney" =0,  "Q_liver"= 0,
           "Q_skin" =0, "Q_rp"=0, "Q_pp"=0,
```

```
          "Q_admin_gills"=0,  "Q_admin_GIT"=(IngestQuantity * frac_abs),
          "Q_met_plasma"=0, "Q_met_liver"=0, "Q_met"=0, "Q_elim_water"=0,
          "Q_excret"=0, "Q_feces"=0, "Q_excret_gills"=0, "Q_bile"=0, "Q_urine"=0, "Q_urine_cum"=0 )

     #================================================
     #(II.2) Environmental and biological scenario
     #================================================

     # Temperature scenarii
     if( length (Temperature) > 1) {
    times = seq(0, length(Temperature)-1, 1)
    import = Temperature
     } else {
    times = Times
    import = rep(Temperature, length(times))}

     Scenario = data.frame(times = times, import = import)
     Temperature.Scenario = approxfun(Scenario$times, Scenario$import, rule = 2)

     # scenario for urine discharge ######################################################################
     if (!is.null(urination_interval)){
    events_urine <- list(data = rbind(data.frame(var = c("V_urine"),
                time = seq(Times[1], rev(Times)[1] , by=urination_interval),
                value = 0,
                method = c("replace")),
              data.frame(var = c("Q_urine"),
                time = seq(Times[1], rev(Times)[1] , by=urination_interval),
                value = 0,
                method = c("replace"))))
     }else{ events_urine <- NULL }

     #================================================
     #(II.3) Exposure scenario :   events_repeated
     #================================================
     events_repeated_f <- NULL

     # repeated dose scenario for oral bolus
     if (!is.null(period) & IngestQuantity!=0 ) {

    # no stop before the end of the experiement
    if (is.null(time_final_dose)){ time_final_dose <- floor(max(Times)/period)*period}

    # First dose NOT at t0 of the experiment
    if (!is.null(time_first_dose)) { Initial.Values["Q_admin_GIT"]<-0 ; Initial.Values["Q_lumen_GIT"]<-0 }

    # First dose at t0 of the experiment
    if (is.null(time_first_dose)){ time_first_dose = period }

    # events : a list with a data frame for each compartment --> Cpt name / Time / Dose / method
    events_repeated_f <- list(data = rbind(data.frame(var = c("Q_lumen_GIT"),
                  time = seq(time_first_dose, time_final_dose , by=period),
                  value = as.numeric(c(parms_chemical["frac_abs"]*parms_exposure["IngestQuantity"])),
                  method = c("add")),
                data.frame(var = c("Q_admin_GIT"),
                  time = seq(time_first_dose, time_final_dose , by=period),
                  value = as.numeric(c(parms_chemical["frac_abs"]*parms_exposure["IngestQuantity"])),
                  method = c("add"))
                  ))
     }

     # repeated dose scenario for water exposure ##########################################################

     events_repeated_w <- NULL


     if (!is.null(period) & WaterQuantity!=0 ) {

    # no stop before the end of the experiement
    if (is.null(time_final_dose)){ time_final_dose <- floor(max(Times)/period)*period}

    # First dose NOT at t0 of the experiment
    if (!is.null(time_first_dose)) { Initial.Values["Q_water"]<-0 }

    # First dose at t0 of the experiment
    if (is.null(time_first_dose)){ time_first_dose = period }

    # events : a list with a data frame for each compartment --> Cpt name / Time / Dose / method
    events_repeated_w <- list(data = rbind(data.frame(var = c("Q_water"),
                  time  = seq(time_first_dose, time_final_dose , by=period),
                  value = (1-frac_renewed),
                  method = c("multiply")),
                data.frame(var = c("Q_water"),
                  time =  0.0000001+seq(time_first_dose, time_final_dose , by=period),
                  value = as.numeric( parms_exposure["WaterQuantity"]* frac_renewed),
                  method = c("add")),
                data.frame(var = c("Q_water"),
                  time  = Time_end_exposure,
                  value = 0,
                  method = c("multiply"))

    #           # In depuration phase, water renewal
    #            ,   data.frame(var = c("Q_water"),
    #              time  = 0.0000001+seq(Time_end_exposure, max(Times) , by=period),
    #              value = (1-frac_renewed),
```

```
#              method = c("multiply"))
 ))
  }

if ((is.null(period))& (WaterQuantity!=0) ){
 events_repeated_w <- list(data = rbind(data.frame(var = c("Q_water"),
              time  = Time_end_exposure,
              value = 0,
              method = c("multiply"))))
  }

  events<-list(data = rbind(events_repeated_f[[1]], events_repeated_w[[1]], events_urine[[1]]))


  #=============================================
  # (III) Numerical resolution and post-calcul
  #=============================================

  out <- ode(times = Times,
    func  = PBPK.model,
    y  = Initial.Values ,
    parms = Parameters,
    input.T = Temperature.Scenario,
    method="lsodes",
    events = events)

  PC = parms_PC

  return( list("Sim"=out, "PC"=PC, "Length" = out[,"L"] / DEB_shape * 1/10 ) ) # Length (cm)
}
```

Example of PBTK model application for TCDD with exposure scenario from Branson et al. (1985)

```
################################
####### 2,3,7,8-Tetrachlorodibenzo-p-dioxin (TCDD)

############################################################
# APPLICATION RAINOW TROUT
##### Data from Branson, 1985
##### Water exposure : 6 h of exposure + 139 days depuration
############################################################

#=============================================
# Observed data
#=============================================

Res_times = c(0.083, 0.25, 7, 22, 42, 64, 78, 118, 134, 136, 139) # days

Times_water = c(0.25, 0.30, 0.75, 1, 1.25,  1.5, 1.75, 2, 3, 4.17, 5, 6) / 24 # h/24 = days
Mean_water = c(362, 330, 337, 320, 321, 354, 316, 327, 307, 296, 310, 291) * 0.63

Mean_value_fish = (c(1.01, 2.58, 2.06, 1.97, 0.98, 0.78, 0.81, 0.583, 0.65, 0.82, 0.49 ) * 10^(-3)) # ng/g * 10^(-3) = microg/g
SD_value_fish = (c(0.09, 0.06, 0.15, 0.07, 0.04, 0.05, NA, 0.1, NA, NA, NA) * 10^(-3)) # ng/g * 10^(-3) = microg/g

#=============================================
# Simulation
#=============================================

Quantity_ext = 107 * 10^(-6) # ng/L * 10^(-6) = microg/mL

tps = sort( unique( c(seq(0,140,0.1), Res_times)))

Res_branson <- PBPK.RT.M( WaterQuantity = Quantity_ext * (145000/30), IngestQuantity= 0, ivQuantity = 0,
      Bw_i    = 35,
      log_Kow    = 6.8,
      Temperature   = 13,
      V_water    = (145000/30), # mL

      Cl_liver   = 0,  # mL/g/d

      K_BG    = 0,
      #Ke_water  = (2 /145) * (24 * 60) * 0.035 , # que dans depuration phase
      Ke_bile    = 1.5, # d-1

      Ku   = (0.58*0.83)/(1-0.58), # d-1
      frac_abs   = 1,

      Times   = tps,
      time_first_dose = NULL,
      time_final_dose = NULL,
      Time_end_exposure= 6/24,
      period  = 140,
      frac_renewed  = 1)
```

Part II Checklist for model evaluation

PBK Model Evaluation Checklist	Checklist assessment	Comments
Name of the PBK model (as in the reporting template)	Generic PB-K model for four fish species	
Model developer and contact details	(1) Remy Beaudouin, (1) Audrey Grech, (1) Cleo Tebby, (2) Frédéric Bois (2) Nadia Quignot, (3) Jean Lou CM Dorne, (1) Celine Brochot (1) INERIS, Paris, France; 2) CERTARA, Paris, France; 3) European Food Safety Authority, Parma, Italy	
Name of person reviewing and contact details	**A Paini**	
Date of checklist assessment	**11/01/2020**	
A. Context/Implementation		
A.1. Regulatory Purpose		
1. What is the acceptable degree of confidence/uncertainty (e.g. high, medium or low) for the envisaged application (e.g. priority setting, screening, full assessment?)	**High**	
2. Is the degree of confidence/uncertainty in application of the PBK model for the envisaged purpose greater or less than that for other assessment options (e.g. reliance on PBK model and *in vitro* data vs. no experimental data)?	**High**	
A.2. Documentation		
3. Is the model documentation adequate, i.e. does it address the essential content of model reporting template, including the following:	**YES**	
• Clear indication of the chemical, or chemicals, to which the model is applicable?	**YES**	
• Is the model being applied for the same scientific purpose as it was developed, or has it been repurposed somehow?	**YES**	
• Model assumptions?	**YES**	
• Graphical representation of the proposed mode of action, if known?	**NO**	
• Graphical representation of the conceptual model?	**YES**	
• Supporting tabulation for parameters (names, meanings, values, mean and standard deviations, units and sources)?	**YES**	
• Relevance and reliability of model parameters?	**YES**	
• Uncertainty and sensitivity analysis?	**YES**	

• Mathematical equations?	**YES**	
• PBK model code?	**YES**	**Reported in the appendix of the peer reviewed article**
• Software algorithm to run the PBK model code?	**NR**	
• Qualification of PBK software platform?	**NA**	
A.3 Software Implementation and Verification		
4. Does the model code express the mathematical model?	**YES**	
5. Is the model code devoid of syntactic and mathematical errors?	**YES**	
6. Are the units of input and output parameters correct?	**YES**	
7. Is the chemical mass balance respected at all times?	**YES**	
8. Is the cardiac output equal to the sum of blood flow rates to the tissue compartments?	**YES**	
9. Is the sum total of tissue volumes equal to total body volume?	**YES**	
10. Is the mathematical solver a well-established algorithm?	**YES**	
11. Does the mathematical solver converge on a solution without numerical error?	**YES**	
12. Has the PBK modelling platform been subjected to a verification process (for a different use, for instance, in the pharmaceutical domain)?	**NA**	
A.4 Peer engagement (input/review)		
13.a Has the model been used previously for a regulatory purpose?	**NO**	
• Is prior peer engagement in the development and review of the model sufficient to support the envisaged application?	**YES**	
• Is additional review required? Peer engagement includes input/review by experts on specific aspects of model development, individual reviews of the model by experts, or collective reviews by peer review panels. Availability of the comments and tracking of revisions to the model in response to peer input contributes to increased confidence in the model for potential application.	**YES**	
B. Assessment of Model Validity		
B.1 Biological Basis (Model Structure and Parameters)		
14. Is the model consistent with known biology?	**YES**	
• Is the biological basis for the model structure provided?	**YES**	
• Is the complexity of the model structure appropriate to address the regulatory application?	**YES**	
• Are assumptions concerning the model structure and parameters clearly stated and justified?	**YES**	
• Is the choice of values for physiological parameters justified?	**YES**	

• Is the choice of methods used to estimate chemical-specific ADME parameters justified?	**YES**	
• Saturable kinetics	**YES**	
B.2 Theoretical Basis of Model Equations		
15. Are the underlying equations based on established theories, .e.g. Michaelis-Menten kinetics, Fick's laws of diffusion?	**YES**	
• In the case of PBK models for particles, does the model take into consideration the properties of particles, e.g. particle size ranges, (poor) solubility, aggregation, partitioning and diffusion/sedimentation behaviour?	**NA**	
B.3. Reliability of input parameters		
16. Has the uncertainty (individual variability, experimental reproducibility and reliability) in the input parameters been characterised?	**YES**	
B.4. Uncertainty and Sensitivity Analysis		
17. Has the impact of uncertainty (individual variability, experimental reproducibility and reliability) in the parameters on the chosen dose metric been estimated?	**YES**	
• Local sensitivity analysis?	**NO**	
• Global sensitivity analysis?	**YES**	
18. Is confidence in influential input parameter estimates (i.e., based on comparison of uncertainty and sensitivity) reasonable (within expected values; similar to those of analogues) in view of the intended application?	**YES**	
B.5. Goodness-of-Fit and Predictivity		
19. For PBK models for which there are sufficient *in vivo* data for the chemical of interest:		
• Suitability of analogue (chemical and biological similarity)?	**NA**	
• Reliable estimation of chosen dose metric for analogue?	**NA**	
• In general is the biological Variability of *in vivo* reference data (from analogue) established?	**NA**	

Part III Overall Evaluation

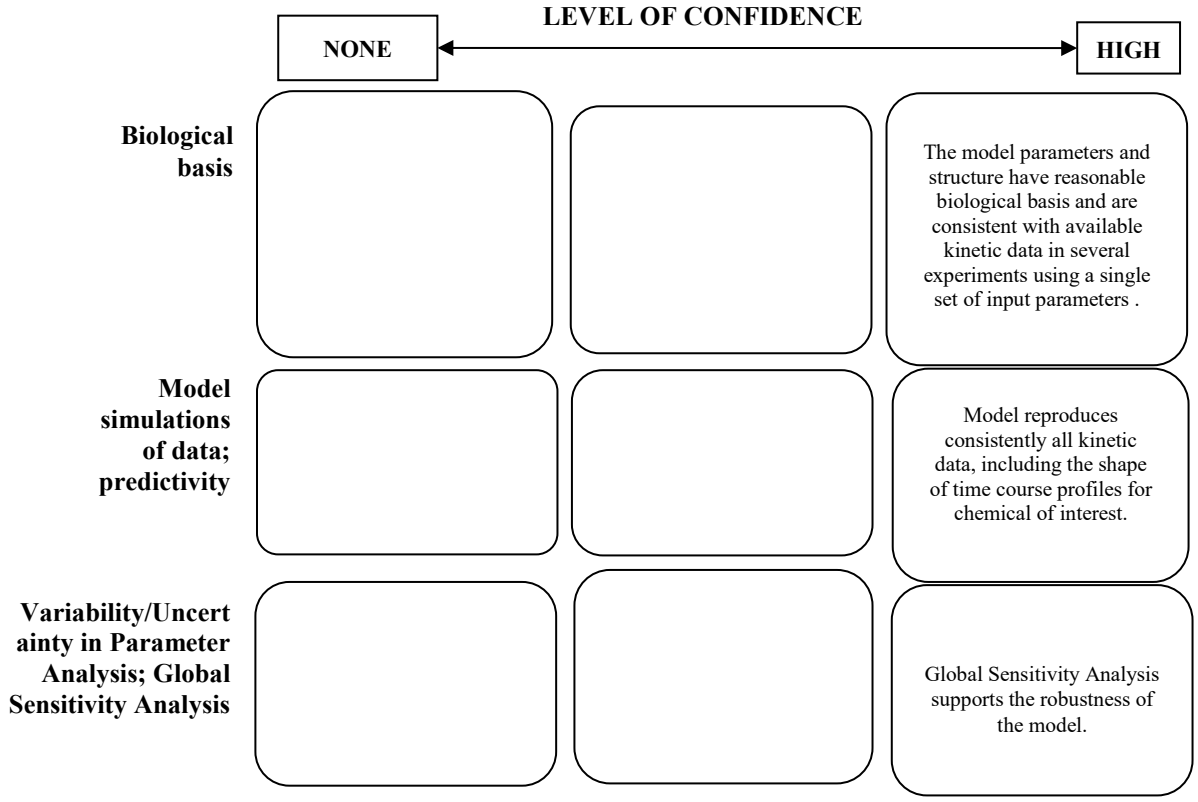

The PBK models reported in the present work were developed to establish blood and organ levels of chemicals in four fish species within food and feed safety context. The documentation provided is strong and the level of confidence scored is high. The models presented here can be applied in chemical risk assessment with high confidence.

Case Study III

In vitro-to *In vivo* extrapolation (IVIVE) by PBTK modelling

Part I. PBK model reporting template

A. Name of model

In vitro-to *In vivo* extrapolation (IVIVE) by PBTK modelling for animal free risk assessment approaches of potential endocrine disrupting compounds – IVIVE by PBTK model.

B. Contact details

Eric Fabian, Caroline Gomes, Barbara Birk, Tzutzuy Ramirez-Hernandez, Tabitha Williford, Christian Haase, Rene Zbranek, Bennard van Ravenzwaay, Robert Landsiedel - BASF SE, Experimental Toxicology and Ecology, 67056 Ludwigshafen, Germany.

C. Summary of model characterisation, development, validation, and potential applicability

We present an *in vitro-in silico*-based reverse dosimetry concept using *in vitro* and *in-silico* based input data for PBTK (physiology based toxicokinetic) modelling and endpoints of endocrine disruption. Ten compounds (acetaminophen, bisphenol A, caffeine, 17-α-ethinylestradiol, fenarimol, flutamide, genistein, ketokonazole, methyltestosterone and trenbolone) were selected since they have been tested in the Yeast Estrogen Screening (YES) or Yeast Androgen Screening (YAS) assays for estrogen and androgen receptor binding, as well as the H295R steroidogenesis assay (OECD test guideline no. 456). The lowest observed effect concentration (LOEC) from these assays was extrapolated to an oral dose by reverse dosimetry using an 8-compartment Physiologically Based Toxicokinetic (PBTK) rat model. The resulting value correlates to a predicted LOEL *in vivo*, which was compared with the measured LOEL in corresponding *in vivo* studies for endocrine disruption (YES/YAS assay versus uterotrophic or Hershberger assay and steroid mapping versus pubertal assay or generation studies). This evaluation resulted in 6 out of 10 compounds for which the *in vitro-in silico*-based LOELs were in the same order of magnitude as the *in vivo* derived LOELs. For 4 compounds, the predicted LOELs differed by >10-fold from the *in vivo*.

Evaluation of potential application of the *in vitro*-to *in vivo* extrapolation (IVIVE) was based on the comparison of estimated lowest observed effect doses versus the measured LOELs in corresponding *in vivo* studies (in the rat -since these data were available in literature). As classical risk assessments are routinely based on defined threshold levels derived from dose-response *in vivo* data, the concept within the current case study was the comparison of estimated lowest observed effect doses versus measured, *in vivo* determined LOELs. Therewith, this comparison is considered to be a basis in parallel also for potentially valid risk assessments based on in vitro data and consequent *in vivo* extrapolation by reverse dosimetry approaches.

D. Model characterisation (structure and parameters, assumptions and limitations)

Step 1 – Scope and purpose of the model (problem formulation)

In vitro testing is used to identify hazards of chemicals, nominal in vitro assay concentrations may misrepresent potential *in vivo* effects and do not provide dose–response data which can be used for a risk assessment. A reverse dosimetry approach was used to compare in vitro effect concentrations-to-*in vivo* doses causing toxic effects related to endocrine disruption.

- 8-compartment model for rats (including the target tissues/organs for endocrine disruption (adrenals and ovaries/testes))
- Chemicals enter the bloodstream as first-order process directly via the liver after uptake in the gastrointestinal tract
- Distribution is diffusion based
- Hepatic clearance reflects the overall clearance. The unbound fraction of the test compound was taken into account for the quantification of metabolic clearance (biliary and renal clearance are not considered in the applied PBTK-model).
- model is focused on the kinetics of the test compounds, which reflects a postulated, parent linked effect. (test chemicals: acetaminophen (APAP); bisphenol A (BPA); caffeine (CAF); 17α-ethynylestradiol (EE); fenarimol (FEN); flutamide (FLU); genistein (GEN); ketoconazole (KET); methyltestosterone (MTT); trenbolone (TRE))

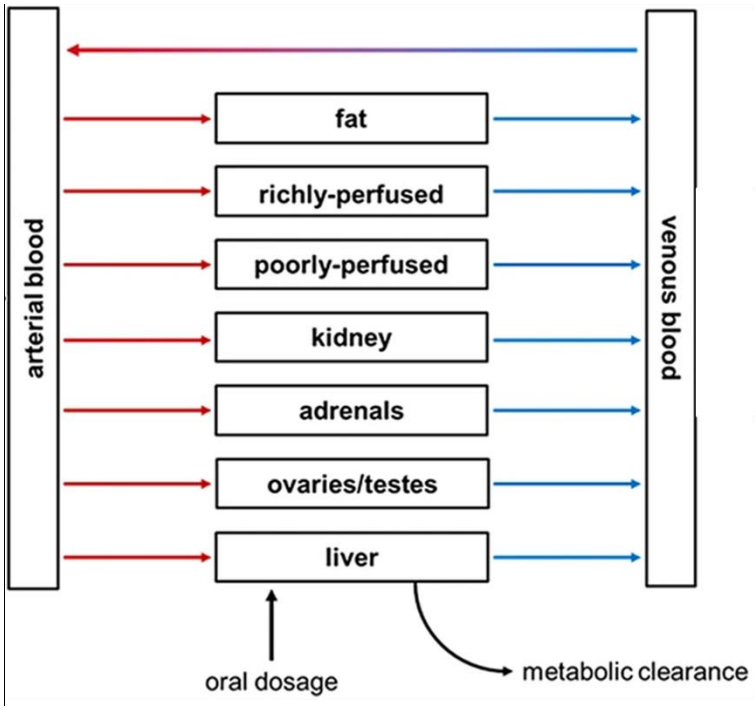

Figure III1. Schematic representation of the PBTK model (taken from Fabian et al., 2019).

Step 2 – Model conceptualisation (model structure, mathematical representation)

The physiological parameters, including body weight, organ volumes, cardiac output, and blood flows, were taken from the literature (Brown et al. 1997; Davies and Morris 1993) and from in house data for male and female Wistar rats (Crl:Han, Charles River, Sulzfeld, Germany) Fabian et al., 2019. Details are listed in Table III1.

The physicochemical input parameters of the test compounds consist of the octanol/water partition coefficient log Kow and molecular weight (Table III1). Log Pow data were predicted using the ALOPGS 2.1 software. The tissue partition coefficients, used to describe and model the distribution between blood and defined tissues, were calculated based on the physicochemical parameters by the following equations as given by DeJongh et al. (1997):

(1) P=(0.081*Kow0.44+0.919)(0.004*Kow0.44+0.996)−0.19

(2) P=(0.8*Kow0.7+0.2)(0.004*Kow0.7+0.996)−0.02

(3) P=(0.056*Kow0.29+0.944)(0.004*Kow0.29+0.996)−0.55.

Equation (1) was used for liver, kidneys, adrenals, ovaries/testes, and richly perfused tissues, Eq. (2) for fat and Eq. (3) for poorly perfused tissue.

Intestinal absorption was predicted using a QSAR model based on Caco-2 data described by the following equation given by Hou et al. (2004):

(4) LogPapp=−4.28−0.011*PSA,

where Papp is the apparent permeability coefficient and PSA is the polar surface area. PSA values were obtained in ChemAxon public database (2016). The results of this calculation in cm/s were thereafter converted to Papp in (cm/s)10^{-6}.

Metabolic clearance was based on hepatic clearance reported in the literature or determined in S9 subcellular fractions of livers from Wistar rats at Cyprotex, Alderley Park, UK (see Table III2). Hence, the intrinsic clearance (CLint) in this model was based on hepatocytes, microsomal, or S9 subcellular hepatic fractions. Since some of the chemicals were expected to be directly conjugated, the microsomal and liver S9 incubations were used that contained cofactors for glucuronidation (UDPGA) and sulfation (PAPS), as well as NADPH for oxidation reactions. CLint data were normalized for hepatocytes as clearance per 10^6 cells, and for S9 and microsomal fraction as clearance per mg of protein. To estimate the *in vivo* hepatic clearance, the CLint values were scaled up using the factors of 135*10^6 cells/g liver for hepatocytes (Houston 1994); 91.3 and 50 mg protein/g liver for liver S9-fraction and microsomes, respectively (BASF internal data).

The fraction unbound to protein in the plasma (fu_p) was experimentally determined by performing rapid equilibrium dialysis (RED). (For more details on the experimental set up see Fabian et al., 2019).

Step 4 – Computer implementation (solving the equations)

The differential equations were solved using the software Berkeley Madonna™, version 8.3.18 (developed by Macey et al. 2009). All the compounds were analyzed in one task using the built ‘batch-run’. Microsoft Excel 2013 (Microsoft®) was used to import and analyze the data.

Equations governing the model

Liver (L) dAL/dt=QL(CA−CLPL)+dAGIdt−dAMintdt; CL=AL/VL;

dAMint/dt=CLint x CVL; CVL=CL/PL; dAGIdt=−Ka*AGI

Fat (F) dAF/dt=QF(CA−CF/PF); CF=AF/VF

Richly perfused (R) dAR/dt=QR(CA−CR/PR); CR=AR/VR

Poorly perfused (P) dAP/dt=QP(CA−CP/PP);CP=AP/VP

Kidneys (K) dAK/dt=QK(CA−CK/PK);CK=AK/VK

Adrenals (A) dAAd/dt=QAd(CA−Cad/PAd);CAd=AAd/VAd

Ovaries (O) dAO/dt=QO(CA−CO/PO);CO=AO/VO

Testes (Te) dATe/dt=QTe(CA−CTe/PTe);CTe=Ate/Vte

Venous blood (V) dAV/dt=(QL*CL/PL + QF*CF/PF + QK*CK/PK + QAd*Cad/Pad + Q(O/Te)*(C(OTe)/P(OTe)) + QR*CR/PR + QP*CP/PP− QC*CV); CV=AV/VB

Arterial blood (A) CA=CV

The fup data were used to calculate the hepatic clearance in the model using the following equation described by Houston (1994):

CLH=QL∗fuP∗CL/QL+fuP∗CL;dAMint/dt=CLH∗CVL,

where CL_H is the hepatic clearance, CL is the intrinsic clearance scaled up, QL is the liver blood flow, AMint is the arterial blood metabolic intrinsic rate, and CVL is the concentration in the venous blood leaving the liver.

For PBTK modelling, oral dose was set to 50 mg/kg bw and differential equations were solved using the software Berkeley Madonna™

Results from PBTK modelling and LOECs from in vitro experiments were used for IVIVE. In a linear manner, dose levels were calculated for respective LOECs based on the estimated plasma C_{max} versus dose plot results from PBTK. For this analysis, the non-protein bound, free fraction of a test compound at the time point of the C_{max} in plasma was considered as correlated tor the endocrine induced effects. In addition, extrapolated dose levels in plasma were compared with *in vivo* LOELs to evaluate the accuracy of the applied PBTK model (Fabian et al., 2019).

Step 5 – Model Performance

To evaluate the PBTK predictions, the results obtained for C_{max} in plasma were compared with measured C_{max} from rats, extracted from the literature. As described above, in the applied PBTK model, the C_{max}/dose ratio is constant and C_{max} values for a given dose, from rat studies, can be calculated in a linear approach from the results obtained at the modeled dose of 50 mg/kg bw by the rule of proportion.

The sensitivity analysis of the model was performed for all compounds based on the description of Evans and Andersen (2000). In this approach, the sensitivity coefficient (SC) is defined by the initial maximum concentration (C) after prediction for plasma or tissue, the initial parameter of the model (P), the maximum concentration after increasing the parameter value by 5% (C′), and the changed parameter (P′) as shown below:

SC=C′−CP′−P∗ PC.

The resulting sensitivity coefficients were analyzed using Microsoft Excel 2013 (Microsoft®). The input parameter was considered to significantly affect the model output when the SC absolute value was higher than 0.5 (Rietjens et al. 2011). The output parameter assessed was the Cmax in plasma.

Step 6 – Model Documentation

The PBTK model was published in peer reviewed journal, Fabian et al., 2019

E. Identification of uncertainties

Model structure

- analysis for estrogen or androgen receptor dependent reporter enzyme activity (agonistic and/or antagonistic) and effects on hormone synthesis in H295R human adrenocortical carcinoma cells from Kolle et al., 2012. LOEC was set as lowest concentration from the available in vitro data, in which an effect was observed without cytotoxicity
- Distribution is based on diffusion (no impact by active transport)

Input parameters

- Hepatic clearance drives overall clearance (negligible extrahepatic metabolism)

Model output

- correlation for c_{max} of test substance (parent compound) in plasma and effect (effective concentration is free (non protein bound) fraction of test substance (parent compound) in plasma)
- Concentration driven toxicodynamic response (comparable in the *in vitro* and *in vivo* environment)
- Target output was the maximal concentration (C_{max}) in plasma and target tissues

Other uncertainties (e.g. model developed for different substance and/or purpose)

- Test substance (parent compound) correlated effect (no metabolic activation; metabolites without contribution to effect)
- Linear extrapolation from LOEC to estimated LOEL based on calculated C_{max} at 50 mg/kg bw (constant C_{max}/dose ratio)

F. Model implementation details

- software (version no) The differential equations were solved using the software Berkeley Madonna™, version 8.3.18 (developed by Macey et al. 2009). All the compounds were analysed in one task using the built ‘batch-run’.
- availability of code: Equations are reported in Fabian et al.,2019. Code is available on demand.

- software verification / qualification. The software verification and qualification was not reported. The software Berkeley Madonna™ is a very well established software to execute ODE and to build PBK models, like the one reported in this work.

G. Peer engagement (input/review)

The model was not peer-reviewed.

Parameter tables

Table III1. Physiological parameters (taken from Fabian et al., 2019)

Physiological parameters	Female Wistar	Male Wistar
Body weight (g)[a]	179	283
Mean % of body weight		
Adrenal[a]	0.04	0.023
Blood[b]	7.4	7.4
Kidney[a]	0.765	0.714
Fat[c]	7	7
Liver[a]	2.668	2.626
Ovary[a]	0.051	–
Testes[a]	–	1.123
Richly perfused[b]	9.034-VLc–VKc–VAdc–(VOc/VTc)	
Slowly perfused[b]	7.34-VFc	
Cardiac output (L/h)[d]	$14.1*BW^{(0.75)}$	
Mean % of cardiac output		
Liver (QLc)[b]	18.3	
Fat (QFc)[b]	7	
Kidney (QKc)[d]	14.1	
Adrenal (QAdc)[d]	0.3	
Ovaries (QOc)[e]	0.665	
Testes (QTc)[f]	0.802	
Richly perfused[b]	47.2-QLc–QKc–QAdc–(QOc/QTc)	
Slowly perfused[b]	52.8-QFc	

[a]Average values from BASF historical control database for Wistar rats Crl:Han, Charles River, Sulzfeld, Germany; [b]Brown et al. (1997); [c]Arms and Travis (1988); [d]Adapted from Arms and Travis (1988) in relation to data for modeled rats; [e]Bruce (1976); [f]Saypol et al. (1981)

Table III2. Permeability, Clearance and Fraction unbound parameters measured (taken from Fabian et al., 2019)

Compound	Permeability (Caco-2)[A]	Clearance		% Fraction unbound (fu_p)	
		Value	Source[a]	Experimental	Literature
Acetaminophen (APAP)	15	15	Hepatocytes[B]	79	82[B]
Bisphenol A (BPA)	19	361	Microsomes[C]	2.8	6.8[G]

Caffeine (CAF)	12	1.4	Hepatocytes[D]	65	84[H]
17α-Ethynylestradiol (EE)	19	243	Microsomes[C]	1.1	1.6[G]
Fenarimol (FEN)	16	1.0	S9[E]	3.2	5.0[I]
Flutamide (FLU)	8.4	4.6	S9[E]	5.7	4.7[I]
Genistein (GEN)	5.8	505	Microsomes[C]	2.7	< 10[J] 3.2[C]
Ketoconazole (KET)	9.1	55	Hepatocytes[F]	0.4	3.7[K]
Methyltestosterone (MTT)	20	110	S9[E]	4.5	4.0[I]
Trenbolone (TRE)	20	43	S9[E]	4.8	9.4[I]

[a]Units of data expressed as: µl/min/10^6 hepatocytes or µl/min/mg microsomal protein or µl/min/mg S9 protein; [A]Calculated based on the equation: Log Papp=−4.28−0.011*PSA; (polar surface area, taken from ChemAxon public database 2016) described by Hou et al. (2004); [B]Naritomi (2003); [C]Punt et al. (2013); [D]Hayes et al. (1995); [E]Cyprotex (2014);' [F]Ito and Houston (2004); [G]Berry et al. (2010); [H]Kilford et al. (2008); [I]Cyprotex UK (2014) [J]Coldham and Sauer (2000) [K]Matthew et al. (1993)

I. References and background information

Arms AD, Travis CC (1988) Reference physiological parameters in pharmacokinetic modeling. Office of Health and Environmental Assessment, Office of Research and Development U.S. Environmental Protection Agency, Washington (EPA/600/6-88/004).

Brown RP, Delp MD, Lindstedt SL, Rhomberg LR, Beliles RP (1997) Physiological parameter values for physiologically based pharmacokinetic models. Toxicol Ind Health 13(4):407–484.

Bruce NW (1976) The distribution of blood flow to the reproductive organs of rats near term. J Reprod Fertil 46(2):359–362.

ChemAxon public database (2016) https://chemaxon.com/. Accessed 01 Feb 2018.

Coldham NG, Sauer MJ (2000) Pharmacokinetics of [(14)C]Genistein in the rat: gender-related differences, potential mechanisms of biological action, and implications for human health. Toxicol Appl Pharmacol 164(2):206–215. https://doi.org/10.1006/taap.2000.8902.

Cyprotex (2014) Cyprotex metabolic stability measurements in S9 subcellular fraction (contract measurement).

Davies B, Morris T (1993) Physiological parameters in laboratory animals and humans. Pharm Res 10(7):1093–1095.

DeJongh J, Verhaar HJ, Hermens JL (1997) A quantitative property–property relationship (QPPR) approach to estimate in vitro tissue-blood partition coefficients of organic chemicals in rats and humans. Arch Toxicol 72(1):17–25.

Evans MV, Andersen ME (2000) Sensitivity analysis of a physiological model for 2,3,7,8-tetrachlorodibenzo-p-dioxin (TCDD): assessing the impact of specific model parameters on sequestration in liver and fat in the rat. Toxicol Sci 54(1):71–80.

Fabian, E., Gomes, C., Birk, B. et al. Arch Toxicol (2019) 93: 401. https://doi.org/10.1007/s00204-018-2372-z.

Hayes KA, Brennan B, Chenery R, Houston JB (1995) In vivo disposition of caffeine predicted from hepatic microsomal and hepatocyte data. Drug Metab Dispos 23(3):349–353.

Hou TJ, Zhang W, Xia K, Qiao XB, Xu XJ (2004) ADME evaluation in drug discovery. 5. Correlation of Caco-2 permeation with simple molecular properties. J Chem Inf Comput Sci 44(5):1585–1600.

Houston B (1994) Utility of in vitro drug metabolism data in predicting in vivo metabolic clearance. Biochem Pharmacol 47:1469–1479. https://doi.org/10.1016/0006-2952(94)90520-7.

Ito K, Houston JB (2004) Comparison of the use of liver models for predicting drug clearance using in vitro kinetic data from hepatic microsomes and isolated hepatocytes. Pharm Res 21(5):785–792. https://doi.org/10.1023/B:PHAM.0000026429.12114.7d.

Kilford PJ, Gertz M, Houston JB, Galetin A (2008) Hepatocellular binding of drugs: correction for unbound fraction in hepatocyte incubations using microsomal binding or drug lipophilicity data. Drug Metab Dispos 36(7):1194–1197. https://doi.org/10.1124/dmd.108.020834.

Kolle et al. (2010) Toxicology in Vitro 24, 2030–40. Kolle et al. (2012) Regulatory Toxicol Pharmaco 63, 259–78. Hou, T. J. et al. (2004) Journal of Chemical Information and Computer Sciences 44, 1585–1600.

DeJongh et al. (1997) Archives in Toxicology 72, 17-25. Brown et al. (1997) Toxicol Ind Health 13, 407.

Evans and Andersen (2000) Toxicological Sciences, 54, 71–80. Rietjens IM, Louisse J, Punt A (2011) Mol Nutr Food Res 55(6): 941-956.

Macey R, Oster G, Zahnley T (2009) Berkeley Madonna user's guide. Berkeley Madonna Webpage, Berkeley.

Naritomi Y (2003) Utility of hepatocytes in predicting drug metabolism: comparison of hepatic intrinsic clearance in rats and humans in vivo and in vitro. Drug Metab Dispos 31(5):580–588. https://doi.org/10.1124/dmd.31.5.580.

Punt A, Brand W, Murk AJ, van Wezel AP, Schriks M, Heringa MB (2013) Effect of combining in vitro estrogenicity data with kinetic characteristics of estrogenic compounds on the in vivo predictive value. Toxicol In Vitro 27(1):44–51. https://doi.org/10.1016/j.tiv.2012.09.014.

Rietjens IM, Louisse J, Punt A (2011) Tutorial on physiologically based kinetic modeling in molecular nutrition and food research. Mol Nutr Food Res 55(6):941–956. https://doi.org/10.1002/mnfr.201000655.

Saypol DC, Howards SS, Turner TT, Miller ED Jr (1981) Influence of surgically induced varicocele on testicular blood flow, temperature, and histology in adult rats and dogs. J Clin Investig 68(1):39–45.

Part II Checklist for model evaluation

PBK Model Evaluation Checklist	Checklist assessment	Comments
Name of the PBK model (as in the reporting template)	**IVIVE by PBTK model**	
Model developer and contact details	**Fabian et al. BASF**	
Name of person reviewing and contact details	**A. Paini**	
Date of checklist assessment	**June 2020**	
A. Context/Implementation		
A.1. Regulatory Purpose		
1. What is the acceptable degree of confidence/uncertainty (e.g. high, medium or low) for the envisaged application (e.g. priority setting, screening, full assessment?)	**High Fill Kinetic data gap in full assessment using IVIVE**	
2. Is the degree of confidence/uncertainty in application of the PBK model for the envisaged purpose greater or less than that for other assessment options (e.g. reliance on PBK model and *in vitro* data vs. no experimental data)?	**high**	
A.2. Documentation		
3. Is the model documentation adequate, i.e. does it address the essential content of model reporting template, including the following:	**Yes**	
• Clear indication of the chemical, or chemicals, to which the model is applicable?	**Yes**	
• Is the model being applied for the same scientific purpose as it was developed, or has it been repurposed somehow?	**Yes**	
• Model assumptions?	**Yes**	
• Graphical representation of the proposed mode of action, if known?	**No**	
• Graphical representation of the conceptual model?	**Yes**	
• Supporting tabulation for parameters (names, meanings, values, mean and standard deviations, units and sources)?	**Yes**	
• Relevance and reliability of model parameters?	**Yes**	
• Uncertainty and sensitivity analysis?	**Yes**	
• Mathematical equations?	**Yes**	
• PBK model code?	**NR**	
• Software algorithm to run the PBK model code?	**NR**	
• Qualification of PBK software platform?	**No**	
A.3 Software Implementation and Verification		
4. Does the model code express the mathematical model?	**NR**	
5. Is the model code devoid of syntactic and mathematical errors?	**NR**	

6. Are the units of input and output parameters correct?	**NR**	
7. Is the chemical mass balance respected at all times?	**NR**	
8. Is the cardiac output equal to the sum of blood flow rates to the tissue compartments?	**Yes**	
9. Is the sum total of tissue volumes equal to total body volume?	**Yes**	
10. Is the mathematical solver a well-established algorithm?	**NR**	
11. Does the mathematical solver converge on a solution without numerical error?	**Yes**	
12. Has the PBK modelling platform been subjected to a verification process (for a different use, for instance, in the pharmaceutical domain)?	**NA**	
A.4 Peer engagement (input/review)		
13. Has the model been used previously for a regulatory purpose?	**No**	
• Is prior peer engagement in the development and review of the model sufficient to support the envisaged application?	**NR**	
• Is additional review required? Peer engagement includes input/review by experts on specific aspects of model development, individual reviews of the model by experts, or collective reviews by peer review panels. Availability of the comments and tracking of revisions to the model in response to peer input contributes to increased confidence in the model for potential application.	**NA**	
B. Assessment of Model Validity		
B.1 Biological Basis (Model Structure and Parameters)		
14. Is the model consistent with known biology?	**YES**	
• Is the biological basis for the model structure provided?	**YES**	
• Is the complexity of the model structure appropriate to address the regulatory application?	**YES**	
• Are assumptions concerning the model structure and parameters clearly stated and justified?	**YES**	
• Is the choice of values for physiological parameters justified?	**YES**	
• Is the choice of methods used to estimate chemical-specific ADME parameters justified?	**YES**	
• Saturable kinetics	**No**	
B.2 Theoretical Basis of Model Equations		
15. Are the underlying equations based on established theories, .e.g. Michaelis-Menten kinetics, Fick's laws of diffusion?	**Yes**	

• In the case of PBK models for particles, does the model take into consideration the properties of particles, e.g. particle size ranges, (poor) solubility, aggregation, partitioning and diffusion/sedimentation behaviour?	**NA**	
B.3. Reliability of input parameters		
16. Has the uncertainty (individual variability, experimental reproducibility and reliability) in the input parameters been characterized?	**YES**	
B.4. Uncertainty and Sensitivity Analysis		
17. Has the impact of uncertainty (individual variability, experimental reproducibility and reliability) in the parameters on the chosen dose metric been estimated?	**Yes**	
• Local sensitivity analysis?	**Yes**	
• Global sensitivity analysis?	**NO**	
18. Is confidence in influential input parameter estimates (i.e., based on comparison of uncertainty and sensitivity) reasonable (within expected values; similar to those of analogues) in view of the intended application?	**Yes**	
B.5. Goodness-of-Fit and Predictivity		
19. For PBK models for which there are sufficient *in vivo* data for the chemical of interest:	**NA**	
• Suitability of analogue (chemical and biological similarity)?	**NA**	
• Reliable estimation of chosen dose metric for analogue?	**NA**	
• In general is the biological Variability of *in vivo* reference data (from analogue) established?	**NA**	

NR = not reported, NA = not applicable

Part III Overall Evaluation

Overall Conclusion on mode evaluation for the intended application

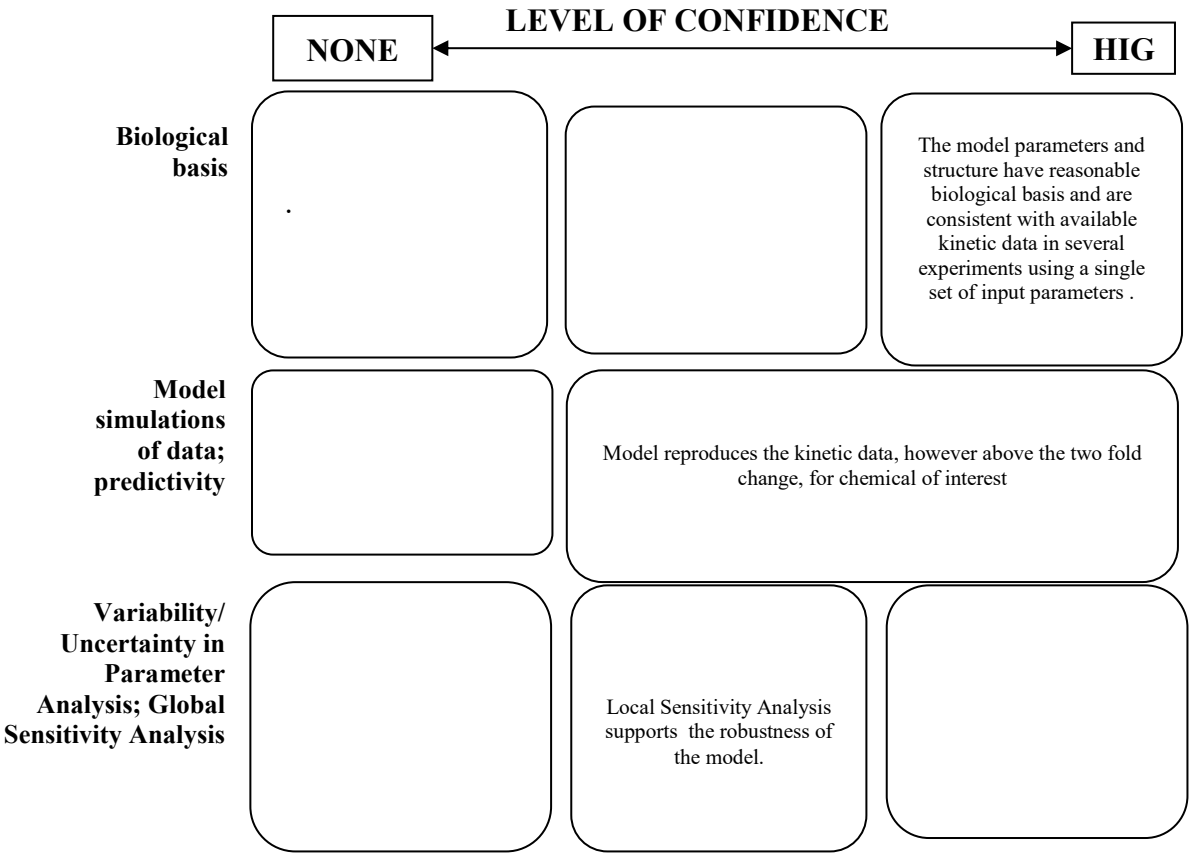

The present study provides an example of application of a PBTK model to extrapolate an external dose (prediction of *in vivo LOELs) for ED chemicals taking into account kinetic information, from in* vitro LOELs. The model equations are described and the model parameters have reasonable biological basis and are consistent with available kinetic data. However, the model reproduces kinetic data, above the two-fold change, including the shape of time course profiles for chemicals of interest. A Local Sensitivity Analysis supports the robustness of the model. The model code was not reported and a full assessment on the model performance could not be conduct.

Case Study IV

PBK model predictions using data from analogues

Part I. PBK model reporting template

A. Name of model

PBK model predictions using data from analogues

B. Contact details

Alicia Paini (1), Sunil Kulkarni (2), Judith Madden (3), and Andrew Worth (1)

1) EC Joint Research Centre; 2) Health Canada; 3) Liverpool John Moore University

C. Summary of model characterisation, development, validation, and potential applicability

The purpose is to provide means to evaluate a PBK model for chemicals for which no *in vivo* reference data are available (toxicity, ADME, TK parameters). This will help to establish safe levels (for humans) for both cases of acute (e.g. acute reference dose) or sub-chronic/chronic (e.g. acceptable daily intake) for regulated compounds (for REACH it is the derived no effect level [DNEL]) or tolerable daily intake for contaminants in food. The approach can be applied for prioritisation of chemicals, and for hazard characterisation, to set a point of departure.

The present study provides an example of PBK model evaluation using (structural) analogues of a chemical under assessment with no *in vivo* data available for the target chemical. On the basis of the results available, it was concluded that using data from one chemical source (estragole) for read across to a target chemical (methyleugenol) is a reasonable approach for a preliminary hazard characterisation, in the absence of *in vivo* data available to fully validate a methyleugenol model. Furthermore, the application of a PBK model that takes into account the kinetics of the chemical understudy reduces the uncertainties of the A, D, M, and E characteristics of the chemical

Disclaimer: In the present case study we report information for two well-known, previously studied chemicals, with valid PBK models, as a proof-of-principle. The chemicals under study are estragole and methyleugenol. Methylegenol will be considered, hypothetically, as a data–poor chemical requiring PBK model validation against human *in vivo* data.

The PBK model code for estragole in humans (Punt et al., 2009, 2016); was used with the following alterations:

1. The MW for parent and hydroxy-metabolite for estragole (known to be the active metabolite) were substituted with the values for methyleugenol as were the partition coefficients, predicted using the approach of Brown et al and the chemical specific LogKow.

2. In addition to the above changes, the in vitro V_{max} and K_m, values measured, for the formation of several metabolites formed in phase I and phase II were also substituted from

those relevant to estragole of those relevant for methyleugenol. These values were available for estragole and methyleugenol (Al-Subeihi et al., (2012) and by Punt et al., (2009; 2016), see table IV2).

We report the information and validation steps for the PBK model of the source chemical estragole and information on the parameters for the target chemical, methyleugenol.

D. Model characterisation (modelling workflow)

Step 1 – Scope and purpose of the model (problem formulation)

Evaluation of PBK models for chemicals that lack data for parametrisation and to assess model validity. In this case study, we need to simulate time and dose concentration response curve of methyleugenol, to assess human exposure after food ingestion – diet – for risk assessment.

Using the Tanimoto index of structural similarity (according to the calculations of the OECD QSAR Toolbox 4.4) estragole and methyleugenol have a similarity score of 0.70.

Premise

Methyleugenol lacks of a valid PBK model, and *in vivo* data are not available*. A PBK model for estragole was developed to assess human exposure and was validated. Data is used from one chemical source (estragole) for read across to a target chemical (methyleugenol).

(*hypothetically posited to enable a proof-of-principle analysis)

Step 2 – Model conceptualisation (model structure, mathematical representation)

A PBK model was developed and evaluated against *in vivo* human data to describe the relative importance of bioactivation and detoxification of estragole in humans at different oral dose levels using in vitro data (Punt et al., 2009). The model used in this case study was developed for estragole and then applied to methyleugenol. (For methyleugenol a PBK model does already exist (Al-Subeihi et al., 2012) and in this case could be used to validate the proof-of-principle. Following the mode of action of the two chemicals being investigated, a similar PBK model structure can be applied to both, focusing on the target organ the liver, but also including lungs and kidney since metabolism also occurs in these organs. The rate of formation of metabolites in lungs and kidney is generally negligible, however they are included in the model to account for wider variation that may be present in a population where some individuals may have higher metabolism in these other organs.

The ADME characteristics of estragole were captured by the following model structure and equations:

a. Organs involved in determining the chemical's ADME profile were identified
b. The model structure is reported in (figure IV2); the model consists of several compartments representing liver, fat tissue, and other rapidly/richly or slowly/poorly perfused tissues) connected via the systemic circulation.
c. The Berkley Madonna PBK model code is available at the end of this document.
d. Metabolism was considered in the target organ (liver) and was based on the proposed biotransformation pathways of estragole.

e. Punt et al., (2009; 2016) developed and parameterised the PBK model for estragole using in vitro data and human physiological information; this model was evaluated on *in vivo* data as described in Punt et al., 2009.

As they are similar in terms of mechanism of toxic action action and similar in structure, the estragole PBK code was used to derive a model for methyleugenol (see figure IV1), since the Tanimoto index of structural similarity estragole and methyleugenol have a similarity score of 0.70.

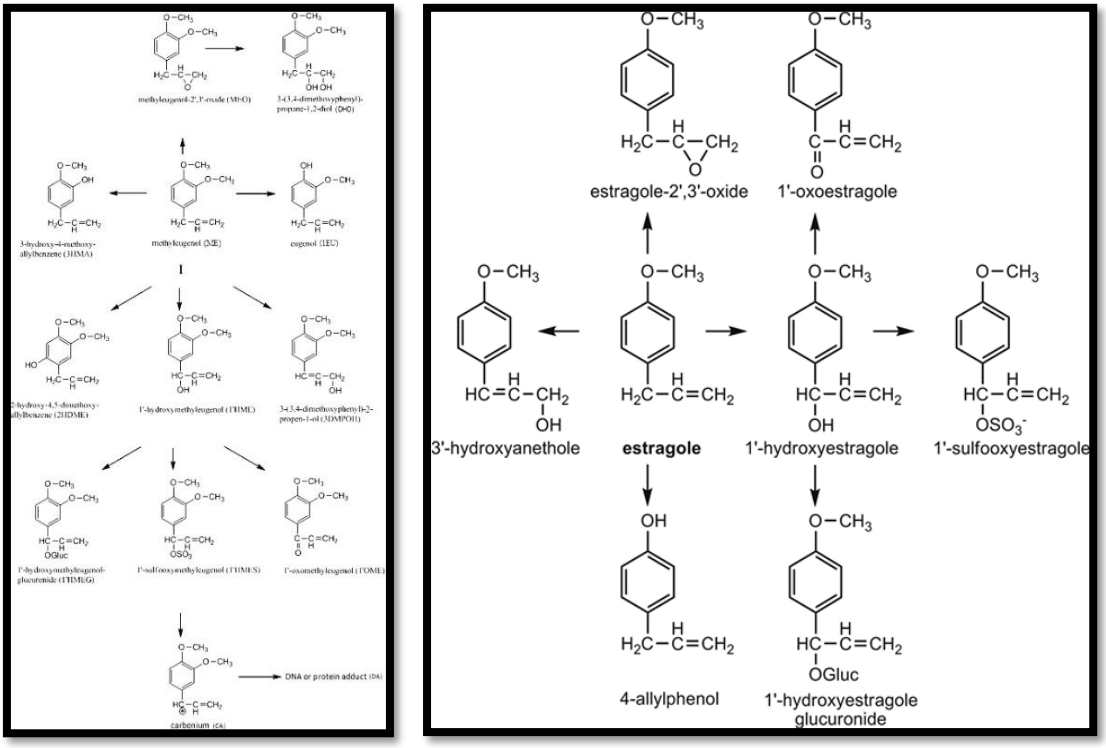

Figure IV1. Proposed metabolic pathways of the alkenylbenzene methyleugenol, taken from Al-Subeihi et al., (2012), and estragole, Punt et al (2009). The two chemicals show same mode of action in metabolism, the difference can be the amount formed of each metabolite

Since similar MOA action and similar in structure the estragole code was applied for methyleugenol.

The PBK Model structure reported in figure IV2 is built by separating in different compartments liver, lung and kidney and lumping remaining organs as either rapidly/richly perfused or slowly/poorly perfused. This division was done in accordance with the capacity of the organ to form metabolites of the parent chemical under investigation and based on the mode of action of the chemicals.

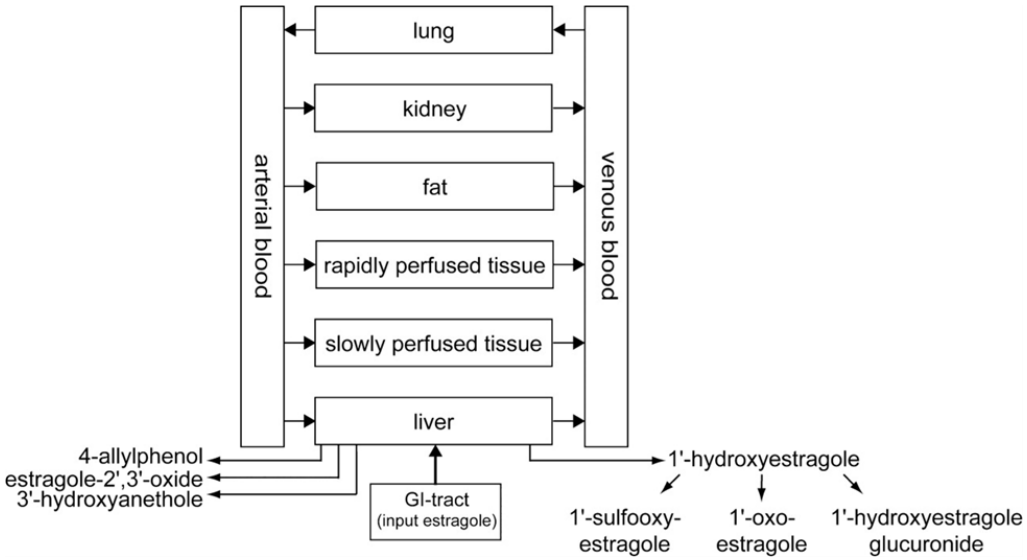

Fig. IV2. Human PBK model structure used to describe mathematically the chemical's (estragole's) fate in the body, taken from Punt et al., 2009.

The PBK model for methyleugenol was based on the proposed biotransformation pathways of estragole as shown in figure IV1. The difference in metabolism between estragole and methyleugenol is that methyleugenol has an additional two metabolites formed, 3-(3,4 – dimethoxyphenyl)-2-propen-1-ol (3-DMPOH) and 2-hydroxy-4,5-dimethoxyallylbenzene (2HDME), that do not appear in estragole pathway so far published in the literature. However, the main pathway leading to adverse outcome, DNA adduct binding, is via hydroxylation, this path is similar path for both chemicals. Using the human PBK models for estragole, a comparison could be made between the model predictions of formation of the 1'-hydroxy metabolite (figure IV1). However, for phase II metabolite formation, both the 1′-sulfoxy metabolite and glucuronide gave the predictions where different using this approach versus the original methyleugenol model.

A summary list of assumptions on the PBK model are reported:

1. First-order kinetics was used to describe the uptake of methyleugenol from the gastrointestinal (GI) tract assuming a direct uptake by the liver with an absorption rate constant (k a) of 1.0 h−1, which is based on the fast and complete absorption of the structurally related alkenylbenzene estragole from the GI tract.
2. Liver was found to be the only target organ for metabolism of estragole and methyleugenol, however, the lack of metabolism in other organs could also be due to low sensitivity of analytics.
3. Because of similar structure and similar MoA to other alkenylbenzenes a read across approach could be applied. However, estragole lacks two metabolites that methyleugenol forms, this could also be due to low sensitivity of analytics.
4. Metabolism plays a crucial role; it is known that the toxic MoA of these chemicals is driven by the hydrolysis pathway with formation of the 1'-hydroxy-metabolite. Here the PBK models for the parent compounds are compared, however toxicity is driven by their metabolites. All alkenyl benzene chemicals will react through the same metabolic pathways, but probably with different rate of formation, via Phase I CYPs and Phase II enzymes.

Step 3 – Model parameterisation (parameter estimation and analysis)

Physiological parameterisation of the PBK model Table IV1. Reports the physiological parameters used in the PBK model (see section i).

Table IV2 reports the physicochemical and kinetic parameters used in the PBK model.

In vitro parameterisation of the PBK model for methyleugenol (Al-Subeihi et al., 2012) these parameters were established by

- Microsomal metabolism of methyleugenol using mixed pooled human S9 fraction.
- Glucuronidation of 1′-hydroxy methyleugenol to 1′-hydroxy methyleugenol glucuronide.
- Oxidation of 1′-hydroxymethyleugenol to 1′-oxo methyleugenol.
- Sulfonation of 1′-hydroxy methyleugenol to 1′-sulfoxy methyleugenol using Paps as a cofactor and GSH as scavenger due to instability of the 1′-sulfoxymetabolite in an aqueous environment.
- Identification and quantification of metabolism of methyleugenol and 1′-hydroxy methyleugenol by UPLC.
- Determination of kinetic constants
- Parameters used in the PBK model for methyleugenol in human
- Physicochemical proprieties, online, Chemspider or EPA Chemistry Dashboard.
- Physiological parameters (Brown et al. 1997)
- Tissue: blood partition coefficients (DeJongh et al.1997) based on Log *K* ow values for methyleugenol and 1′-hydroxy methyleugenol

Step 4 – Computer implementation (solving the equations)

The equations were coded and numerically integrated in Berkeley Madonna 8.3.18 (Macey and Oster, UC Berkeley, CA) using Rosenbrock's algorithm for stiff systems. PBK models in human liver were run for 72h, because that would be the time for total clearance of methyleugenol in human tissues after one dose.

The code was run using Berkeley Madonna version 8.3.23.0, on august 2018 (the code is available at the end of this document).

The Code of the model is reported in the appendix of this template.

Step 5 – Model Performance

Model performance was assessed by checking the estragole PBK model:

1. The mass balance equation was used to evaluate the model description/stability.
2. A local sensitivity analysis was performed (figure IV3), normalized sensitivity coefficients (SCs) were determined using the following equation:

$$SC = (C' - C)/(P' - P) \times (P/C)$$

where C is the initial value of the model output, C′ is the modified value of the model output resulting from an increase in parameter value, P is the initial parameter value, and P′ represents the modified parameter value. An increase of 5 % in parameter values was used to analyze the effect of a change in parameter on the formation of 1′-hydroxy metabolite and 1′-sulfoxymetabolite (expressed as a percentage of the dose). Each parameter was analyzed individually, while the other parameters were kept at their initial value.

Comparison was made of the PBK model-based prediction of bioactivation of methyleugenol to the PBK model-based predictions for bioactivation of the structurally related compound estragole.

3. The human PBK model was validate by comparing historical data available for excretion of the glucuronidation in humans. In addition the model was also compared to the rodent PBK model that was validated using *in vivo* data.

We believe that once the PBK model for estragole passed the model performance and gained confidence it can be applied in a read across manner to incorporate the data of methyleugenol.

Step 6 – Model Documentation

The following models were previously published in peer review journals (Punt, A. et al., 2009. Al-Subeihi et al., 2011. The read across approach described within this case study will be published soon (Paini et al., in preparation).

E. Identification of uncertainties

The methyleugenol predictions were run using a "valid" PBK model built for estragole, results were compared to the estragole outcomes, but also compared to the "valid" methyleugenol model (Al-Subeihi et al., 2011).

Model structure

The structure of the PBK model was simplified to capture the only organs and metabolic pathways that were relevant for the source chemical estragole. The authors report that only the liver, and to a minor capacity also lungs and kidney, showed a significant metabolic rate of exchange compared to the other organs, metabolism in kidney was neglected. The PBK Model structure reported in figure IV2 is built by separating in different compartments liver, lung and kidney and lumping up in rapidly/richly perfused and slowly perfused the remaining organs. This division was done in accordance of their –organ- capacity in metabolising – biotransformation of the parent/chemicals understudy and based on the mode of action of the chemicals.

Input parameters

1. Although a well-established protocol to assess the formation of metabolite(s), the application of mixed gender human pooled S9 could be restricted to a few donors and therefore not be reflective of the overall variability in the population; variability in metabolic pathways may be much greater with more donors.

2. The in vitro V_{max} and K_m can carry additional uncertainty based on human variability (in ADME or metabolism) (although pooled batches are often used) and differences in sample preparation and sensitivity in the analytical (method) to measure the samples, in also quantification of concentrations of the chemical and its metabolite(s).
3. Sensitivity analysis (OAT) was conducted on the estragole PBK model, to identify the most sensitive parameters, which were identified as the V_{max} and K_m Kinetic constant. Figure IV3.

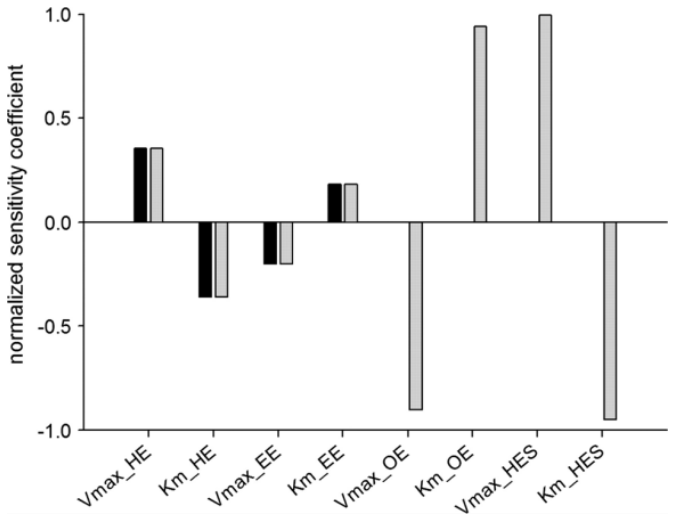

Figure IV3. Sensitivity of the predicted formation of 1′-hydroxymetabolite (black bars) and 1′-sulfooxymetabolite (gray bars) to different model parameters. The V_{max} and K_m correspond to the maximum rate of formation and the Michaelis-Menten constant for the formation of the different metabolites in the liver for estragole: 1′-hydroxyestragole (HE), estragole-2′,3′-oxide (EE), 1′-oxoestragole (OE) and 1′-sulfooxyestragole (HES), taken from Punt et al., 2009 .

Model output

Uncertainties in output: Variability in model output (over prediction and under prediction, depending on the metabolite) between using the read-across model versus the original model. Due to model input data and model structure. Sensitivity analysis was conducted on the estragole PBK model, to identify the most sensitive parameters, which were identified as the V_{max} and K_m constant for the formation of the different metabolites in the liver: 1′-hydroxyestragole (HE), and 1′-sulfooxyestragole (HES). A change in this value can lead to a change in model output.

Other uncertainties (e.g. model developed for different substance and/or purpose)

Other uncertainties: Although in this example we used two chemicals for which we had a valid PBK model, still some uncertainties can be found in the process proposed.

Overall evaluation of uncertainties: On the basis of the results available it was concluded that the using data and available model code from one chemical (source) to read across to the target is a reasonable approach for a preliminary risk assessment, where *in vivo* data are

not available. Furthermore, the application of a PBK model that takes into account the kinetics of the chemical understudy reduces the uncertainties of A, D, M, and E.

F. Model implementation details

- software (version no): The code was run using Berkeley Madonna version 8.3.23.0, on August 2018 (the code is available at the end of this document).
- availability of code: Yes, reported below in appendix.
- software verification / qualification : was done by peer reviewed publication.

G. Peer engagement (input/review)

Was not performed but the model was published in peer reviewed journals, see reference list

H. Parameter tables

Table IV1. Reports the physiological parameters used in the PBK model.

Parameter name	Value	Unit
Body weight	60	Kg
Cardiac output	15	(L/hr-1kg)
Fractional blood flow to fat - QFC	0.052	
Fractional blood flow to liver -QLC	0.227	
Fractional blood flow to richly perfused tissues QRC	0.70-QLC	
Fractional blood flow to slowly perfused tissues - QSC	0.30-QFC	
Fraction fat tissue VFC	0.214	
Fraction of liver - VLC	0.026	
Fraction richly perfused tissue - VRC	0.076-VLC	
Fraction slowly perfused tissue - VSC	0.81-VFC-VBC	
Fraction of blood Quick and Shuler 1999	VBC = 0.079	

Table IV2. Reports the physicochemical and kinetic parameters used in the PBK model.

	MW/ Hydroxyl metabolite MW	V_{max}/K_m	PC
Estragole source Punt et al., (2009; 2016)	148.2/164.2	{Phase I} V_{max}LHEc = 0.7; HE = 1'-hydroxyestragole, Max rate of metabolism (nmol min-1(mg protein)-1) V_{max}LAPc = 0.4; AP = 4-allylphenol, V_{max}LEEc = 0.9; EE = estragole-2',3'-oxide, V_{max}LHAc = 1.4; HA = 3'-hydroxyanethole, K_mLHE = 21;Affinity constant (umol/L) K_mLAP = 290 K_mLEE = 83 K_mLHA = 350 {Phase II} V_{max}LHEGc = 0.29; HEG = 1'-hydroxyestragoleglucuronide, Max rate of metabolism (nmol min-1(mg protein)-1)	PFE = 105; Fat/blood partition coefficient PRE = 6.5;Richly perfused tissues/blood partition coefficient PSE = 4.0;Slowly perfused tissues/blood partition coefficient PLE = 6.5;Liver/blood partition coefficient {1'-hydroxy-met} PLHE = 1.6; Liver/blood partition coefficient

		V_{max}LHESc = 0.0074; AHE = 1'-sulfooxyestragole, V_{max}LOEc = 5 K_mLHEG = 708; Affinity constant (umol/L) K_mLHES = 727 K_mLOE = 345	
Methyleugenol target (Al-Subeihi et al., 2012)	178.2/194.2	{Phase I} V_{max}LHEc = 1.38; HE = 1'-hydroxyestragole, Max rate of metabolism (nmol min-1(mg protein)-1) V_{max}LAPc = 0.15; AP = 4-allylphenol, V_{max}LEEc = 0.66; EE = estragole-2',3'-oxide, V_{max}LHAc = 0.39; HA = 3'-hydroxyanethole, K_mLHE = 404;Affinity constant (umol/L) K_mLAP = 13.6 K_mLEE = 23.7 K_mLHA =161 {Phase II} V_{max}LHEGc = 0.66; HEG = 1'-hydroxyestragoleglucuronide, Max rate of metabolism (nmol min-1(mg protein)-1) V_{max}LHESc = 0.0009; AHE = 1'-sulfooxyestragole, V_{max}LOEc = 2.1 K_mLHEG = 2393; affinity constant (umol/L) K_mLHES = 139 K_mLOE = 1774	PFE = 103; Fat/blood partition coefficient PRE =6.2;Richly perfused tissues/blood partition coefficient PSE = 3.9;Slowly perfused tissues/blood partition coefficient PLE = 6.2;Liver/blood partition coefficient {1'-hydroxy-met} PLHE = 1.4; Liver/blood partition coefficient

Strategy for reducing overall uncertainty (excluding generation of data based on new animal test)

Generate data using volunteer human subjects.

Application of methyleugenol *in vitro* metabolic parameters

To make the read-across approach more robust - apply the approach using more analogues, which have valid model codes and check the results.

Based on the local sensitivity analysis performed V_{max} and K_m were the parameters identified that could influence the model output most significantly. The following table shows the uncertainty/variability of the parameter estimates.

		Variability/Uncertainty in the Parameter Estimates		
		High	Medium	Low
SENSITIVITY	High	Variability in V_{max} and K_m from *in vitro* studies from different donors or pooled		
	Medium		Analytics - Measurement of V_{max} and K_m	
	Low			Extrapolation from *in vitro* to *in vivo* of V_{max} and K_m

		Variability/Uncertainty in the Parameter Estimates		
		High	Medium	Low
SENSITIVITY	High			
	Medium			
	Low			PC and Physic chemical proprieties from literature and QSARs

In conclusion the present study provides an example of PBK model evaluation using (structural) analogues of a chemical under assessment with no *in vivo* data available for the target chemical.

On the basis of the results available, it was concluded that using data from one chemical source (estragole) for read across to methyleugenol is a reasonable approach for a preliminary hazard characterisation, in the absence of *in vivo* data available to fully validate a methyleugenol model. Furthermore, the application of a PBK model that takes into account the kinetics of the chemical understudy reduces the uncertainties of A, D, M, and E.

I. References and background information

Punt, A. Paini, A., Boersma, M.G Freidig, A.P. Delatour T., Scholz G., Schilter B., van Bladeren P.J., Rietjens I.M.C.M.(2009) Use of physiologically based biokinetic (PBBK)

modeling to study estragole bioactivation and detoxification in humans as compared to male rats Toxicological Sciences, 110 (2009), pp. 255-269

Al-Subeihi, A.A Spenkelink, B. Rachmawati N., Boersma M.G, Punt A., Vervoort J., van Bladeren P. J., Rietjens I. M.C.M., (2011) Physiologically based biokinetic model of bioactivation and detoxification of the alkenylbenzene methyleugenol in rat, Toxicology in Vitro, Volume 25, Issue 1, 2011, Pages 267-285.

PBK model code

Estragole PBK model code written in Berkeley Madonna (Punt et al., 2009 and 2016)

{Punt et al., 2009; Physiological Parameters: Krishnan and Andersen, 2001; Brown et al., 1997}

QCC = 15;	Cardiac output (L/hr-1kg)
QFC = 0.052;	Fractional blood flow to fat
QLC = 0.227;	Fractional blood flow to liver
QRC = 0.70-QLC;	Fractional blood flow to richly perfused tissues
QSC = 0.30-QFC;	Fractional blood flow to slowly perfused tissues
	;Total fractions is 1
BW = 60;	Body weight, kg
VFC = 0.214;	Fraction fat tissue
VLC = 0.026;	Fraction of liver
VRC = 0.076-VLC;	Fraction richly perfused tissue
VSC = 0.81-VFC-VBC;	Fraction slowly perfused tissue
	;Total fractions tissues is 0.91

VBC = 0.079; Fraction of blood Quick and Shuler 1999 (13.2 mL min-1 k.o.m. 0.06) Fraction of blood (zie TCDD model cursus)

{Partition Coefficients: DeJongh et al., 1997}

{Estragole}

PFE = 105; Fat/blood partition coefficient

PRE = 6.5; Richly perfused tissues/blood partition coefficient

PSE = 4.0; Slowly perfused tissues/blood partition coefficient

PLE = 6.5; Liver/blood partition coefficient

{1'-hydroxyestragole}

PLHE = 1.6; Liver/blood partition coefficient

{Biochemical parameters} {Metabolism Liver} {Phase I}

VmaxLHEc = 0.7; HE = 1'-hydroxyestragole, Max rate of metabolism (nmol min-1(mg protein)-1)

VmaxLAPc = 0.4; AP = 4-allylphenol, Max rate of metabolism (nmol min-1(mg protein)-1)

VmaxLEEc = 0.9; EE = estragole-2',3'-oxide, Max rate of metabolism (nmol min-1(mg protein)-1)

VmaxLHAc = 1.4; HA = 3'-hydroxyanethole, Max rate of metabolism (nmol min-1(mg protein)-1)

KmLHE = 21; Affinity constant (umol/L)

KmLAP = 290

KmLEE = 83

KmLHA = 350

{Phase II}

VmaxLHEGc = 0.29; HEG = 1'-hydroxyestragoleglucuronide, Max rate of metabolism (nmol min-1(mg protein)-1)

VmaxLHESc = 0.0074;AHE = 1'-sulfooxyestragole, Max rate of metabolism (nmol min-1(mg protein)-1)

VmaxLOEc = 5

KmLHEG = 708; Affinity constant (umol/L)

KmLHES = 727

KmLOE = 345

{Linear uptake rate constant}

Ka = 1; hr-1

{Experimental Parameters/Conditions}

{Molecular weight}

MWE = 148.2; Molecular weight estragole

MWHE=164.2; Molecular weight 1'-hydroxyestragole

{Given dose (mg/ kg bw) and oral dose umol/ kg bw}

GDOSE = 0.07 {mg/ kg bw}

ODOSE = GDOSE*1E-3/MWE*1E6 {umol/ kg bw}

{Time}

Starttime = 0; in hrs

Stoptime = 24; in hrs

{Calculated parameters}

{Blood flow}

QC = QCc*BW**0.74; Cardiac output - L/hr

QF = QFC*QC; Fat blood flow - L/hr

QR = QRC*QC; Richly perfused tissue blood flow - L/hr

```
        QS = QSC*QC;                    Slowly perfused tissue blood flow - L/hr
        QL = QLC*QC;                    Liver blood flow - L/hr
 {Tissue volume}
 VF = VFC*BW;                   Volume of fat - L
        VR = VRC*BW;            Volume of richly perfused tissues - L
        VS = VSC*BW;            Volume of slowly perfused tissues - L
        VL = VLC*BW;                    Volume of liver - L
        VB = VBC*BW;                    Volume of blood-L
{Metabolism liver}
 {Scaling factors}
 S9PL=143;      Liver S9 protein yield (mg/gram liver) Pang et al.1985
 MPL=35;        Liver microsomal protein yield (mg/gram liver) Atio et al. 1976
 L=VLC*1000;  Liver = 34 (gram/kg BW)
  {Phase I}
 VMaxLHE = VMaxLHEC/1000*60*MPL*L*BW;       Max rate of metabolism
(umol/hr)
 VMaxLAP = VMaxLAPC/1000*60*MPL*L*BW
 VMaxLEE = VMaxLEEC/1000*60*MPL*L*BW
 VMaxLHA = VMaxLHAC/1000*60*MPL*L*BW
  {Phase II}
 VMaxLHEG = VMaxLHEGC/1000*60*MPL*L*BW
 VMaxLHES = VMaxLHESC/1000*60*S9PL*L*BW
 VMaxLOE = VMaxLOEC/1000*60*MPL*L*BW
 {Dose in umol}
 DOSE=ODOSE*BW;             umol
{Equations}
{MR = Amount Estragole remaining in stomach, umol}
MR' =-Ka*MR
Init MR = DOSE
{AO = Amount Estragole entering the body, umol}
AO' = Ka*MR
Init AO = 0
{AF = Amount estragole in fat tissue, umol}
     AF' = QF*(CA-CVF)
```

```
    Init AF = 0
    CF = AF/VF
    CVF = CF/PFE
{AR = Amount Estragole in richly perfused tissue, umol}
    AR' = QR*(CA-CVR)
    Init AR = 0
    CR = AR/VR
    CVR = CR/PRE
{AS = Amount Estragole in slowly perfused tissue, umol}
    AS' = QS*(CA-CVS)
    Init AS = 0
    CS = AS/VS
    CVS = CS/PSE
{AL = Amount Estragole in liver tissue, umol}
    AL' = AO' + QL*(CA -CVL) - AMLEE' - AMLHE' - AMLAP' - AMLHA'
    Init AL = 0
    CL = AL/VL
    CVL = CL/PLE
{AMLEE=Amount estragole metabolized in liver to epoxide metabolite (EE)}
                AMLEE' = VmaxLEE*CVL/(KmLEE + CVL)
                init AMLEE = 0
{AMLHE = Amount Estragole metabolized in liver to 1'-hydroxyestragole (HE)}
                AMLHE' = VmaxLHE*CVL/(KmLHE + CVL)
                init AMLHE = 0
        CMLHE= AMLHE/VL
{AMLAP = Amount Estragole metabolized in liver to 4-allyphenol (AP)}
                AMLAP' = VmaxLAP*CVL/(KmLAP + CVL)
                init AMLAP = 0
{AMLHA = Amount Estragole metabolized in liver to 3'-hydroxyanethole (HA)}
                AMLHA' = VmaxLHA*CVL/(KmLHA + CVL)
                init AMLHA = 0
{CV = Concentration venous blood estragole (umol/L)}
    AB' = (QF*CVF + QR*CVR + QS*CVS + QL*CVL  - QC*CA)
    Init AB = 0
```

```
    CA = AB/VB
{1'OHestragole submodel}
{ALHE=Amount 1'-Hydroxyestragole in liver tissue, mg}
    ALHE' =  AMLHE' - AMHEG' - AMHES'  - AMOE'
    Init ALHE = 0
    CLHE=ALHE/VL
    CVLHE =CLHE/PLHE
  {AMHEG= Amount 1'-hydroxyestragole conjugated with glucuronic acid, umol}
                AMHEG'=VmaxLHEG*CVLHE/(KmLHEG + CVLHE)
                init AMHEG = 0
        CLHEG = AMHEG/VL
        {AMHES= Amount 1'-hydroxyestragole conjugated with sulfate}
                AMHES'=VmaxLHES*CVLHE/(KmLHES + CVLHE)
                init AMHES = 0
        CLHES=AMHES/VL
{AMOE= Amount 1'-hydroxyestragole oxidated to 1'-oxoestragole, umol}
                AMOE'=VmaxLOE*CVLHE/(KmLOE + CVLHE)
                init AMOE = 0
        CLOE = AMOE/VL
{Mass Balance}
Total = DOSE
Calculated = AF + AS + AR+ AL+ MR + AMLEE + AMLHA+ AMLHE + AMLAP  +
AB
ERROR=((Total-Calculated)/Total+1E-30)*100
MASSBBAL=Total-Calculated + 1
PercAP= AMLAP*100/DOSE
PercEE= AMLEE*100/DOSE
PercHE= AMLHE*100/DOSE
PercHA= AMLHA*100/DOSE

PercHEG= AMHEG*100/DOSE
PercHES= AMHES*100/DOSE
PercOE= AMOE*100/DOSE
```

Part II Checklist for model evaluation

PBK Model Evaluation Checklist	Checklist assessment	Comments
Name of the PBK model (as in the reporting template)	PBK model predictions using data from analogues	
Model developer and contact details	Alicia Paini (1), Sunil Kulkarni (2), Judith Madden (3), and Andrew Worth(1) 1) EC Joint Research Centre; 2) Health Canada; 3) Liverpool John Moore University	
Name of person reviewing and contact details	**L. Rossi**	
Date of checklist assessment	**04/04/2020**	
A. Context/Implementation		
A.1. Regulatory Purpose		
1. What is the acceptable degree of confidence/uncertainty (e.g. high, medium or low) for the envisaged application (e.g. priority setting, screening, full assessment?)	**High**	
2. Is the degree of confidence/uncertainty in application of the PBK model for the envisaged purpose greater or less than that for other assessment options (e.g. reliance on PBK model and *in vitro* data vs. no experimental data)?	**High**	
A.2. Documentation		
3. Is the model documentation adequate, i.e. does it address the essential content of model reporting template, including the following:	**Yes**	
• Clear indication of the chemical, or chemicals, to which the model is applicable?	**Yes**	
• Is the model being applied for the same scientific purpose as it was developed, or has it been repurposed somehow?	**Yes**	
• Model assumptions?	**Yes**	
• Graphical representation of the proposed mode of action, if known?	**Yes**	
• Graphical representation of the conceptual model?	**Yes**	
• Supporting tabulation for parameters (names, meanings, values, mean and standard deviations, units and sources)?	**Yes**	
• Relevance and reliability of model parameters?	**No**	
• Uncertainty and sensitivity analysis?	**Yes**	
• Mathematical equations?	**No**	
• PBK model code?	**Yes**	
• Software algorithm to run the PBK model code?	**Yes**	
• Qualification of PBK software platform?	**No**	

A.3 Software Implementation and Verification		
4. Does the model code express the mathematical model?	**-**	**We do not have the two so we cannot asses, but the code represents the chemical MoA**
5. Is the model code devoid of syntactic and mathematical errors?	**Yes**	
6. Are the units of input and output parameters correct?	**Yes**	
7. Is the chemical mass balance respected at all times?	**Yes**	
8. Is the cardiac output equal to the sum of blood flow rates to the tissue compartments?	**Yes**	
9. Is the sum total of tissue volumes equal to total body volume?	**No**	**Equals to 0.91**
10. Is the mathematical solver a well-established algorithm?	**Yes**	
11. Does the mathematical solver converge on a solution without numerical error?	**Yes**	
12. Has the PBK modelling platform been subjected to a verification process (for a different use, for instance, in the pharmaceutical domain)?	**No**	
A.4 Peer engagement (input/review)		
13. Has the model been used previously for a regulatory purpose?	**No**	
• Is prior peer engagement in the development and review of the model sufficient to support the envisaged application?	**-**	
• Is additional review required? Peer engagement includes input/review by experts on specific aspects of model development, individual reviews of the model by experts, or collective reviews by peer review panels. Availability of the comments and tracking of revisions to the model in response to peer input contributes to increased confidence in the model for potential application.	**No**	
B. Assessment of Model Validity		
B.1 Biological Basis (Model Structure and Parameters)		
14. Is the model consistent with known biology?	**Yes**	
• Is the biological basis for the model structure provided?	**Yes**	
• Is the complexity of the model structure appropriate to address the regulatory application?	**Yes**	
• Are assumptions concerning the model structure and parameters clearly stated and justified?	**Yes**	
• Is the choice of values for physiological parameters justified?	**Yes**	
• Is the choice of methods used to estimate chemical-specific ADME parameters justified?	**Yes**	

• Saturable kinetics	**Yes**	**By means of K_m and V_{max}**
B.2 Theoretical Basis of Model Equations		
15. Are the underlying equations based on established theories, .e.g. Michaelis-Menten kinetics, Fick's laws of diffusion?	**Yes**	
• In the case of PBK models for particles, does the model take into consideration the properties of particles, e.g. particle size ranges, (poor) solubility, aggregation, partitioning and diffusion/sedimentation behaviour?	**NA**	
B.3. Reliability of input parameters		
16. Has the uncertainty (individual variability, experimental reproducibility and reliability) in the input parameters been characterised?	**Partially**	**In the measured one yes**
B.4. Uncertainty and Sensitivity Analysis		
17. Has the impact of uncertainty (individual variability, experimental reproducibility and reliability) in the parameters on the chosen dose metric been estimated?	**Yes bySA**	
• Local sensitivity analysis?	**Yes**	
• Global sensitivity analysis?	**No**	
18. Is confidence in influential input parameter estimates (i.e., based on comparison of uncertainty and sensitivity) reasonable (within expected values; similar to those of analogues) in view of the intended application?	**Yes**	
B.5. Goodness-of-Fit and Predictivity		
19. For PBK models for which there are sufficient *in vivo* data for the chemical of interest:		
• Suitability as analogue (chemical and biological similarity) been assessed?	**Yes**	
• Reliable estimation of chosen dose metric for analogue?	**Yes**	
• In general is the biological Variability of *in vivo* reference data (from analogue) established?	**Yes**	

Part III Overall Evaluation

Overall conclusion on mode evaluation for the intended application

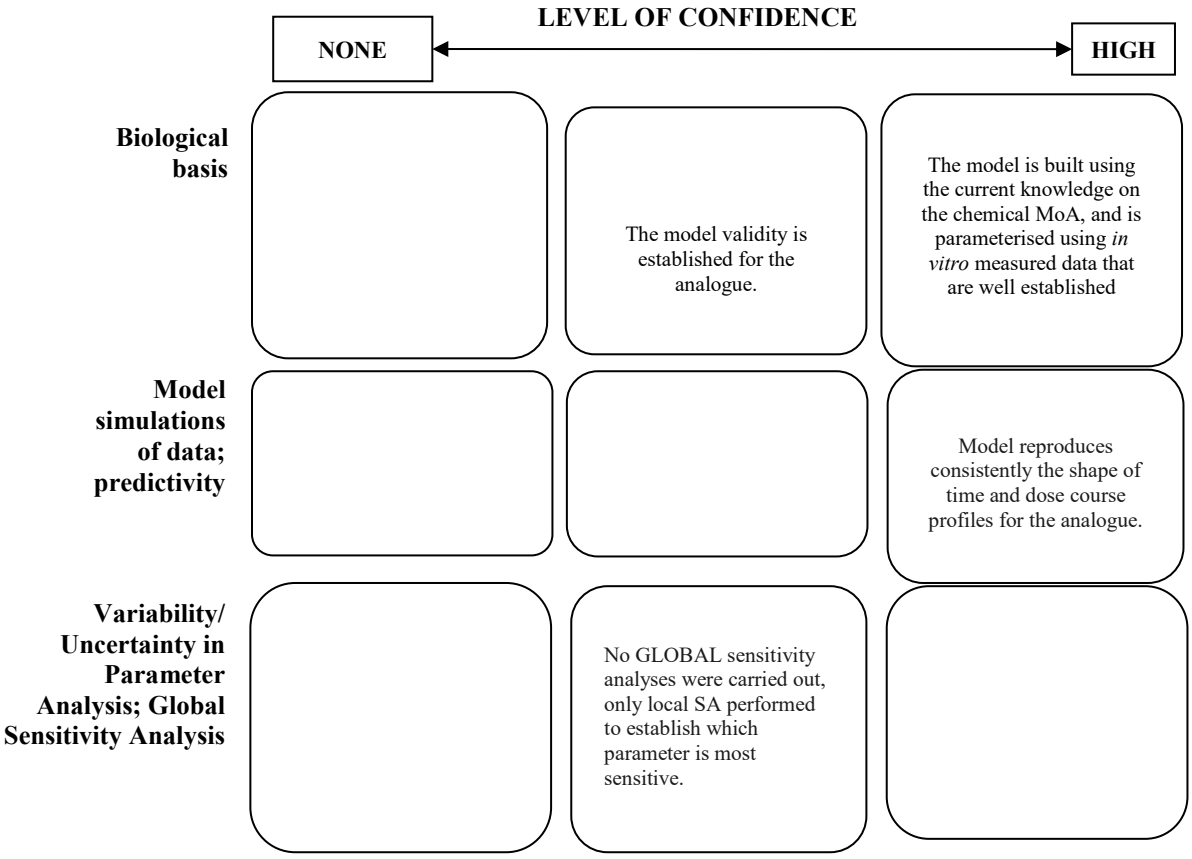

The model is built using the current knowledge on the source chemical MoA (estragole), and is parametrise using *in vitro* metabolic measured data (for the target methyleugenol) using well established assays. The PBK model reproduces consistently the shape of time and dose course profiles for the analogue. The PBK model validity is established for source chemical, thus we assume that the PBK model is valid also for the target chemicals (methyleugenol).

Recommendation is to gain more confidence in dose metric prediction probably a GSA should have been performed. However, by running an OAT SA we identified the key parameter that can perturb the model output most significantly.

Case Study V

Physiologically based pharmacokinetic (PBK) model for acrylonitrile in humans

Part I. PBK model reporting template

A. Name of model

Blood concentrations of acrylonitrile in humans after oral administration extrapolated from *in vivo* rat pharmacokinetics, *in vitro* human metabolism, and physiologically based pharmacokinetic modelling.

B. Contact details

Authors: Ryohji Takano, Norie Murayama, Kana Horiuchi, Masato Kitajima, Masatoshi Kumamoto, Fumiaki Shono, Hiroshi Yamazaki*

Affiliation: *Laboratory of Drug Metabolism and Pharmacokinetics, Showa Pharmaceutical University, Machida, Tokyo 194-8543, Japan

C. Summary of model characterisation, development, validation, and regulatory applicability

The present study defined a simplified physiologically based pharmacokinetic (PBK) model for acrylonitrile in humans based on *in vitro* metabolic parameters determined using relevant liver microsomes, coefficients derived *in silico*, physiological parameters derived from the literature, and a prior previously developed PBK model in rats. The model basically consists of a chemical absorption compartment, a metabolizing compartment, and a central compartment for acrylonitrile. Evaluation of a previous rat model was performed by comparisons with experimental pharmacokinetic values from blood and urine obtained from rats *in vivo* after oral treatment with acrylonitrile (30 mg/kg, a no-observed-adverse-effect level) for 14 days. Elimination rates of acrylonitrile *in vitro* were established using data from rat liver microsomes and from pooled human liver microsomes. Acrylonitrile was expected to be absorbed and cleared rapidly from the body *in silico*, as was the case for rats confirmed experimentally *in vivo* with repeated low-dose treatments. These results indicate that the simplified PBK model for acrylonitrile is useful for a forward dosimetry approach in humans. This model may also be useful for simulating blood concentrations of other related compounds resulting from exposure to low chemical doses.

D. Model characterisation (modelling workflow)

Step 1 – Scope and purpose of the model (problem formulation)

Acrylonitrile is widely used, principally as a monomer in the industrial manufacture of synthetic polymers and as a precursor of acrylamide and acrylic acid. It has been recently reported that more than 20 studies examining mortality and/or cancer incidence rates among people who had been exposed to acrylonitrile do not collectively support a causal relationship between acrylonitrile exposure and cancers. The International Agency for Research on Cancer has concluded that there is inadequate evidence in humans for the carcinogenicity of acrylonitrile and downgraded its classification to a Class 2B carcinogen

(possibly carcinogenic); however, its primary metabolite, 2-cyanoethylene oxide, was supposed to be a reactive metabolite. Therefore, the purpose of this study was to carry out a forward dosimetry approach (shown in Figure V1) using data from chemical doses administered to animals and *in vitro* experiments with liver microsomes from humans and animals to predict acrylonitrile concentrations in humans. The adjusted animal biomonitoring equivalents after orally administered doses at a no-observed-adverse-effect level (NOAEL) in rat studies were scaled to human biomonitoring equivalents using known species allometric scaling factors and human metabolic data with a simple PBK model.

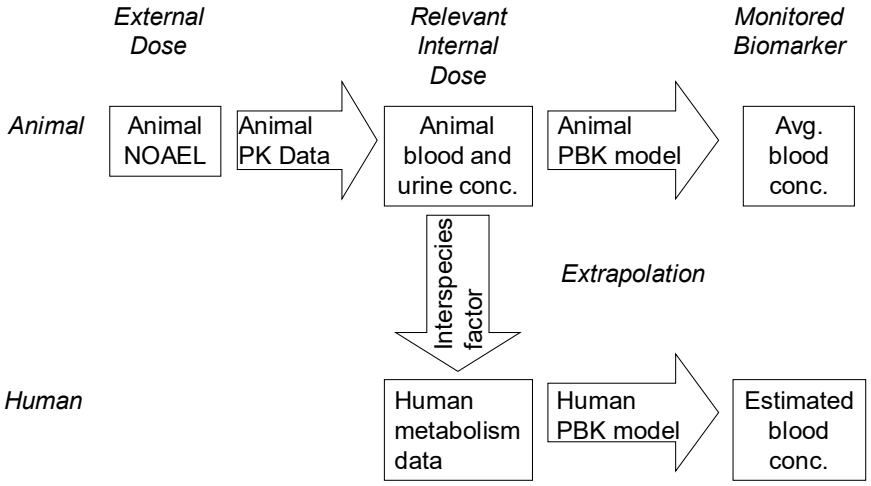

Figure V1. Approach for calculating blood-based biomonitoring equivalents for acrylonitrile. NOAEL, no-observed-adverse-effect level; PK, pharmacokinetics; PBK, physiologically based pharmacokinetic.

Step 2 – Model conceptualisation (model structure, mathematical representation)

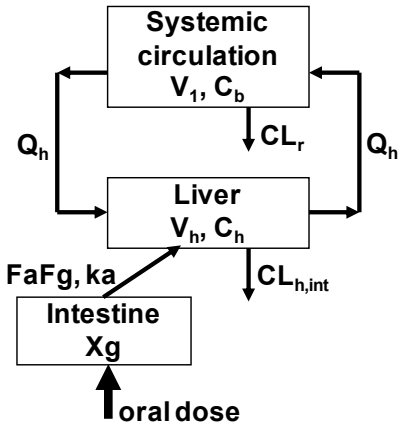

Figure V2. PBK model established in this study for rats and humans.

- The same values for the plasma unbound fraction, blood-to-plasma ratio, and liver-to-plasma ratio of the substrate were used for rats and humans by *in silico* estimation.

- Pooled liver microsomes from rats and humans are representative of liver cells given to interspecies factors.
- 70 kg male is representative of adult population

Step 3 – Model parameterisation (parameter estimation and analysis)

The simplified PBK models employed in the current study (Figure V1) consisted of a chemical receptor compartment, a metabolizing compartment, and a central compartment and were set up. Parameter values for the physicochemical properties of compounds ($f_{u,p}$, log$P$, $K_{p,h}$, and R_b) are shown in TableV1. Values of $f_{u,p}$ and log$P$ were obtained by *in silico* estimation using SimCYP and ChemDrawBioUltra software; the liver–plasma concentration ratio (Kp,h) and the ratio of the blood to plasma concentration (Rb) were calculated from its fu,p and logP values.

$$K_{p,h} = \frac{0.02289 \cdot P + 0.72621}{0.00396 \cdot P + 0.960581} \times \frac{1 + f_{\mathrm{u,p}}}{2}$$

$$\mathrm{R_b} = 0.45 \cdot \left(\mathrm{K_b} \cdot \mathrm{f_{u,p}} - 1\right) + 1 \text{ where } \log \mathrm{K_b} = 0.617 \cdot \log\left(\frac{1-\mathrm{f_{u,p}}}{\mathrm{f_{u,p}}}\right) + 0.208$$

where P is the water–octanol partition ratio and was estimated from the computer-calculated log P as neutral (clog P). A value of $\frac{1+f_{u,p}}{2}$ is corresponded to $f_{\mathrm{u,p}}$ over tissue fraction unbound. Accepted values for the physiological hepatic blood flow rates (Qh) in rats (0.853 L/h) and humans (96.6 L/h) were used.

Experimental plasma concentrations of acrylonitrile in rats were analyzed by WinNonlin software (Professional version 5.01) with a one-compartment model and yielded primary k_a, and k_{el} values as pharmacokinetic parameters (abbreviations used are also shown in Table V1). Values of total clearance (CL_{tot}), hepatic clearance (CL_h), hepatic intrinsic clearance ($CL_{h,int}$), and V_1 were also calculated. Subsequently, final parameter values for the rat PBK model were calculated using the initial values mentioned above by the user model in WinNonlin and are shown in Table V1.

To define a simplified PBK model for acrylonitrile in humans based on the rat PBK model, we used relevant liver microsomes and physiological parameters (CL_r, k_a, and V_1) derived from the literature and applied the systems approaches to fit them into the traditional parallelogram for risk assessment, as shown in Figure V1. Rodent k_a was multiplied by 0.744 to give the human k_a value. The human systemic circulation volume ($V_{1,human}$) was estimated using V_h and the blood volume (V_b), with $V_{h,human}$, $V_{b,rat}$, and $V_{b,human}$ values of 1.50, 0.0160, and 4.90 L, respectively:

$$V_{ss,human}(\mathrm{L}) = V_{ss,rodent}(\mathrm{L}) \cdot \frac{\mathrm{Body\ weight_{human}}}{\mathrm{Body\ weight_{rodent}}}$$

$$V_1 = (V_{ss} - V_b - V_h \cdot \frac{K_{p,h} \times F_h}{R_b}) / \frac{1+f_{u,p}}{2}$$

where V_{ss} is the volume of distribution, and F_h is the unmetabolized fraction in liver. The *in vivo* hepatic intrinsic clearance ($CL_{h,int}$) of acrylonitrile in humans was estimated by multiplying the calculated initial parameters for *in vitro* hepatic intrinsic clearance values in humans by the ratio of *in vivo* to *in vitro* hepatic intrinsic clearance in rats, as mentioned above for modeling in rats. The human renal clearance $CL_{,human}$ was estimated using the equation, where BW_{rodent} = 0.25 kg (rat) and BW_{human} = 70 kg:

$$\mathrm{CL_{r,human}} = \frac{\mathrm{CL_{r,rodent}}}{\mathrm{Body\ weight_{rodent}}^{\left(\frac{2}{3}\right)}} \cdot \mathrm{Body\ weight_{human}}^{\left(\frac{2}{3}\right)}$$

Then, the final parameters for the PBK model in humans were calculated using these initial values by the user model in WinNonlin and are shown in Table V2.

Step 4 – Computer implementation (solving the equations)

The following systems of differential equations were solved to conduct the modelling shown in Figure V1.

$$\frac{dX_g(t)}{dt} = -k_a \cdot X_g(t) \quad \frac{\mathrm{dX_g(t)}}{\mathrm{dt}} = -\mathrm{k_a} \cdot \mathrm{X_g(t)} \quad \text{when at } t = 0,\ X_g(0) = Fa \cdot\ Fg \cdot\ dose$$

$$V_h \frac{dV_h}{dt} = Q_h \cdot C_b - \frac{Q_h \cdot C_h \cdot R_b}{K_{p,h}} + k_a \cdot X_g - CL_{h,int} \cdot \frac{C_h}{K_{p,h}} \cdot f_{u,p}$$

$$V_1 \frac{dC_b}{dt} = -Q_h \cdot C_b + \frac{Q_h \cdot C_h \cdot R_b}{K_{p,h}} - CL_r \cdot C_b$$

where X_g is substance amount in gut, C_h is hepatic substance concentration, and C_b is blood substance concentration.

As was done for the rat model, systems of differential equations were solved to achieve concentrations in each compartment in humans.

Step 5 – Model Performance

Typical parameter values for acrylonitrile in rat PBK model, absorption rate constant, volume of systemic circulation, and hepatic intrinsic clearance, were determined within 30% standard deviations. To evaluate the predictive ability of the PBK model, the maximum plasma concentration (C_{max}) and area under the concentration versus time curve (AUC) values predicted by the PBK model after a virtual oral administration were within 2-fold errors of the corresponding values calculated using the one-compartment models.

Step 6 – Model Documentation

Information reported in the peer-reviewed publication in the references section.

E. Identification of uncertainties

Model structure

The model basically consists of a chemical absorption compartment, a metabolizing compartment, and a central compartment.

Input parameters

- Several physiological parameters of acrylonitrile were estimated using *in silico* tools.
- Metabolic clearance *in vitro* was based on data using pooled rat or human liver microsomal fractions to give to interspecies factors.
- Using the allometric scaling methods, a human PBK model for acrylonitrile was set up based on the PBK model for rats.

Model output

- Output in human PBK model for acrylonitrile was estimated values bases on PBK results in rats experimentally obtained.
- Elimination rates of acrylonitrile in vitro were established using data from rat liver microsomes and from pooled human liver microsomes for human PBK modeling.

Other uncertainties (e.g. model developed for different substance and/or purpose)

- Inter-individual variability was not taken into account.

F. Model implementation details

- software (version no), WinNonlin software (Professional version 5.01)
- availability of code, Not reported
- software verification / qualification, YES. Part of the Certara portfolio.

G. Peer engagement (input/review)

Not reported

H. Parameter tables

Table V1. Parameters used for the rat PBK model.

Parameter	Symbol	Value	Unit
Octanol–water partition coefficient	log *P*	0.850	–
Hepatic intrinsic clearance	$CL_{h,int}$	76.2	L/h
Liver–plasma concentration ratio	$K_{p,h}$	0.710	–
Renal clearance	CL_r	0.00204	L/h
Plasma unbound fraction	$f_{u,p}$	0.556	–
Ratio of the blood to plasma concentration	R_b	1.00	–
Volume of systemic circulation	V_1	1.87	L
Hepatic volume	V_h	0.00850	L
Hepatic blood flow rate of systemic circulation to the tissue compartment	Q_h	0.853	L/h
Absorption rate constant	k_a	3.32	h^{-1}
Fraction absorbed × intestinal availability	F_aF_g	1.00	–
Dose	Dose	7.50	mg

Table V2. Parameters used for the human PBK model.

Parameter	Symbol	Value	Unit
Hepatic intrinsic clearance	$CL_{h,int}$	18,600	L/h
Renal clearance	CL_r	0.0873	L/h
Volume of systemic circulation	V_1	524	L
Hepatic volume	V_h	1.50	L
Hepatic blood flow rate of systemic circulation to the tissue compartment	Q_h	96.6	L/h
Absorption rate constant	k_a	2.47	h^{-1}

Dose	Dose	2100	mg

Other chemical parameters are the same as those shown in Table V1 for the rat PBK model.

I. References and background information

Takano, R.; Murayama, N.; Horiuchi, K.; Kitajima, M.; Kumamoto, M.; Shono, F.; Yamazaki, H. Blood concentrations of acrylonitrile in humans after oral administration extrapolated from in vivo rat pharmacokinetics, in vitro human metabolism, and physiologically based pharmacokinetic modeling. *Regul. Toxicol. Pharmacol.* 2010, 58, 252-258. https://doi.org/10.1016/j.yrtph.2010.06.008

Links to other resources

Cases for similar human PBK modeling for general chemicals from the rat models are:

Takano, R.; Murayama, N.; Horiuchi, K.; Kitajima, M.; Shono, F.; Yamazaki, H. Blood concentrations of 1,4-dioxane in humans after oral administration extrapolated from in vivo rat pharmacokinetics, in vitro human metabolism, and physiologically based pharmacokinetic modeling. J. Health Sci. 2010, 56, 557-565.

Yamazaki, H.; Horiuchi, K.; Takano, R.; Nagano, T.; Shimizu, M.; Kitajima, M.; Murayama, N.; Shono, F. Human blood concentrations of cotinine, a biomonitoring marker for tobacco smoke, extrapolated from nicotine metabolism in rats and humans and physiologically based pharmacokinetic modeling. Int. J. Environ. Res. Public Health 2010, 7, 3406-3421.

Yamazaki, H.; Takano, R.; Horiuchi, K.; Shimizu, M.; Murayama, N.; Kitajima, M.; Shono, F. Human blood concentrations of dichlorodiphenyltrichloroethane (DDT) extrapolated from metabolism in rats and humans and physiologically based pharmacokinetic modeling. J. Health Sci. 2010, 56, 566-575.

Miura, T., Uehara, S., Nakazato, M., Kusama, T., Toda, A., Kamiya, Y., Murayama, N., Shimizu, M., Suemizu, H., and Yamazaki, H. Human plasma and liver concentrations of styrene estimated by combining a simple physiologically based pharmacokinetic model with rodent data. J. Toxicol. Sci. 2019, 44, 543-548.

Kamiya, Y.; Otsuka, S.; Miura, T.; Takaku, H.; Yamada, R.; Nakazato, M.; Nakamura, H.; Mizuno, S.; Shono, F.; Funatsu, K.; Yamazaki, H. Plasma and hepatic concentrations of chemicals after virtual oral administrations extrapolated using rat plasma data and simple physiologically based pharmacokinetic models, Chem.Res.Toxicol. 2019, 32, 211-218.

Kamiya, Y.; Otsuka, S.; Miura, T.; Yoshizawa, M.; Nakano, A.; Iwasaki, M.; Kobayashi, Y.; Shimizu, M.; Kitajima, M.: Shono, F.; Funatsu, K.; Yamazaki, H. Physiologically based pharmacokinetic models predicting renal and hepatic concentrations of industrial chemicals after vrtual oral doses in rats, Chem.Res.Toxicol. 2020, 33, 736-1751.

Part II Checklist for model evaluation

PBK Model Evaluation Checklist	Checklist assessment	Comments
Name of the PBK model (as in the reporting template)	**PBK model for acrylonitrile in humans**	
Model developer and contact details	**Authors**: Ryohji Takano, Norie Murayama, Kana Horiuchi, Masato Kitajima, Masatoshi Kumamoto, Fumiaki Shono, Hiroshi Yamazaki* **Affiliation:** *Laboratory of Drug Metabolism and Pharmacokinetics, Showa Pharmaceutical University, Machida, Tokyo 194-8543, Japan	
Name of person reviewing and contact details	**L. Rossi**	
Date of checklist assessment	**June 2020**	
A. Context/Implementation		
A.1. Regulatory Purpose		
1. What is the acceptable degree of confidence/uncertainty (e.g. high, medium or low) for the envisaged application (e.g. priority setting, screening, full assessment?)	**High**	
2. Is the degree of confidence/uncertainty in application of the PBK model for the envisaged purpose greater or less than that for other assessment options (e.g. reliance on PBK model and *in vitro* data vs. no experimental data)?	**High**	
A.2. Documentation		
3. Is the model documentation adequate, i.e. does it address the essential content of model reporting template, including the following:		
• Clear indication of the chemical, or chemicals, to which the model is applicable?	**Yes**	
• Is the model being applied for the same scientific purpose as it was developed, or has it been repurposed somehow?	**Yes**	
• Model assumptions?	**Yes**	
• Graphical representation of the proposed mode of action, if known?	**Yes**	
• Graphical representation of the conceptual model?	**Yes**	
• Supporting tabulation for parameters (names, meanings, values, mean and standard deviations, units and sources)?	**Yes**	
• Relevance and reliability of model parameters?	**Yes**	

• Uncertainty and sensitivity analysis?	**Yes**	
• Mathematical equations?	**Yes**	
• PBK model code?	**NO**	
• Software algorithm to run the PBK model code?	**Yes**	
• Qualification of PBK software platform?	**No**	
A.3 Software Implementation and Verification		
4. Does the model code express the mathematical model?	**-**	**code represents the chemical MoA**
5. Is the model code devoid of syntactic and mathematical errors?	**Yes**	
6. Are the units of input and output parameters correct?	**Yes**	
7. Is the chemical mass balance respected at all times?	**Yes**	
8. Is the cardiac output equal to the sum of blood flow rates to the tissue compartments?	**Yes**	
9. Is the sum total of tissue volumes equal to total body volume?	**No**	
10. Is the mathematical solver a well-established algorithm?	**Yes**	
11. Does the mathematical solver converge on a solution without numerical error?	**Yes**	
12. Has the PBK modelling platform been subjected to a verification process (for a different use, for instance, in the pharmaceutical domain)?	**No**	**Is part of the CERTARA well establish commercial PBK model platform**
A.4 Peer engagement (input/review)		
13. Has the model been used previously for a regulatory purpose?	**No**	
• Is prior peer engagement in the development and review of the model sufficient to support the envisaged application?	**-**	
• Is additional review required? • Peer engagement includes input/review by experts on specific aspects of model development, individual reviews of the model by experts, or collective reviews by peer review panels. Availability of the comments and tracking of revisions to the model in response to peer input contributes to increased confidence in the model for potential application.	**No**	
B. Assessment of Model Validity		
B.1 Biological Basis (Model Structure and Parameters)		
14. Is the model consistent with known biology?	**Yes**	
• Is the biological basis for the model structure provided?	**Yes**	
• Is the complexity of the model structure appropriate to address the regulatory application?	**Yes**	
• Are assumptions concerning the model structure and parameters clearly stated and justified?	**Yes**	

• Is the choice of values for physiological parameters justified?	**Yes**	
• Is the choice of methods used to estimate chemical-specific ADME parameters justified?	**Yes**	
• Saturable kinetics	**No**	
B.2 Theoretical Basis of Model Equations		
15. Are the underlying equations based on established theories, .e.g. Michaelis-Menten kinetics, Fick's laws of diffusion?	**Yes**	
• In the case of PBK models for particles, does the model take into consideration the properties of particles, e.g. particle size ranges, (poor) solubility, aggregation, partitioning and diffusion/sedimentation behaviour?	**NA**	
B.3. Reliability of input parameters		
16. Has the uncertainty (individual variability, experimental reproducibility and reliability) in the input parameters been characterised?	**Partially**	**In the measured one yes**
B.4. Uncertainty and Sensitivity Analysis		
17. Has the impact of uncertainty (individual variability, experimental reproducibility and reliability) in the parameters on the chosen dose metric been estimated?	**Yes**	
• Local sensitivity analysis?	**Yes**	
• Global sensitivity analysis?	**No**	
18. Is confidence in influential input parameter estimates (i.e., based on comparison of uncertainty and sensitivity) reasonable (within expected values; similar to those of analogues) in view of the intended application?	**Yes**	
B.5. Goodness-of-Fit and Predictivity		
19. For PBK models for which there are sufficient *in vivo* data for the chemical of interest:		
• Suitability as analogue (chemical and biological similarity) been assessed?	**Yes**	
• Reliable estimation of chosen dose metric for analogue?	**Yes**	
• In general is the biological Variability of *in vivo* reference data (from analogue) established?	**Yes**	

NA= not applicable, NR=not reported, NK=not known

Part III Overall Evaluation

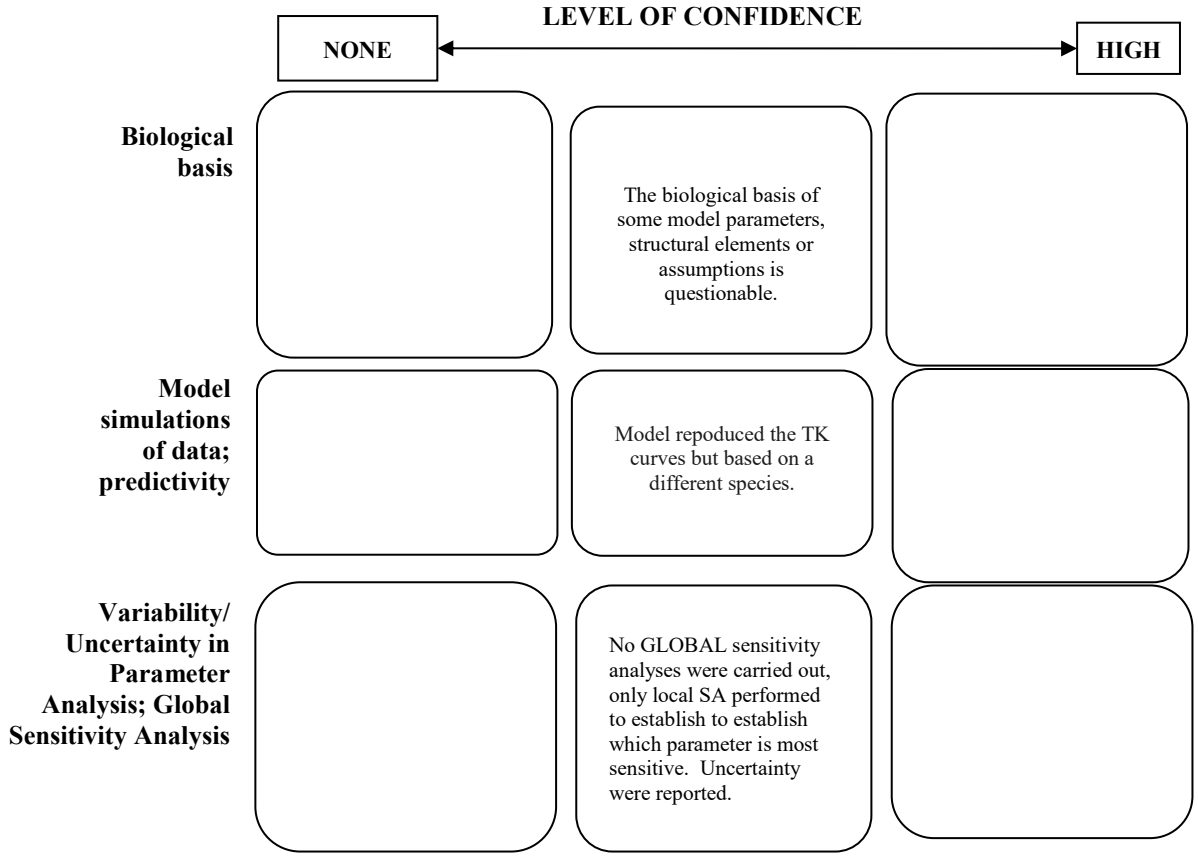

A simplified PBK model was developed for acrylonitrile for a forward dosimetry approach in humans based on rat tk data scaled to human. The discrepancy between the *in vitro* and *in vivo* measurements of the hepatic clearance in the rat remains to be clarified, as well as its justification cq. scaling, to humans. Assumptions are reported to underline the uncertainties. Based on all the evidence provided the following model will have a medium/standard level of confidence. The model code is not reported and a full assessment cannot be performed. It is therefore recommended that the PBK model and relative output be used in a regulatory framework only as information on the acrylonitrile.

Case Study VI

PBK model predictions for monoisononyl phthalate

Part I. PBK model reporting template

A. Name of model

Human urinary concentrations of monoisononyl phthalate estimated using physiologically based pharmacokinetic modeling and experimental pharmacokinetics in humanized-liver mice orally administered with diisononyl phthalate

B. Contact details

Authors: Tomonori Miura, Hiroshi Suemizu, Masatomo Goto, Norifumi Sakai, Hiroshi Iwata, Makiko Shimizu and Hiroshi Yamazaki*

Affiliation: *Laboratory of Drug Metabolism and Pharmacokinetics, Showa Pharmaceutical University, Machida, Tokyo 194-8543, Japan

C. Summary of model characterisation, development, validation, and regulatory applicability

Diisononyl phthalate (DINP) used as a plasticizer is a mixture of compounds consisting of isononyl esters of phthalic acid. There are concerns about the bioaccumulation of such esters in humans. A [phenyl-U-^{14}C]DINP mixture was synthesized and orally administered (50 mg/kg body weight) to control and humanized-liver mice and their pharmacokinetics were determined. Monoisononyl phthalate (MINP, a primary metabolite of DINP), oxidized MINP (isomers with hydroxy, carbonyl, and carboxy functional groups), and their glucuronides were detected in plasma from control and humanized-liver mice. Biphasic plasma concentration–time curves of MINP and its glucuronide were seen in control mice. In contrast, no such biphasic relationship was seen in humanized-liver mice, in which MINP and oxidized MINP were extensively excreted in the urine within 48 h. Animal biomonitoring equivalents of MINP and oxidized MINP from humanized-liver mice studies were scaled to human equivalents using known species allometric scaling factors with a simple physiologically based pharmacokinetic (PBK) model. Estimated urinary oxidized MINP concentrations in humans were roughly consistent with reported concentrations of MINP (with a different side chain). The simplified PBK model could estimate human urinary concentrations of MINP after ingestion of DINP and was capable of both forward and reverse dosimetry.

D. Model characterisation (Modelling workflow)

Step 1 – Scope and purpose of the model (problem formulation)

Typical phthalate plasticizers include di(2-ethylhexyl) phthalate (DEHP), dibutyl phthalate (DBP), and diisononyl phthalate (DINP). DBP or DEHP has been replaced with DINP as the new major plasticizer for polyvinylchloride polymers. Although no information is available on the antiandrogenic effects of DINP in humans, animal studies have reported that oral exposure to high doses has resulted in developmental or reproductive effects in

rodents. The primary and/or secondary phthalate monoester metabolites have been detected in human urine samples. Daily tolerable intake levels of DINP (150 μg/kg/day) has been set in humans. Therefore, the purpose of this study was to carry out a forward dosimetry approach (shown in Figure VI1) using data from chemical doses administered to animals to estimate human plasma and urine concentrations of MINP and oxidized MINP (isomers with hydroxy, carbonyl, and carboxy functional groups) after ingestion of DINP, capable of reverse dosimetry to facilitate the risk assessment of phthalates.

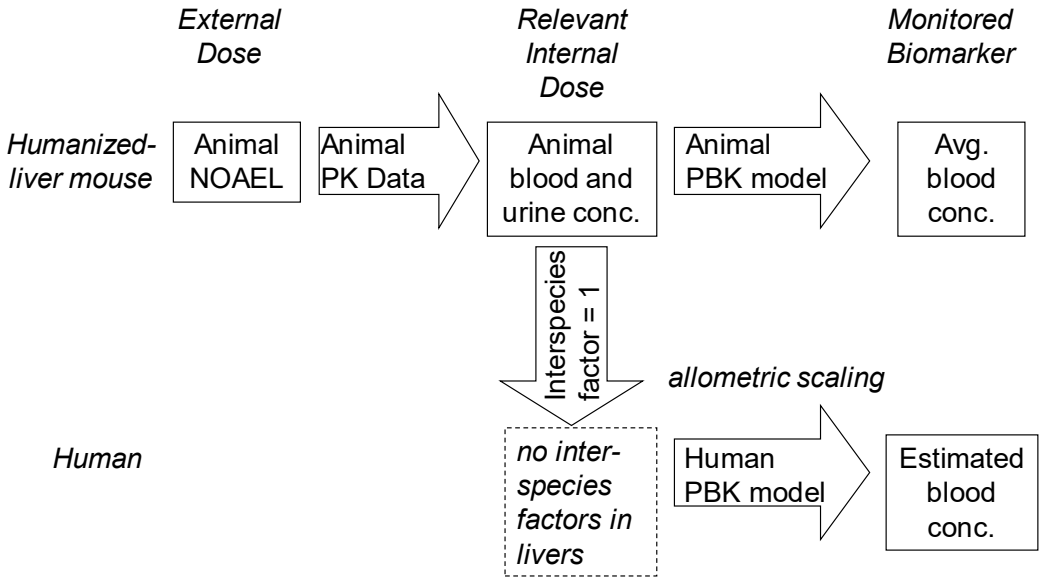

Figure VI1. Approach for calculating blood-based biomonitoring equivalents for phthalates. NOAEL, no-observed-adverse-effect level; PK, pharmacokinetics; PBK, physiologically based pharmacokinetic

Step 2 – Model conceptualisation (model structure, mathematical representation)

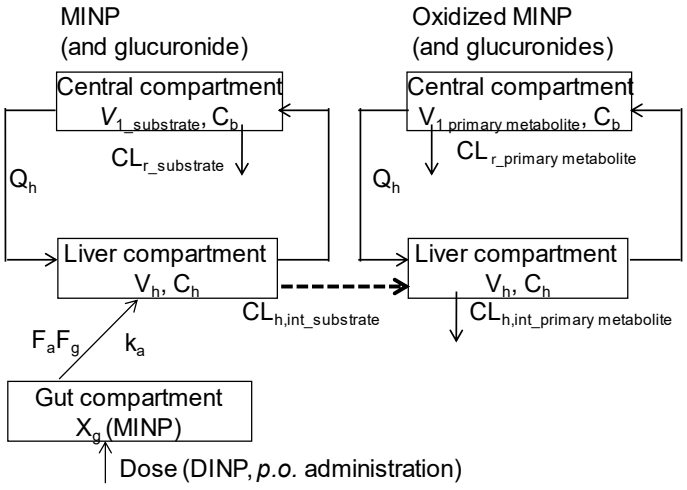

Figure VI2. PBK model established in this study for humanized-live mice and humans.

- The same values for the plasma unbound fraction, blood-to-plasma ratio, and liver-to-plasma ratio of the substrate and metabolite(s) were used for mice and humans by *in silico* estimation.
- In this conversion process from mice to humans, no consideration was given to interspecies factors when using *in vitro* liver clearances based on humanized-liver mice.
- 70 kg male is representative of adult population.

Step 3 – Model parameterisation (parameter estimation and analysis)

The simplified PBK models employed in the current study (Figure VI1) consisted of a chemical receptor compartment, a metabolizing compartment, and a central compartment and were set up. The chemical properties (Table VI1) were estimated using *in silico* tools(SimCYP and ChemDrawBioUltra software). The liver–plasma concentration ratio ($K_{p,h}$) and the ratio of the blood to plasma concentration (R_b) were calculated from their $f_{u,p}$ and log*P* values.

$$K_{p,h} = \frac{0.02289 \cdot P + 0.72621}{0.00396 \cdot P + 0.960581} \times \frac{1 + f_{u,p}}{2}$$

$$R_b = 0.45 \cdot \left(K_b \cdot f_{u,p} - 1\right) + 1 \text{ where } \log K_b = 0.617 \cdot \log\left(\frac{1 - f_{u,p}}{f_{u,p}}\right) + 0.208$$

where *P* is the water–octanol partition ratio and was estimated from the computer-calculated log *P* as neutral (clog *P*). A value of $\frac{1+f_{u,p}}{2}$ is corresponded to $f_{u,p}$ over tissue fraction unbound. Accepted values for the physiological hepatic blood flow rates (Q_h) in mice (0.160 L/h) and humans (96.6 L/h) were used. Values of the fraction absorbed (F_a) × intestinal availability (F_g) were estimated as 1 by fitting curves to plasma concentrations at several sampling points for humanized-liver mice. Subsequently, final parameter values and standard deviations for such as absorption rate constant (k_a), the systemic circulation volume (V_1), and the hepatic intrinsic clearance ($CL_{h,int}$) for the humanized-liver mouse models were calculated by the user model in WinNonlin ver. 5 (Certara, Princeton, NJ) so as to give the best fit to measured blood substrate concentrations in humanized-liver mice by simplex and modified Marquardt methods (with standard deviation values) and are shown in Table VI2.

To define a similar simplified PBK model for humans, the values of k_a, V_1, and $CL_{h,int}$ for the human PBK model shown in Table VI2 were estimated using a scale-up strategy from humanized-liver mice to humans as following. Rodent k_a was multiplied by 0.744 to give the human k_a value. The values for $V_{1,human}$ were calculated using the equation derived from a human steady-state volume of distribution (V_{ss}) and fixed values of the liver volume ($V_{h,human}$, 1.50 L) and blood volume ($V_{b,human}$, 4.90 L):

$$V_{ss,human}(\text{L}) = V_{ss,rodent}(\text{L}) \cdot \frac{\text{Body weight}_{\text{human}}}{\text{Body weight}_{\text{rodent}}}$$

$$V_1 = (V_{ss} - V_b - V_h \cdot \frac{K_{p,h} \times F_h}{R_b}) / \frac{1 + f_{u,p}}{2}$$

The *in vivo* hepatic intrinsic clearance ($CL_{h,int}$) in humans was generally estimated by multiplying the calculated initial parameters for *in vitro* hepatic intrinsic clearance values in humans by the ratio of *in vivo* to *in vitro* hepatic intrinsic clearance in humanized-liver

mice. However, in this conversion process, no consideration was given to interspecies factors when using *in vitro* liver clearances based on humanized-liver mice. The human renal clearance CLr,human was estimated using the equation, where BWrodent = 0.025 kg (mouse) and BWhuman = 70 kg:

$$\mathrm{CL_{r,human}} = \frac{\mathrm{CL_{r,rodent}}}{\mathrm{Body\ weight_{rodent}}^{\left(\frac{2}{3}\right)}} \cdot \mathrm{Body\ weight_{human}}^{\left(\frac{2}{3}\right)}$$

Then, the final parameters for the PBK model in humans were calculated using these initial values by the user model in WinNonlin.

Step 4 – Computer implementation (solving the equations)

The system of differential equations was solved to conduct the modeling for concentrations of the apparent substrate (MINP) and primary metabolite (hydroxylated MINP, indicated with subscript $_m$):

$$\frac{dX_g(t)}{dt} = -k_a \cdot X_g(t) \quad \frac{\mathrm{dX_g(t)}}{\mathrm{dt}} = -\mathrm{k_a} \cdot \mathrm{X_g(t)} \quad \text{when at } t = 0,\ X_g(0) = Fa \cdot\ Fg \cdot\ dose$$

$$V_h \frac{dV_h}{dt} = Q_h \cdot C_b - \frac{Q_h \cdot C_h \cdot R_b}{K_{p,h}} + k_a \cdot X_g - CL_{h,int} \cdot \frac{C_h}{K_{p,h}} \cdot f_{u,p}$$

$$V_1 \frac{dC_b}{dt} = -Q_h \cdot C_b + \frac{Q_h \cdot C_h \cdot R_b}{K_{p,h}} - CL_r \cdot C_b$$

$$V_u \frac{dC_u}{dt} = CL_r \cdot C_b$$

$$V_{h,m} \frac{dV_{h,m}}{dt} = Q_h \cdot C_{b,m} - \frac{Q_h \cdot C_{h,m} \cdot R_{b,m}}{K_{p,h,m}} + CL_{h,int} \cdot \frac{C_h}{K_{p,h}} \cdot f_{u,p} \ - CL_{h,int,m} \cdot \frac{C_{h,m}}{K_{p,h,m}} \cdot f_{u,p,m}$$

$$V_{1,m} \frac{dC_{b,m}}{dt} = -Q_h \cdot C_{b,m} + \frac{Q_h \cdot C_{h,m} \cdot R_{b,m}}{K_{p,h,m}} - CL_{r,m} \cdot C_{b,m}$$

$$V_{u,m} \frac{dC_{u,m}}{dt} = CL_{r,m} \cdot C_{b,m}$$

where Xg is the amount of compound in the gut, V_h and V_u are the volumes of liver and urine, respectively, C_h is the hepatic substrate concentration, and C_b is the blood substrate concentration.

As was done for the mouse models, systems of differential equations were solved to determine the concentrations in each compartment in humans.

Step 5 – Model Performance

Typical parameter values for monoisononyl phthalate and its oxidized metabolites in humanized-mouse PBK model, absorption rate constant, volume of systemic circulation, and hepatic intrinsic clearance, were determined within 30% standard deviations. To evaluate the predictive ability of the PBK model, the maximum plasma concentration (C_{max}) and area under the concentration versus time curve (AUC) values predicted by the PBK model after a virtual oral administration were within 2-fold errors of the corresponding values calculated using the one-compartment model.

Step 6 – Model Documentation

Information reported in the peer-reviewed publication in the references section

E. Identification of uncertainties

Model structure

- The model basically consists of a chemical absorption compartment, a metabolizing compartment, and a central compartment.

Input parameters

- Several physiological parameters of diisononyl phthalate were estimated using *in silico* tools.
- Using the allometric scaling methods, a human PBK model for MINP and oxidized MINP were set up based on the PBK models for humanized-liver mice.

Model output

- Output in human PBK model for monoisononyl phthalate and its oxidized metabolites after oral administrations of diisononyl phthalate was estimated values bases on PBK results in humanized-liver mice experimentally obtained.

Other uncertainties (e.g. model developed for different substance and/or purpose)

- Inter-individual variability was not taken into account.
- DINP comes in two forms, depending on the composition of the isononyl alcohol moieties, DINP-1 (CAS 68515-48-0) and DINP-2 (CAS 28553-12-0).

F. Model implementation details

- software (version no) WinNonlin software (Professional version 5.01)
- availability of code Not reported
- software verification / qualification YES. Part of the Certara portfolio.

G. Peer engagement (input/review)

Not reported

H. Parameter tables

Table VI1. Chemical properties of MINP and its primary hydroxylated metabolite.

Parameter	Symbol	MINP	Hydroxylated MINP
Molecular weight	MW	292	308
Octanol–water partition coefficient	logP	5.23	3.25
Plasma unbound fraction	$f_{u,p}$	0.005	0.0244

Blood-to-plasma concentration ratio	R_b	0.645	0.723
Liver-to-plasma concentration ratio	$K_{p,h}$	2.90	3.29

Table VI2. Experimental and calculated parameters for PBK models of MINP disposition.

Parameter	Symbol (unit)	Humanized-liver mouse	Human (from humanized-liver mouse)
Absorption rate constant	k_a (1/h)	1.50 ± 0.06	1.12
Volume of systemic circulation for MINP	$V_{1\_substrate}$ (L)	0.0182 (± 0.0023)	270
Hepatic intrinsic clearance for MINP	$CL_{h,int\_substrate}$ (L/h)	4.56 (± 0.06)	457
Hepatic clearance for MINP	$CL_{h,\_substrate}$ (L/h)	0.0200	2.23
Renal clearance for MINP	$CL_{r,\_substrate}$ (L/h)	0.0020	0.397
Metabolic ratio to primary metabolite	mRatio	1.0	1.0
Volume of systemic circulation for primary metabolite	$V_{1\_primary\ metabolite}$ (L)	0.0195 (± 0.0030)	54.8
Hepatic intrinsic clearance for primary metabolite	$CL_{h,int\_primary\ metabolite}$ (L/h)	0.576 (± 0.051)	57.7
Hepatic clearance for primary metabolite	$CL_{h,\_primary\ metabolite}$ (L/h)	0.0129	1.39
Renal clearance for primary metabolite	$CL_{r,\_primary\ metabolite}$ (L/h)	0.0129	2.57

Values in parentheses are standard deviations.

I. References and background information

Miura, T.; Suemizu, H.; Goto, M.; Sakai, N.; Iwata, H.; Shimizu, M.; Yamazaki, H. Human urinary concentrations of monoisononyl phthalate estimated using physiologically based pharmacokinetic modeling and experimental pharmacokinetics in humanized-liver mice orally administered with diisononyl phthalate. *Xenobiotica*, 2019. May;49(5):513-520 https://doi.org/10.1080/00498254.2018.1471753

Links to other resources

Using both simple PBK models and humanized-liver mice, a biomonitoring strategy was developed for evaluation of human exposure to DINP similar to that previously reported for di(2-ethylhexyl)phthalate (Adachi et al., 2015) and extended to dibutyl phthalate (Miura et al., 2019).

Adachi K, Suemizu H, Murayama N, Shimizu M, and Yamazaki H. Human biofluid concentrations of mono(2-ethylhexyl)phthalate extrapolated from pharmacokinetics in chimeric mice with humanized liver administered with **di(2-ethylhexyl)phthalate** and physiologically based pharmacokinetic modeling. *Environ Toxicol Pharmacol* **2015,** *39*, 1067–73.

Miura, T., Uehara, S., Mizuno, S., Yoshizawa, M., Murayama, N., Kamiya, Y., Shimizu, M., Suemizu, H., and Yamazaki, H. Steady-state human pharmacokinetics of monobutyl phthalate predicted by physiologically based pharmacokinetic modeling using single-dose

data from humanized-liver mice orally administered with **dibutyl phthalate**. *Chem.Res.Toxicol*. **2019,** *32*, 333-340.

Cases for similar human PBK modeling for chemicals from the humanized-liver mice models are:

Yamashita M, Suemizu H, Murayama N, Nishiyama S, Shimizu M, Yamazaki H. Human plasma concentrations of herbicidal carbamate molinate extrapolated from the pharmacokinetics established in in vivo experiments with chimeric mice with humanized liver and physiologically based pharmacokinetic modeling. Regul. Toxicol. Pharmacol. 2014, 70, 214-221.

Miyaguchi T, Suemizu H, Shimizu M, Shida S, Nishiyama S, Takano R, Murayama N, Yamazaki H. Human urine and plasma concentrations of bisphenol A extrapolated from pharmacokinetics established in in vivo experiments with chimeric mice with humanized liver and semi-physiological pharmacokinetic modeling. Regul. Toxicol. Pharmacol. 2015, 72, 71-76.

Shimizu M, Suemizu H, Mizuno S, Kusama T, Miura T, Uehara S, Yamazaki H. Human plasma concentrations of trimethylamine N-oxide extrapolated using pharmacokinetic modeling based on metabolic profiles of deuterium-labeled trimethylamine in humanized-liver mice. J. Toxicol. Sci. 2018, 43, 387-393.

Part II Checklist for model evaluation

PBK Model Evaluation Checklist	Checklist assessment	Comments
Name of the PBK model (as in the reporting template)	**PBK model for monoisononyl phthalate in humans**	
Model developer and contact details	**Authors**: Tomonori Miura, Hiroshi Suemizu, Masatomo Goto, Norifumi Sakai, Hiroshi Iwata, Makiko Shimizu and Hiroshi Yamazaki* **Affiliation:** *Laboratory of Drug Metabolism and Pharmacokinetics, Showa Pharmaceutical University, Machida, Tokyo 194-8543, Japan	
Name of person reviewing and contact details	**L. Rossi**	
Date of checklist assessment	**June 2020**	
A. Context/Implementation		
A.1. Regulatory Purpose		
1. What is the acceptable degree of confidence/uncertainty (e.g. high, medium or low) for the envisaged application (e.g. priority setting, screening, full assessment?)	**High**	
2. Is the degree of confidence/uncertainty in application of the PBK model for the envisaged purpose greater or less than that for other assessment options (e.g. reliance on PBK model and *in vitro* data vs. no experimental data)?	**High**	
A.2. Documentation		
3. Is the model documentation adequate, i.e. does it address the essential content of model reporting template, including the following:	**Yes**	
• Clear indication of the chemical, or chemicals, to which the model is applicable?	**Yes**	
• Is the model being applied for the same scientific purpose as it was developed, or has it been repurposed somehow?	**Yes**	
• Model assumptions?	**Yes**	
• Graphical representation of the proposed mode of action, if known?	**Yes**	
• Graphical representation of the conceptual model?	**Yes**	
• Supporting tabulation for parameters (names, meanings, values, mean and standard deviations, units and sources)?	**Yes**	
• Relevance and reliability of model parameters?	**Yes**	
• Uncertainty and sensitivity analysis?	**Yes**	
• Mathematical equations?	**Yes**	

• PBK model code?	**No**	
• Software algorithm to run the PBK model code?	**Yes**	
• Qualification of PBK software platform?	**No**	
A.3 Software Implementation and Verification		
4. Does the model code express the mathematical model?	**No**	**code represents the chemical MoA**
5. Is the model code devoid of syntactic and mathematical errors?	**Yes**	
6. Are the units of input and output parameters correct?	**Yes**	
7. Is the chemical mass balance respected at all times?	**Yes**	
8. Is the cardiac output equal to the sum of blood flow rates to the tissue compartments?	**Yes**	
9. Is the sum total of tissue volumes equal to total body volume?	**No**	**Equals to 0.91**
10. Is the mathematical solver a well-established algorithm?	**Yes**	
11. Does the mathematical solver converge on a solution without numerical error?	**Yes**	
12. Has the PBK modelling platform been subjected to a verification process (for a different use, for instance, in the pharmaceutical domain)?	**No**	**Is part of the CERTARA well establish commercial PBK model platform**
A.4 Peer engagement (input/review)		
13. Has the model been used previously for a regulatory purpose?	**No**	
• Is prior peer engagement in the development and review of the model sufficient to support the envisaged application?	**-**	
• Is additional review required? Peer engagement includes input/review by experts on specific aspects of model development, individual reviews of the model by experts, or collective reviews by peer review panels. Availability of the comments and tracking of revisions to the model in response to peer input contributes to increased confidence in the model for potential application.	**No**	
B. Assessment of Model Validity		
B.1 Biological Basis (Model Structure and Parameters)		
14. Is the model consistent with known biology?	**Yes**	
• Is the biological basis for the model structure provided?	**Yes**	
• Is the complexity of the model structure appropriate to address the regulatory application?	**Yes**	
• Are assumptions concerning the model structure and parameters clearly stated and justified?	**Yes**	
• Is the choice of values for physiological parameters justified?	**Yes**	

• Is the choice of methods used to estimate chemical-specific ADME parameters justified?	**Yes**	
• Saturable kinetics	**No**	
B.2 Theoretical Basis of Model Equations		
15. Are the underlying equations based on established theories, .e.g. Michaelis-Menten kinetics, Fick's laws of diffusion?	**Yes**	
• In the case of PBK models for particles, does the model take into consideration the properties of particles, e.g. particle size ranges, (poor) solubility, aggregation, partitioning and diffusion/sedimentation behaviour?	**NA**	
B.3. Reliability of input parameters		
16. Has the uncertainty (individual variability, experimental reproducibility and reliability) in the input parameters been characterised?	**Partially**	**In the measured one yes**
B.4. Uncertainty and Sensitivity Analysis		
17. Has the impact of uncertainty (individual variability, experimental reproducibility and reliability) in the parameters on the chosen dose metric been estimated?	**Yes**	
• Local sensitivity analysis?	**Yes**	
• Global sensitivity analysis?	**No**	
18. Is confidence in influential input parameter estimates (i.e., based on comparison of uncertainty and sensitivity) reasonable (within expected values; similar to those of analogues) in view of the intended application?	**Yes**	
B.5. Goodness-of-Fit and Predictivity		
19. For PBK models for which there are sufficient *in vivo* data for the chemical of interest:		
• Suitability as analogue (chemical and biological similarity) been assessed?	**Yes**	
• Reliable estimation of chosen dose metric for analogue?	**Yes**	

Part III Overall Evaluation

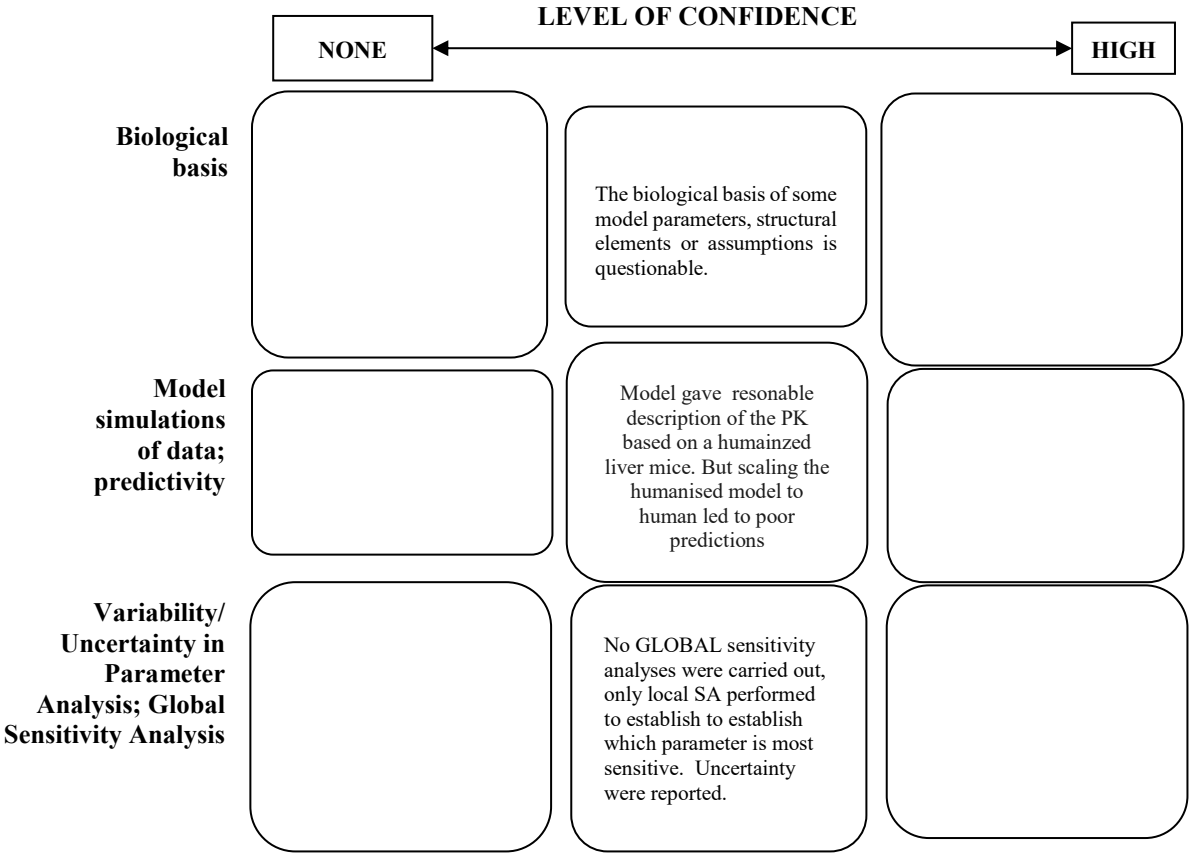

Application of PBK modelling in the interspecies scaling of the urinary excretion in rodent of the diisononyl phthalate (DINP) metabolite monoisononyl phthalate (MINP) was reported. Though the PBK model gave a reasonable description of the plasma kinetics of MINP after a single oral dose of DINP corresponding predictions in plasma of humanized liver mice were less. Scaling the humanized rodent PBK model to humans led to a poor prediction of experimentally observed time course of the excretion of MINP and oxidized MINP in human urine. Assumptions are reported to underline the uncertainties. Based on all the evidence provided the following model will have a medium/standard level of confidence. The model code is not reported and a full assessment cannot be performed. Thus, it is recommended that the PBK model and relative output can be used in a regulatory framework only as information on the DINP.

Case Study VII

Quantitative Proteomics-based Bottom-up PBK Modelling to Predict Chemical Exposure in Humans

Part I. PBK model reporting template

A. Name of model

Quantitative Proteomics-based Bottom-up PBK Modelling to Predict Chemical Exposure in Humans

B. Contact details

Authors: James Chun Yip Chan[1,2], Shawn Pei Feng Tan[2,3], Eric Chun Yong Chan[2,3]

Affiliation: [1]Skin Research Institute of Singapore, Agency for Science Technology and Research, Singapore [2]Innovations in Food and Chemical Safety, Agency for Science Technology and Research, Singapore [3]Department of Pharmacy, National University of Singapore, Singapore

C. Summary of model characterisation, development, validation, and regulatory applicability

This case study examines the feasibility of a fully bottom-up PBK strategy based on quantitative proteomics measurements of metabolic enzyme and transporter expression levels to perform *in vitro*-to-*in vivo* extrapolation (IVIVE) for predicting the exposure of chemicals in humans. The Simcyp® software was used to build bottom-up PBK models for a series of structurally-related, data-rich statins without empirically fitting any parameters to *in vivo* human biokinetic (BK) data. Subsequently, simulations were compared with plasma time-course data as well as *in vivo* parameters such as the maximum peak concentration (C_{max}) and area under the curve (AUC) and clearance using a two-fold acceptance criterion to ascertain the predictivity of the models.

In this case study, a bottom-up PBK model was built for rosuvastatin, fluvastatin and pitavastatin. These statins are differentially eliminated. Rosuvastatin's disposition is largely driven by multiple uptake and efflux transporters (intestinal, hepatic and renal) with minimal metabolism. Fluvastatin's disposition is driven mainly by CYP3A4, CYP2C9 and CYP2C8 metabolism while still requiring transporters for uptake into hepatocytes for metabolism. Finally, pitavastatin's disposition is driven by both transporters and metabolism. Given that IVIVE for transporters is poorly established, in this case study we emphasize the use of quantitative proteomics to address this gap.

Our simulations revealed that utilizing intrinsic clearance (CL_{int}) values alone to inform transporter kinetics result in a poor prediction of exposure. Predictions improved significantly (within two-fold of measured values) when absolute transporter abundance levels in the *in vitro* system, isolated hepatocytes and fresh liver tissue were taken into account via the mechanistic scaling of the maximal transport rate (J_{max}) values. Crucially, the differences in expression levels between isolated and fresh hepatocytes, that were frequently unaccounted in most studies, was found to be significant for our case study. This approach also accounted for biliary excretion, enterohepatic recirculation and renal

excretion in the simulations. Similarly, CL_{int} values for metabolism were scaled based on the CYP450 abundances in the *in vitro* system to *in vivo* liver and intestinal abundances, which allowed for extrapolation of metabolic clearance at the organ level. Importantly, for fluvastatin and pitavastatin whose metabolic clearance depends on transporter-mediated uptake into hepatocytes, clearance was correctly predicted only when appropriate scaling of transporter J_{max} values were performed.

Additionally, we optimized the prediction of rosuvastatin and pitavastatin distribution profiles by using tissue-to-plasma equilibrium distribution ratios (K_p) obtained from rat distribution studies. This was done as the Rodgers and Rowland method (Rodgers *et al.*, 2007) was unable to adequately predict the volume of distribution at steady state (V_{ss}) and distribution profile for these two statins. However, the prediction of biokinetic parameters such as CL, $AUC_{0h-\infty}$, C_{max} and T_{max} were unaffected whether the Rodgers and Rowland method or rat K_p values were used. (T_{max} is defined as the Time of maximum drug concentration, peak time).

In conclusion, we demonstrate that IVIVE of transporters can be performed accurately when transporter kinetics were measured, accompanied by measurements of transporter abundances in the *in vitro* system using quantitative proteomics, which are then scaled to transporter abundances *in vivo*. This example illustrates that thorough collection of high quality *in vitro* data is necessary for predictive IVIVE to be performed in a fully bottom-up setting. Finally, while our case study has shown that the use of K_p values obtained from animal distribution studies may improve the prediction of V_{ss}, we also demonstrated that reasonable predictions of the various biokinetic parameters could be performed without the use of such animal data.

D. Model characterisation (modelling workflow)

Step 1 – Scope and purpose of the model (problem formulation)

We hypothesized that accounting for differences in transporter and metabolic enzyme expression between *in vitro* and *in vivo* systems measured using quantitative proteomics is crucial for the accuracy of PBK models for chemicals.

Step 2 – Model conceptualisation (model structure, mathematical representation)

A general description of the Simcyp® simulator has been published previously (Jamei *et al*., 2009, 2013, 2014). An in depth description of the PBK model input parameters and the derivation of proteomics-based scaling factors have been published and may be found here (Chan *et al.*, 2019). The following assumptions are reported:

1) K_p values of HMG-CoA reductase inhibitors are best predicted by the equation put forth by Rodgers and Rowland (Rodgers *et al.*, 2007).

2) Perfusion rate-limited distribution occurs in all organs other than the liver/intestine/kidney.

3) 100% of biliary excreted drug is available for enterohepatic reabsorption.

4) In the case of rosuvastatin, the kinetic parameters of the following transporters involved in its disposition were used:

a) Hepatic sinusoidal uptake: OATP1B1[1], OATP1B3, OATP2B1

b) Hepatic sinusoidal efflux: MRP4[2]

c) Hepatic canalicular efflux: BCRP[3], MRP2

d) Renal basolateral uptake: OAT3[4]

e) Renal apical efflux: MRP4

5) In the case of fluvastatin, metabolism is assumed to be its rate-limiting step in its disposition, hence overall CL_{int} value is used to define its hepatic uptake transport.

6) In the case of pitavastatin, the kinetic parameters of the following transporters involved in its hepatic disposition were used:

a) Sinusoidal uptake: OATP1B1, OATP1B3, OATP2B1, NTCP[5]

b) Sinusoidal efflux: MRP3

c) Canalicular efflux: BCRP

d) Renal basolateral uptake: OAT3

e) Renal apical efflux: MRP4

7) Fraction unbound in the *in vitro* incubation system ($f_{u,inc}$) is equal to 1 if not stated.

8) Mean expression of transporters measured from pooled samples of isolated and fresh hepatocytes were representative of mean population transporter levels.

9) Tissue concentrations of pitavastatin (excluding the liver) obtained from rat radiolabelled distribution studies (used to calculate K_p) values reflect only the unchanged parent compound.

Step 3. Model parameterisation (parameter estimation and analysis)

1) Comprehensive literature search and selection of relevant preclinical (*in vitro* or *in vivo* animal) data for input into our PBK model.

2) Establishment of step-wise scaling factors for uptake and efflux hepatic/intestinal/renal transporters measured using quantitative proteomics to obtain the absolute expression level of transporters:

a) Scaling *in vitro* kinetic data to isolated hepatocytes/renal tubular cells/intestinal enterocytes based on absolute expression level or activity of transporters (in a small number of instances where absolute expression level data were unavailable)

b) Scaling isolated to fresh hepatocytes/renal tubular cells/intestinal enterocytes based on absolute expression level of transporters.

[1] OATP: Organic Anion-Transporting Polypeptide

[2] MRP: Multidrug Resistance Associated Protein

[3] BCRP: Breast Cancer Resistant Protein

[4] Organic Anion Transporters

[5] NTCP: Sodium-Taurocholate Cotransporting Polypeptide

c) Scaling fresh hepatocytes/renal tubular cells/intestinal enterocytes to *in vivo* human liver/kidney/intestinal tissue based on expression level of transporters.

3) Establishment of scaling factors for hepatic metabolism.

a) Scaling kinetic data obtained from *in vitro* systems to cryopreserved or primary hepatocytes based on relative activity of enzymes.

b) Scaling kinetic data from hepatocytes to *in vivo* human liver tissue based on proteomics informed, relative expression of enzymes.

4) Obtain K_p values from rat radiolabelled distribution studies for rosuvastatin and pitavastatin for selected organs (where appropriate).

Step 4 – Computer implementation (solving the equations)

Development of PBK model with IVIVE scaling factors to simulate plasma concentrations after a single IV, single oral and repeated oral dosing using the Simcyp® simulator.

Step 5 – Model Performance

Extensive verification of PBK models with observed biokinetic data from human clinical trials, based on intravenous, single oral and multiple oral dosing was performed for all 3 compounds. A two-fold criterion was used to judge the accuracy of predicted biokinetic parameters against the observed biokinetic parameters.

1) Bottom-Up Simulations of Single and Multiple Dose Biokinetics of Rosuvastatin

Figure VII1 shows the simulated plasma concentration-time profile of rosuvastatin after a single 8 mg IV infusion, a single 20 mg oral dose and a 10 mg once daily dosing for 14 days (clinical plasma data obtained from Martin et al., 2002, 2003). For all 3 dosing scenarios, the simulated biokinetic parameters (C_{max}, T_{max}, AUC_{0h-t}, $AUC_{0h-\infty}$ and CL) were within 1.5-fold of the observed data (Table VII1).

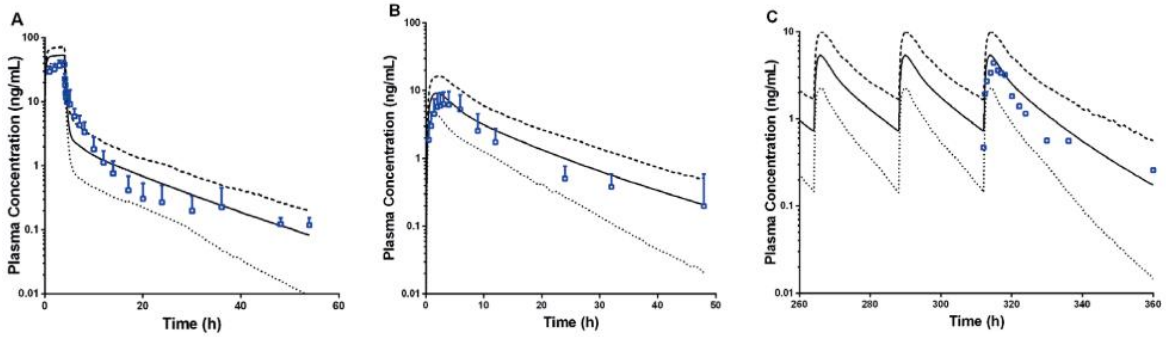

Figure VII1: Bottom-up simulated rosuvastatin model and observed plasma concentration-time profile of rosuvastatin after (A) 8 mg IV infusion, (B) 20 mg single oral dose, and (C) 10 mg once daily oral dosing for 14 days. The continuous line represents the predicted mean concentration for the simulated population. The dotted and dashed lines represent the 5th and 95th percentile of the predicted mean concentration. The blue boxes represent the observed rosuvastatin concentration with error bars (SD) if available.

2) Bottom-Up Simulations of Single and Multiple Dose Biokinetics of Fluvastatin

As shown in Table VII1, the predicted biokinetic parameters after a 2 mg IV infusion, 10 mg single oral dose and 40 mg once daily oral dosing for 6 days fell within two-fold of the observed parameters (Tse, 1992). Only the T_{max} for the 10 mg single oral dosing was beyond the two-fold criteria with a fold difference of 2.35 versus the observed value. Similarly, the plasma concentration-time profile (Figure VII2) shows that the simulations are in close agreement with the observed profile.

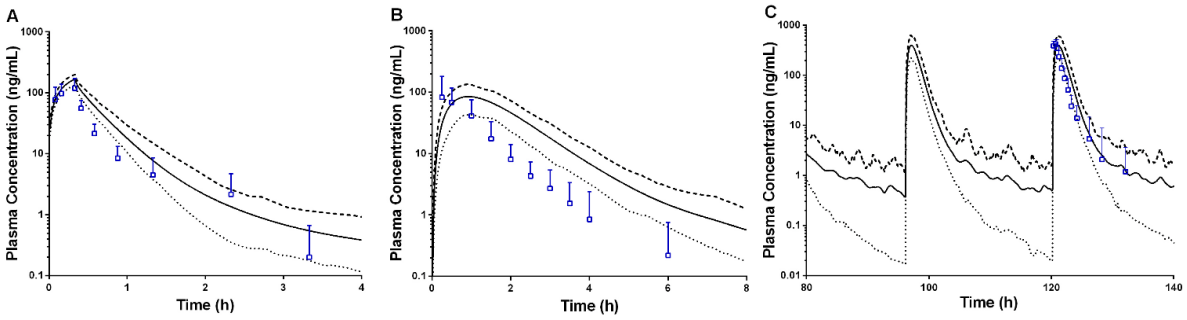

Figure VII2. Bottom-up fluvastatin model simulated and observed plasma concentration-time profile of fluvastatin after (A) 2 mg IV infusion, (B) 10 mg single oral dose and (C) 40 mg once daily oral dosing for 6 days. The continuous line represents the predicted mean concentration for the simulated population. The dotted and dashed lines represents the 5th and 95th percentile of the predicted mean concentration. The blue boxes represent the observed fluvastatin concentration with error bars (SD) if available.

3) Bottom-Up Simulations of Single and Multiple Dose Biokinetics of Pitavastatin

The plasma concentration-time profile of pitavastatin after a 2 mg IV infusion over 1 hour, 2 mg single oral dosing and 4 mg once daily dosing for 5 days are shown in Figure VII3. Simulated biokinetic parameters for the IV infusion and single oral dose were well predicted, with the simulated biokinetic parameters within 2-fold of the observed data (FDA, 2012) (Table VII1).

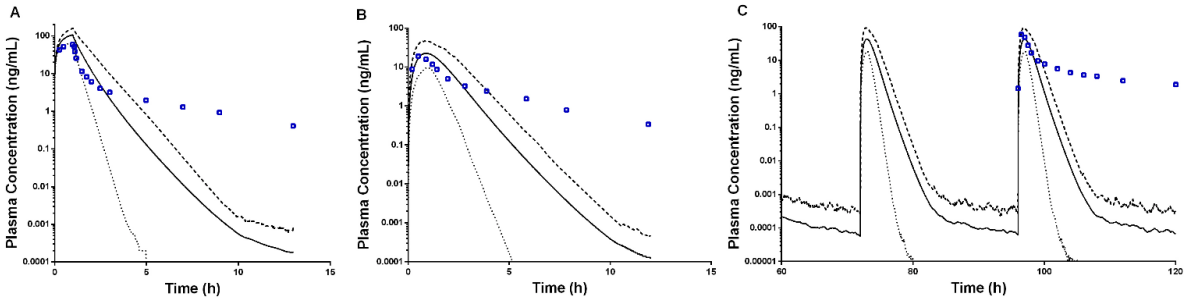

Figure VII3. Bottom-up pitavastatin model simulated and observed plasma concentration-time profile of pitavastatin after (A) 2 mg IV infusion, (B) 2 mg single oral dose and (C) 4 mg once daily oral dosing for 5 days. The continuous line represents the predicted mean concentration for the simulated population. The dotted and dashed lines represents the 5th and 95th percentile of the predicted mean concentration. The blue boxes represent the observed pitavastatin concentration.

Study Design	Rosuvastatin 8 mg IV infusion			Rosuvastatin 20 mg single oral dose			Rosuvastatin 10 mg once daily oral dose for 14 days		
Biokinetic Parameter (unit)	Observed	Simulated	F/D	Observed	Simulated	F/D	Observed	Simulated	F/D
C_{max} (ng/ml)	37.10	52.90	**1.43**	7.60	8.68	**1.14**	4.58	5.03	**1.10**
T_{max} (h)	4.00	3.98	**1.00**	3.00	1.93	**0.64**	3.00	1.95	**0.65**
AUC_{0h-t} (ng.h/ml)	164.00	236.69	**1.44**	77.20	84.33	**1.09**	40.10	54.49	**1.36**
$AUC_{0h-\infty}$ (ng.h/ml)	-	-	**-**	83.50	87.09	**1.04**	71.80	58.36	**0.81**
CL or CL/F (L/h)	48.90	33.80	**0.69**	239.50	229.65	**0.96**	139.28	171.35	**1.23**

Study Design	Fluvastatin 2 mg IV infusion			Fluvastatin 10 mg single oral dose			Fluvastatin 40 mg once daily oral dose for 6 days		
Biokinetic Parameter (unit)	Observed	Simulated	F/D	Observed	Simulated	F/D	Observed	Simulated	F/D
C_{max} (ng/ml)	118.80	166.80	**1.40**	88.20	84.12	**0.95**	438.00	395.61	**0.90**
T_{max} (h)	0.33	0.33	**1.00**	0.40	0.94	**2.35**	0.50	0.95	**1.90**
AUC_{0h-t} (ng.h/ml)	48.00	83.16	**1.73**	86.40	168.98	**1.96**	568.00	798.47	**1.41**
$AUC_{0h-\infty}$ (ng.h/ml)	-	-	-	-	-	-	-	-	-
CL or CL/F (L/h)	37.72	24.05	**0.64**	115.74	59.18	**0.51**	70.42	50.10	**0.71**

Study Design	Pitavastatin 2 mg IV infusion			Pitavastatin 2 mg single oral dose			Pitavastatin 4 mg once daily oral dose for 5 days		
Biokinetic Parameter (unit)	Observed	Simulated	F/D	Observed	Simulated	F/D	Observed	Simulated	F/D
C_{max} (ng/ml)	59.83	102.95	**1.72**	18.58	21.43	**1.15**	62.39	40.68	**0.65**
T_{max} (h)	0.97	0.99	**1.02**	0.75	0.96	**1.28**	0.50	1.06	**2.12**
AUC_{0h-t} (ng.h/ml)	76.07	114.78	**1.51**	33.57	30.90	**0.92**	147.33	62.64	**0.43**
$AUC_{0h-\infty}$ (ng.h/ml)	83.9	114.78	**1.37**	42.95	30.91	**0.72**	-	-	**-**
CL or CL/F (L/h)	23.67	17.42	**0.74**	45.85	64.71	**1.41**	27.15	63.86	**2.35**

Table VII1: Simulated versus observed biokinetic parameters and the fold difference (simulated/observed) after bottom-up simulations

F/D refers to fold difference

Step 6 – Model Documentation

The PBK model for rosuvastatin, fluvastatin and pitavastatin has been published and reported in a peer-reviewed journal (Chan *et al.*, 2019).

E. Identification of uncertainties

Model structure

Absolute abundance and distribution of transporters in different segments of the kidney is currently unknown. Current knowledge is largely confined to the proximal tubule.

Input parameters

The type of *in vitro* system and methodology used (suspension hepatocytes, membrane vesicles or transporter expressing immortalised cell lines) will influence the value and type of transporter kinetic parameters obtained. For efflux transporters, it was unknown whether the unbound intracellular concentration was measured.

Transporter and metabolic enzyme expression data depends on the methodology used by the researcher. Different proteomics methodology and instrumentation used can result in varying measurements of transporter abundance levels.

Appropriate J_{max} and K_m kinetic data are not available for selected transporters.

a) Intestinal transporter data is unavailable and unaccounted for rosuvastatin and fluvastatin

b) Individual hepatic canalicular efflux transporter data for rosuvastatin was unavailable. Overall canalicular efflux from sandwich-cultured hepatocyte data was used.

c) Hepatic uptake and efflux transporter data for fluvastatin were available but CL_{int} was used instead.

$f_{u,inc}$ for certain assays are unknown or not available. Sensitivity analysis was conducted to determine the importance of $f_{u,inc}$ in our PBK models. Using the MRP4 mediated transport of rosuvastatin as an example, sensitivity analysis was conducted for $f_{u,inc}$ from 0.01 to 1.

a) AUC is insensitive to changes in $f_{u,inc}$ when $f_{u,inc}$ is above 0.23.

b) AUC increased from 171.43 to 578.8 ng·h/mL as $f_{u,inc}$ decreased from 0.23 to 0.01.

c) Although not measured experimentally, the value of $f_{u,inc}$ is likely to be closer to 1 in the *in vitro* system (sandwich-cultured human hepatocytes) as the experimental buffer used was protein-free, hence the margin of tolerance for variability in the value of $f_{u,inc}$ for this transporter and *in vitro* system is high.

For rosuvastatin, there is conflicting information of the role of P-gp (MDR1) transporter in its efflux.

Model output

The effects of transporter genetic polymorphisms (such as OATP1B1 and BCRP) have not been accounted for in simulations.

The influence of transporters and enterohepatic recirculation on the prediction of K_p and volume of distribution is not accounted for by the Rodgers and Rowland method.

Other uncertainties (e.g. model developed for different substance and/or purpose)

The amount of biliary excreted chemical that is reabsorbed in the intestinal lumen is uncertain due to a possible deconjugation of the chemical in the colonic lumen by gut microflora and lack of appropriate *in vitro* assays to estimate the extent of enterohepatic recirculation.

For pitavastatin, the extent and rate of non-enzymatic breakdown of the pitavastatin lactone metabolite to pitavastatin in the *in vitro* metabolic assays are unknown.

The sensitivity analyses on the major assumptions and uncertainties indicate that these do not have a major impact on the simulations (except for the breakdown of pitavastatin lactone to pitavastatin, which may account for increased exposure in the multiple dosing scenario). The simulations are robust and the quantitative proteomics-based scaling factors permit fully bottom-up, mechanistic IVIVE to accurately predict *in vivo* chemical disposition. Strategies for reducing overall uncertainty includes:

a) Generate missing *in vitro* data and perform proteomics quantification of transporter expression levels. For example, measure transport kinetics for renal uptake and efflux transporters for fluvastatin and quantify transporters and enzymes in the *in vitro* system and kidney tissue.

b) Meta-analysis of available liver/kidney/intestinal transporter expression data in the literature to reduce variability arising from differences in analytical methodologies.

c) Measure $f_{u,inc}$ whenever conducting any *in vitro* metabolic and transporter kinetics assays.

F. Model implementation details

- Simcyp® Version 17, Release 1
- Code is not publically available, but the mathematical equations underlying the model are available (Jamei *et al.,* 2009; Chan *et al.*, 2019)
- The software has been verified with pharmaceutical compounds and their results published in peer-reviewed journals. It is used regularly by pharmaceutical companies and regulatory bodies such as the US FDA and EMA. A list of PBPK analyses generated with Simcyp® that has been accepted by the US FDA and EMA has been published (Shebley *et al.*, 2018).

G. Peer engagement (input/review)

- A manuscript based on this case study has been published in a peer-reviewed journal (Chan *et al.*, 2019).

H. Parameter tables

- Refer to the supplementary material (Table S1 to S3) of our publication (Chan *et al.*, 2019).

I. References and background information

Bosgra, S., Van De Steeg, E., Vlaming, M. L. et al. (2014). Predicting carrier-mediated hepatic disposition of rosuvastatin in man by scaling from individual transfected cell-lines in vitro using absolute transporter protein quantification and PBPK modeling. Eur J Pharm Sci 65, 156–166. https://doi.org/10.1016/j.ejps.2014.09.007.

Chan, J. C. Y., Tan, S. P. F., Upton, Z., & Chan, E. C. Y. (2019). Bottom-up physiologically-based biokinetic modelling as an alternative to animal testing. ALTEX, 36(4), 597–612. https://doi.org/10.14573/altex.1812051

FDA (2012). Livalo Clinical Pharmacology and Biopharmaceutics Review. , 1–5. Available at: https://www.accessdata.fda.gov/drugsatfda_docs/nda/2009/022363s000TOC.cfm [Accessed August 13, 2018].

Fischer, V., Johanson, L., Heitz, F. et al. (1999). The 3-hydroxy-3-methylglutaryl coenzyme A reductase inhibitor fluvastatin: effect on human cytochrome P-450 and implications for metabolic drug interactions. Drug Metab Dispos 27, 410–416. Available at: http://dmd.aspetjournals.org/content/27/3/410.abstract.

Fujino, H., Nakai, D. and Nakagomi, R. (2004). Metabolic stability and uptake by human hepatocytes of pitavastatin, a new inhibitor of HMG-CoA reductase. Lipid Reducers 388, 382–388. Available at: https://www.thieme-connect.com/ejournals/abstract/10.1055/s-0031-1296988.

Fujino, H., Saito, T., Tsunenari, Y. et al. (2004). Metabolic properties of the acid and lactone forms of HMGCoA reductase inhibitors. Xenobiotica 34, 961–971. https://doi.org/10.1080/00498250400015319.

Hirano, M. (2004). Contribution of OATP2 (OATP1B1) and OATP8 (OATP1B3) to the Hepatic Uptake of Pitavastatin in Humans. J Pharmacol Exp Ther 311, 139–146. https://doi.org/10.1124/jpet.104.068056.

Izumi, S., Nozaki, Y., Kusuhara, H. et al. (2018). Relative Activity Factor (RAF)-based Scaling of Uptake Clearance Mediated by Organic Anion Transporting Polypeptide (OATP) 1B1 and OATP1B3 in Human Hepatocytes. Mol Pharm 15, 2277–2288. https://doi.org/10.1021/acs.molpharmaceut.8b00138.

Jamei, M., Bajot, F., Neuhoff, S. et al. (2014). A mechanistic framework for in vitro-in vivo extrapolation of liver membrane transporters: Prediction of drug-drug interaction between rosuvastatin and cyclosporine. Clin Pharmacokinet 53, 73–87. https://doi.org/10.1007/s40262-013-0097-y.

Jamei M, Dickinson GL, Rostami-Hodjegan A. (2009). A framework for assessing inter-individual variability in pharmacokinetics using virtual human populations and integrating general knowledge of physical chemistry, biology, anatomy, physiology and genetics: A tale of “bottom-up” vs “top-down” recognition. Drug Metab Pharmacokinet 24(1), 53-75. https://doi:10.2133/dmpk.24.53.

Jamei, M., Marciniak, S., Edwards, D., Wragg, K., Feng, K., Barnett, A., & Rostami-Hodjegan, A. (2013). The Simcyp Population Based Simulator: Architecture, Implementation, and Quality Assurance. In Silico Pharmacology, 1(1), 9. https://doi.org/10.1186/2193-9616-1-9

Kitamura, S., Maeda, K., Wang, Y. et al. (2008). Involvement of multiple transporters in the hepatobiliary transport of rosuvastatin. Drug Metab Dispos 36, 2014–2023. https://doi.org/10.1124/dmd.108.021410.

Martin, P. D., Mitchell, P. D. and Schneck, D. W. (2002). Pharmacodynamic effects and pharmacokinetics of a new HMG-CoA reductase inhibitor, rosuvastatin, after morning or evening administration in healthy volunteers. Br J Clin Pharmacol 54, 472–477. https://doi.org/10.1046/j.1365-2125.2002.01688.x.

Martin, P. D., Warwick, M. J., Dane, A. L. et al. (2003). Absolute Oral Bioavailability of Rosuvastatin in Healthy White Adult Male Volunteers. Clin Ther 25, 2553–2563. https://doi.org/10.1016/S0149-2918(03)80316-8.

Rodgers, T. and Rowland, M. (2007). Mechanistic approaches to volume of distribution predictions: Understanding the processes. Pharm Res 24, 918–933. https://doi.org/10.1007/s11095-006-9210-3.

Schirris, T. J. J. et al. (2015). Statin Lactonization by Uridine 5′-Diphospho-glucuronosyltransferases (UGTs). Mol Pharm 12, 4048–4055. https://doi.org/10.1021/acs.molpharmaceut.5b00474.

Shebley, M., Sandhu, P., Emami Riedmaier, A., Jamei, M., Narayanan, R., Patel, A., … Rowland, M. (2018). Physiologically Based Pharmacokinetic Model Qualification and Reporting Procedures for Regulatory Submissions: A Consortium Perspective. Clinical Pharmacology and Therapeutics, 104(1), 88–110. https://doi.org/10.1002/cpt.1013

Tse, F. L. S., Jaffe, J. M. and Troendle, A. (1992). Pharmacokinetics of Fluvastatin After Single and Multiple Doses in Normal Volunteers. J Clin Pharmacol 32, 630–638. https://doi.org/10.1002/j.15524604.1992.tb05773.x.

Vildhede, A., Wiśniewski, J. R., Norén, A. et al. (2015). Comparative Proteomic Analysis of Human Liver Tissue and Isolated Hepatocytes with a Focus on Proteins Determining Drug Exposure. J Proteome Res 14, 3305– 3314. https://doi.org/10.1021/acs.jproteome.5b00334.

Part II Checklist for model evaluation

PBK Model Evaluation Checklist	Checklist assessment	Comments
Name of the PBK model (as in the reporting template)	Quantitative Proteomics-based Bottom-up PBK Modeling to Predict Chemical Exposure in Humans	
Model developer and contact details	Chan Chun Yip James* Tan Pei Feng Shawn Chan Chun Yong Eric * james_chan@sris.a-star.edu.sg	
Name of person reviewing and contact details	**A. Paini**	
Date of checklist assessment	June 2020	
A. Context/Implementation		
A.1. Regulatory Purpose		
1. What is the acceptable degree of confidence/uncertainty (e.g. high, medium or low) for the envisaged application (e.g. priority setting, screening, full assessment?)	**High**	
2. Is the degree of confidence/uncertainty in application of the PBK model for the envisaged purpose greater or less than that for other assessment options (e.g. reliance on PBK model and *in vitro* data vs. no experimental data)?	**High**	
A.2. Documentation		
3. Is the model documentation adequate, i.e. does it address the essential content of model reporting template, including the following:	**Yes**	
• Clear indication of the chemical, or chemicals, to which the model is applicable?	**Yes**	
• Is the model being applied for the same scientific purpose as it was developed, or has it been repurposed somehow?	**Yes**	
• Model assumptions?	**Yes**	
• Graphical representation of the proposed mode of action, if known?	**Yes**	
• Graphical representation of the conceptual model?	**Yes**	
• Supporting tabulation for parameters (names, meanings, values, mean and standard deviations, units and sources)?	**Yes**	
• Relevance and reliability of model parameters?	**Yes**	
• Uncertainty and sensitivity analysis?	**Yes**	
• Mathematical equations?	**Yes**	(Jamei *et al.*, 2009; Chan *et al.*, 2019)
• PBK model code?	**Yes**	
• Software algorithm to run the PBK model code?	**Yes**	

• Qualification of PBK software platform?	**Yes**	(Jamei *et al.,* 2009; Shebley *et al.*, 2018)
A.3 Software Implementation and Verification		
4. Does the model code express the mathematical model?	**-**	**We do not have the two so we cannot asses, but the code represents the chemical MoA**
5. Is the model code devoid of syntactic and mathematical errors?	**Yes**	
6. Are the units of input and output parameters correct?	**Yes**	
7. Is the chemical mass balance respected at all times?	**Yes**	
8. Is the cardiac output equal to the sum of blood flow rates to the tissue compartments?	**Yes**	
9. Is the sum total of tissue volumes equal to total body volume?	**No**	
10. Is the mathematical solver a well-established algorithm?	**Yes**	
11. Does the mathematical solver converge on a solution without numerical error?	**Yes**	
12. Has the PBK modelling platform been subjected to a verification process (for a different use, for instance, in the pharmaceutical domain)?	**Yes**	Verified extensively in pharmaceutical domain
A.4 Peer engagement (input/review)		
13. Has the model been used previously for a regulatory purpose?	**Yes**	Use of Simcyp by the US FDA for regulatory purposes has been extensively published in peer-reviewed journals
• Is prior peer engagement in the development and review of the model sufficient to support the envisaged application?	**-**	
• Is additional review required? Peer engagement includes input/review by experts on specific aspects of model development, individual reviews of the model by experts, or collective reviews by peer review panels. Availability of the comments and tracking of revisions to the model in response to peer input contributes to increased confidence in the model for potential application.	**No**	
B. Assessment of Model Validity		
B.1 Biological Basis (Model Structure and Parameters)		
14. Is the model consistent with known biology?	**Yes**	
• Is the biological basis for the model structure provided?	**Yes**	
• Is the complexity of the model structure appropriate to address the regulatory application?	**Yes**	
• Are assumptions concerning the model structure and parameters clearly stated and justified?	**Yes**	
• Is the choice of values for physiological parameters justified?	**Yes**	

• Is the choice of methods used to estimate chemical-specific ADME parameters justified?	**Yes**	
• Saturable kinetics	**No**	
B.2 Theoretical Basis of Model Equations		
15. Are the underlying equations based on established theories, .e.g. Michaelis-Menten kinetics, Fick's laws of diffusion?	**Yes**	
• In the case of PBK models for particles, does the model take into consideration the properties of particles, e.g. particle size ranges, (poor) solubility, aggregation, partitioning and diffusion/sedimentation behaviour?	**NA**	
B.3. Reliability of input parameters		
16. Has the uncertainty (individual variability, experimental reproducibility and reliability) in the input parameters been characterised?	**Partially**	**In the measured one yes**
B.4. Uncertainty and Sensitivity Analysis		
17. Has the impact of uncertainty (individual variability, experimental reproducibility and reliability) in the parameters on the chosen dose metric been estimated?	**Yes by SA**	
• Local sensitivity analysis?	**Yes**	
• Global sensitivity analysis?	**No**	
18. Is confidence in influential input parameter estimates (i.e., based on comparison of uncertainty and sensitivity) reasonable (within expected values; similar to those of analogues) in view of the intended application?	**Yes**	
B.5. Goodness-of-Fit and Predictivity		
19. For PBK models for which there are sufficient *in vivo* data for the chemical of interest:		
• Suitability as analogue (chemical and biological similarity) been assessed?	**Yes**	
• Reliable estimation of chosen dose metric for analogue?	**Yes**	
• In general is the biological Variability of *in vivo* reference data (from analogue) established?	**Yes**	

Part III Overall Evaluation

Overall Conclusion on mode evaluation for the intended application

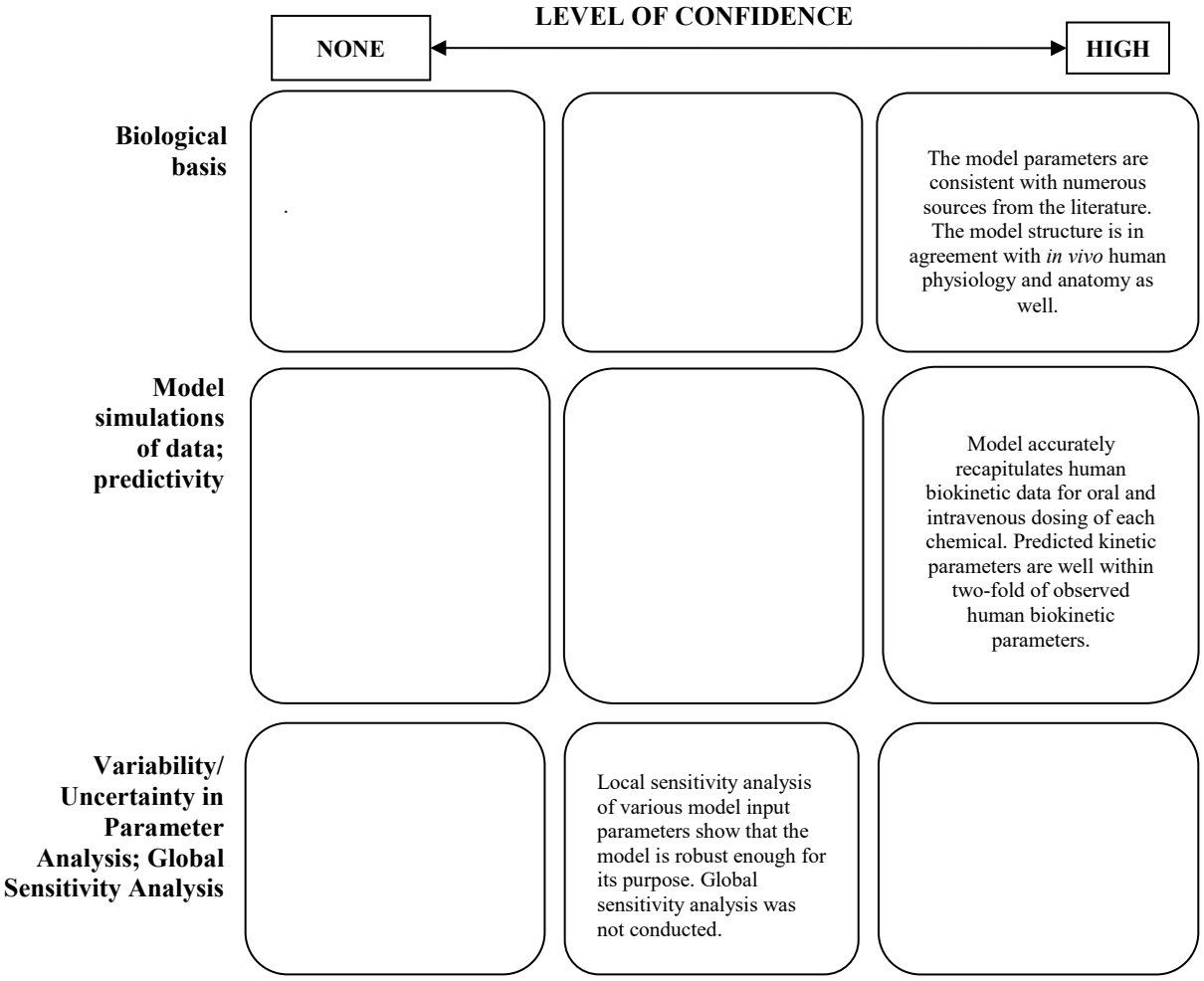

The PBK model was developed account for differences in transporter and metabolic enzyme expression between *in vitro* and *in vivo* systems measured using quantitative proteomics is crucial for the accuracy of PBK models for chemicals. The model is well characterised, the biological basis of some model parameters, model structural elements are consistent with what is reported in literature. Assumptions are reported to underline the uncertainties; the Model reproduces consistently all kinetic data, including the shape of time course profiles for chemical of interest, for the calibrated person. Based on all the evidence provided the following model will have a medium/standard level of confidence. Thus, it is recommended that the PBK model described here and relative output, can be used in a regulatory framework only as supporting information.

Case Study VIII

PBK model application in species and route-to-route extrapolation

Part I. PBK model reporting template

A. Name of model

PBK model application in interspecies and route-to-route extrapolation

B. Contact details

Authors: Jos G.M.Bessems, AliciaPaini, Monika Gajewska, Andrew Worth.

Affiliation: European Commission, Joint Research Centre, Ispra, Italy

C. Summary of model characterisation, development, validation, and regulatory applicability

The present paper presents a methodological case study following the is margin of internal exposure (MOIE) approach to characterise the risk of caffeine exposure in a dermal product using data based on an oral bioassay (Figure VIII1). Caffeine was chosen for this case study for oral-to-dermal extrapolation since it is an ingredient in cosmetics and oral animal toxicity data are present. A rat PBK model was developed for caffeine to convert the chosen oral NOAEL to the internal dose metrics AUC and C_{max} of caffeine, as well as of its most relevant metabolite paraxanthine. Secondly, we used an oral human PBK model (Gajewska et al., 2014, Gajewska et al., 2015) to predict human internal dose metrics. Data from an oral human volunteer study were used to calibrate some of the PBK model parameters. Subsequently, the calibrated human oral model was extended with a dermal compartment to accommodate a few realistic exposure scenarios involving the topical use of cosmetic products. QSARs were used to simulate human dermal penetration. Finally, the resulting internal dose metrics for the rat (oral) and the human (dermal) were compared in terms of resulting MOIE. With the present work we cover the extrapolations oral to dermal, high rat to low human as well as single to repeated.

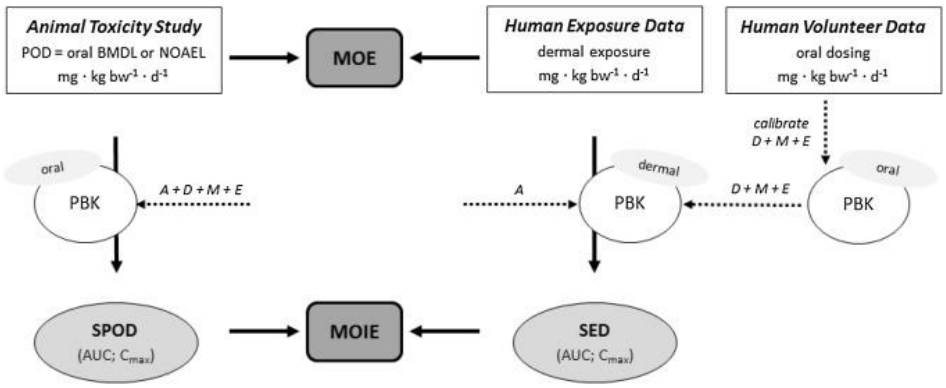

Figure VIII1. Conceptual depiction of the margin of internal exposure (MOIE) approach based on comparison of internal dose metrics. The individual assessment factor (AF) of 4

that should cover interspecies differences in toxicokinetics (TK) can be left out in the MOIE approach as these differences are taking into account using the PBK approach (animal PBK model and human PBK model). aPBK = animal PBK model; hPBK = human PBK model. SED = Systemic exposure dose; SPOD = Systemic Point of Departure.

D. Model characterisation (modelling workflow)

Step 1 – Scope and purpose of the model (problem formulation)

Route-to-route extrapolation is a common part of human risk assessment. Data from oral animal toxicity studies are commonly used to assess the safety of various but specific human dermal exposure scenarios. Using theoretical examples of various user scenarios, it was concluded that delineation of a generally applicable human dermal limit value is not a practicable approach, due to the wide variety of possible human exposure scenarios, including its consequences for internal exposure. Using physiologically based kinetic (PBK) modelling approaches to predict animal as well as human internal exposure dose metrics excellent opportunities to investigate the consequences of variations in human dermal exposure scenarios.

Step 2 – Model conceptualisation (model structure, mathematical representation)

A rat PBK model was developed for caffeine to convert the chosen oral NOAEL to the internal dose metrics AUC and C_{max} of caffeine, as well as of its most relevant metabolite paraxanthine. Secondly, we used an oral human PBK model (Gajewska et al., 2014, Gajewska et al., 2015) to predict human internal dose metrics. Data from an oral human volunteer study were used to calibrate some of the PBK model parameters. Subsequently, the calibrated human oral model was extended with a dermal compartment to accommodate a few realistic exposure scenarios involving the topical use of cosmetic products. QSARs were used to simulate human dermal penetration. Finally, the resulting internal dose metrics for the rat (oral) and the human (dermal) were compared in terms of resulting MOIE. With the present work we cover the extrapolations oral to dermal, high rat to low human dose metric as well as single to repeated.

QSAR modelling was used to predict dermal absorption, these information were needed for the human dermal PBK model. The various theoretical models were applied and integrated in order to develop an approach for assessing dermal bioavailability. Parts of the human PBK model were published before (Gajewska et al., 2014, Gajewska et al., 2015). The dermal human model was based on the oral human PBK model (Gajewska et al., 2014). The oral rat model was developed for the current project by replacing in the human model the human parameters with the rat parameters (rat physiology and anatomy, see appendix). Chemical specific parameters were kept the same as in the human model, which had been set after optimization to the human volunteer blood data (Gajewska et al., 2014). See figure VIII2 for the overall PBK model structures. PBK model assumptions are reported under (D) Model characterisation.

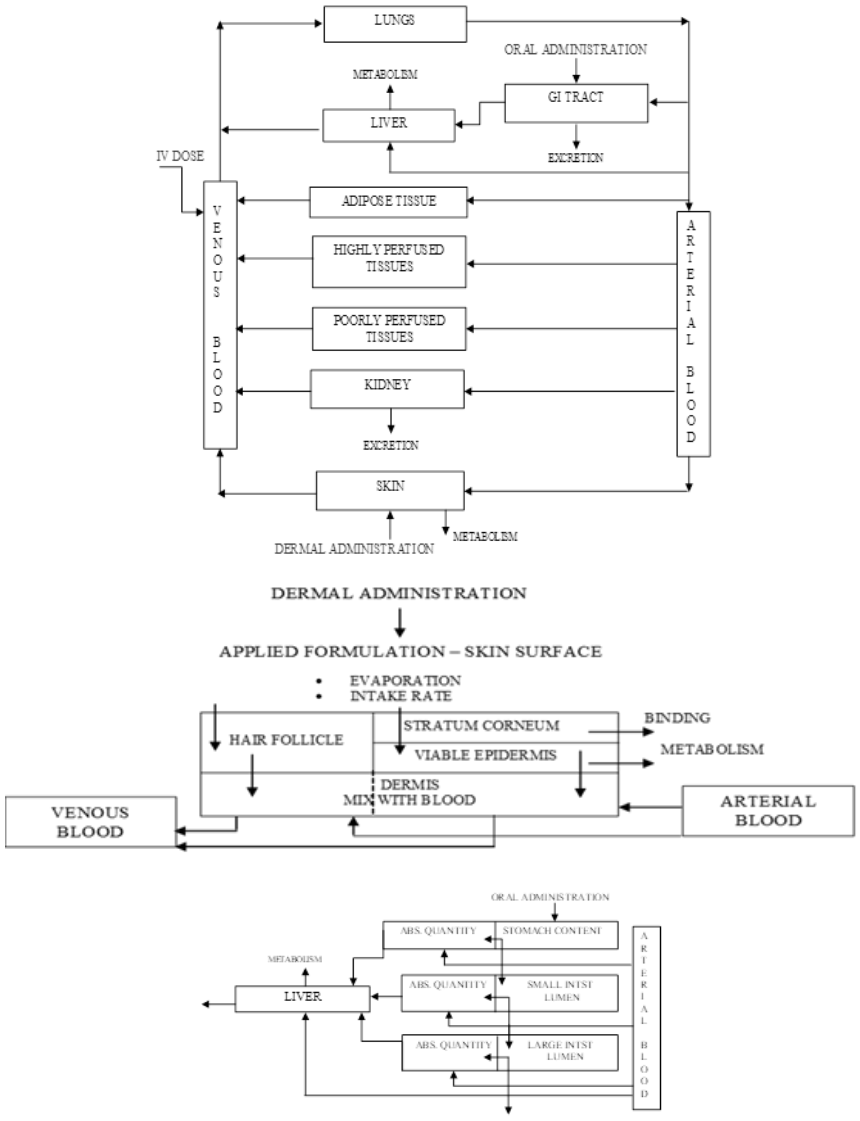

Figure VIII2. Overall PBK model structures.

We illustrate the integrated use of different modelling approaches to simulate the *in vivo* kinetics of dermally applied caffeine. At the heart of this are a series of PBK models that were developed here or earlier: an oral rat model and a dermal human model for which some elimination parameters were calibrated using oral human volunteer data and the dermal absorption by using dermal human volunteer data.

The PBK modelling approach was based on the following assumptions:

a) In the human models, skin and GI tract are represented by sub-compartments, FigureVIII2. The sub-compartments account for the complexity of the absorption process (especially the time-lag in absorption). In the rat PBK model the GI tract is represented by a single compartment and a first order rate absorption is assumed.

b) In the human PBK model for oral absorption, the GI tract is represented by 6 sub-compartments (Figure VIII2). In modelling absorption along the GI tract following gavage administration dissolution from matrix, stomach emptying rate and a first order rate of absorption from stomach, small and large intestine were taken into account.

c) In the rat PBK model for oral absorption, the GI tract is represented by a single compartment with first order rate of absorption following administration via food or water for caffeine (light meal followed directly by intake of a little water in which the caffeine was dissolved which means that exposure of the stomach is actually represented as food exposure). The value of this absorption rate and of metabolic parameters (liver metabolism) were obtained by fitting to oral rat experimental data for caffeine (Mohiuddin et al., 2009).

d) For PBK modelling of human dermal exposure, 4 compartments were used for dermal exposure (surface compartment for the product formulation and 3 skin sub-compartments: *stratum corneum*, viable epidermis and dermis perfused by blood), with the addition of one extra skin sub-compartment representing hair follicles (see Figure VIII2). This model was selected because it gave the best goodness of fit (Gajewska et al., 2014).

e) Unidirectional diffusion describes the one-way transport in fine skin (skin without hair follicles) and hair follicles according to Fick's second law with specified initial and boundary conditions. The diffusion coefficients are different for the *stratum corneum*, viable epidermis and hair follicles and assumed constant throughout the skin absorption process. It is assumed that the test compound is applied onto the skin surface in a pure solvent (vehicle) to account for a simple formulation (i.e. in ethanol, acetone). No mixture effects are considered and the vehicle is assumed to disappear from the skin surface (in model constructed as separate compartment) only due to possible evaporation.

f) Metabolism is assumed to occur only in the liver.

g) The liver metabolism was assumed to follow Michaelis–Menten kinetics. The V_{max} and K_m used in the present work are reported in Gajewska et al., 2014.

h) Excretion via urine is described by a first order rate constant.

i) Tissues are assumed to be homogenised compartments with respect to the concentration of a chemical (instantaneous distribution of chemical or metabolite once it is delivered by the arterial blood). Transport between blood and tissues is assumed to be flow-limited (assuming that transport barriers between free molecules of chemical in blood and tissue are negligible) and equilibrium between free and bound fractions in blood and tissue is instantaneous. We used the QSAR-based Schmitt approach to calculate a partition between the blood and the organs of interest (Schmitt, 2008). The model calculates steady-state tissue:plasma partition coefficients based on the composition of the tissues in terms of water, neutral lipids, neutral and acidic phospholipids and proteins using the lipophilicity, the binding to phospholipid membranes, the pKa and the unbound fraction in blood plasma as compound specific parameters. For caffeine, calculations were done for pKa 10.4, LogPoct = −0.07 (octanol-water partition coefficient) and fu = 0.65 (fraction bound to proteins).

j) Inter-individual differences in metabolism and excretion are not explicitly considered (only deterministic modelling). To partially account for such variations, the metabolic rates are corrected by the subject's body weight.

Step 3 – Model parameterisation (parameter estimation and analysis)

Anatomical/physiological parameters for rat and humans (reference woman and reference man) were taken from literature (Brown et al., 1997) and listed in the table VIII1. All physiological parameters for a reference man, woman and rat that are independent of the chemical and constitute a constant part of the model equations (see step 3). The ADME parameters for oral and dermal absorption of caffeine are given in table VIII2. For the oral human model, the most sensitive parameters (GIT dissolution rates, first order uptake rate constants and metabolism parameters for liver) were optimized using measured human data. Liver metabolism parameters were taken from the literature and were optimized with respect to *in vivo* blood concentrations using human data for the main metabolites (Gajewska et al., 2015).

As reported in Gajewska et al. (2015) *in vivo* plasma concentrations of caffeine following oral absorption were taken from: (i) Lelo et al. (1986) where a non-smoking male volunteer ingested only once 270 mg of caffeine in a gelatin capsule followed by 150 mL of water; (ii) Csajka et al. (2005) where caffeine was given orally in a gelatin capsule (200 mg of caffeine sulphate) to 16 subjects and in a commercial dietary supplement (a mixture containing 200 mg caffeine and 20 mg ephedrine alkaloids) to 8 subjects. For model validation, plasma concentrations from the oral study by Newton et al. (1981) were selected, in which a gelatin capsule containing 300 mg of caffeine was administered to one male subject. Plasma caffeine levels after dermal absorption were taken from Otberg et al. (2008). In this experiment, caffeine in an ethanol/propylene glycol vehicle was administered to 6 male volunteers by applying the liquid onto a chest area of 25 cm^2 for 24 h. In contrast to other dermal absorption studies, the additional impact of hair follicles in the overall absorption process was considered.

The equations of the QSARs applied for assessing dermal bioavailability are given in Gajewska et al. (2014). A review of *in vitro* and QSAR methods for predicting dermal absorption is given in Dumont et al. (2015). In order to explore models for predicting liver and skin metabolism the OECD QSAR Toolbox was applied. For caffeine, five metabolites were predicted by a QSAR approach for liver metabolism and one for skin metabolism. However, in case of skin metabolism, neither *in vitro* nor *in vivo* data were found with respect to the relevance, quantity and/or the metabolic rate constants (V_{max}, K_m). Therefore, the formation of these metabolites was not included in the PBK model.

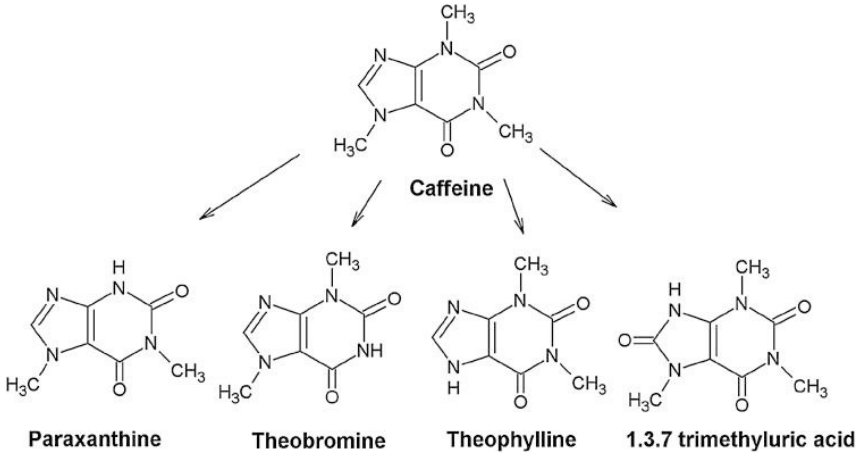

Figure VIII3. Caffeine MoA: metabolites formation

Step 4 – Computer implementation (solving the equations)

The mathematical equations were programmed in R language by combining functionalities of the following R packages available from "The Comprehensive R Archive Network" website (http://cran.r-project.org): deSolve, ReacTran, PK, FME, rgenoud and AICcmodavg. Ordinary differential equations (ODEs) were solved by the method *lsoda* available in the deSolve package. The method of lines was used to solve partial differential equations (PDEs). Further details of the mathematical equations are given in Appendix A1 in Supplementary material of the publication Bessems et al., 2017.

Mathematical equations for the PBK models (Gajewska et al., 2014; 2015)

- Adipose tissue and highly- and poorly-perfused tissues

$$\frac{dA_{org}}{dt} = f_{org} \cdot \left(C_{art} - \frac{C_{org}}{PC_{org}} \right), \quad A_{org}(t=0) = 0, \quad C_{art} = \frac{C_{art}}{V_{art}} \quad C_{org} = \frac{A_{org}}{V_{org}} \tag{A1.1}$$

where: org = organ name (adp, hpt, ppt)

- Metabolism is assumed to occur mainly in the liver

$$\frac{dA_{liv}}{dt} = Fl_{GIT} + FORM_{liv} + f_{liv} \cdot \left(C_{art} - \frac{C_{liv}}{PC_{liv}} \right) - MET_{liv}, \quad A_{liv}(t=0) = 0, \quad C_{liv} = \frac{A_{liv}}{V_{liv}} \tag{A1.2}$$

Where, for a parent compound:

$$Human: Fl_{GIT} = fra \cdot f_{git} \cdot \frac{C_{stm}}{PC_{git}} + frb \cdot f_{git} \cdot \frac{C_{SI}}{PC_{git}} + frc \cdot f_{git} \cdot \frac{C_{LI}}{PC_{git}}$$

$$Rat: Fl_{GIT} = ka_{GI,rat} \cdot \frac{C_{GI,rat}}{PC_{GI,rat}}$$

$FORM_{liv} = 0$ (rate of formation of metabolites)

In most cases, metabolism was assumed to follow Michaelis–Menten kinetics (A1.3) or was described by the first order reaction (A1.4). The liver metabolic parameter values as

calibrated and optimised using the oral human volunteer data were taken unchanged to the human dermal model.

$$\frac{\mathrm{V}_{\max} \cdot \frac{C_{liv}}{PC_{liv}}}{\mathrm{K}_{\mathrm{m}} + \frac{C_{liv}}{PC_{liv}}} \qquad \text{(A1.3)}$$

$$K_{\mathrm{met}} \cdot \frac{C_{liv}}{PC_{liv}} \qquad \text{(A1.4)}$$

where:

Cliv is the liver concentration and PCliv is the liver-to-blood partition coefficient of a substance undergoing metabolism.

$$\frac{dA_{kid}}{dt} = f_{kid} \cdot \left(C_{art} - \frac{C_{kid}}{PC_{kid}} \right) - CLR \cdot \frac{C_{kid}}{PC_{kid}} \qquad \text{(A1.5)}$$

Venous blood mass balance is as follows:

$$\frac{dA_{ven}}{dt} = f_{liv} \cdot \frac{C_{liv}}{PC_{liv}} + f_{ppt} \cdot \frac{C_{ppt}}{PC_{ppt}} + f_{hpt} \cdot \frac{C_{hpt}}{PC_{hpt}} + f_{adp} \cdot \frac{C_{adp}}{PC_{adp}} + f_{kid} \cdot \frac{C_{kid}}{PC_{kid}} + Fl_{skn} - f_{crd} \cdot C_{ven}, \quad A_{ven}(t=0) = 0, \quad C_{ven} = \frac{A_{ven}}{V_{ven}} \qquad \text{(A1.6)}$$

where, for dermal absorption only: $Fl_{skn} = \frac{3}{4} \cdot f_{skn} \cdot \frac{C_{skn}}{PC_{skn}} + \frac{1}{4} \cdot f_{skn} \cdot \frac{C_{sknhf}}{PC_{skn}}$ otherwise $Fl_{skn} = 0$

We assume that plasma accounts for 55% of blood volume.

Plasma quantification: $C_{ven,PL} = \frac{A_{ven} \big/ (0.55 \cdot V_{ven})}{RBP}$ (A1.7)

Arterial blood mass balance:

$$\frac{dA_{\ln g}}{dt} = f_{\ln g} \cdot \left(C_{ven} - \frac{C_{\ln g}}{PC_{\ln g}} \right); \quad A_{\ln g}(t=0) = 0; \quad C_{\ln g} = \frac{A_{\ln g}}{V_{\ln g}} \qquad \text{(A1.8)}$$

$$\frac{dA_{art}}{dt} = f_{crd} \cdot \left(\frac{C_{\ln g}}{PC_{\ln g}} - C_{art} \right); \quad A_{art}(t=0) = 0 \qquad \text{(A1.9)}$$

Oral Rat absorption

A single compartment representing the GI tract with first order rate of absorption:

$$\frac{dA_{GI,rat}}{dt} = -ka_{GI,rat} \cdot \frac{C_{GI,rat}}{PC_{GI,rat}} \qquad \text{(A1.10)}$$

Human GI tract model consists of sub-compartments:

Stomach content: $\frac{dA_{stm,cont}}{dt} = D_{rt} - ka_{stm} \cdot C_{stm,cont} - kGIT \cdot A_{stm,cont}$ (A1.11)

with: $C_{stm,cont} = \frac{A_{stm,cont}}{V_{stm}}, \quad kGIT = \frac{k_{\max}}{(1 + k_{\min} \cdot C_{stm})}$

and:

administration via gavage: $D_{rt} = 0$ and $A_{stm,cont}(t=0) = Dose$

administration by a coated tablet:

$$D_{rt} = Diss \cdot \frac{dA_{stm,cont,diss}}{dt} \text{ and } A_{stm,cont,diss}(t=0) = dose,\ A_{stm,cont}(t=0) = 0$$

Stomach tissue:

$$\frac{dA_{stm}}{dt} = ka_{stm} \cdot C_{stm,cont} + fra \cdot f_{git} \cdot \left(C_{art} - \frac{C_{stm}}{PC_{git}} \right), \quad A_{stm}(t=0) = 0, \quad C_{art} = \frac{A_{art}}{V_{art}}, \quad C_{stm} = \frac{A_{stm}}{V_{stm}} \tag{A1.12}$$

Small intestine lumen and absorbed quantity:

$$\frac{dA_{SI,lumen}}{dt} = kGIT \cdot A_{stm,cont} - (ka_{SI} + flow_{LI}) \cdot C_{SI,lumen}, \qquad A_{SI,lument}(t=0) = 0, \qquad C_{SI,lumen} = \frac{A_{SI,lumen}}{\left(\frac{3}{4} \cdot V_{\text{int}}\right)}$$

(A1.13)

$$\frac{dA_{SI}}{dt} = ka_{SI} \cdot C_{SI,lumen} + frb \cdot f_{git} \cdot \left(C_{art} - \frac{C_{SI,}}{PC_{git}} \right), \qquad A_{SI}(t=0) = 0, \qquad C_{SI} = \frac{A_{SI}}{\left(\frac{3}{4} \cdot V_{\text{int}}\right)}$$

(A1.14)

Large intestine lumen and absorbed quantity:

$$\frac{dA_{LI,lumen}}{dt} = flow_{LI} \cdot C_{SI,lumen} - \left(kel_{LI} + ka_{LI}\right) \cdot C_{LI,lumen}, \qquad A_{LI,lumen}(t=0) = 0, \qquad C_{LI,lumen} = \frac{A_{LI,lumen}}{\left(\frac{1}{4} \cdot V_{\text{int}}\right)}$$

(A1.15)

$$\frac{dA_{LI}}{dt} = ka_{LI} \cdot C_{LI,lumen} + frc \cdot f_{git} \cdot \left(C_{art} - \frac{C_{LI}}{PC_{git}} \right), \qquad A_{LI}(t=0) = 0, \qquad C_{LI} = \frac{A_{LI}}{\left(\frac{1}{4} \cdot V_{\text{int}}\right)} \tag{A1.16}$$

Skin surface:

$$or(t < t_{appl})\ AbsRate = -(ka_{form} \cdot C_{form} + ka_{hf} \cdot C_{form}) \text{ and } for(t > t_{appl})\ AbsRate = 0$$

(A1.17)

Where: tappl is the application time of a formulation on the skin.

Evaporation of a vehicle (EvapRate) is calculated for volatile substances according to Tibaldi et al., (Tibaldi, ten Berge, & Drolet, 2011):

$$EvapRate = \frac{-k_{evp}}{TL} \tag{A1.18}$$

For a vehicle (solvent) this evaporation is quantified in terms of decrease of an applied solution volume in time rather than mass of the solvent:

$$\frac{dV_{appliedFom}}{dt} = -\frac{k_{evp} \cdot Area}{1000 \cdot \sigma_{form}} \qquad V_{appliedFom}(t=0) = V_{0,appliedFom} \tag{A1.19}$$

where: $k_{evp} = \frac{\beta \cdot MW \cdot V_p}{R \cdot T \cdot 10} \left[\frac{mg}{h \cdot cm^2} \right]$ $\qquad \beta = \frac{0.0111 \cdot \nu_{air}^{0.96} \cdot D_g^{0.19}}{\upsilon^{0.15} \cdot X^{0.04}}$

where β is the mass transfer coefficient in vapour phase (m h^{-1}), MW the molecular weight, V_p the vapour pressure of the liquid at skin temperature (Pa), R the gas constant in J $mol^{-1}K^{-1}$, T the skin temperature (assumed to be 303K which equals 29.85°C), V_{air} the velocity of air (at workplaces it ranges from 0.3-0.6 m s^{-1}), D_g the diffusivity of the liquid in gas phase (range: 0.03 to 0.06 m^2h^{-1}), ϑ the kinematic viscosity of air (literature value of 0.054 m^2 h^{-1}), X the length of evaporation area in the direction of air stream, TL a thickness of applied substance layer (cm), $Area$ the application area (cm^2) and δ_{form} the density of solvent (g cm^{-3}).

Stratum corneum (SC):

Passive diffusion is modelled according to Fick's second law of unidimensional diffusion with initial and boundary conditions (tappl is a time of experiment duration, after which the remaining formulation is wiped off from skin surface). The diffusion coefficient is assumed to be constant throughout the process:

$$\frac{dC_{SC,i}}{dt} \approx -\frac{q_{SC,i+1} - 2 \cdot q_{SC,i} + q_{SC,i-1}}{\left(\frac{Lsc}{N}\right)}; i = 1:N \qquad C_{SC,i} = \frac{A_{SC,i}}{V_{SCi}} \tag{A1.20}$$

$$q_{SC.,i} = -Dsc_i \cdot \frac{C_{SC,i+1} - 2 \cdot C_{SC,i} + C_{SC.,i-1}}{\left(\frac{Lsc}{N}\right)}; i = 1:N$$

where:

Initial and boundary conditions:

$$C_{SC}(t=0)|_{0 \le x \le L_{SC}} = 0$$

$$\frac{dC_{SC}}{dt}(t>0)|_{x=0} = ka_{form} \cdot C_{form}$$

$$D_{SC} \cdot \frac{dC_{SC}}{dx}(t > t_{appl})|_{x=0} = 0$$

$$C_{SC}(t>0)|_{x=0} = PC_{SC} \cdot C_{form}$$

$$C_{SC}(t>0)|_{x=L_{SC}} = PC_{SCVE} \cdot C_{VE}$$

Viable epidermis (VE):

The reaction-diffusion partial differential equations for viable epidermis are solved in the same manner, by means of the methods of lines approach:

$$\frac{dC_{VE,j}}{dt} \approx -\frac{q_{VE,j+1} - 2 \cdot q_{VE,j} + q_{VE,j-1}}{\left(\frac{Lve}{M}\right)} - \frac{BioC_{VE,j}}{V_{VE,j}}; j = 1:M \qquad C_{VE,j} = \frac{A_{VE,,j}}{V_{VE\,j}} \tag{A1.21}$$

$$q_{VE,j} = -D_{VE,j} \cdot \frac{C_{VE,j+1} - 2 \cdot C_{VE,j} + C_{VE,j-1}}{\left(\frac{L_{VE}}{M}\right)}; j = 1:M \quad \text{and} \quad BioC_{VE,j} = \frac{V\max_{m,j} \cdot C_{VE,j}}{Km_m + C_{VE,j}}$$

Where:

Initial and boundary conditions:

$$C_{VE}(t=0)|_{0 \le y \le L_{VE}} = 0$$

$$C_{VE}(t>0)|_{y=0} = \frac{C_{SC,i=N}}{PC_{SCVE}}$$

$$D_{SC}\frac{dC_{SC}}{dx}|_{x=L_{SC}} = D_{VE} \cdot \frac{dC_{VE}}{dy}|_{y=0}$$

$$C_{VE}(t>0)|_{y=L_{VE}} = PC_{skn} \cdot C_{skn}$$

If skin metabolism occurs, its rate is assumed to follow first order kinetics (until more data become available). The model simulations were run for N=M=10 layers.

Dermis and mix with blood:

$$\frac{dA_{skn}}{dt} = \frac{3}{4} \cdot f_{skn} \cdot \left(C_{art} - \frac{C_{skn}}{PC_{skn}} \right) + q_{VE,j=M} \cdot \frac{100 - nf}{100} \cdot Area \qquad A_{skn}(t=0) = 0 \qquad C_{skn} = \frac{A_{skn}}{10^{-3} \cdot \frac{2}{3} \cdot Vde} \tag{A1.22}$$

Hair follicles compartment (Bookout Jr., Quinn, & McDougal, 1997):

$$\frac{dC_{hf,i}}{dt} \approx -\frac{q_{hf,i+1} - 2 \cdot q_{hf,i} + q_{hf,i-1}}{\left(\frac{Lhf}{K}\right)}; i = 1:K \qquad L_{hf} = \frac{388}{560} \cdot L$$

$$q_{hf.,i} = -D_{hf_i} \cdot \frac{C_{hf,i+1} - 2 \cdot C_{hf,i} + C_{hf.,i-1}}{\left(\frac{L_{hf}}{K}\right)}; i = 1:K \tag{A1.23}$$

The initial and boundary conditions:

$$C_{hf}(t=0)|_{0 \le x \le L_{hf}} = 0$$

$$\frac{dC_{hf}}{dt}(t>0)|_{x=0} = ka_{hf} \cdot C_{form}$$

$$D_{hf} \cdot \frac{dC_{hf}}{dx}(t > t_{appl})|_{x=0} = 0$$

$$C_{hf}(t>0)|_{x=0} = PC_{hf,} \cdot C_{form}$$

$$C_{hf}(t>0)|_{x=L_{hf}} = PC_{Skn} \cdot C_{sknhf}$$

Hair follicles: mix with blood

$$\frac{dA_{skinhf}}{dt} = \frac{1}{4} \cdot f_{skn} \cdot \left(C_{art} - \frac{C_{sknhf}}{PC_{skn}} \right) + q_{hf,i=K} \cdot \frac{nf}{100} \cdot Area \qquad A_{sknhf}(t=0) = 0 \qquad C_{sknhf} = \frac{A_{sknhf}}{10^{-3} \cdot \frac{1}{3} \cdot Vde} \tag{A1.24}$$

List of symbols

Symbol	Parameter [unit]
A_{org}	amount of a chemical in organ/tissue [mg]
Area	application area on skin [cm^2]
CLR	renal clearance rate [L/h]
C_{org}	concentration of a chemical in organ/tissue [mg/L]
D_{HF}	diffusion coefficient in coefficient in hair follicles [cm^2/h]
Diss	dissolution from a coated matrix [L/h]
D_{SC}	diffusion coefficient *in stratum corneum* [cm^2/h]
Dt	drinking rate [L/h]
D_{VE}	diffusion coefficient in viable epidermis [cm^2/h]
f_{crd}	cardiac output [L/h]
$flow_{LI}$	flow rate from small intestine into large intestine [L/h]

f_{org}	regional blood flow rates [L/h]
Fl_{GIT}	amount from the GI tract [mg]
Flskn	amount from the skin [mg]
ka_{form}	intake rate of chemical from formulation by stratum corneum [mL/h]
ka_{HF}	intake rate of a chemical from formulation by hair follicles [mL/h]
ka_{LI}	absorption rate from large intestine lumen [L/h]
ka_{SI}	absorption rate from small intestine lumen [L/h]
ka_{stm}	absorption rate into stomach tissue [L/h]
$ka_{GI,rat}$	absorption rate into GI tract for rat [L/h]
kel_{LI}	elimination rate in large intestine lumen [L/h]
K_m	chemical concentration at which the reaction rate is half of the maximal
K_{met}	first order rate of formation of metabolites [L/h]
K_{min}, K_{max}	kinetic constants of stomach emptying rate of a chemical to small intestine
L_{sc}	thickness of *stratum corneum* [cm]
L_{ve}	thickness of viable epidermis [cm]
$PC_{bloodair}$	blood/air partition coefficient
PC_{HF}	partition coefficient hair follicle /solvent
PC_{org}	tissue-to- blood partition coefficients
PC_{SC}	partition coefficient *stratum corneum*/ solvent
PC_{SCVE}	partition coefficient *stratum corneum*/ viable epidermis
RBP	Blood-to-plasma concentration ratio
Rem_{bld}	bladder emptying rate [L/h]
$Rform_{Creat}$	formation rate of creatinine[mg/h]
V_{max}	the maximum rate metabolic rate at maximum (saturating) concentration of
V_{org}	volume of organ/tissue

Step 5 – Model Performance

Parameters were analysed using the sensitivity analysis as reported in Gajewska et al. (2014). Briefly, the sensitivity analysis and parameter identifiability were performed to identify the most important and sensitive parameters with respect to the blood/plasma AUC for caffeine according to Soetaert and Petzoldt (Soetaert and Petzoldt, 2010) prior to their optimization. In local sensitivity analysis Eq. (1), all parameters were evaluated individually in a very small region close to their nominal value. A parameter value divided by the average of simulated outputs was used as a scaling factor (SF).

x=f(x,u,φ)y=g(x,φ)Sij=(φj0SF)∂yi∂φj|φ=φ0 (1)

L1=∑||Sij||NL2=√∑S2ijN (2)

γ=1√min(EV)[ˆsT⋅ˆs] (3)

where y is vector of function outputs for a specific variable; x is vector of state variables; θ is vector of parameters (θ 0parameter estimate); u is vector of inputs; N is number of time points;ˆs is the columns of the sensitivity matrix that correspond to the parameters included in the set; EV is estimation of the eigenvalues.

The following kinetic and compound-specific parameters were analyzed: GItract absorption rates (D_{iss} (or D_t), k_{astm}, k_{aSI}, k_{aLI}, k_{elLI}, k_{max}, k_{min}), liver metabolic rates (V_{max}, kK_m, K_{met}), skin absorption parameters (D_{sc}, D_{ve}, D_{hf}, k_{aform}, k_{ahf}, PC_{sc},PC_{scve}, PC_{hf}), blood-to-plasma ratio and tissue-to-blood partition coefficients: PC_{liv}, PC_{adp}, PC_{ppt}, PC_{hpt}, PC_{kid}, PC_{lng}, PC_{git}, PC_{skn}. The higher the absolute sensitivity value, the more important is the parameter. These sensitivity functions are collapsed into summary values (L1 and L2 are used as selection criteria) (Eq. (2)). Based on the sensitivity functions of blood AUC to selected parameters, the identifiability of a set of parameters to be fine-tuned by calibration is then calculated. As a rule of thumb, a collinearity value (y) less than about 20 means "identifiable" (in general, when the collinearity index exceeds 20, the linear dependence is assumed to be critical (Eq. (3)) (Brun et al., 2001). The collinearity is a measure of approximate linear dependence between sets of parameters. The higher its value, the more the parameters are related. In this context, "related" means that several parameter combinations may produce similar values of the output variables.

Monte Carlo simulations were used to quantify the impact of variability and uncertainty in parameter distributions separately by drawing parameter values according to a predefined distribution (normally distributed random samples), running the model with each of these parameter combinations, and calculating the values of the selected output variables at each output interval. The parameters were optimised according to the Levenberg-Marquardt algorithm for nonlinear data fitting (Moré, 1978).

With an oral exposure to caffeine, the tissue-to-blood partition coefficients show comparable sensitivity to kinetic parameters in terms of blood/plasma AUC; however, lower sensitivity is observed in the case of dermal absorption. The most sensitive kinetic parameters are caffeine metabolic rate to paraxanthine (V_{max}), skin absorption rates (D_{sc}, D_{ve}, D_{hf}) and blood-to-plasma ratio. The most sensitive partition coefficients are: PC_{adp}, PC_{ppt}, PC_{kid} (oral model) and PC_{lng}, PC_{adp}, PC_{ppt} (dermal model).

Simulation graphs are available in the paper by Bessems et al., 2017.

Step 6 – Model Documentation

Bessems et al., 2017

E. Identification of uncertainties

Model structure

- The human models, skin and GI tract are represented by sub-compartments, Figure VIII2. The sub-compartments account for the complexity of the absorption process (especially the time lag in absorption). In the rat PBK model, the GI tract is represented by a single compartment and a 1st order rate absorption is assumed.
- Metabolism is assumed to occur only in the liver.
- First order oral absorption has been stated to be applicable to many pharmaceuticals. However, for non-pharmaceuticals, this is uncertain. In addition, the value for the first order absorption rate constant used may change for

significantly different exposure conditions. Predicted AUC as well as C_{max} values may deviate significantly from the real AUC and C_{max} (rat, human). The potential risk is significant over- or underestimation of actual risk

- No human first pass metabolism in skin. First pass metabolism reduces the internal exposure to the parent chemical. Internal exposure to the parent chemical is overestimated (either as AUC or as C_{max}). No consequence in comparison to default approach (just using total external dose). Larger risks predicted compared to when first pass metabolism in skin would have been taken into account.

Input parameters

- The model calculates steady-state tissue:plasma partition coefficients based on the composition of the tissues in terms of water, neutral lipids, neutral and acidic phospholipids and proteins using the lipophilicity, the binding to phospholipid membranes, the pKa and the unbound fraction in blood plasma as compound specific parameters. For caffeine, calculations were done for pKa 10.4, LogPoct = −0.07 (octanol-water partition coefficient) and fu = 0.65 (fraction bound to proteins).
- No genetic polymorphism in the human population. The values used for V_{max} and K_m in the present work are not representative for whole human population (it is known that there is genetic polymorphism).

Model output

- No genetic polymorphism in the human population
- Predicted AUC and V_{max} are not valid for whole human population. Risks maybe over- or under predicted for part of the human population.

Other uncertainties (e.g. model developed for different substance and/or purpose)

None reported.

F. Model implementation details

- software (version no) Not reported
- availability of code Available upon request, SEURAT 1 /COSMOS output
- software verification / qualification Not applicable

G. Peer engagement (input/review)

Not peer reviewed.

H. Parameter tables

Table VIII1. Anatomical and physiological parameters for a reference woman, a reference man and rat (Brown et al., 1997)

Parameter	Reference woman	Reference man	Rat
Average body weight [kg]	65	75	0.265
Organ weights fractions (fractions of body weight)			
Liver	0.026	0.026	0.0253
Adipose tissue	0.278	0.155	0.07
Lungs	0.0105	0.012	0.005
Kidney	0.0044	0.0044	0.0073
GI tract total	0.0265 *	0.025 *	0.046
Stomach	0.00337	0.00318	
Small intestine	0.0146	0.0138	
Large intestine	0.0085	0.0080	
Poorly perfused tissues + skin	0.436	0.525	0.667
Highly perfused tissues	0.153	0.181	0.1254
Blood total	0.065	0.072	0.054
Venous blood	0.04875	0.054	0.018
Thickness of skin [cm]			
Whole skin	0.204	0.2906	0.17
Viable epidermis	0.0032	0.0047	0.001
Stratum corneum	0.0018	0.0017	0.002
Dermis	?	?	?
Organ and tissue blood flow rates [fraction of cardiac output [L/h]			
Cardiac output [L/h]	$15 \cdot BW^{0.74}$		5.208
Liver	0.25	0.24	0.009
Adipose tissue	0.055	0.04	0.07
Skin	0.05	0.05	0.058
Highly perfused tissues	0.155	0.155	0.222
Poorly perfused tissues	0.135	0.16	0.4
Kidney	0.19	0.2	0.14
GI tract	0.14	0.13	0.08
Lungs	0.025	0.025	0.021

* Sum of stomach, small intestine and large intestine

Table VIII2. Human and Rat oral physiological parameters and ADME parameters for caffeine[1]

Parameter	Value
Physiological parameters oral	
Stomach emptying maximum rate k_{max} [L/h]	8.16 (Loizou & Spendiff, 2004)
Stomach emptying rate k_{min} [L/h]	0.005 (Loizou & Spendiff, 2004)
Release from formulation/matrix/capsule	
Dissolution from matrix Diss [L/h]	3.2
Absorption oral	
Stomach 1st order absorption rate constant ka_{stm} [L/h]	0.2
Small intestine 1st order absorption rate constant ka_{si} [L/h]	1.5
Large intestine elimination kel_{li} [L/h]	0.1
Absorption dermal	
Diffusion coefficient in stratum corneum D_{sc} [cm^2/h]	1.4e-07 (Hansen et al., 2008)
Diffusion coefficient in viable epidermis D_{ve} [cm^2/h]	1.5e-05 [2]
Diffusion coefficient in hair follicles D_{hf} [cm^2/h]	1.243e-05
Formulation intake rate from stratum corneum ka_{form} [mL/h]	0.2
Formulation intake rate from hair follicles ka_{hf} [mL/h]	0.153
Partition coefficient stratum corneum/vehicle PC_{sc}	2.5 (Hansen et al., 2008)
Partition coefficient stratum corneum/viable epidermis PC_{scve}	0.6 [2]
Partition coefficient hair follicles/vehicle PC_{hf}	1 [3]
% of hair follicles in skin (nf)	20

Blood/plasma ratio and tissue to blood partition coefficients (Schmitt, 2008)	
Blood-to-plasma ratio RBP	0.28-0.35 (Newton et al., 1981)
Liver: PC_{liv}	4.25
Poorly-perfused tissues: PC_{ppt}	0.995
Highly-perfused tissues:PC_{hpt}	1
Skin: PC_{skn}	1
Lungs: PC_{lng}	1.23
Kidney: PC_{kid}	3.76
GI tract: PC_{git}	1.49
Adipose tissue: PC_{adp}	0.68
Michaelis-Menten parameters	
caffeine to paraxanthine	V_{max} = 0.351[4]; K_m= 1
caffeine to theobromine	V_{max} = 0.0432; K_m=1 (Lelo et al., 1986; Zandvliet et al., 2005)
caffeine to theophylline	V_{max} = 0.0072; K_m=1 (Lelo et al., 1986; Zandvliet et al., 2005)
caffeine to trimethyluric acid	K_{met}=0.001 (Lelo et al., 1986; Zandvliet et al., 2005)

[1] Values without footnote or reference were fitted to experimental data; [2] Estimated by QSPRs; [3] PC_{hf} was set at 1 as no QSARs were found to predict it. Optimising it to a calibration set did not make sense as the diffusion coefficient had to be optimised as well and the two are strongly correlated. As the model is more sensitive to diffusion coefficient it was decided to optimise only that value in the usual range of values of diffusion coefficient (10^{-5}) and to set PC_{hf} for caffeine at 1, being a reasonable value between the usual boundaries of approx. 0.5 and 8 seen so far with this sort of chemicals; [4] Predicted by ADMET Predictor (https://www.simulations-plus.com/)

I. References and background information

Bookout Jr., R.L. Quinn, D.W. McDougal J.N. (1997) Parallel dermal subcompartments for modeling chemical absorption. SAR QSAR Environ. Res., 7, 259–279.

Brown, R.P., Delp, M.D Brown, R.P., Delp, M.D., Lindstedt, S.L., Rhomberg, L.R., Beliles, R.P., 1997. Physiological parameter values for physiologically based pharmacokinetic models. Toxicol. Ind. Health 13, 407–484.

Gajewska, M., Worth, A., Urani, C., Briesen, H., & Schramm, K. (2014). Application of physiologically-based toxicokinetic modelling in oral-to-dermal extrapolation of threshold doses of cosmetic ingredients. Toxicol Lett., 227(3).

Gajewska, M., Paini A., Sala Benito J, Burton J, Worth, A., Urani, C., Briesen, H., & Schramm, K. (2015). In vitro to in vivo correlation of the skin penetration, liver clearance and hepatotoxicity of caffeine. Food and Chemical Toxicology, 75, 39–49.

Hansen, S., Henning, A., Naegel, A., Heisig, M., Wittum, G., Neumann, D., Schaefer, U. F. (2008). In-silico model of skin penetration based on experimentally determined input parameters. Part I: Experimental determination of partition and diffusion coefficients. European Journal of Pharmaceutics and Biopharmaceutics, 68(2), 352–367.

Lelo, A., Birkett, D. J., Robson, R. A., & Miners, J. O. (1986). Comparative pharmacokinetics of caffeine and its primary demethylated metabolites paraxanthine, theobromine and theophylline in man. British Journal of Clinical Pharmacology, 22(2), 177–182.

Loizou, G. D., & Spendiff, M. (2004). A human PBPK model for ethanol describing inhibition of gastric motility. Journal of Molecular Histology, 35(7), 687–696.

Newton, R., Broughton, L. J., Lind, M. J., Morrison, P. J., Rogers, H. J., & Bradbrook, I. D. (1981). Plasma and salivary pharmacokinetics of caffeine in man. European Journal of Clinical Pharmacology, 21(1), 45–52.

Tibaldi, R., ten Berge, W., & Drolet, D. (2011). IH SkinPerm Help Manual.

Zandvliet, A. S., Huitema, A. D. R., De Jonge, M. E., Den Hoed, R., Sparidans, R. W., Hendriks, V. M., … Beijnen, J. H. (2005). Population pharmacokinetics of caffeine and its metabolites theobromine, paraxanthine and theophylline after inhalation in combination with diacetylmorphine. Basic and Clinical Pharmacology and Toxicology, 96(1), 71–79. Retrieved from http://www.scopus.com/inward/record.url?eid=2-s2.0-13844310313&partnerID=40&md5=b27d1606e33e9ae71c458ac3421c660f

Part II Checklist for model evaluation

PBK Model Evaluation Checklist	Checklist assessment	Comments
Name of the PBK model (as in the reporting template)	PBK model application in species and route to route extrapolation	
Model developer and contact details	**Authors:** Jos G.M.Bessems AliciaPaini, Monika Gajewska, Andrew Worth. **Affiliation:** European Commission, Joint Research Centre, Ispra, Italy	
Name of person reviewing and contact details	**L. Rossi**	
Date of checklist assessment	**June 2020**	
A. Context/Implementation		
A.1. Regulatory Purpose		
1. What is the acceptable degree of confidence/uncertainty (e.g. high, medium or low) for the envisaged application (e.g. priority setting, screening, full assessment?)	**High**	
2. Is the degree of confidence/uncertainty in application of the PBK model for the envisaged purpose greater or less than that for other assessment options (e.g. reliance on PBK model and *in vitro* data vs. no experimental data)?	**Standard**	
A.2. Documentation		
3. Is the model documentation adequate, i.e. does it address the essential content of model reporting template, including the following:	**Yes**	
• Clear indication of the chemical, or chemicals, to which the model is applicable?	**Yes**	
• Is the model being applied for the same scientific purpose as it was developed, or has it been repurposed somehow?	**Yes**	
• Model assumptions?	**Yes**	
• Graphical representation of the proposed mode of action, if known?	**Yes**	**Only metabolite formation**
• Graphical representation of the conceptual model?	**Yes**	
• Supporting tabulation for parameters (names, meanings, values, mean and standard deviations, units and sources)?	**Yes**	
• Relevance and reliability of model parameters?	**No**	
• Uncertainty and sensitivity analysis?	**Yes**	
• Mathematical equations?	**YES**	
• PBK model code?	**No**	**Available upon request**
• Software algorithm to run the PBK model code?	**Yes**	
• Qualification of PBK software platform?	**No**	

A.3 Software Implementation and Verification		
4. Does the model code express the mathematical model?	**NR**	**Without the model code we cannot establish this**
5. Is the model code devoid of syntactic and mathematical errors?	**NR**	**Without the model code we cannot establish this**
6. Are the units of input and output parameters correct?	**NR**	**Without the model code we cannot establish this**
7. Is the chemical mass balance respected at all times?	**NR**	**Without the model code we cannot establish this**
8. Is the cardiac output equal to the sum of blood flow rates to the tissue compartments?	**Yes**	
9. Is the sum total of tissue volumes equal to total body volume?	**Yes**	
10. Is the mathematical solver a well-established algorithm?	**Yes**	
11. Does the mathematical solver converge on a solution without numerical error?	**NA**	**Without the model code we cannot establish this**
12. Has the PBK modelling platform been subjected to a verification process (for a different use, for instance, in the pharmaceutical domain)?	**NA**	
A.4 Peer engagement (input/review)		
13. Has the model been used previously for a regulatory purpose?	**No**	
• Is prior peer engagement in the development and review of the model sufficient to support the envisaged application?	**No**	
• Is additional review required? Peer engagement includes input/review by experts on specific aspects of model development, individual reviews of the model by experts, or collective reviews by peer review panels. Availability of the comments and tracking of revisions to the model in response to peer input contributes to increased confidence in the model for potential application.	**Yes**	
B. Assessment of Model Validity		
B.1 Biological Basis (Model Structure and Parameters)		
14. Is the model consistent with known biology?	**Yes**	
• Is the biological basis for the model structure provided?	**Yes**	
• Is the complexity of the model structure appropriate to address the regulatory application?	**Yes**	

• Are assumptions concerning the model structure and parameters clearly stated and justified?	**Yes**	
• Is the choice of values for physiological parameters justified?	**Yes**	**Taken from *in vivo* human studies**
• Is the choice of methods used to estimate chemical-specific ADME parameters justified?	**No**	**Most of the input parameter where taken from literature we are not sure how reliable these are.**
• Saturable Kinetics	**Yes**	**By means of K_m and V_{max}**
B.2 Theoretical Basis of Model Equations		
15. Are the underlying equations based on established theories, .e.g. Michaelis-Menten kinetics, Fick's laws of diffusion?	**Yes**	
• In the case of PBK models for particles, does the model take into consideration the properties of particles, e.g. particle size ranges, (poor) solubility, aggregation, partitioning and diffusion/sedimentation behaviour?	**NA**	
B.3. Reliability of input parameters		
16. Has the uncertainty (individual variability, experimental reproducibility and reliability) in the input parameters been characterised?	**YES**	**Assumptions and uncertainties are reported**
B.4. Uncertainty and Sensitivity Analysis		
17. Has the impact of uncertainty (individual variability, experimental reproducibility and reliability) in the parameters on the chosen dose metric been estimated?	**Yes bySA**	
• Local sensitivity analysis?	**Yes**	
• Global sensitivity analysis?	**No**	
18. Is confidence in influential input parameter estimates (i.e., based on comparison of uncertainty and sensitivity) reasonable (within expected values; similar to those of analogues) in view of the intended application?	**Standard**	
B.5. Goodness-of-Fit and Predictivity		
19. For PBK models for which there are sufficient *in vivo* data for the chemical of interest:		
• Suitability as analogue (chemical and biological similarity) been assessed?	**NA**	
• Reliable estimation of chosen dose metric for analogue?	**NA**	
• In general is the biological Variability of *in vivo* reference data (from analogue) established?	**NA**	

Part III Overall Evaluation

Overall Conclusion on mode evaluation for the intended application

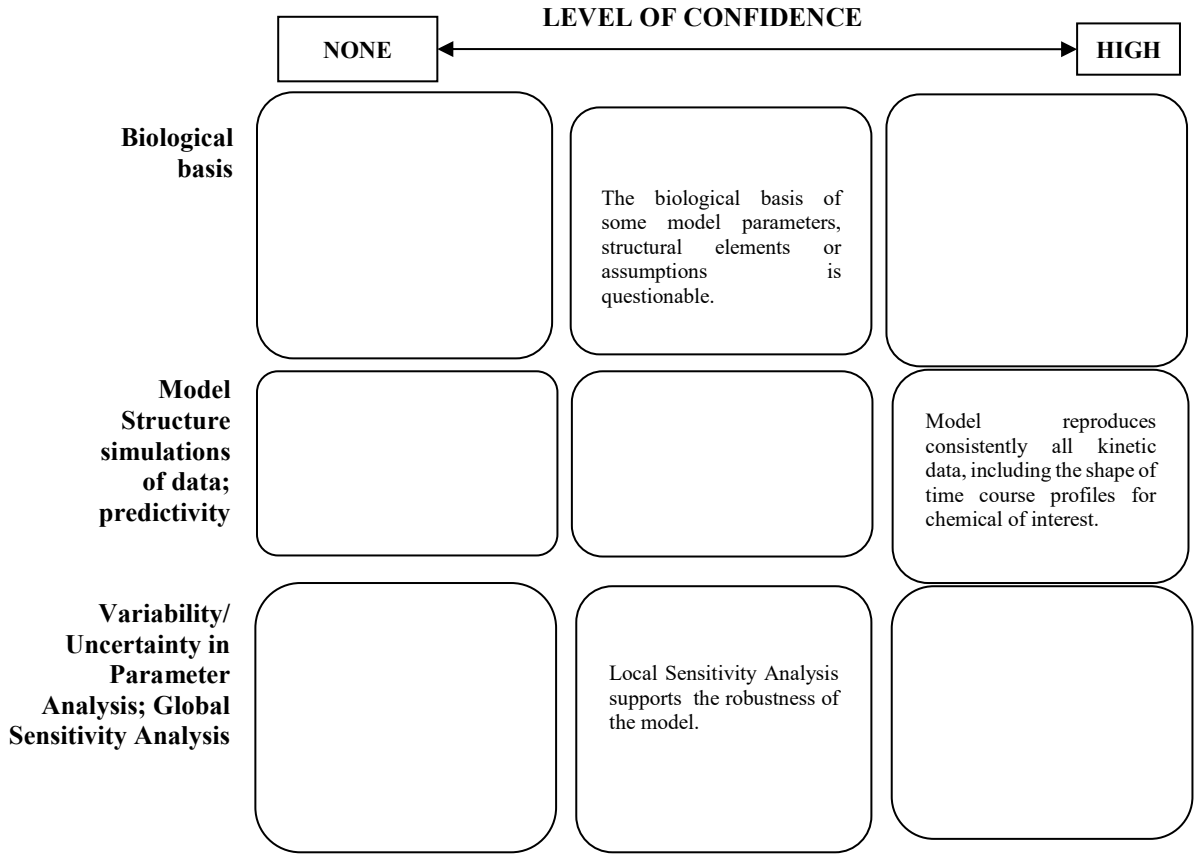

The PBK model was developed to illustrate an approach to apply MoIE. The model is well characterised however, the biological basis of some model parameters, model structural elements are questionable. Assumptions are reported to underline the uncertainties; the Model reproduces consistently all kinetic data, including the shape of time course profiles for chemical of interest, for the calibrated person. A local SA with a montecarlo simulation where performed. Based on all the evidence provided the following model will have a medium/standard level of confidence. The model code is not reported and a full assessment cannot be performed. Thus, it is recommended that the PBK model and relative output can be used in a regulatory framework only as supporting information.

Case Study IX

Caffeine PBBK model to predict MoIE for risk assessment

Part I. PBK model reporting template

A. Name of model

Caffeine PBBK model to predict MoIE for risk assessment

B. Model developer and contact details

Eric Hack[1], Alina Efremenko[1], Harvey Clewell[2]

[1]Scitovation LLC, Durham NC, USA

[2]Ramboll, Durham NC, USA

C. Summary of model characterisation, development, validation, and regulatory applicability

A PBBK model was developed to estimate blood concentrations following exposures to caffeine in experimental animals and humans and to obtain a point of departure as the Margin of Internal Exposure (MoIE).

The prediction are part of a risk assessment based on only *in vitro*, *in silico* and historical *in vivo* data to demonstrate how read-across can be applied in order to fill data gaps in an assessment of the potential risk for the consumer from exposure to caffeine. For this purpose, *in vivo* data from structural analogues have been used while assuming that no *in vivo* repeated dose toxicity data were available for the target substance caffeine. The physiologically-based biokinetic (PBBK) model to estimate blood concentrations following exposures to caffeine in experimental animals and humans, a Margin of Internal Exposure (MoIE).

D. Model characterisation (Modelling workflow)

Step 1 – Scope and purpose of the model (problem formulation)

The physiological structure of PBBK models provides a particularly useful framework for conducting cross species extrapolations (Clewell and Andersen 1985). To apply a PBBK model for interspecies extrapolation, the model is first used to simulate the exposure of interest (dose, route, and duration) in the experimental species, and the internal dose metric (peak or average concentration) is calculated. The parameters in the PBBK model are then changed to those for the target species of concern and the dose is adjusted until the same internal dose metric is achieved. The dose that produces the same internal dose metric (MoIE) is then considered the kinetically equivalent dose (Clewell et al. 2002).

Step 2 – Model conceptualisation (model structure, mathematical representation)

The PBBK model developed is structured with perfusion-limited compartments for skin, liver, fat, lung, kidney, blood, and lumped compartments for the remaining richly and slowly perfused tissues. Consistent with common practice, tissue:venous equilibration is assumed, and the tissues are assumed to be well-mixed reservoirs. Exposure is characterized in exposed skin (dermal) and gastrointestinal (GI, oral) compartments, and metabolism is described as a first-order clearance process in the liver. The model structure is shown schematically in Figure IX1.

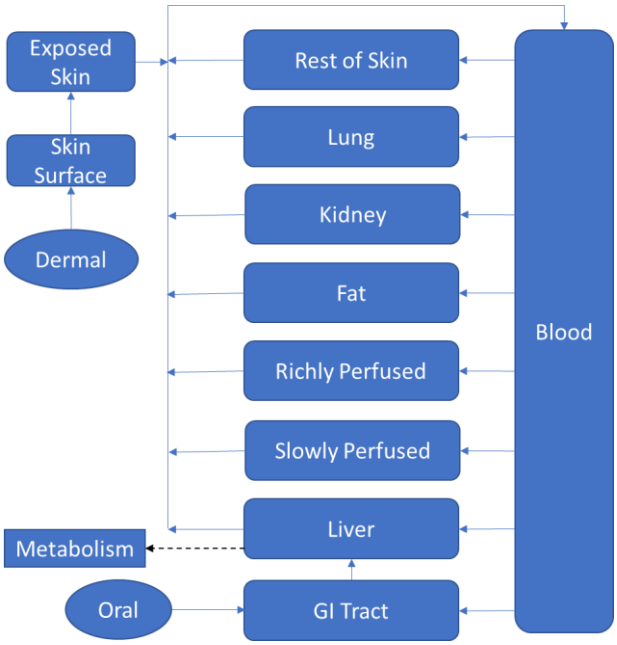

Figure IX1. PBK model schematic for caffeine showing the representation of the main organs considered with various sub-compartments in the skin and GI tract for oral and dermal exposure

Caffeine by the GI tract or by the skin becomes systemically available, and is metabolized in the liver by CYP450 1A2 mainly to three metabolites, i.e. theophylline (1,3-dimethylxanthine), theobromine (3,7-dimethylxanthine), and paraxanthine (1,7-dimethylxanthine) (see Figure IX2), corresponding respectively to 4%, 12% and 84% of the parent caffeine (Puchem and DrugBank). Metabolism in the skin is regarded as negligible for caffeine since skin expresses little amount of CYP450 1A2 (Gajewska et al, 2014 & 2015, Genies et al 2019). Caffeine is metabolically converted into, theophylline, theobromine, and paraxanthine, primarily in the liver where ca. 90-99 % of the metabolism takes place.

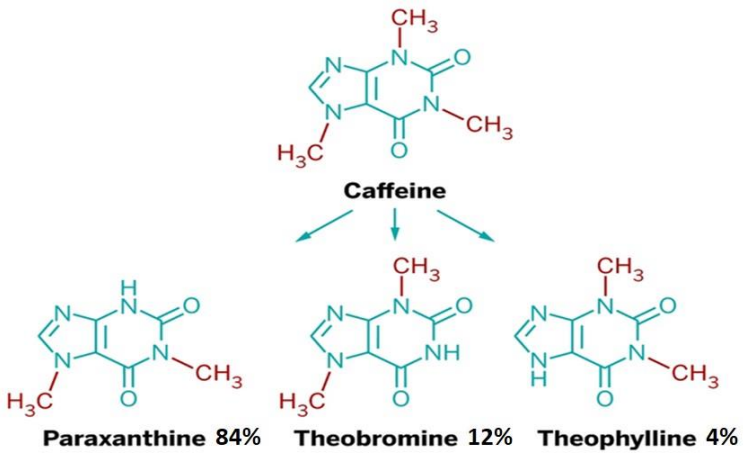

Figure IX2. Caffeine metabolism.

Step 3 – Model parameterisation (parameter estimation and analysis)

A list of physiological parameters is shown in Table IX4, and chemical-specific parameters are shown in Table IX5. Tissue blood flows and volumes are set to values in Brown et al. (1997, Tables 21 and 23), except for skin. Skin volume was calculated as the product of surface area and average skin thickness. Skin thickness was taken from Brown et al. (1997) and skin surface area was calculated using the following allometric relationship from Livingston and Lee (2001):

SA = 0.1173 * BW 0.6466 (m^2).

Blood flow to the exposed skin was calculated as the total skin blood flow adjusted by the ratio of volume exposed skin to volume of total skin. Exposed skin volume and blood flow was subtracted from the total skin to derive the parameters for the unexposed skin compartment.

Tissue:blood partition coefficients (PC) were estimated by Gajewska using the algorithm of Schmitt (2008), except for skin. Skin:blood PC was estimated as a weighted average of liver and fat PCs (i.e. 0.7*PL + 0.3*PF).

Oral exposure is modelled using a 1-compartment, first-order absorption model, with the gastrointestinal (GI) tract acting as a reservoir for the oral dose. All oral doses are simulated as bolus doses (i.e. all chemical ingested at once per dosing event). The blood flow from the GI enters the liver via the portal vein.

Dermal exposure is modelled using a skin surface compartment to house the applied dose in terms of the volume and surface area, and a single skin compartment. Transfer to the systemic circulation occurs in the skin compartment. The skin is separated into exposed and unexposed compartments. Dermal absorption is driven by a permeability coefficient for uptake from the surface into the skin (units of cm/hr), the exposure area and volume of application, the amount of chemical applied, duration of application, and the fraction absorbed. Transfer from the skin to the blood is modelled assuming a well-mixed, blood flow-limited exposed skin compartment and a skin:blood partition coefficient.

The liver clearance was calculated by scaling the *in vitro* intrinsic clearance value to the whole body. The liver clearance rate is calculated as the uL/min/million cells, times hepatocellularity, times the volume of the liver:

$$\mathrm{CLint\ (L/h)} = \mathrm{CLint\_invitro} * \mathrm{hpgl} * 10^{-6}\ \mathrm{(L/\mu L)} * 60\ \mathrm{(min/h)} * 10^{3}\ \mathrm{(g/kg)} * \mathrm{VLc} * \mathrm{BW\ (kg)}$$

where CLint_invitro is the uL/min/million cells cleared *in vitro*, hpgl is the number of million hepatocytes per gram of liver, and VLc*BW is the volume of the liver.

Step 4 – Computer implementation (solving the equations)

The physiologically-based biokinetic (PBBK) model was developed in Berkeley Madonna software (version 8.3.18; University of California, Berkeley, CA; www.berkeleymadonna.com).

A typical equation for a perfusion-limited tissue describes the mass balance for the uptake and clearance of the chemical in the tissue, in this case the liver:

dALiver/dt = QL*(CArterial – CVenous) – ClLiver

This equation can be interpreted as: The rate of change in the mass of the chemical (ALiver) in the liver is equal to the liver blood flow (QL) multiplied by the difference between the concentrations in the blood entering and leaving the liver (CArterial – CVenous), minus the metabolic clearance of the chemical in the liver (ClLiver).

These models typically rely on three types of parameters; physiological (e.g. tissue volumes, blood flows), physicochemical (e.g. octanol:water portioning, vapor pressure, water solubility), and biochemical (e.g. absorption rates, metabolism, clearances). The particular parameters needed depend on factors such as the chemical properties and the purpose of the model. Various guidance documents for the application, use, and reporting of PBBK models have been published (WHO, 2010; USEPA, 2006; USFDA, 2018).

Step 5 – Model Performance

A qualitative evaluation of the agreement between experimental plasma concentration and simulations was conducted through visual inspection of the time-course concentration curves (USEPA, 2006). Good agreement, with model predictions generally within a factor of two of the data (WHO 2010) was obtained for both the oral and dermal route (figures IX3, 4 and 5).

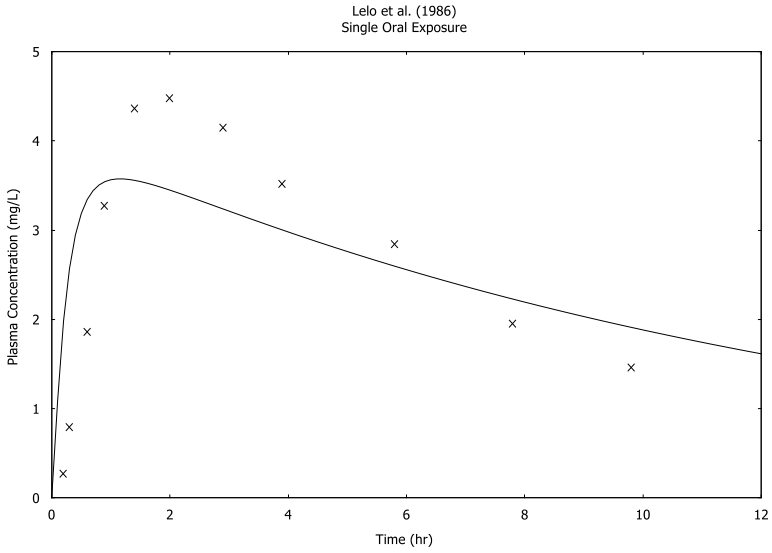

Figure IX3. Caffeine PBBK simulations compared to oral exposure data of Lelo et al. (1986). Plasma concentration following ingestion of 3.25 mg/kg body weight caffeine in a gelatin capsule. Study subjects included 6 non-smoking, male volunteers aged 19-21 years and weighing 62-104 kg (average body weight of 83 kg used for the simulation).

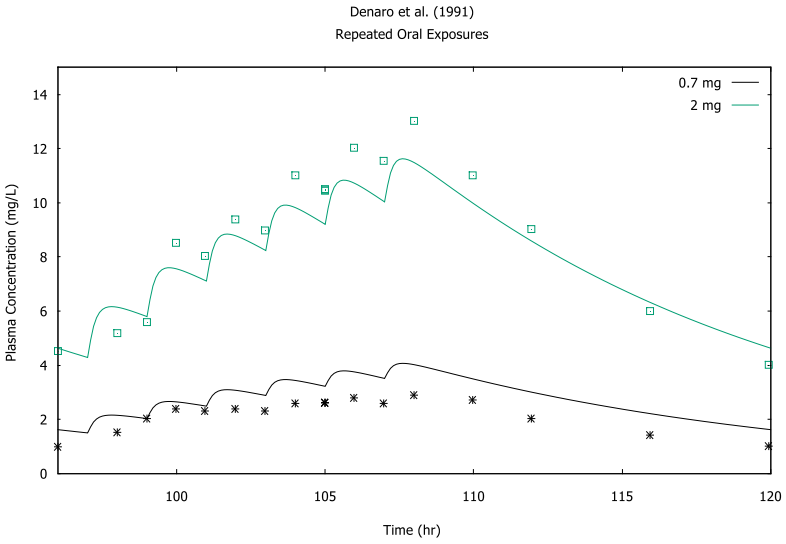

Figure IX4. Caffeine PBBK simulations compared to repeated oral exposure data of Denaro et al. (1991). Nine healthy nonsmokers who regularly drank 4 or more cups of coffee were admitted for 16 days. There were 7 males and 2 females, with ages ranging from 19 to 55 years of age. No body weights were reported, and a value of 70 kg was assumed for the simulation. Each subject participated in 3 treatment blocks of a placebo, low and high dose of caffeine. Plasma concentration of caffeine was determined following ingestion of a cup of coffee (0.7 and 2 mg/kg caffeine) every 2 hours (a total of 6 cups of coffee per day) over 5 days.The last day of a low and high dose treatment block is shown in the figure.

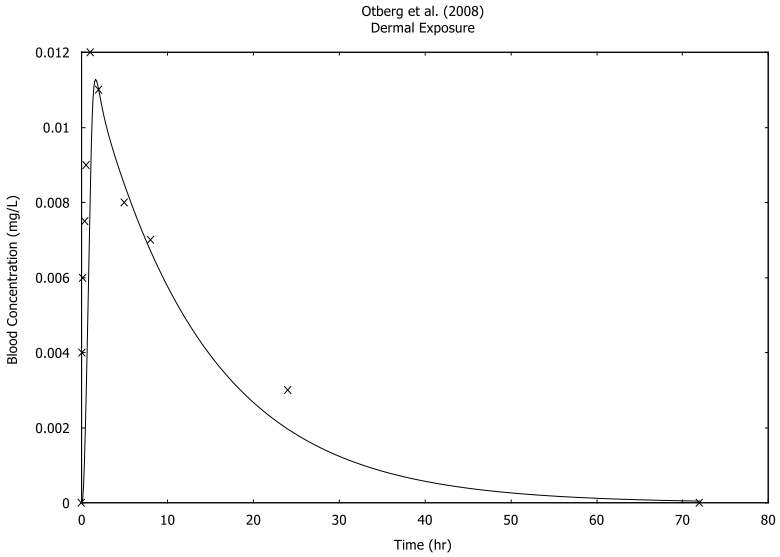

Figure IX5. Caffeine PBBK simulations compared to dermal exposure data of Otberg et al. (2008). Plasma concentration was determined following application of 50 mg (0.05 mL) of ethanol/propylene glycol formulation containing 2.5% caffeine (1.25 mg caffeine) to 25 cm^2 of the chest of 6 healthy Caucasian male volunteers. Hair was clipped, and hair follicle density averaged between 20 and 32 follicles/cm^2. Volunteers were 26-39 years of age with a normal BMI between 21 and 24. Body weight was not reported, and default value of 70 kg used for the simulation.

A local sensitivity analysis for model parameters was conducted with the cosmetic exposure scenario using the built-in tool in the Berkeley Madonna software. The sensitivity coefficients were then normalized by the output and input parameter values according to the following equation:

$$\text{Normalized Sensitivity Coefficient} = \frac{\Delta Y/Y}{\Delta X/X}$$

where Y is the output (i.e., C_{max} or AUC), X is the input parameter (e.g., Ka, Kp), ΔX is the change in the parameter value, and ΔY is the resulting change in the output value. Normalization of the sensitivity coefficients is necessary to make comparisons across parameters of different scales (Clewell et al. 1994).

Table IX1. Summary of the largest normalized sensitivity coefficients. The sensitivity of the maximum plasma concentration (C_{max}) and area under the plasma concentration curve (AUC) are shown.

Parameter	Symbol	Cmax Sensitivity	AUC Sensitivity
Fraction Absorbed	FracAvail	0.18	0.16
Body Weight	BW	-0.15	-0.16
Liver Volume	VLC	-0.68	-0.96
Cardiac Output	QCC	-0.06	-
Liver:Blood Partition	PCLiv	-0.08	-
Slowly-perfused:Blood Partition	PSC	-0.09	-
Oral Absorption Rate	Ka	0.11	-
Fraction Unbound in Blood	fub	-0.67	-0.96
Hepatic Intrinsic Clearance	hep_CLint_invitro	-0.67	-0.96
Hepatocellularity	hpgl	-0.67	-0.96

Step 6 – Model Documentation

The following PBBK model is also part of the IATA case study (2/2019, Case Study on the use of Integrated Approaches for Testing and Assessment for Systemic Toxicity Arising from Cosmetic Exposure to Caffeine for repeated dose toxicity) and as peer review paper by Cosmetic Europe (in preparation).

E. Identification of uncertainties

Model structure

A PBBK model with relatively simple oral and dermal absorption models was developed. The model simulations agreed reasonably well across multiple oral and dermal exposure data sets using a common set of parameter values. The model did tend to underpredict the plasma concentration at the higher oral doses, though it was consistently within a factor of 2 from the data. This is likely due to saturation of oxidative metabolism, and there are also potential vehicle effects that are not being captured by the model (Lelo et al. used gelatin capsules, while Denaro et al. put anhydrous caffeine into decaffeinated coffee). A more complex description of the oral absorption model could potentially improve the accuracy of the simulations at high doses, though more data or assumptions would be required to parameterize the model, bringing with them uncertainties of their own.

Input parameters

The fraction available for dermal absorption was set to 50% based on extrapolation of the trend found using *in vitro* testing. It is noted, however, that the fraction absorbed has been observed as high as 67%, which would lead to higher predictions of C_{max} and AUC. To estimate the impact of this assumption, the model was run again with 67% available for absorption. There is a 10% increase in C_{max}, and approximately a 6% increase in AUC.

Table IX2. Comparison of internal dose metrics with 67% dermal absorption vs 50%. The exposure scenario is the cosmetic use scenario described in Table IX3.

Fraction Absorbed	50%	67%
C_{max} (mg/L)	10	11
AUC (mg-h/L)	180	180

Model output

A simulation of the worst-case exposure estimated for caffeine via oral and dermal routes was conducted. Upper bound oral (13.1 mg/kg/d) and dermal (4.8 mg/kg/d) exposure estimates were determined and used as input to the model. Twice daily exposures were simulated, 12 hours apart, as bolus ingestions or applications. A 4 mL volume was used to simulate whole body exposure to lotion, as reported by Troutman et al. (2015). Caffeine concentration in the dermal formulation was assumed to be 2%, which corresponds to approximately 20 mg/mL caffeine. Using trends from *in vitro* dermal penetration data, 50% of the caffeine was assumed available for dermal absorption. A default body weight of 60 kg was also assumed.

The simulated internal dose metrics (C_{max} and AUC) are shown in Table IX3. The dosing simulation was run for 3 (simulated) days to achieve steady periodicity, as shown in Figure IX6. The maximum concentration in blood (C_{max}) was 10 mg/L, the daily area under the concentration curve (AUC, calculated over the time period from 48 hours to 72 hours) was 180 mg-h/L, and the average daily concentration (C_{avg}) was 7.3 mg/L.

Table IX3. Summary of the worst-case cosmetic exposure scenario. Daily oral and dermal doses are split into 2 equal doses, administered at 12-h intervals.

Exposure	
Single Oral Dose (mg/kg)	6.55
Single Dermal Dose (mg/kg/d)	2.4
Dermal Exposure Area cm^2	16560[a]
Doses/day	2
Daily Oral Dose (mg/kg/d)	13.1
Daily Dermal Dose (mg/d)	4.8
Internal Dose Metrics	
C_{max} (mg/L)	10
AUC (mg-h/L)	180
C_{avg} (mg/L)	7.3

[a] Whole body surface area for a 60 kg human calculated using the equation of Livingston and Lee (2001)

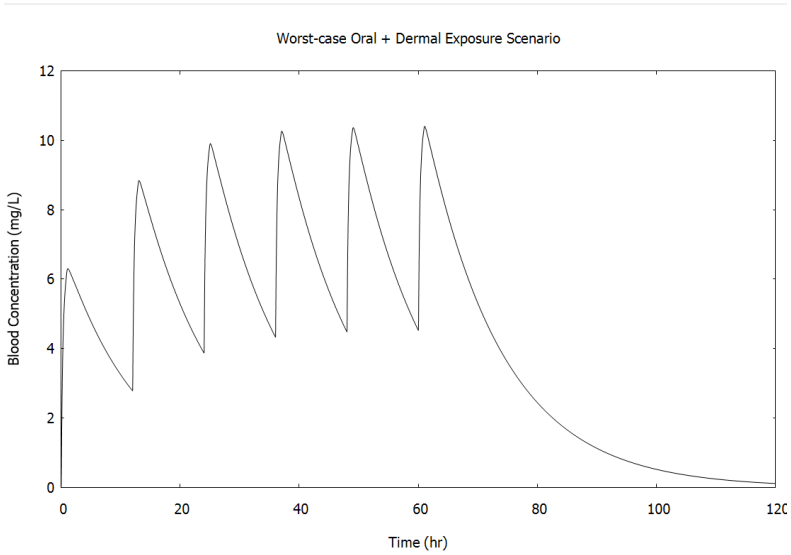

Figure IX6. PBBK simulation of internal plasma concentration of caffeine following estimated oral and whole body dermal exposure in Table IX3. Oral exposure = 13.1 mg/kg/d, whole body dermal exposure = 4.8 mg/kg/d in 4 mL of product, twice daily exposure. BW = 60 kg. C_{max} = 10 mg/L, AUC = 180 mg-h/L, C_{avg} = AUC/24 = 7.3 mg/L.

The sensitivity analysis identified 6 parameters to which the AUC and C_{max} were sensitive, and an additional 4 to which C_{max} only was sensitive. The parameters driving absorption (FracAvail and K_a) had positive coefficients (i.e., increase parameter → increase C_{max}), while parameters increasing clearance (e.g., liver parameters and intrinsic clearance) had negative coefficients.

Other uncertainties (e.g. model developed for different substance and/or purpose)

Simulation of the product use scenario was conducted for adult consumers using parameters for an average individual. Previous evaluations of the impact of inter-individual variability in pharmacokinetics on PBK modelling of the relationship of internal dose to external exposure (Clewell and Andersen 1996) suggest that the resulting variability in internal dose is consistent with the recommended default factor of three recommended by IPCS (2005). Age-dependent variations in pharmacokinetics can also be expected. However, a study of the impact of age-dependence pharmacokinetics on internal dose (Clewell et al. 2004) found that, in general, predictions of average pharmacokinetic dose metrics for a chemical across life stages were within a factor of two, although larger transient variations were predicted, particularly during the neonatal period.

F. Model implementation details

- software (version no): Berkeley Madonna software (version 8.3.18; University of California, Berkeley, CA; www.berkeleymadonna.com).
- availability of code Yes
- software verification / qualification not applicable

H. Peer engagement (input/review)

None.

G. Parameter tables

Table IX4. Human PBBK physiological parameter values for caffeine. Source for values is Brown et al. (1997) unless otherwise specified.

Parameter	Units	Symbol	Value
Body mass [d]	kg	BW	-
Skin thickness	cm	Depth	0.1
Blood Flows (Fraction of Cardiac Output) [a]			
Cardiac Output	$L/h/kg^{0.75}$	QCc	15
Fat	1	QFc	0.052
Kidney	1	QKc	0.175
Liver	1	QLc	0.227
Skin	1	QSkc	0.058
Lung	1	QLuc	0.025
Volumes (fraction of BW) [b]			
Fat	1	VFc	0.21
Kidney	1	VKc	0.004
Liver	1	VLc	0.026
Lung	1	VLuc	0.008
Blood [c]	1	VAc, VVc	0.079
Hepatocellularity [e]	millions of hepatocytes per gram liver	hpgl	99

[a] Richly perfused blood flow = 70% of QC minus liver, kidney, and lung volumes.

[a] Slowly perfused blood flow = 30% of QC minus fat, and skin volumes.

[b] Richly perfused tissue volume = 70% of BW minus liver, kidney, and lung volumes.

[b] Slowly perfused tissue volume = 83.6% of BW minus fat, blood, and skin volumes.

[c] Blood is divided into 3/4 arterial and 1/4 venous.

[d] Simulation specific

[e] Barter et al. (2007)

Table IX5. Chemical-specific PBBK parameters for caffeine

Parameter	Units	Symbol	Value	Source
Molecular weight	g/mol	MWC	194.2	PubChem
Partition Coefficients				
Fat	1	PF	0.68	Schmitt (2008)
Kidney	1	PK	3.76	Schmitt (2008)
Liver	1	PL	4.25	Schmitt (2008)
Lung	1	PLu	1.23	Schmitt (2008)
Rich	1	PR	2.4	Schmitt (2008)
Slow	1	PS	0.995	Schmitt (2008)
Blood and Plasma				
Fraction unbound in blood	%	fub	96	Lave et al. (1997)
Fraction unbound in plasma	%	fup	68	Lelo et al. (1986)
Blood:plasma ratio	%	RBP	71	fup/fub
Oral absorption				
GI -> liver	1/h	Ka	1.6	fit
Dermal absorption				
Fraction available	%	FracAvail	50	Genies et al, Hewitt et al.
Permeability	cm/h	Kp	6E-3	Doucet et al. (1998)[1]
Metabolism				
Hepatocyte clearance	uL/min/million cells	hep_Clint_invitro	0.68	fit

[1] The value from Doucet et al. (1998) was 6E-4 cm/h. However, this value was adjusted upward an order of magnitude to obtain results matching the in human data of Otberg et al. (2008). Doucet used frozen female abdominal skin tissue, while Otberg exposed male chests with "pronounced terminal hair on the chest". The adjustment was considered reasonable, as there are known absorption differences and hair follicle densities across body locations.

H. References and background information

Case Study on the use of Integrated Approaches for Testing and Assessment for Systemic Toxicity Arising from Cosmetic Exposure to Caffeine. Series testing and assessment No. 321 [ENV/JM/MONO(2020)17].

Cosmetic Europe (in preparation).

Links to other resources

PBK Model code

;Caffeine PBBK model

;Created for CosEu case study by Eric Hack, Alina Efremenko, Alicia Paini, and Harvey Clewell

;Model units

;time = hr

;volumes = L

;mass = mmole

{

Instructions for running the model simulations

Denaro repeated oral exposure simulation:

STOPTIME = 120

BW = 70

Bolus = 0.7 or 2

start = 1

ostop = 12

repeat = 2

allstop = 109

Lelo single oral exposure simulation:

STOPTIME = 24

BW = 83

Bolus = 3.25

start = 0

repeat > STOPTIME

Otberg dermal exposure simulation:

STOPTIME = 72

BW = 70

Bolus = 0

DermalGDose = 1.25

VolApp = 0.05

AreaE = 25

```
DRepeat > STOPTIME
tinf = 0.1

Cosmetic oral and dermal exposure simulation:
STOPTIME = 72
BW = 60
Bolus = 6.55
repeat = 12
ostop > STOPTIME
DermalGDose = 144
DRepeat = 12
DStop > STOPTIME
VolApp = 4
AreaE = 16560
tinf = 0.1
}
;-------------------------------------------------------------------------------------------------------
---------------------------------
; Solver settings
 METHOD RK4          ; Runge-Kutta 4th-order solver (not using stiff system integrator
because of pulsed oral repeated dose)
 STARTTIME = 0       ; hours
 STOPTIME = 24       ; hours
; Molecular weight
 MWC = 194.2;        Molecular weight caffeine
;-------------------------------------------------------------------------------------------------------
---------------------------------
; Exposure calculations

; Control all exposure
 allstop = 1e6                          ; hours
 exposurezone = (Time <= allstop)       ; hours
;-------------------------------------------------------------------------------------------------------
---------------------------------
; Oral exposure - repeated bolus dose
```

```
 bolus = 6.55                    ; mg/kg per application
 start = 0                       ; initial bolus time (hr)
 ostop = 12                      ; time to stop oral dosing (hr)
 repeat = 1e6                    ; bolus repeat interval (hours)
 ondaily = if MOD(time-1, 24) <= ostop then 1 else 0

 GDOSE' = pulse(bolus, start, repeat) * ondaily * exposurezone    ; mg/kg/h
 init GDOSE = 0                  ; initial amount in stomach (mg/kg)
 ODOSE = GDOSE/MWC               ; mmole/kg bw
 DOSE=ODOSE*BW                   ; mmole
;-------------------------------------------------------------------------------------------------------
; Dermal exposure
 DermalGDose = 243.6             ; mg
 VolApp = 0.1                    ; application volume (mL)
 DermalDose  = DermalGDose/MWC   ; mmole
 FracAvail = 0.67          ; Fraction of applied dose available for absorption, from CE study
 tinf = 1.0                      ; Time to apply dermal dose (h)
 DStart = 0                      ; time to start dermal dosing (hr)
 DRepeat = 999                   ; time interval to repeat dermal exposure (hr)
 DStop = 1         ; time of last dermal exposure + delta t (hr) {e.g., DStop = 97 for last daily
dose at 96 hr}
 DZone = IF MOD(TIME, DRepeat) < tinf THEN 1 ELSE 0          ; flag for dermal
exposure on/off
 applddose' = DZone*(DermalDose*FracAvail)/tinf * (TIME <= DStop) * exposurezone
 ; mmole/h
 INIT applddose = 0.0    ; initial dermal dose
;-------------------------------------------------------------------------------------------------------
; Body weight
 BW = 60                         ; kg
;-------------------------------------------------------------------------------------------------------
; Skin parameters
; Total Area of Skin (cm^2), Livingston and Lee (2001)
```

```
 SA = (0.1173*(BW)**0.6466) * 10**4  ; total body surface area, cm2 (the 10**4 converts m2 to cm2)
 AreaE = 25                          ; surface area of skin exposed cm2
 SA_exposed = min(AreaE, SA) ; limit exposed SA to <= total SA
 Depth = 0.10                        ; skin thickness (cm), Brown 1997
 Kp = 6e-4        ; skin permeability (cm/hr), Table III Doucet et al 1998, frozen human skin (female abdomen), simple O/W emulsion
 VSk = SA*Depth / 1000               ; total skin volume (L)
 VSkc = VSk/BW                       ; fractional skin volume (for slowly perfused volume calculation)
 VSkE = SA_exposed*Depth / 1000      ; exposed skin volume (L)
;-------------------------------------------------------------------------------------------------------------------------
; Other tissue volume fractions (L or kg per kg body weight)
 VLc = 0.026                         ; fraction of  liver tissue
 VKc = 0.004                         ; fraction of kidney tissue
 VLuc = 0.012                        ; fraction of lung tissue
 VFc = 0.214                         ; fraction of fat tissue
 VAc = 0.0185                        ; fraction of arterial blood  0.074*1/4
 VVc = 0.0555                        ; fraction of venous blood 0.074*3/4
 VRc = 0.08-VLc-VLuc-VKc             ; fraction of richly perfused tissue
 VSc = 0.836-VFc-VAc-VVc-VSkc        ; Fraction of blood flow to slowly perfused tissue
                                     ; total of fractions = 0.91
; Volume check = 0.91?
 VBal = VLc + VKc + VLuc + VFc + VSkc + VAc + VVc + VRc + VSc
;-------------------------------------------------------------------------------------------------------------------------
; Allometric scaling of tissue volumes (L or kg)
 VL = VLc*BW
 VLu= VLuc*BW
 VK = VKc*BW
 VF = VFc*BW
 VR = VRc*BW
 VS = VSc*BW
 VV = VVc*BW
```

```
 VA = VAc*BW
;-----------------------------------------------------------------------------------------------------------
----------------------------------
; Blood flow rates
 QCc = 15
 QC = QCc*BW**0.74          ; Reference: Brown et al 1997, L/hr
 QLc = 0.259                ; Fraction of blood flow to liver
 QKc = 0.19                         ; Fraction of blood flow to kidney
 QFc = 0.055                ; Fraction of blood flow to fat
 QSKc = 0.058               ; Fraction of blood flow to all skin (Brown)
 QSkeC = QSKc * (VSke/VSk)  ; Fraction blood flow to exposed skin
 QLuc = 0.025               ; Fraction of blood flow to Lungs
 QRc = 0.70-QLc-QKc-QLuc            ; Fraction of blood flow to richly perfused tissue
 QSc = 0.30-QFc-QSKc        ; Fraction of blood flow to slowly perfused tissue
;-----------------------------------------------------------------------------------------------------------
----------------------------------
; Scale blood flows by total cardiac output
 QL = QLc*QC                {L/hr}
 QK = QKc*QC                        {L/hr}
 QF = QFc*QC                {L/hr}
 QR = QRc*QC                {L/hr}
 QS = QSc*QC                {L/hr}
 QLu = QLuc*QC                      {L/hr}
 QSke = QSkeC*QC            {L/hr}
 QSk = (QSkC - QSKeC)*QC    {L/hr}

; Blood flow balance check = 0?
 QBal = QL + QK + QF + QR + QS + QSK + QSke + QLu - QC
;-----------------------------------------------------------------------------------------------
; Partition Coefficients
 PCLiv = 4.25               ; liver/blood partition coefficient based on Schmitt 2008
 PCLu = 1.23                ; lung/blood partition coefficient
 PCK = 3.76                 ; kidney/blood partition coefficient
 PCF = 0.68                         ; fat/blood partition coefficient
```

```
 PCR = 2.4                          ; richly perfused tissues/blood partition coefficient
 PCS = 0.995                        ; slowly perfused tissues/blood partition coefficient
 PCSk = 0.7*PCLiv + 0.3*PCF         ; correlation from parabens model (See Campbell et al)
; Protein binding
 fub = 0.96                         ; fraction caffeine unbound in blood (Lave et al. 1997)
 fup = 0.68                         ; fraction unbound in plasma (Lelo et al 1986)
 RBP = fup/fub                      ; blood to plasma concentration ratio (assumes Cup = Cub)
;-----------------------------------------------------------------------------------------
; Linear hepatic in vitro clearance (uL/min/million hepatocytes)
 hep_CLint_invitro = 0              ; ul/min/million hepatocytes
 hpgl = 99                          ; 10^6 Hepatocytes per gram liver (human value from PLETHEM)
 hep_CLint_invivo = hep_CLint_invitro * (10^-6) * 60 * hpgl * 1000      ; L/h/kg Liver
 CLintC = hep_CLint_invivo                  ; L/hr/kg liver
 CLint = CLintC*VL                          ; L/hr
;=========================================================================
; Tissue compartment dynamic equations
;=========================================================================
; Oral uptake from gut
 Ka = 5                             ; 1st-order oral absorption rate constant (1/hr)
 AGI' = GDOSE'*BW/MWC - Ka*AGI      ; mmol/hr
 Init AGI = 0                       ; mmol
;-----------------------------------------------------
; Liver
; Linear Metabolism
 AMTot' = CLint * fub * CVL                 ; mmole/hr
 init AMTot = 0                             ; mmole
 AL' = QL * (CA - CVL)  + Ka * AGI - AMTot' ; mmole/hr
 init AL= 0                                 ; mmole
 CL = AL / VL                               ; mmole/L
 CVL = CL / PCLiv                           ; mmole/L
```

```
;-------------------------------------------------------
; Skin
; Surface exposed (mmol)
; Rate absorbed (mmol/hr) = Permeability coeff (cm/hr) / Volume applied (cm3) * SA exposed (cm2) * amount of surface (mmole)
 ASFC' =  applddose' - (Kp / VolApp * SA_exposed)*ASFC        ; mmole/hr
 INIT ASFC = 0.0                                              ; mmole
; Amount in Exposed Skin (mmole)
 ASke' = (Kp * SA_exposed / VolApp)*ASFC + (QSke * (CA - CVSke)) ; mmole/hr
 INIT ASke = 0.0                                                  ;
mmole
 CSke = ASke / (VSke+1.0e-23)                                     ; mmole/L
 CVSke = CSke / PCSk                                              ; mmole/L
; ASK = Amount in unexposed skin (mmole)
 ASK' = QSK*(CA - CVSK)                    ; mmole/hr
 INIT ASK = 0.0                            ; mmole
 CSK = ASK/(VSK-VSke+1.0e-23)              ; mmole/L
 CVSK = CSK/PCSk                    ; mmole/L
;-------------------------------------------------------
; Blood
; arterial blood
 AA' = QC*CV - QC*CA          ; mmole/hr
 Init AA = 0                  ; mmole
 CA = AA/VA             ; mmole/L
; venous blood
 AV' = ( QL*CVL + QS*CVS + QR*CVR + QF*CVF + QK*CVK + QLu*CVLu +
QSK*CVSk + QSke*CVSke) -  QC*CV                ; mmole/hr
 Init AV = 0                  ; mmole
 CV = AV/VV             ; mmole/L
;-------------------------------------------------------
; Slowly perfused tissue
 AS' = QS * (CA - CVS); mmole/h
 init AS=0                    ; mmole
 CS = AS / VS           ; mmole/L
 CVS = CS/PCS           ; mmole/L
```

```
;-------------------------------------------------------
; Richly perfused tissue
 AR' = QR * (CA - CVR)          ; mmole/hr
 init AR=0                      ; mmole
 CR = AR / VR             ; mmole/L
 CVR = CR/PCR                   ; mmole/L
;-------------------------------------------------------
; Lung
 ALu' = QLu * (CA - CVLu)       ; mmole/hr
 init ALu=0                     ; mmole
 CLu = ALu / VLu                ; mmole/L
 CVLu = CLu / PCLu      ; mmole/L
;-------------------------------------------------------
; Fat
 AF' = QF * (CA - CVF) ; mmole/hr
 init AF=0                      ; mmole
 CF = AF / VF             ; mmole/L
 CVF = CF / PCF                 ; mmole/L
;-------------------------------------------------------
; Kidney
 AK' = QK * (CA -CVK )          ; mmole/hr
 init AK=0                      ; mmole
 CK = AK / VK             ; mmole/L
 CVK = CK / PCK                 ; mmole/L
;=======================================================
; Dose metrics
 CVmgpl = CV*MWC                ; mg/L
 CVPlas = CV/RBP                        ; mmol/L
 CVPlasmgpl = CVPlas*MWC    ; mg/L
 AUCV' = CV                     ; mmole/L
 init AUCV = 0                  ; mmole*hr/L
 AUCmghpl = AUCV*MWC                    ; mg*hr/L
; ********************** Calculate last 24-hr AUC ************************
init AUC24 = 0
```

```
AUC24' = IF (STOPTIME - time < 24) THEN (CV*MWC) ELSE 0        ; mg*h/L
;=============================================================
; Mass balance
 In = DOSE + applddose ; mmole
 Stored = AF + AS + AR + AL + AK + AV +AA + ALu +AGI + ASfc + ASk + ASke
 ; mmole
 Out = AMTot                    ; mmole
 MASSBAL = In - Stored - Out   ; mmole
```

Part II Checklist for model evaluation

PBK Model Evaluation Checklist	Checklist assessment	Comments
Name of the PBK model (as in the reporting template)	Caffeine PBBK model to predict MoIE for risk assessment	
Model developer and contact details	Eric Hack[1], Alina Efremenko[1], Harvey Clewell[2] [1]Scitovation LLC, Durham NC, USA [2]Ramboll, Durham NC, USA	
Name of person reviewing and contact details	A.Paini	
Date of checklist assessment	04/05/2020	
A. Context/Implementation		
A.1. Regulatory Purpose		
1. What is the acceptable degree of confidence/uncertainty (e.g. high, medium or low) for the envisaged application (e.g. priority setting, screening, full assessment?)	**High** **Fill gap for full assessment**	
2. Is the degree of confidence/uncertainty in application of the PBK model for the envisaged purpose greater or less than that for other assessment options (e.g. reliance on PBK model and *in vitro* data vs. no experimental data)?	**greater**	
A.2. Documentation		
3. Is the model documentation adequate, i.e. does it address the essential content of model reporting template, including the following:	**Y**	
• Clear indication of the chemical, or chemicals, to which the model is applicable?	**Y**	
• Is the model being applied for the same scientific purpose as it was developed, or has it been repurposed somehow?	**Y**	
• Model assumptions?	**Y, reported**	
• Graphical representation of the proposed mode of action, if known?	**Reported**	
• Graphical representation of the conceptual model?	**Y**	

• Supporting tabulation for parameters (names, meanings, values, mean and standard deviations, units and sources)?	**Y**	
• Relevance and reliability of model parameters?	**Y**	
• Uncertainty and sensitivity analysis?	**Y**	
• Mathematical equations?	**Y**	**Sample example was reported**
• PBK model code?	**Y**	
• Software algorithm to run the PBK model code?	**Yes**	**Reported in the model code**
• Qualification of PBK software platform?	**NA**	
A.3 Software Implementation and Verification		
4. Does the model code express the mathematical model?	**YES**	
5. Is the model code devoid of syntactic and mathematical errors?	**YES**	
6. Are the units of input and output parameters correct?	**YES**	
7. Is the chemical mass balance respected at all times?	**YES**	
8. Is the cardiac output equal to the sum of blood flow rates to the tissue compartments?	**YES**	
9. Is the sum total of tissue volumes equal to total body volume?	**YES**	
10. Is the mathematical solver a well-established algorithm?	**YES**	
11. Does the mathematical solver converge on a solution without numerical error?	**YES**	
12. Has the PBK modelling platform been subjected to a verification process (for a different use, for instance, in the pharmaceutical domain)?	**NO**	
A.4 Peer engagement (input/review)		
13. Has the model been used previously for a regulatory purpose?	**NO**	
• Is prior peer engagement in the development and review of the model sufficient to support the envisaged application?	**YES**	**Was developed by experts in the field**
• Is additional review required? Peer engagement includes input/review by experts on specific aspects of model development, individual reviews of the model by experts, or collective reviews by peer review panels. Availability of the comments and tracking of revisions to the model in response to peer input contributes to increased confidence in the model for potential application.	**NO**	**But independent peer review of the model and model code would enhance credibility**
B. Assessment of Model Validity		
B.1 Biological Basis (Model Structure and Parameters)		
14. Is the model consistent with known biology?	**YES**	
• Is the biological basis for the model structure provided?	**YES**	
• Is the complexity of the model structure appropriate to address the regulatory application?	**YES**	

• Are assumptions concerning the model structure and parameters clearly stated and justified?	**YES**	
• Is the choice of values for physiological parameters justified?	**YES**	
• Is the choice of methods used to estimate chemical-specific ADME parameters justified?	**YES**	
• Saturable Kinetics	**No**	
B.2 Theoretical Basis of Model Equations		
15. Are the underlying equations based on established theories, .e.g. Michaelis-Menten kinetics, Fick's laws of diffusion?	**YES**	
• In the case of PBK models for particles, does the model take into consideration the properties of particles, e.g. particle size ranges, (poor) solubility, aggregation, partitioning and diffusion/sedimentation behaviour?	**NA**	
B.3. Reliability of input parameters		
16. Has the uncertainty (individual variability, experimental reproducibility and reliability) in the input parameters been characterised?	**YES**	
B.4. Uncertainty and Sensitivity Analysis		
17. Has the impact of uncertainty (individual variability, experimental reproducibility and reliability) in the parameters on the chosen dose metric been estimated?	**YES**	
• Local sensitivity analysis?	**YES**	
• Global sensitivity analysis?	**NO**	
18. Is confidence in influential input parameter estimates (i.e., based on comparison of uncertainty and sensitivity) reasonable (within expected values; similar to those of analogues) in view of the intended application?	**YES**	
B.5. Goodness-of-Fit and Predictivity		
19. For PBK models for which there are sufficient *in vivo* data for the chemical of interest:		
• Suitability as analogue (chemical and biological similarity) been assessed?	**NA**	
• Reliable estimation of chosen dose metric for analogue?	**NA**	
• In general is the biological Variability of *in vivo* reference data (from analogue) established?	**YES**	

NA= Not applicable; NR = Not Reported

Part III Overall Evaluation

Overall Conclusion on mode evaluation for the intended application

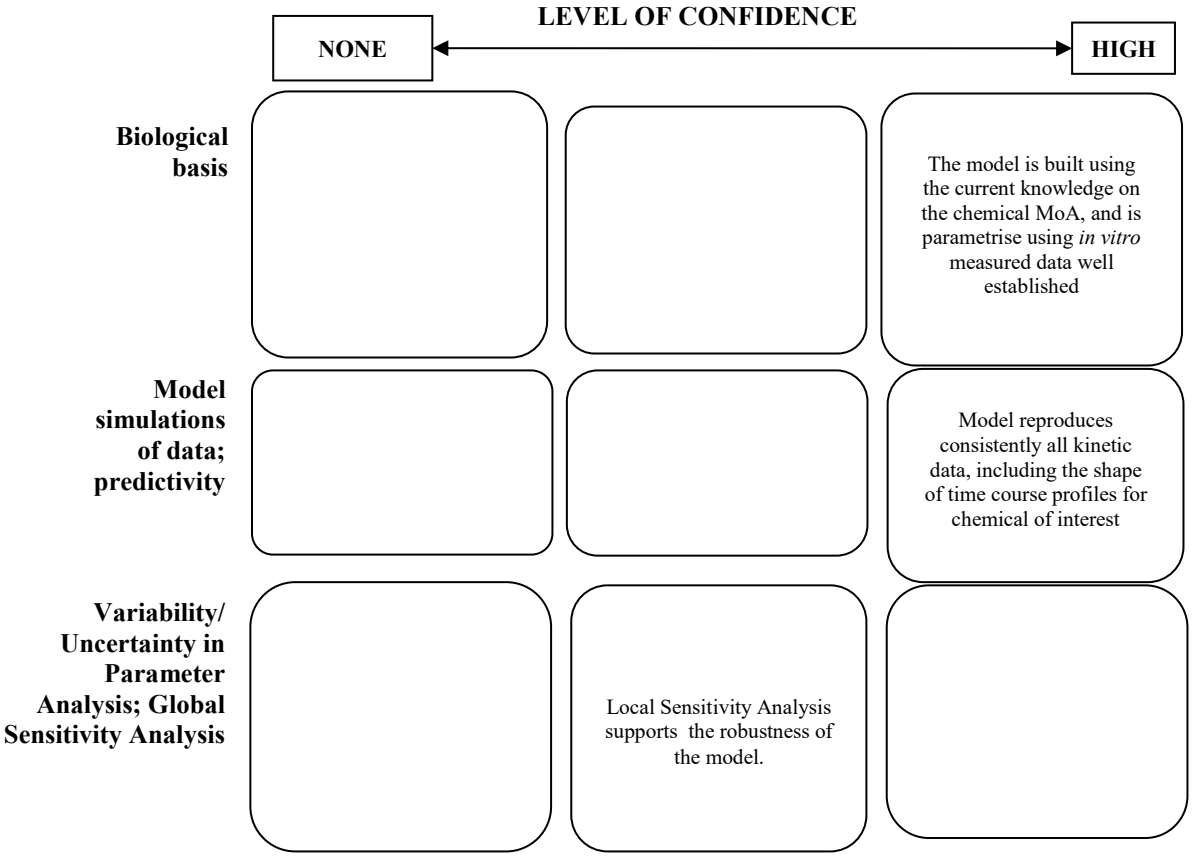

A PBK model with relatively simple oral and dermal absorption models was developed in order to conduce cross species extrapolations and route-to-route extrapolation. The model is built using solid knowledge on the chemical MoA, and is parametrise using good *in vitro* measured data well established. The model reproduces the shape time and dose course of the chemical of interest. A Local Sensitivity Analysis supports the robustness of the model.

Based on the results available, it was concluded that, the application of this PBK model for cross-species extrapolation is a reasonable approach for a preliminary hazard characterisation. A global SA would have given a more global overview on the key parameters that can perturb the model output.

Case Study X

IVIVE-PBPK model for phenyl-1,4-dihydropyridine calcium channel antagonists

The following document captures the information of a case study that used an in *vitro-in vivo* extrapolation approach coupled with a physiologically based kinetic (PBK) model to predict the plasma exposure and pharmacokinetic parameters of a series of seven structurally related phenyl-1,4-dihydropyridine compounds. Initial choices about IVIVE-PBK model structure and appropriate methods to predict the tissue distribution and intestinal metabolism were verified using available clinical data for nifedipine. The model was parameterized with appropriate physicochemical data and *in vitro* metabolism and binding data to predict the pharmacokinetic parameters of the six remaining compounds. The intravenous and oral clearance and steady-state volume of distribution (Vss) were predicted with a reasonable degree of accuracy (predicted parameters within 2.2-fold of observed) for all of the compounds apart from the Vss of nimodipine (predicted with a 10-fold error). Sensitivity analysis showed that the predicted Vss for nimodipine was very sensitive to the lipophilicity of the compound and the predicted values matched the observed value when a range of measured and predicted lipophilicities of the compound were tested. The predicted concentration time profile for the compounds when administered at the same oral dose (10 mg) showed marked differences in the maximum free concentration in plasma Cmax,free (> 100-fold) and time course of exposure.

Part I. PBK model reporting template

A. Name of model:

IVIVE-PBPK model for phenyl-1,4-dihydropyridine calcium channel antagonists

B. Contact details.

Iain Gardner, Certara UK Ltd, Simcyp Division, Level 2-Acero, 1 Concourse Way, Sheffield, S1 2BJ, United Kingdom.

C. Summary of model characterisation, development, validation, and regulatory applicability

This modelling exercise was undertaken to explore the concept of using IVIVE-PBK models in a pharmacokinetic/Toxicokinetic (PK/TK) read across exercise using a category approach. A series of structurally related phenyl-1,4-dihydropyridine compounds with measured human pharmacokinetics were used in this exercise. One compound (nifedipine) was selected as a source compound and a PBK model constructed using available *in vitro* data. The PBK model results were compared to available *in vivo* human PK data and the model refined if needed. Using the same workflow and refinements as used for the nifedipine model, PBK models were constructed for a series of chemically related phenyl-1,4-dihydropyridine compounds and the PBK model results were compared to observed PK parameters in humans. No further modifications of the PBK models were made for the

analogue compounds. To explore the concept of biological read across the same process was also followed for 4 structurally unrelated compounds that are predominantly cleared by the same mechanism (CYP 3A4 metabolism).

The chemical structures used in the case study are shown in Figure X1.

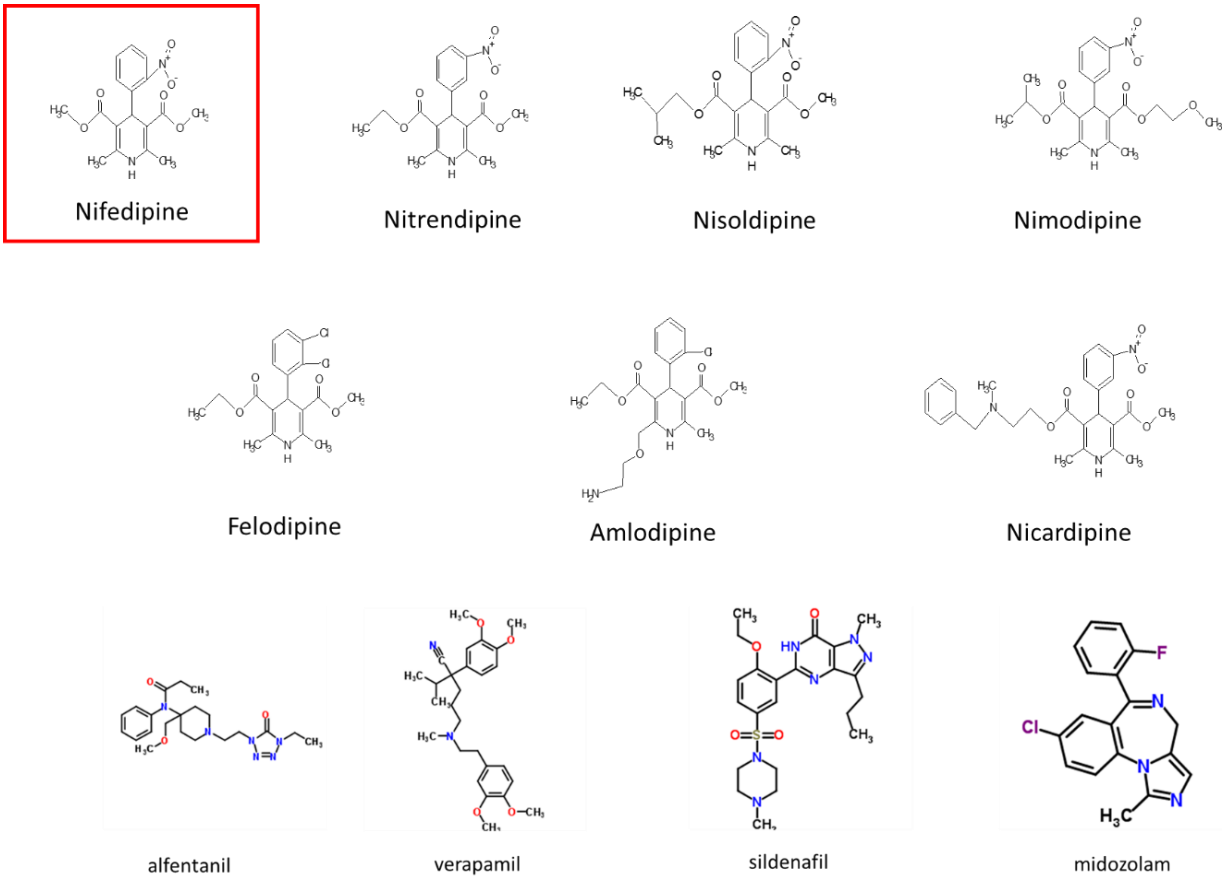

Figure X1 Chemical structure of the source compound nifedipine and the structurally related phenyl-1,4-dihydropyridine analogue compounds (nitrendipine, nisoldipine and nimodipine, felodipine, amlodipine and nicardipine) as well as the 4 structurally unrelated CYP 3A4 compounds (alfentanil, verapamil, sildenafil and midazolam).

D. Model characterisation (modelling workflow)

Step 1 – Scope and purpose of the model

The purpose of this case study was to examine the utility of IVIVE-PBK models in a read across (RAX) approach where human data is available and can be used to refine the PBK model of the source compound but is not available (or in this case was not used) to refine the PBK model for the analogue compounds. The metrics of interest for this case study were those parameters that define the PK of the compounds (C_{max}, AUC etc.) and no further risk or biological effect assessment was considered.

The following assumptions were made:

1) Parent compound was assumed to be the moiety of interest in the case study, concentrations of metabolites were not considered.
2) Based on experimental observations metabolism is thought to be the major clearance pathway of the compounds in this case study and active transport processes were not considered. The clearance in human subjects was predicted using an *in vitro – in vivo* extrapolation approach using intrinsic clearance data generated *in vitro* in human liver microsomes.
3) The physiology (i.e. tissue weights and blood flow rates) of the human populations of interest were the default values in the Simcyp human simulator (V16; further details below).
4) No differences in the disposition of the individual enantiomers of racemic compounds was considered.

Step 2 – Model Conceptualisation

The model structure used for this exercise was a whole body PBPK model (figure X2) with each of the compartments described as a well-stirred perfusion limited compartment.

Oral absorption

Oral absorption was predicted using a first order absorption model where the oral absorption was described by an absorption rate and a value for the fraction absorbed. The method used to predict the rate and extent of absorption varied from compound to compound depending on the *in vitro* data or physicochemical available (see input tables in section I). The preferred method was to predict effective permeability in humans using the apparent permeability (P_{app} ($cm*10^{-6}/s$)) measured *in vitro* in a Caco-2 cell system with the permeability in the *in vitro* system calibrated against a compound (propranolol). Where *in vitro* permeability has been measured in the same *in vitro* system and the effective permeability of the compound in the human intestine has also been determined. When this data was unavailable the rate and extent of absorption was calculated using a mechanistic permeability model (Mech P_{eff}) that uses compound lipophilicity as an input. The MechPeff Model is a fully mechanistic model that predicts passive intestinal permeability using a compound's physicochemical parameters such as LogP, pKa, molecular weight and compound type. The MechPeff model within Simcyp is adapted from the original structure described by Sugano[1]. In brief, the model considers:

Intrinsic transcellular permeability according to the pH-partition hypothesis (default setting) but allows the user to select an additional model permitting transcellular ion permeation if desired;

Paracellular permeability based on the chemical's molecular size in relation to paracellular pore sizes (modelled via a Renkin function [46]). In addition pore charge-charge interactions are considered (ionic species as well as neutral species can pass through the paracellular pathways)

The luminal Unstirred Boundary Layer (UBL) which may be the rate limiting barrier for otherwise highly permeable compounds.

A scaling procedure is used to account for the impact of the varying regional gastrointestinal tract (GI) morphology and physiology along the small intestine upon P_{eff}. A further scaling of effective available absorptive surface area, according to epithelial permeability, is provided. This accounts for the fact that highly permeable compounds may be almost entirely absorbed at the villi tips while less permeable compounds will tend to diffuse down the inter-villus spaces and thus be exposed to a larger effective surface area. This scaling procedure is based upon the model described by Oliver et al.[2]. The model also considers the impact of partitioning of the compound into bile salt micelles upon P_{eff}.

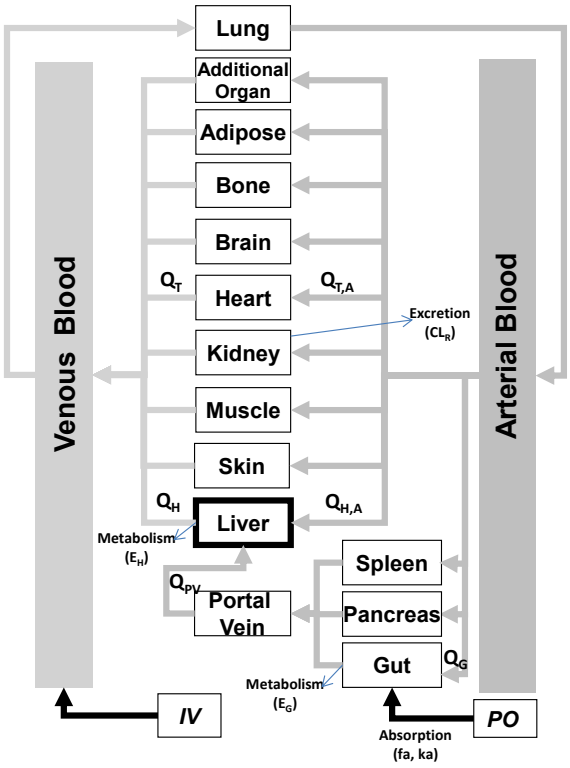

Figure X2. A physiologically based kinetic model. QH, QH,A, QPV, QG, QT,A and QT are blood flows in the hepatic vein, hepatic artery, hepatic portal vein, gut and blood flows into and out of the other tissue (T) compartments, respectively; EG and EH are the fractions undergoing first pass metabolism in the gut and liver, respectively; CLR is the renal clearance; fa and ka are the fraction absorbed and the first order absorption rate constant, respectively.

Intestinal metabolism

The metabolism of nifedipine occurring in human liver microsomes was assumed to be catalysed by CYP 3A4 (see tables in section I). The same information can be used to predict the metabolism of a compound in the intestine by accounting for differences in expression of the CYP 3A4 enzyme in the intestine and in the liver Equation 1 and 2 [3]. Metabolism via multiple enzymes can be accounted for by the summation of the respective enzyme contributions (Equation 3).

$$CL_{int,u,enz} = \frac{CL_{int,u,LM}}{Abundance_{Le}} \quad \text{Equation 1}$$

$$CL_{int,u,G,e} = CL_{int,u,enz} \cdot Abundance_{Ge} \cdot MPPI \quad \text{Equation 2}$$

$$CL_{int,u,G} = \sum_{e=1}^{n} CL_{int,u,G,e} \quad \text{Equation 3}$$

Where CLint,u,enz is in units of L/h/pmol enzyme and CLint,u,G is in units of L/h, CLint,u,lm is the intrinsic clearance in the human liver microsmes and the abundanceLe is the abundance of the isozyme in the liver and AbundanceGe is the abundance of the enzyme in the intestine.

When the first order absorption models are used, the metabolism in the intestine is estimated using the Qgut model. The Qgut model (**Error! Reference source not found.**) can be used to predict intestinal metabolism under the assumption of a homogenous intestinal compartment. Whilst this dramatically simplifies the regional differences in metabolism and transport expression and activities, the Qgut model has been shown a useful approach to predict intestinal metabolism of compounds [3]. The model considers the impact of Qgut, a hybrid parameter consisting of both Qvilli (villus blood flow) and cellular permeability through the enterocyte (CLperm) (**Error! Reference source not found.**) and the net intrinsic metabolic clearance in the gut based on unbound drug concentration (CLuint,G) to drive prediction of FG [3]. Utilisation of this strategy provided reasonable predictions for low to medium intestinal extraction drugs using the assumption of fuG (the fraction of drug unbound in the enterocyte) is 1 (i.e. all unbound) [3, 4]. However, the predictions were less accurate for drugs with moderate to high intestinal extractions (FG <0.5) [4].

$$F_G = \frac{Q_{GUT}}{Q_{GUT} + fu_G \times CLu_{int,G}} \quad \text{Equation 4}$$

$$Q_{GUT} = \frac{Q_{villi} \times CL_{perm}}{Q_{villi} + CL_{perm}} \quad \text{Equation 5}$$

The metabolism of nifedipine within the intestine was predicted using the Qgut model [3, 5], with the assumption that the binding of compound within the intestine (fugut) was equal to the fraction unbound in blood. As it is challenging to directly measure fugut, other possible values for fugut were evaluated using local sensitivity analysis and the results from these evaluations are discussed further within the results and discussion sections of the accompanying manuscript.

Tissue distribution

In the Simcyp human simulator inter-individual variability in tissue distribution is accounted for through relationships between tissue volume and age, sex, weight and height [6]. The *in vivo* volume of distribution at steady state (Vss) is predicted using Equation 6 from Sawada et al. [7]:

$$V_{ss} = (\sum V_T \times P_{T:p}) + (V_e \times E:P) + V_p$$

Equation 6

Where V is the fractional body volume (L/kg) of a tissue (T), erythrocytes (e), and plasma (p), E:P is the erythrocyte:plasma drug concentration ratio and $P_{T:p}$ is the partition coefficient of drug between tissues and plasma components.

In this study the $P_{T:P}$ value for each compound in each tissue was calculated using the methods described by Rodgers and Rowland and co-workers (this is designated as method 2 within the Simcyp simulator) [8-11]. These prediction models split the tissue water volume into intra- and extracellular components and account for binding of basic compounds to the tissue acidic phospholipid fraction. The extent of ionization of the compound of interest at the pH of the compartment of interest is considered within the model and the pH of the tissue space and plasma are specified independently. The methods proposed by Rodgers and Rowland and co-workers were developed primarily using pharmaceutical compounds and so are relevant for the drug compounds considered in this exercise. Both basic and neutral compounds were included in the set of analogue compounds and previous studies have shown that the Rodgers and Rowland methods can improve the prediction of unbound $P_{T:P}$ and consequently Vss for strong bases (pKa >7) [8-11].

Prediction of hepatic clearance

Elimination of a compound can be characterized by various inputs of clearance such as intravenous or oral clearance (CL_{iv} or CL_{po}), whole organ metabolic clearance via hepatocytes (CL_{int}; µL/min/10^6 cells), liver microsomes (CL_{int}; µL/min/mg) or recombinant enzymes (CL_{int}; µL/min/pmol enzyme). In the current study literature data from human liver microsomes was used to calculate the *in vivo* intrinsic clearance ($CL_{intu,h}$) as an input to the PBK model using the scaling procedure in equation 7. *In vitro* intrinsic clearance values measured *in vitro* were corrected for non-specific microsomal binding using the *in silico* prediction methods contained within the Simcyp simulator (see later for details). On a general basis the *in vivo* hepatic metabolic clearance is predicted using *in vitro-in vivo* extrapolation (IVIVE) as shown schematically in Figure X3 followed by scaling for the specific metabolising tissue blood flow (liver in this case) and fraction of unbound drug in blood.

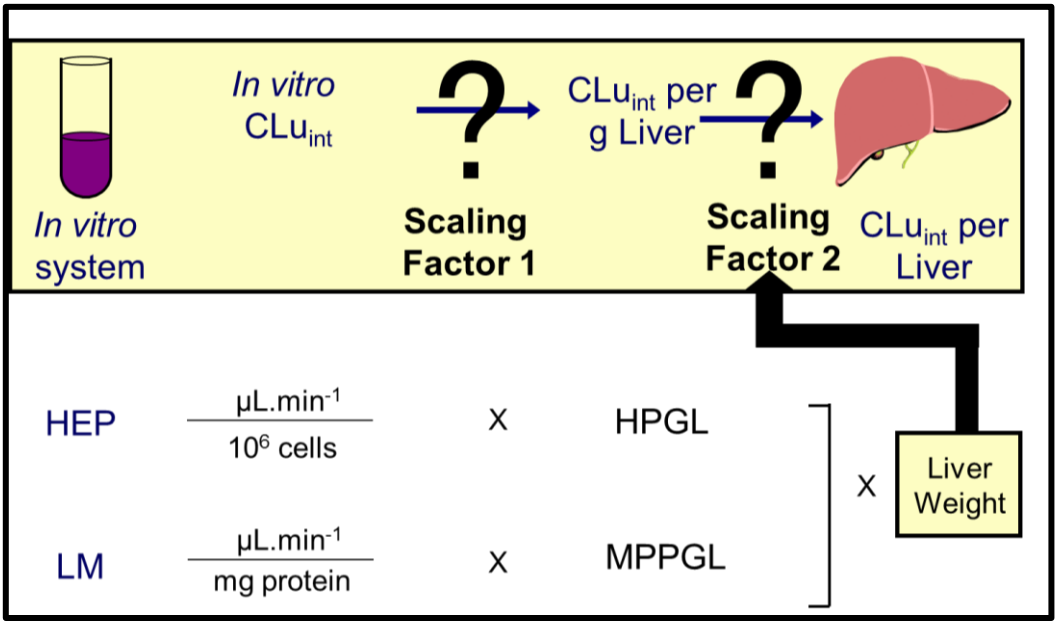

Figure X3. Schematic of IVIVE for scaling of *in vitro* intrinsic clearance available for the Simcyp simulator.

$$CLint_{u,H} = \frac{CLint,mic}{fu,mic} \times Uptake \times MPPGL\ Scaling\ Factor \times Liver\ Weight \times 10^{-6}\ x\ 60 \qquad \text{Equation 7}$$

Where fu_{mic} is the fraction unbound of the compound in the micorosomal incubation, MPPGL is the amount of microsomal protein per gram of liver, uptake was assumed to be only due to passive processes in these simulations (set =1), and 10^{-6} and 60 are to adjust units from µl/min per mg protein to L/h in the whole liver.

Correction for non-specific protein binding is important for IVIVE [12, 13]. $Fu_{,mic}$ may be determined experimentally by equilibrium dialysis, ultrafiltration or ultracentrifugation methods[14]. Measured values of fu_{mic} were not available for the compounds studied in this exercise, and therefore in order to account for non-specific binding of the compound in the incubation, fu_{mic} was predicted using the QSAR model implemented within the Prediction toolbox in the Simcyp Simulator. The Simcyp fu_{mic} prediction is based on a dataset of both human and rat liver microsomes. It has been shown that there are no species differences in microsomal binding once corrections for any differences in protein content in the incubation are accounted for [15]. The fu_{mic} prediction model with Simcyp uses separate models for fully ionised acids, bases and neutral compounds[16]. The fu_{mic} for a partially ionised compound is calculated as described by Gao et al.[17].

The hepatic clearance (CL_H) in humans was calculated from the whole liver scaled *in vivo* $CL_{int,u}$ using the well-stirred model (equation 8).

$$CL_H = \frac{Q_H * Clint_{u,h} * fu_B}{Q_H + (Clint_{u,h} * fu_B)} \qquad \text{Equation 8}$$

Where QH = hepatic blood flow, CLintu,h is the *in vivo* hepatic intrinsic clearance and fuB = fu/(B/P).

Simulations of plasma concentration time profiles for nifedipine after IV and oral exposure were performed using a population of 100 simulated individuals in the default healthy volunteer population within the Simcyp simulator (Version 16).

General description of equations for eliminating and non-eliminating organs

Each compartment within the full body PBK model was initially described as a perfusion limited model with representative equations for an eliminating and non-eliminating organ as shown below. The equations describing the behaviour of the compound within the intestine following oral absorption are as described by Jamei at al [18]. The basic principles for a PBK model outlined on P19 of the WHO guidance on PBPK modelling were adhered to.

Namely

1) the mixing of the chemical in the effluent blood from the tissues is instantaneous and complete;
2) blood flow is unidirectional, constant and non-pulsatile; and
3) the presence of chemicals in the blood does not alter the blood flow rate

In non-eliminating tissues the compound concentration (C) at a given time (t) is defined as follows

$$\frac{dC_{tissue}}{dt} = \frac{Q_{tissue}}{V_{tissue}}\left(C_{ab} - \frac{C_{tissue}}{P_{tissue:p}/_{BP}}\right) \qquad \text{Equation 9}$$

Where Q = blood flow to the tissue, V = tissue volume, Cab = arterial blood concentration, BP = blood to plasma ratio and PTissue:p – partition coefficient of drug between tissues and plasma

In the liver the following equation is applied

$$\frac{dC_{liver}}{dt} = \frac{1}{V_{liver}}\left((Q_{liver} - Q_{pv})C_{ab} + Q_{pv}C_{pv} - \frac{Q_{liver}C_{liver}}{P_{liver:p}/_{BP}} - \frac{f_u}{BP} * \frac{Clu_{int}}{P_{liver:p}/_{BP}} * C_{liver}\right)$$

Equation 10

Where Q_{liver} = sum of blood flow to the liver by the hepatic artery and hepatic portal vein, Q_{pv} = hepatic portal blood vein flow, C_{pv} = hepatic portal compound vein concentration, fu = fraction unbound in plasma, $CL_{int,u}$ = intrinsic clearance.

Within each simulated human subject the sum of the tissue blood flow rates (excluding the lung) are equal to cardiac output. In line with accepted mammalian physiology the lung also receives a blood flow equal to total cardiac output. Subject demographics are within the documented range for human adult subjects Table X1[6].

Table X1. Mean and range of physiological values generated in a population of 100 Healthy adults (50% female) using an age range of 20-50 as input.

Parameter	Mean value	Range
Age (y)	29.6	20 - 48
Weight (kg)	72.45	45 - 118
Height (cm)	168.4	149 - 189
Cardiac output (L/h)	321.8	252 - 416
Serum albumin (g/L)	45.98	35.6 – 58.8

PBK models for other compounds

The structure of the PBK model used for the nifedipine analogue compounds was the same as that used for the simulations of nifedipine. Absorption was predicted using a first order absorption model with metabolism in the intestine described using the Q_{gut} model (fu_{gut} was set equal to the fraction unbound in blood), distribution of the compounds into the tissues was predicted using the approach outlined by Rodgers and Rowland [8-11] with a whole-body PBK model was used for each compound.

The intravenous clearance of four structurally unrelated compounds (sildenafil, verapamil, alfentanil and midazolam) that are each cleared predominantly by CYP 3A4 in humans were also made. The *in vitro* data used in the IVIVE approach (HLM CL_{int}, fu_{mic}, fu_p and BP) was taken from the data generated in laboratory 1 in the publication by Beaumont et al [19]. The clinical data for comparison with the simulated results were taken from literature reports [19, 20].

Step 3 – Model parameterisation

The compound specific input parameters are listed in tables in section H for nifedpine and the related structural compounds. The impact of a number of compound and physiological model input parameters on the plasma AUC of nifedipine following IV and oral dosing were assessed using a one at a time local sensitivity analysis. The results are presented in Tables X2 and X3.

Table X2. Parameter sensitivity and uncertainty table for the effect of changing different model parameters on total plasma AUC of nifedipine after IV dosing. Sensitivity analysis results are presented as high (absolute value greater than or equal to 0.5), medium (absolute value greater than or equal to 0.2 but less than 0.5) or low (absolute value less than 0.2). A sensitivity ratio of 1 implies that a 1% change in input of a parameter value leads to a 1% change in AUC. Uncertainty is a subjective assessment of how reliable the input parameters are. A formal uncertainty analysis as suggested in the WHO PBPK guidance is difficult to perform with a bottom up PBK model as the ratio of median to 95th percentile reflects a measure of variability rather than true uncertainty as could be obtained if the PBK model parameters were fitted to an observed dataset.

		Uncertainty in variability of the input parameter estimates		
		High	Medium	Low
SENSITIVITY	High		Unbound Intrinsic clearance	fu, Liver weight/Volume, MPPGL
	Medium		Portal vein blood flow	BP ratio, Cardiac output,
	Low		Log P, Vss	Molecular weight

Table X3. Parameter sensitivity and uncertainty table for the effect of changing different model parameters on total plasma AUC of nifedipine after oral dosing. Sensitivity analysis results are presented as high (absolute value greater than or equal to 0.5), medium (absolute value greater than or equal to 0.2 but less than 0.5) or low (absolute less than 0.2). A sensitivity ratio of 1 implies that a 1% change in input of a parameter value leads to a 1% change in AUC. Uncertainty is a subjective assessment of how reliable the input parameters are. A formal uncertainty analysis as suggested in the WHO PBPK guidance is difficult to perform with a bottom up PBK model as the ratio of median to 95th percentile reflects a measure of variability rather than true uncertainty as could be obtained if the PBK model parameters were fitted to an observed dataset. The majority of parameters used in the model are based on measured *in vitro* values or are based on mathematical relationships that recapitulate known physiology of the human body. Some parameters are unknown (eg fu_{gut}) and are difficult to measure. For this type of parameter sensitivity analysis was conducted and different possible values (eg fu_{gut} = 1, fu blood, fu plasma or an *in silico* predicted value) were tried. The final model parameter selection was based on the ability of the model to describe the PK of nifedipine after oral dosing (data shown below). The sensitivity of the model to changes in fu_{gut} is not linear and depends on the value of fu_{gut} being used i.e. a 10% change in parameter value does not always have the same impact on the AUC. Depending on the values used the impact was either of moderate or low sensitivity and for this reason fu_{gut} is included in the matrix twice. The same parameter choice was then applied to all of the other analogue compounds i.e. this parameter for the analogues was informed by the PK of the source compound.

SENSITIVITY				
	High		Unbound Intrinsic clearance	
	Medium	fu_{gut}		
	Low	fu_{gut}	Vss, Caco-2 permeability	

Step 4 – Computer implementation (Solving the equations)

The PBK models described in this report were run using the default solver in V16 of the Simcyp simulator, which is based on the 5th order Runge-Kutta solver widely used for solving this type of numerical problem.

Step 5 – Model Performance

The ability of the PBK model to describe the plasma pharmacokinetics of nifedipine after IV and oral dosing are shown in the following figures and tables.

Table X4. Observed and simulated pharmacokinetic parameters for nifedipine

Parameter	Observed[a]	Simulated[b]
Clearance intravenous (L/h)	32.4 +/- 16.8	29.2 +/- 8.7
Clearance Oral (L/h)	62.2 +/- 25.8	63.6 +/- 38.0
Vss (L/kg)	0.77 +/- 0.30	0.88 +/- 0.17

[a] Results are presented as mean +/- SD. Intravenous data come from a meta-analysis of 17 published studies (n=113 individual subjects) and oral clearance from a meta-analysis of 33 studies (n=469 individual subjects). The meta-analyses was conducted using the approach outlined in Howgate et al [5].[b] Simulations were conducted in the Simcyp simulator V16 using a virtual population of 100 healthy subjects aged 20 to 50 years old with 50% of the subjects being female.

(A)

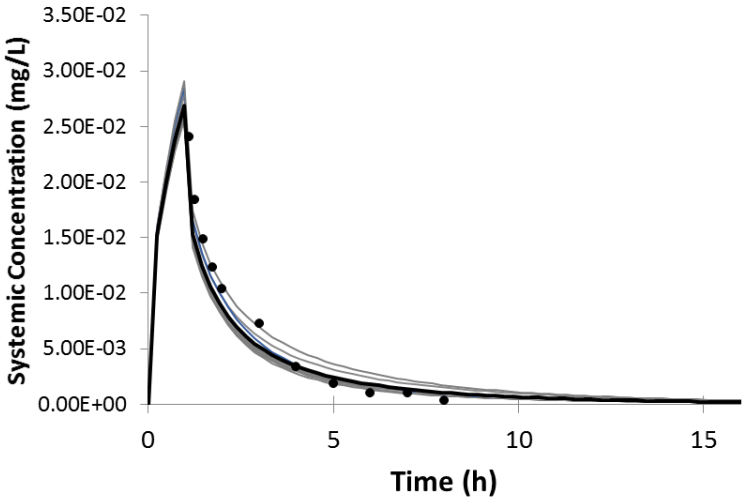

(B)

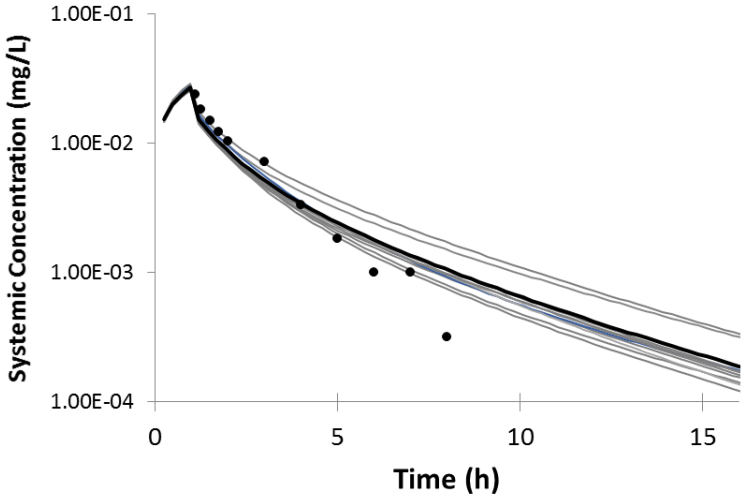

Figure X4. Simulated and observed (black dots) plasma concentration versus time profiles of nifedipine following dosing by intravenous infusion (1.5 mg over 1 hour). Observed data are taken from Lemmer et al [21]. Panel (A) shows the data on a linear y axis and panel (B) shows the data using a log y-axis. Simulations were performed of 10 trials with 12 healthy male individuals 20-30 years old to match the demographic of the subjects used in the clinical study. The thick black line is the mean simulated concentration time profile for the total simulated population the thin grey lines represent the mean simulated concentration time profile for each of the 10 simulated trials.

(A)

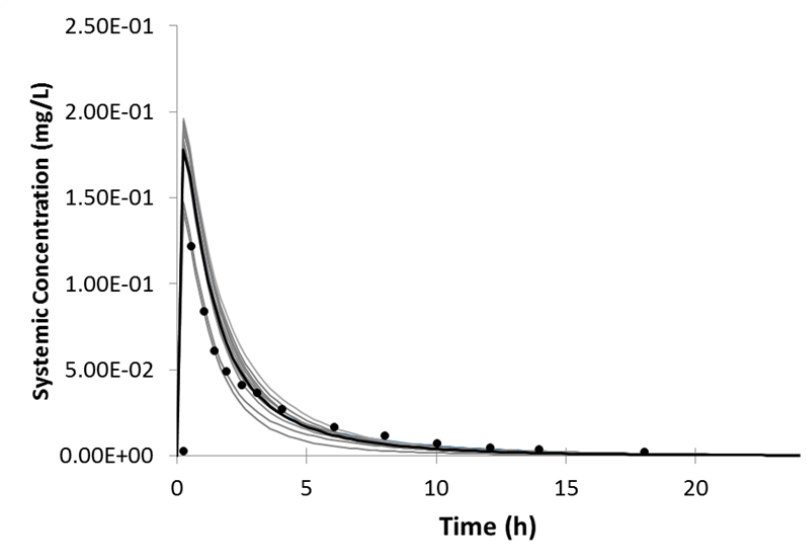

(B)

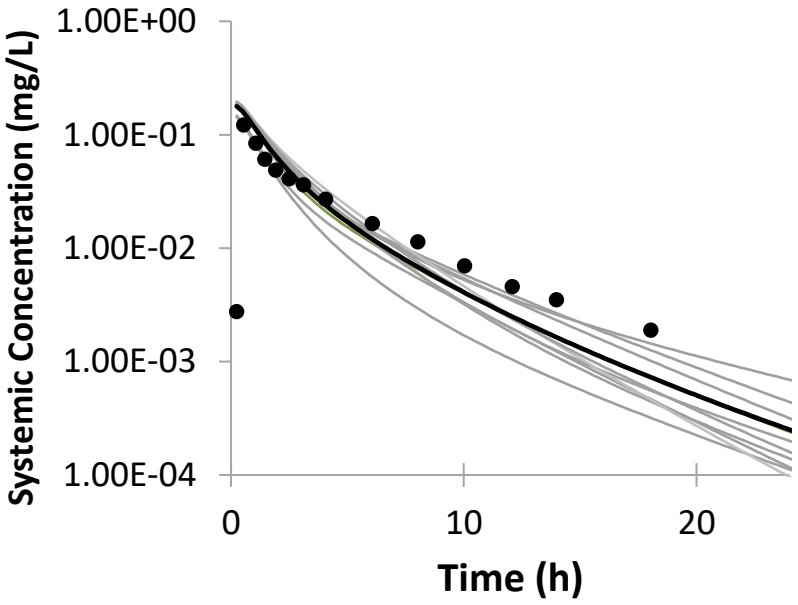

Figure X5. Simulated and observed (black dots) plasma concentration versus time profiles of nifedipine following oral dosing (20 mg). Observed data are taken from Harris et al [22]. Panel (A) shows the data on a linear y-axis and panel (B) shows the data using a log y-axis. Simulations were performed of 10 trials with 10 healthy male individuals 20-50 years old. The thick black line is the mean simulated concentration time profile for the total simulated population the thin grey lines represent the mean simulated concentration time profile for each of the 10 simulated trials.

The results for the analogue compounds used the same model construct and assumptions (model choices) as the nifedipine PBK model. The results are shown in the accompanying draft manuscript and summarized below.

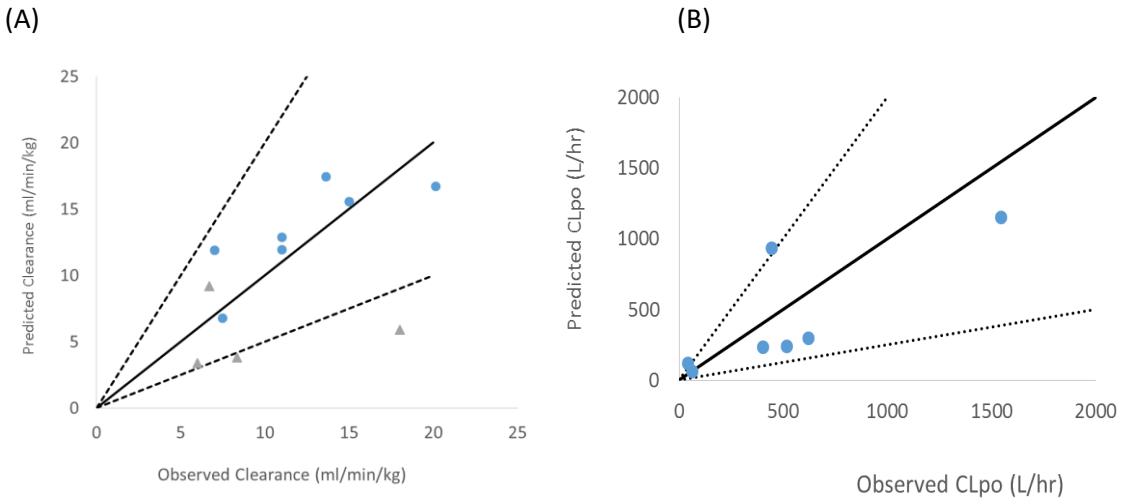

Figure X6. Predicted and observed clearance for the series of phenyl-1,4-dihydropyridine calcium channel antagonists (blue circles) after (A) intravenous and (B) oral dosing. The thick black line is the line of unity and the dotted lines in panel B represent predicted/observed 0.5 and 2-fold ratios. The grey triangles in panel A represent the predicted and observed intravenous clearance values for the four structurally unrelated compounds (alfentanil, midazolam, sildenafil and verapamil).

Step 6 – Model documentation

The results are described in this document and in the in the draft manuscript (in preparation).

E. Identification of uncertainties

Uncertainties are described within the workflow under section D.

F. Model implementation details

The PBK models used in this exercise were constructed in the Simcyp Simulator V16. The Simcyp simulator is a commercial software programme and the model code is not directly exported or visible. However, all of the equations used in the code are published in peer reviewed literature and/or stated in the text of this document. If further details of any particular equation are needed, they can be obtained from the author.

The Simcyp simulator has been extensively tested and used by a consortium of industry, regulatory and academic scientists. Lists of known bugs within the code of the Simcyp simulator are maintained on our website (https://members.simcyp.com/account/softwareIssues/). The QA system used to support the production of each version of the Simcyp simulator has been described in detail [23].

G. Peer engagement (input/review)

This study was done as part of the EU-Toxrisk project funded *from the European Union's Horizon 2020 research and innovation programme under grant agreement No 681002.* The work was presented at the ECOPA meeting in Helsinki, Finland, 2017.

H. Parameter tables

Table X5. Input parameters for the nifedipine PBK model.

Parameter	Value	Method/Reference
Molecular weight (g/mol)	346.3	https://pubchem.ncbi.nlm.nih.gov/compound/4485
log $P_{o:w}$	2.69	
Compound type	Monoprotic Base	
pKa	2.39	
BP	0.74	[24]
fu_p	0.04	[25]
Main plasma binding protein	Human serum albumin	
Fa	0.99	Predicted
ka (1/h)	2.31	Predicted
fu_{gut}	0.054	Assumed
Q_{gut} (L/h)	15.82	Predicted
$P_{eff,man}$ (10^{-4}cm/s)	5.62	Predicted
Permeability Assay	Caco-2	
Apical pH : Basolateral pH	7.4 : 7.4	
Activity	Passive & Active	
$P_{appA:B}$(10^{-6} cm/s)	52.3	[26]
Reference Compound	Propranolol	
Reference Compound $P_{appA:B}$ (10^{-6} cm/s)	40.5	[26]
Scalar	1.06	

Distribution Model	Full PBPK Model	
VSS (L/kg)	0.86	Predicted[8-11]
Enzyme	CYP3A4	
Pathway	Oxidation	
CL_{int} (µL/min/mg protein)	382.5	[24]
CL_R (L/h)	0	assumed

Table X6. Input parameters for the PBK models for the structurally related phenyl-1,4-dihydropyridine calcium antagonist compounds

Compound	Nitrendipine	Nisoldipine	Nimodipine	Felodipine	Amlodipine	Nicardipine
Smiles	CCOC(=O)C1=C(NC(=C(C1c2cccc(c2)[N+](=O)[O-])C(=O)OC)C)C	CC1=C(C(C(=C(N1)C)C(=O)OCC(C)C)c2ccccc2[N+](=O)[O-])C(=O)OC	CC1=C(C(C(=C(N1)C)C(=O)OC(C)C)c2cccc(c2)[N+](=O)[O-])C(=O)OCCOC	CCOC(=O)C1=C(NC(=C(C1c2cccc(c2Cl)Cl)C(=O)OC)C)C	CCOC(=O)C1=C(NC(=C(C1c2ccccc2Cl)C(=O)OC)C)COCCN	CC1=C(C(C(=C(N1)C)C(=O)OCCN(C)Cc2ccccc2)c3cccc(c3)[N+](=O)[O-])C(=O)OC
Similarity to nifedipine % (RD_Kit_MACCS_DICE)	95	95	87	73	63	85
Similarity to nifedipine % (RD_KIT_MACCS_Tanimoto)	90	91	77	57	46	73
MW	360.4 (1)	388.4 (1)	418.4 (1)	384.3 (1)	408.9 (1)	479.5 (1)
Log P	3.5 (1)	4.4 (1)	3.86 (1)	4.83 (S-isomer) (1)	3.64 (7)	3.82 (1)
pKa	Neutral (1)	Neutral (1)	Neutral (1)	Neutral (1)	Basic (pKa =9.1) (8)	Basic (pKa = 8.18)(6)
BP	1.46 (2)	1 (3)	1.34 (4)	0.78 (4)	1.48 (8)	0.69 (4)
fu	0.02 (2)	0.003 (3)	0.029 (4)	0.0036 (5)	0.05 (8)	0.016 (4)
fa	0.98	1.00	1.0	1.0	0.91	0.98
fu_{gut}	0.0137	0.003	0.022	0.0046	0.034	0.023
Q_{gut} (L/h)	13.0	18.3	17.9	16.0	9.9	13.3

$P_{eff,man}$ (10^{-4}cm/s)	3.35	9.85	8.95	5.85	1.95	3.50
$P_{eff,man}$ prediction method	Caco-2 *in vitro* data[27]	Mechanistic permeability model (Simcyp simulator V16)	Mechanistic permeability model (Simcyp simulator V16)	Caco-2 *in vitro* data [4]	Caco-2 data [28]	Caco-2 data calibrated against midazolam [26]
Vss prediction method	Simcyp Method 2 [8-11]	Simcyp Method 2 [8-11])	Simcyp Method 2 [8-11]	Simcyp Method 2 [8-11]	Simcyp Method 2 [8-11]	Simcyp Method 2 [8-11]
$CLint_u$ HLM 3A4 (µl/min/mg protein)	2591(2)	57211 (scaled from the data in [4] using felodipine as a calibrator)	1684 (4)	16700 (4)	497 (4)	9414 (4,9)
Clinical Data	[29-33]	[4, 34, 35]	[36]	[37]	[38-40]	[40-42]

Where BP = blood to plasma ratio, fu = fraction unbound in plasma. For all compounds the major binding protein in plasma was assumed to be albumin and renal clearance was assumed to be negligible, volume of distribution at steady state (V_{ss}) was predicted using the approach outlined by Rodgers and Rowland [8, 10]. The intrinsic clearance measured *in vitro* in human liver microsomes was assumed to be exclusively catalysed by CYP 3A4 and was corrected for non-specific binding using the microsomal binding prediction model within the Simcyp simulator (V16). Sources of data: (1) http://www.chemspider.com (2) [43] (3) [4], (4) [19], (5)[20] (6) https://www.ebi.ac.uk/chembl/compound_report_card/CHEMBL1484/ (7) calculated from Log D and pKa reported in [44], (8) [44], (9)[45] (10)[8, 10]. Unless stated otherwise all values in the table are based on measurements/predictions made for the racemic compound.

I. References and background information

The work is described in a draft publication made available alongside the completed PBK template. See reference list below.

1. Sugano, K., Theoretical investigation of passive intestinal membrane permeability using Monte Carlo method to generate drug-like molecule population. Int J Pharm, 2009. 373(1-2): p. 55-61.

2. Oliver, R.E., A.F. Jones, and M. Rowland, What surface of the intestinal epithelium is effectively available to permeating drugs? J Pharm Sci, 1998. 87(5): p. 634-9.

3. Yang, J., et al., Prediction of intestinal first-pass drug metabolism. Curr Drug Metab, 2007. 8(7): p. 676-84.

4. Gertz, M., et al., Prediction of human intestinal first-pass metabolism of 25 CYP3A substrates from *in vitro* clearance and permeability data. Drug Metab Dispos, 2010. 38(7): p. 1147-58.

5. Howgate, E.M., et al., Prediction of *in vivo* drug clearance from *in vitro* data. I: impact of inter-individual variability. Xenobiotica, 2006. 36(6): p. 473-97.

6. Jamei, M., G.L. Dickinson, and A. Rostami-Hodjegan, A framework for assessing inter-individual variability in pharmacokinetics using virtual human populations and integrating general knowledge of physical chemistry, biology, anatomy, physiology and genetics: A tale of 'bottom-up' vs 'top-down' recognition of covariates. Drug Metab Pharmacokinet, 2009. 24(1): p. 53-75.

7. Sawada, Y., et al., Prediction of the volumes of distribution of basic drugs in humans based on data from animals. J Pharmacokinet Biopharm, 1984. 12(6): p. 587-96.

8. Rodgers, T., D. Leahy, and M. Rowland, Physiologically based pharmacokinetic modeling 1: predicting the tissue distribution of moderate-to-strong bases. J Pharm Sci, 2005. 94(6): p. 1259-76.

9. Rodgers, T., D. Leahy, and M. Rowland, Tissue distribution of basic drugs: accounting for enantiomeric, compound and regional differences amongst beta-blocking drugs in rat. J Pharm Sci, 2005. 94(6): p. 1237-48.

10. Rodgers, T. and M. Rowland, Physiologically based pharmacokinetic modelling 2: predicting the tissue distribution of acids, very weak bases, neutrals and zwitterions. J Pharm Sci, 2006. 95(6): p. 1238-57.

11. Rodgers, T. and M. Rowland, Mechanistic approaches to volume of distribution predictions: understanding the processes. Pharm Res, 2007. 24(5): p. 918-33.

12. Brown, H.S., A. Chadwick, and J.B. Houston, Use of isolated hepatocyte preparations for cytochrome P450 inhibition studies: comparison with microsomes for Ki determination. Drug Metab Dispos, 2007. 35(11): p. 2119-26.

13. McGinnity, D.F., et al., Evaluation of time-dependent cytochrome P450 inhibition using cultured human hepatocytes. Drug Metab Dispos, 2006. 34(8): p. 1291-300.

14. Giuliano, C., et al., Direct determination of unbound intrinsic drug clearance in the microsomal stability assay. Drug Metab Dispos, 2005. 33(9): p. 1319-24.

15. Zhang, Y., et al., Lack of appreciable species differences in nonspecific microsomal binding. J Pharm Sci, 2010. 99(8): p. 3620-7.

16. Turner DB, et al. Prediction of non-specific microsomal binding from readily available physicochemical properties. in 9th European ISSX meeting. 2006. Manchester, UK. 2006:June 4-7.

17. Gao, H., et al., In silico modeling of nonspecific binding to human liver microsomes. Drug Metab Dispos, 2008. 36(10): p. 2130-5.

18. Jamei, M., et al., Population-based mechanistic prediction of oral drug absorption. AAPS J, 2009. 11(2): p. 225-37.

19. Beaumont, K., et al., Toward an integrated human clearance prediction strategy that minimizes animal use. J Pharm Sci, 2011. 100(10): p. 4518-35.

20. Obach, R.S., F. Lombardo, and N.J. Waters, Trend analysis of a database of intravenous pharmacokinetic parameters in humans for 670 drug compounds. Drug Metab Dispos, 2008. 36(7): p. 1385-405.

21. Lemmer, B., et al., Chronopharmacokinetics and cardiovascular effects of nifedipine. Chronobiol Int, 1991. 8(6): p. 485-94.

22. Harris, R.Z., et al., Rosiglitazone has no clinically significant effect on nifedipine pharmacokinetics. J Clin Pharmacol, 1999. 39(11): p. 1189-94.

23. Jamei, M., et al., The simcyp population based simulator: architecture, implementation, and quality assurance. In Silico Pharmacol, 2013. 1: p. 9.

24. Akabane, T., et al., A comparison of pharmacokinetics between humans and monkeys. Drug Metab Dispos, 2010. 38(2): p. 308-16.

25. Krecic-Shepard, M.E., et al., Race and sex influence clearance of nifedipine: results of a population study. Clin Pharmacol Ther, 2000. 68(2): p. 130-42.

26. Lau, Y.Y., et al., Evaluation of a novel in vitro Caco-2 hepatocyte hybrid system for predicting in vivo oral bioavailability. Drug Metab Dispos, 2004. 32(9): p. 937-42.

27. Heikkinen, A.T., et al., In vitro to in vivo extrapolation and physiologically based modeling of cytochrome P450 mediated metabolism in beagle dog gut wall and liver. Mol Pharm, 2013. 10(4): p. 1388-99.

28. Dennison, T.J., et al., Fixed-dose combination orally disintegrating tablets to treat cardiovascular disease: formulation, in vitro characterization and physiologically based pharmacokinetic modeling to assess bioavailability. Drug Des Devel Ther, 2017. 11: p. 811-826.

29. Ankermann, T., et al., Elimination and haemodynamic effects of nitrendipine in patients with chronic renal failure. Eur J Clin Pharmacol, 1989. 36(5): p. 433-7.

30. Antolic, G., F. Kozjek, and S. Primozic, The relevance of nitrendipine erythrocyte partitioning for the variability of its bioavailability parameters. Int J Pharm, 2001. 215(1-2): p. 147-52.

31. Aronoff, G.R., Pharmacokinetics of nitrendipine in patients with renal failure: comparison to normal subjects. J Cardiovasc Pharmacol, 1984. 6 Suppl 7: p. S974-6.

32. Soons, P.A., et al., Oral absorption profile of nitrendipine in healthy subjects: a kinetic and dynamic study. Br J Clin Pharmacol, 1989. 27(2): p. 179-89.

33. Mikus, G., et al., Application of stable isotope methodology to study the pharmacokinetics, bioavailability and metabolism of nitrendipine after i.v. and p.o. administration. Br J Clin Pharmacol, 1987. 24(5): p. 561-9.

34. van Harten, J., et al., The influence of infusion rate on the pharmacokinetics and haemodynamic effects of nisoldipine in man. Br J Clin Pharmacol, 1988. 25(6): p. 709-17.

35. Friedel, H.A. and E.M. Sorkin, Nisoldipine. A preliminary review of its pharmacodynamic and pharmacokinetic properties, and therapeutic efficacy in the treatment of angina pectoris, hypertension and related cardiovascular disorders. Drugs, 1988. 36(6): p. 682-731.

36. Varma, M.V., et al., Physicochemical space for optimum oral bioavailability: contribution of human intestinal absorption and first-pass elimination. J Med Chem, 2010. 53(3): p. 1098-108.

37. Dunselman, P.H. and B. Edgar, Felodipine clinical pharmacokinetics. Clin Pharmacokinet, 1991. 21(6): p. 418-30.

38. Abernethy, D.R., The pharmacokinetic profile of amlodipine. Am Heart J, 1989. 118(5 Pt 2): p. 1100-3.

39. Murdoch, D. and R.C. Heel, Amlodipine. A review of its pharmacodynamic and pharmacokinetic properties, and therapeutic use in cardiovascular disease. Drugs, 1991. 41(3): p. 478-505.

40. Vincent, J., et al., Lack of effect of grapefruit juice on the pharmacokinetics and pharmacodynamics of amlodipine. Br J Clin Pharmacol, 2000. 50(5): p. 455-63.

41. Graham, D.J., et al., Pharmacokinetics of nicardipine following oral and intravenous administration in man. Postgrad Med J, 1984. 60 Suppl 4: p. 7-10.

42. Laurent-Kenesi, M.A., et al., Influence of CYP2D6-dependent metabolism on the steady-state pharmacokinetics and pharmacodynamics of metoprolol and nicardipine, alone and in combination. Br J Clin Pharmacol, 1993. 36(6): p. 531-8.

43. Mitsui, T., et al., A useful model capable of predicting the clearance of cytochrome 3A4 (CYP3A4) substrates in humans: validity of CYP3A4 transgenic mice lacking their own Cyp3a enzymes. Drug Metab Dispos, 2014. 42(9): p. 1540-7.

44. Small, H., et al., Measurement of binding of basic drugs to acidic phospholipids using surface plasmon resonance and incorporation of the data into mechanistic tissue composition equations to predict steady-state volume of distribution. Drug Metab Dispos, 2011. 39(10): p. 1789-93.

45. Naritomi, Y., et al., Prediction of human hepatic clearance from in vivo animal experiments and in vitro metabolic studies with liver microsomes from animals and humans. Drug Metab Dispos, 2001. 29(10): p. 1316-24.

46. Renkin EM. Filtration, diffusion, and molecular sieving through porous cellulose membranes. J Gen Physiol. 1954;38(2):225–243.

Part II Checklist for model evaluation

PBK Model Evaluation Checklist	Checklist assessment	Comments
Name of the PBK model (as in the reporting template)	**IVIVE-PBPK model for phenyl-1,4-dihydropyridine calcium channel antagonists**	
Contact details	**Iain Gardner, Simcyp Certara**	
Name of person reviewing and contact details	**Alicia Paini**	
Date of checklist assessment	**29/04/2020**	
A. Context/Implementation		
A.1. Regulatory Purpose		
1. What is the acceptable degree of confidence/uncertainty (e.g. high, medium or low) for the envisaged application (e.g. priority setting, screening, full assessment?)	**High**	
2. Is the degree of confidence/uncertainty in application of the PBK model for the envisaged purpose greater or less than that for other assessment options (e.g. reliance on PBK model and *in vitro* data vs. no experimental data)?	**High**	
A.2. Documentation		
3. Is the model documentation adequate, i.e. does it address the essential content of model reporting template, including the following:		
• Clear indication of the chemical, or chemicals, to which the model is applicable?	**Yes**	
• Is the model being applied for the same scientific purpose as it was developed, or has it been repurposed somehow?	**Yes**	**Platform is used that was built for different applications**
• Model assumptions?	**Yes**	
• Graphical representation of the proposed mode of action, if known?	**Yes**	
• Graphical representation of the conceptual model?	**Yes**	
• Supporting tabulation for parameters (names, meanings, values, mean and standard deviations, units and sources)?	**Yes**	
• Relevance and reliability of model parameters?	**Yes**	
• Uncertainty and sensitivity analysis?	**Yes**	**OAT**
• Mathematical equations?	**Yes**	
• PBK model code?	**No**	**Is part of the Simcyp software**
• Software algorithm to run the PBK model code?	**Yes**	
• Qualification of PBK software platform?	**Yes**	

A.3 Software Implementation and Verification		
4. Does the model code express the mathematical model?	**Yes**	
5. Is the model code devoid of syntactic and mathematical errors?	**Yes**	
6. Are the units of input and output parameters correct?	**Yes**	
7. Is the chemical mass balance respected at all times?	**Yes**	
8. Is the cardiac output equal to the sum of blood flow rates to the tissue compartments?	**Yes**	
9. Is the sum total of tissue volumes equal to total body volume?	**Yes**	
10. Is the mathematical solver a well-established algorithm?	**Yes**	
11. Does the mathematical solver converge on a solution without numerical error?	**Yes**	
12. Has the PBK modelling platform been subjected to a verification process (for a different use, for instance, in the pharmaceutical domain)?	**Yes**	**Simcyp, Well established platform**
A.4 Peer engagement (input/review)		
13. Has the model been used previously for a regulatory purpose?	**Yes**	**Drug submission**
• Is prior peer engagement in the development and review of the model sufficient to support the envisaged application?	**Yes**	
• Is additional review required? Peer engagement includes input/review by experts on specific aspects of model development, individual reviews of the model by experts, or collective reviews by peer review panels. Availability of the comments and tracking of revisions to the model in response to peer input contributes to increased confidence in the model for potential application.	**No**	
B. Assessment of Model Validity		
B.1 Biological Basis (Model Structure and Parameters)		
14. Is the model consistent with known biology?	**Yes**	
• Is the biological basis for the model structure provided?	**Yes**	
• Is the complexity of the model structure appropriate to address the regulatory application?	**Yes**	
• Are assumptions concerning the model structure and parameters clearly stated and justified?	**Yes**	
• Is the choice of values for physiological parameters justified?	**Yes**	
• Is the choice of methods used to estimate chemical-specific ADME parameters justified?	**Yes**	
• Saturable kinetics	**Not present**	
B.2 Theoretical Basis of Model Equations		
15. Are the underlying equations based on established theories, .e.g. Michaelis-Menten kinetics, Fick's laws of diffusion?	**Yes**	

• In the case of PBK models for particles, does the model take into consideration the properties of particles, e.g. particle size ranges, (poor) solubility, aggregation, partitioning and diffusion/sedimentation behaviour?	**N.A.**	
B.3. Reliability of input parameters		
16. Has the uncertainty (individual variability, experimental reproducibility and reliability) in the input parameters been characterised?	**Yes**	
B.4. Uncertainty and Sensitivity Analysis		
17. Has the impact of uncertainty (individual variability, experimental reproducibility and reliability) in the parameters on the chosen dose metric been estimated?	**Yes by SA**	
• Local sensitivity analysis?	**Yes**	
• Global sensitivity analysis?	**No**	
18. Is confidence in influential input parameter estimates (i.e., based on comparison of uncertainty and sensitivity) reasonable (within expected values; similar to those of analogues) in view of the intended application?	**Yes**	
B.5. Goodness-of-Fit and Predictivity		
19. For PBK models for which there are sufficient *in vivo* data for the chemical of interest:		
• Suitability as analogue (chemical and biological similarity) been assessed?	**Yes**	
• Reliable estimation of chosen dose metric for analogue?	**Yes**	
• In general is the biological Variability of *in vivo* reference data (from analogue) established?	**Yes**	

NA= Not applicable; NR = Not Reported

Part III Overall Evaluation

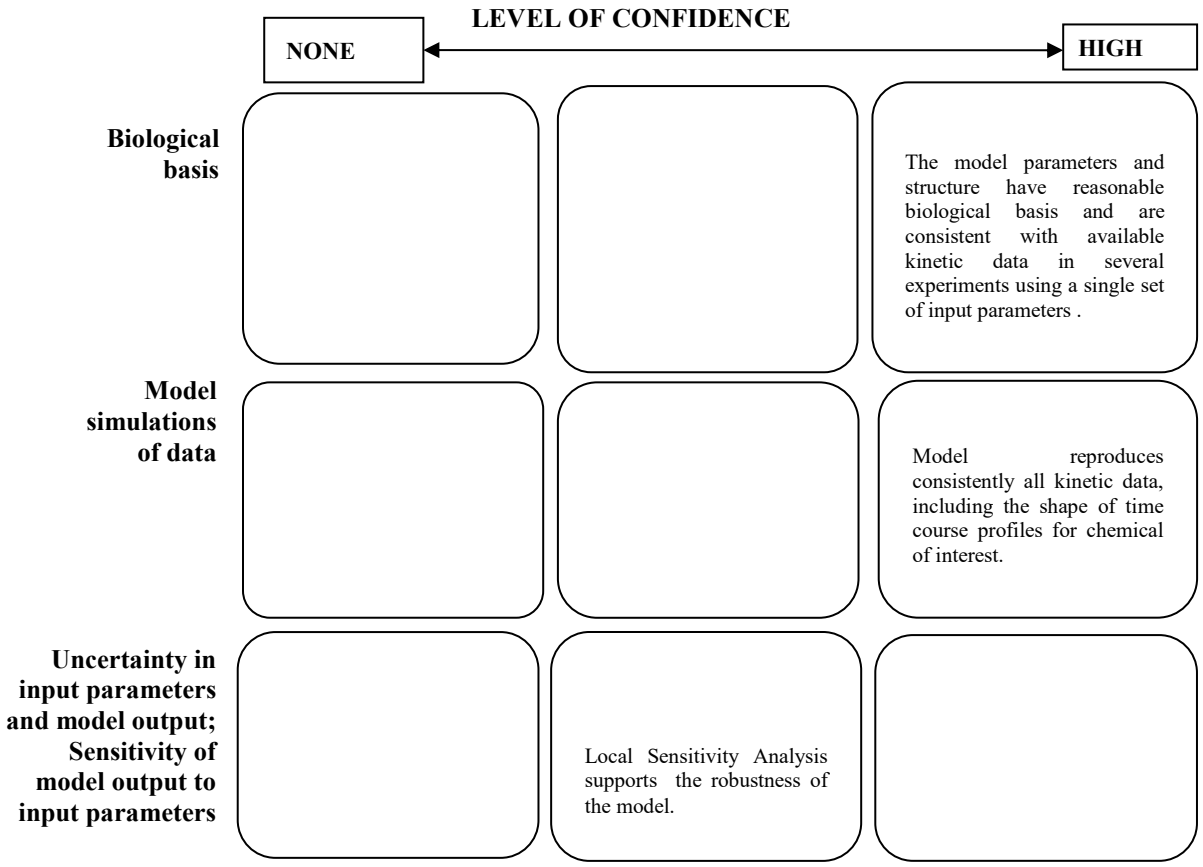

An *in vitro-in vivo* extrapolation approach coupled with a physiologically based kinetic (PBK) model to predict the plasma exposure and pharmacokinetic parameters of a series of seven structurally related phenyl-1,4-dihydropyridine compounds was developed. The model is built using solid knowledge on the chemicals MoA, and is parametrise using good *in vitro* measured data well established. The model reproduces the shape time and dose course of the chemical(s) of interest. A Local Sensitivity Analysis supports the robustness of the model.

Based on the results available, it was concluded that, the application of this PBK model for IVIV extrapolation to read across is a reasonable approach to inform hazard characterisation. A global SA would have given a more global overview on the key parameters that can perturb the model output.

Case Study XI

Using high-throughput pharmacokinetic simulation and *in silico* property predictions to predict herbicide absorption and bioavailability

Part I. PBK model reporting template

A. Name of model

Using high-throughput pharmacokinetic simulation and *in silico* property predictions to predict herbicide absorption and bioavailability.

B. Contact details

Author: Robert D. Clark

Affiliation: Simulations Plus, Inc.

C. Summary of model characterisation, development, validation, and regulatory applicability

Key compound-specific physicochemical and metabolic properties needed to run a rat pharmacokinetic (PK) simulation were calculated using ADMET Predictor™ 9.0 for a representative group of herbicides drawn from the literature. The predicted properties were fed into the program's high-throughput pharmacokinetic (HTPK) Simulation Module. The Module links the Advanced Compartmental Absorption and Transit (ACAT™) model developed for GastroPlus™ to three other compartments: one for first-pass liver metabolism, one for renal excretion, and a central compartment that accounts for the systemic circulation and other tissues. The effective volume of the central compartment was calculated mechanistically from the predicted compound properties and the known compositions of the tissues it represents.

Simulations were run on a dose of 2.5 mg for each herbicide and the predicted percentages absorbed (%Fa) and reaching the systemic circulation (%Fb) were estimated. They were compared to published values for the percentages of radiolabel not recovered in the feces and of parent recovered in the urine, which represent lower bounds for %Fa and %Fb, respectively.

The observed %Fa was within 2-fold of the observed value for 81% of the compounds examined, and an additional 3% (one compound) was within the reported experimental variation. The observed %Fb was within 2-fold of the predicted value for 59% of the compounds. Only a quarter of the compounds falling outside that range (10% of the total) represented underestimates of systemic exposure. Most of the molecules for which %Fb was overestimated by more than 2-fold are known to be subject to non-cytochrome P450 metabolism or enterohepatic circulation or both; failing to account for those factors was likely responsible for the overestimations in these cases.

The herbicides analyzed have already received regulatory approval and undergone risk assessments, but there is no reason to think that the method's applicability is limited to them or to that kind of compound. The approach could be used in the future by end-users

in support of chemical registration applications in general or by regulators in evaluating such applications.

D. Model characterisation (Modelling workflow)

Step 1 – Scope and purpose of the model (problem formulation)

The fully *in silico* systemic exposure assessment described here can be augmented by measured ADME properties where good experimental values – e.g., solubility, pKa, lipophilicity, microsomal clearance - are available. Even when that is not feasible, the exposure estimates obtained can be used to generate hypotheses that can be tested with reduced numbers of test animals. It can also highlight cases where *in vivo* results from animals are unlikely to be directly translatable to human beings.

Property predictions can identify measured properties that need to be reevaluated for use in other simulations, and sensitivity analyses carried out within the framework can identify properties in need of particularly accurate determination.

Step 2 – Model conceptualisation (model structure, mathematical representation)

- The QSAR models used are based on artificial neural network ensembles (ANNE) regression and classification models.
- The pharmacokinetic simulation is based on the ACAT model from GastroPlus plus a liver compartment, a kidney compartment and a central compartment. Compartment properties and flows are taken from the literature for gut, liver and kidney. The effective volume of the central compartment is calculated from the estimated lipophilicity and pKa of the compound and literature tissue compositions of each organ.
- A schematic of the HTTPK Simulation model is shown in Figure XI1.
- Results are shown graphically in Figure XI2

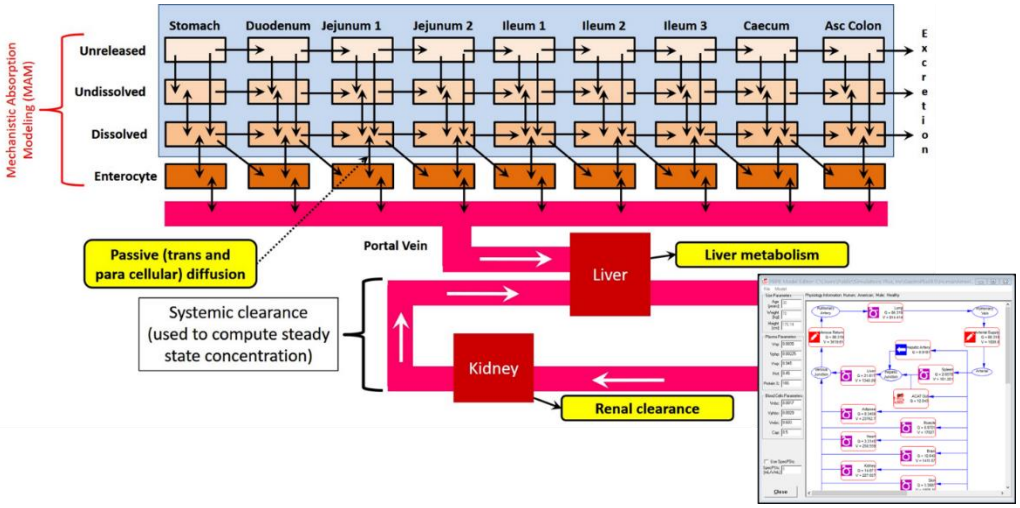

.

Figure XI1. Schematic representative of the compartmental layouts and flow used in the HTTPK Simulation Module of ADMET Predictor 9.0.

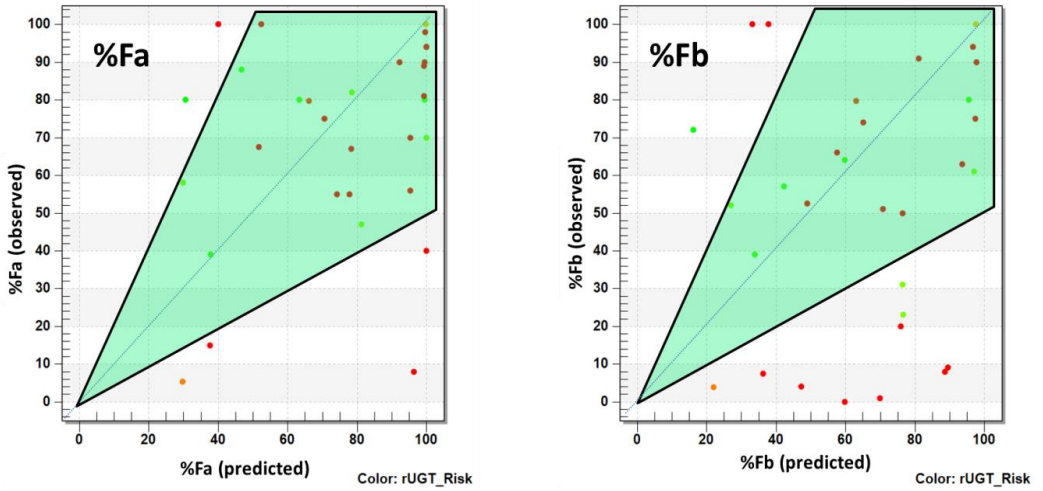

Figure XI2. Plots of observed (Y-axis) vs predicted (X-axis) %Fa and %Fb estimated for herbicides based on *in silico* property predictions for a typical male rat.

Assumptions

- Formulation effects in gavage dosing are negligible at the doses examined.
- Active influx and efflux transport did not dominate intestinal uptake for these compounds.
- Metabolism is predominantly hepatic and mediated by CYPs.
- Biliary excretion and enterohepatic circulation are negligible.
- Metabolism within the gut lumen is negligible.

Step 3 – Model parameterisation

1) Searches of EPA, EFSA and WHO risk assessments and databases provided observed %Fa and %Fb estimates for 31 of 37 representative herbicides cited by Zhang et al.
2) Fasted rat physiology details (gastrointestinal compartment sizes and transit times, liver volumes, etc.) were taken from the ACAT model in GastroPlus 9.0.
3) Rat HTPK simulations were run for each herbicide in ADMET Predictor 9.0 using predicted logP, pKa, aqueous solubility, effective jejunal permeability, fraction unbound in microsomes (fumic), fraction unbound in rat plasma (fup), and the ratio of blood to plasma for rat. Hepatic clearance was based on the predicted total cytochrome P450 (CYP) clearance in rat liver microsomes (RLM). Renal clearance was taken as glomerular filtration rate (GFR) * fup. Calculated fractions ionized and molecular size parameters were used to account for paracellular permeability.
4) The predicted %Fa was compared graphically to the percentage of radiolabel not recovered in the feces and the predicted %Fb was compared with the amount of parent recovered from the urine. Note that both "observed" values are lower bounds for the values that would be obtained by sampling the blood.

5) Points in the predicted vs. observed plots were color-coded by a qualitative measure of their predicted susceptibility to glucuronidation in rat liver and by whether or not they were predicted to be substrates for P-glycoprotein (P-gp). This was done to flag cases where the simplifying assumptions made may break down. Classification models are also available that can indicate where active transport is likely to enhance first-pass metabolism; these are calibrated for human beings but are probably reasonably applicable to rats as well.

Step 4 – Computer implementation (solving the equations)

The equations are executed using the ADMET Predictor 9.0.

Step 5 – Model Performance

- Sensitivity to dose can be examined by specifying multiple doses in the user interface.
- Graphical sensitivity analysis with respect to solubility and permeability inputs is available for fraction absorbed, bioavailability, Cmax, Tmax and AUC.
- Sensitivity to hepatic clearance, lipophilicity, fraction unbound in plasma, blood:plasma ratio and volume of distribution can readily be varied manually.
- System parameters such as body weight, compartment dimensions and transit times are accessible in parameter files but are not directly exposed to the casual user.

Step 6 – Model Documentation

The model information are reported in the peer review articles in the reference list.

E. Identification of uncertainties

Model structure

- The HTPK Simulation model does not attempt to take biliary excretion or enterohepatic circulation into account, nor is metabolism outside the liver considered.
- Species-specific system parameters are set based on literature values for the chosen species. A broad range of applications has shown them to be suitable and robust in a pharmaceutical setting.
- Variations in physiology between strains, sexes and individuals are not taken into account.
- **Note**: where such effects are known to occur, a full PBPK simulation can be run in GastroPlus.

Input parameters

- Predictions for compounds falling outside the applicability domains of the QSAR models used to predict properties may not be reliably predicted, but such predictions are flagged by the program.

- Classification models for being a P-gp or UGT substrate are available to indicate when either or both may complicate the analysis. Individualized confidence estimates are provided for all in-scope predictions.
- A quantitative measure of predictivity for a held-out test set is provided in the ADMET Predictor spreadsheet for each classification and regression QSAR model.
- A dose of 2.5 mg per animal was used in the analysis described here and a body weight of 0.25 kg was assumed. This was representative of the reported doses in most cases and usually fell within the dose-proportional absorption and excretion range, where that was reported. Both can be varied as appropriate.

Model output

See Sensitivity analysis above.

Other uncertainties (e.g. model developed for different substance and/or purpose)

The "observed" values are approximations in all cases and rather poor ones in some due to the biology involved.

The system is completely mechanistic, so the number of freely adjustable parameters is minimal; none are fitted to data for the compound in question. The species-specific compartmental parameters are well documented and, other than the central compartment, are not compound-specific. Compound-specific property inputs can be checked by *in vitro* measurements if necessary. Moreover, the differential equations that define how the inputs interact constrain the output substantially, thereby limiting the effective number of degrees of freedom.

The biggest source of uncertainty is attributable to unknown contributions from active efflux, active hepatic uptake, and non-CYP metabolism. Fortunately, the model is conservative for most scenarios in which these factors do contribute substantially – i.e., the systemic exposure is lower than predicted (Figure XI2).

A strategy to reduce the overall uncertainty: Rodent exposure assays are not always directly relevant to human beings. A validated *in silico* comparison of predicted exposures in rats and humans can serve to generate hypotheses that can be tested *in vitro* more efficiently than in animal tests. At a minimum, such simulations will support a shift to hypothesis-driven testing that should minimize the number of animal tests that need to be done. More thorough validation of the workflow is needed to build confidence in its general applicability.

Good quantitative QSAR models need to be developed for major metabolic pathways other than CYPs, especially UGTs and esterases. Kinetic models are also needed for efflux transporters and those involved in biliary excretion. These would substantially improve predictions for acids and simple esters.

Develop a way to estimate uncertainties for individual predictions rather than average reliability statistics for held-out test sets.

Validate the use of the dose optimization function in ADMET Predictor for use in estimating systemic concentrations after chronic exposure to potential toxins.

F. Model implementation details

- software (version no) ADMET Predictor (9.0).
- availability of code: the code is available under an annual commercial license from Simulations Plus, Inc. Academic and non-profit licenses are heavily discounted.
- software verification / qualification YES

G. Peer engagement (input/review)

Dr. Michael Bolger and John DiBella (Simulations Plus, Inc.; review)

H. Parameter tables

No customization was involved. Default program settings were used except dose 0.25 mg and specifying default rat physiology

I. References and background information

PR Daga, MB Bolger, IS Haworth, RD Clark & J Martin (2018). Physiologically Based Pharmacokinetic Modeling in Lead Optimization. 1. Evaluation and Adaptation of GastroPlus To Predict Bioavailability of Medchem Series. Mol Pharmaceutics 15, 821-830.

PR Daga, MB Bolger, IS Haworth, RD Clark & J Martin (2018). Rational Bioavailability Design by Global Sensitivity Analysis To Identify Properties Affecting Bioavailability. Mol Pharmaceutics 15, 831-839.

R Clark (2018). Predicting mammalian metabolism and toxicity of pesticides *in silico*. Pest Management Science 74, 1992-2003.

Y Zhang, BA Lorsbach, S Castetter, WT Lambert, J Kister, NX Wang, CJR Klittich, J Roth, TC Sparks & MR Loso (2018). Physicochemical property guidelines for modern agrochemicals. Pest Management Science 74, 1979-1991.

Links to other resources

https://www.simulations-plus.com/

Part II Checklist for model evaluation

PBK Model Evaluation Checklist	Checklist assessment	Comments
Name of the PBK model (as in the reporting template)	Using high-throughput pharmacokinetic simulation and *in silico* property predictions to predict herbicide absorption and bioavailability.	
Model developer and contact details	Robert D. Clark Simulations Plus, Inc. bob@simulations-plus.com	
Name of person reviewing and contact details	**A. Paini**	
Date of checklist assessment	**June 2020**	
A. Context/Implementation		
A.1. Regulatory Purpose		
1. What is the acceptable degree of confidence/uncertainty (e.g. high, medium or low) for the envisaged application (e.g. priority setting, screening, full assessment?)	**Medium**	The intended use is to estimate exposure (bioavailability) at an early stage of pesticide development.
2. Is the degree of confidence/uncertainty in application of the PBK model for the envisaged purpose greater or less than that for other assessment options (e.g. reliance on PBK model and *in vitro* data vs. no experimental data)?	**Varies**	Experimental values can readily be incorporated as they become available.
A.2. Documentation		
3. Is the model documentation adequate, i.e. does it address the essential content of model reporting template, including the following:		
• Clear indication of the chemical, or chemicals, to which the model is applicable?	**Yes**	
• Is the model being applied for the same scientific purpose as it was developed, or has it been repurposed somehow?	**It has been repurposed somewhat**	The model was originally designed for drugs PK in humans but applied to herbicides in rats. The commercial QSAR models used were trained on a range of pharmaceuticals, agrochemicals and other environmentally

		relevant small molecules.
• Model assumptions?	**Yes**	
• Graphical representation of the proposed mode of action, if known?	**NA**	Mode of action is not modelled, just systemic exposure
• Graphical representation of the conceptual model?	**Yes**	
• Supporting tabulation for parameters (names, meanings, values, mean and standard deviations, units and sources)?	**NA**	The model is fully mechanistic with no adjustable parameters other than species and dose.
• Relevance and reliability of model parameters?	**Yes**	
• Uncertainty and sensitivity analysis?	**Yes**	Uncertainties of property estimates are provided, and accuracy fit a 2-fold uncertainty window.
• Mathematical equations available?	**No**	
• PBK model code available?	**No**	Commercial software used, not customizable.
• Software algorithm to run the PBK model code reported?	**No**	Commercial software used, not customizable.
• Qualification of PBK software platform?	**No**	The case study was developed to help validate the approach.
A.3 Software Implementation and Verification		
4. Does the model code express the mathematical model?	**NA**	
5. Is the model code devoid of syntactic and mathematical errors?	**NA**	
6. Are the units of input and output parameters correct?	**Yes**	
7. Is the chemical mass balance respected at all times?	**Yes**	
8. Is the cardiac output equal to the sum of blood flow rates to the tissue compartments?	**Yes**	
9. Is the sum total of tissue volumes equal to total body volume?	**Yes**	
10. Is the mathematical solver a well-established algorithm?	**Yes**	
11. Does the mathematical solver converge on a solution without numerical error?	**Yes**	
12. Has the PBK modelling platform been subjected to a verification process (for a different use, for instance, in the pharmaceutical domain)?	**Yes**	
A.4 Peer engagement (input/review)		

13. Has the model been used previously for a regulatory purpose?		
• Is prior peer engagement in the development and review of the model sufficient to support the envisaged application?	**Yes**	The core code is based on GastroPlus and ADMET Predictor, which have been used in a wide range of applications.
• Is additional review required? Peer engagement includes input/review by experts on specific aspects of model development, individual reviews of the model by experts, or collective reviews by peer review panels. Availability of the comments and tracking of revisions to the model in response to peer input contributes to increased confidence in the model for potential application.	**Yes**	Likely susceptibility to active uptake and metabolism for which quantitative models are not available (e.g., UGTs) must be evaluated outside the model.
B. Assessment of Model Validity		
B.1 Biological Basis (Model Structure and Parameters)		
14. Is the model consistent with known biology?		
• Is the biological basis for the model structure provided?	**Yes**	
• Is the complexity of the model structure appropriate to address the regulatory application?	**Yes**	
• Are assumptions concerning the model structure and parameters clearly stated and justified?	**Yes**	
• Is the choice of values for physiological parameters justified?	**Yes**	
• Is the choice of methods used to estimate chemical-specific ADME parameters justified?	**Yes**	
• Saturable kinetics	**Not present**	
B.2 Theoretical Basis of Model Equations		
15. Are the underlying equations based on established theories, .e.g. Michaelis-Menten kinetics, Fick's laws of diffusion?	**Yes**	
• In the case of PBK models for particles, does the model take into consideration the properties of particles, e.g. particle size ranges, (poor) solubility, aggregation, partitioning and diffusion/sedimentation behaviour?	**Yes**	Particle size is adjustable but is not generally recommended this early in discovery.
B.3. Reliability of input parameters		
16. Has the uncertainty (individual variability, experimental reproducibility and reliability) in the input parameters been characterised?	**Yes**	
B.4. Uncertainty and Sensitivity Analysis		

17. Has the impact of uncertainty (individual variability, experimental reproducibility and reliability) in the parameters on the chosen dose metric been estimated?		
• Local sensitivity analysis?	**YES**	Is supported in more recent versions.
• Global sensitivity analysis?	**No**	It can readily be done manually but was not in this application**.**
18. Is confidence in influential input parameter estimates (i.e., based on comparison of uncertainty and sensitivity) reasonable (within expected values; similar to those of analogues) in view of the intended application?	**Yes**	Bioavailability was correct within 2-fold in cases where oxidative CYP metabolism is predicted to dominate.
B.5. Goodness-of-Fit and Predictivity		
19. For PBK models for which there are sufficient *in vivo* data for the chemical of interest:		
• Suitability as analogue (chemical and biological similarity) been assessed?	**No**	
• Reliable estimation of chosen dose metric for analogue?	**NA**	
• In general is the biological Variability of *in vivo* reference data (from analogue) established?	**NA**	

Part III Overall Evaluation

Overall Conclusion on mode evaluation for the intended application as reported in chapter 3 of the GD

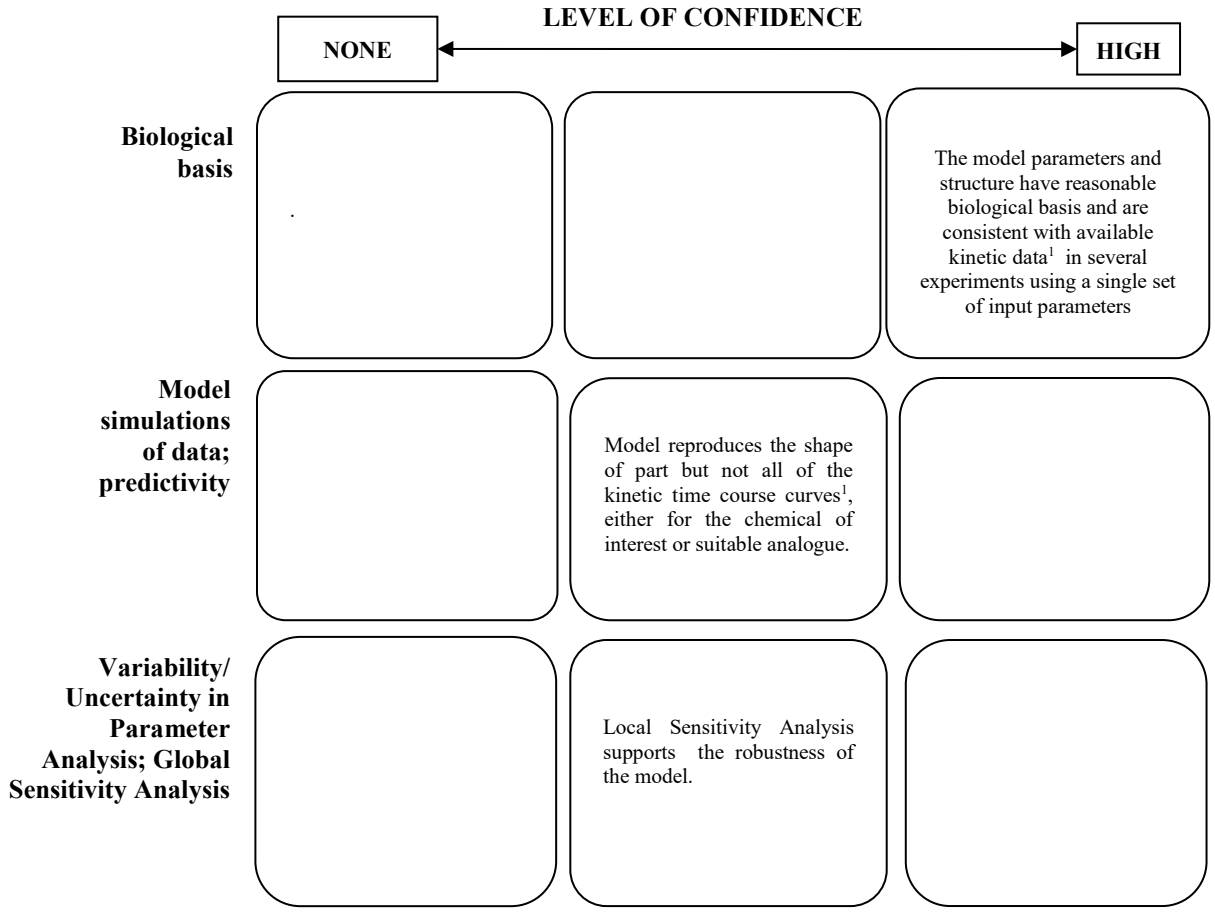

Notes: 1. Only integrated pharmacokinetic data (biovailability) was available and used in this study, and – as detailed in Step 2.4 above – those were approximations based on surrogate endpoints, not time courses.

Case Study XII

Application of physiologically based kinetic (PBK) modelling in the next generation risk assessment of dermally applied consumer products

The following document captures the information of a case study to evaluate PBK models for topical application

Part I. PBK model reporting template

A. Name of model

Application of physiologically based kinetic (PBK) modelling in the next generation risk assessment of dermally applied consumer products.

B. Contact details

Authors: Thomas E. Moxon, Hequn Li, Mi-Young Lee, Przemyslaw Piechota, Beate Nicol, Juliette Pickles, Ruth Pendlington, Ian Sorrell, Maria Teresa Baltazar

Affiliation: Unilever Safety and Environmental Assurance Centre, Colworth Science Park, Sharnbrook, Bedfordshire MK44 1LQ, UK

C. Summary of model characterisation, development, validation, and regulatory applicability

Models were built to predict systemic of three chemicals (coumarin, caffeine and sulforaphane) used as hypothetical ingredients in four consumer goods product types (kitchen cleaner liquid, face cream, shampoo, and body lotion). This illustrated how PBK modelling could be employed for the risk assessment of an ingredient for inclusion in a consumer product where the only significant exposure route is dermal absorption. The risk assessment would be carried out using NAMs and this has been illustrated for one of the compounds (coumarin, manuscript submitted Baltazar). The PBK models were built in the commercial software Gastroplus 9.6. The models were parameterised following a tiered framework. Initially the models are built with *in silico* only estimates of model parameters. Sensitivity analysis is then used to determine the most sensitive parameters. For the final model, key parameters were then determined using *in vitro* data on skin absorption, hepatic metabolism and protein binding. The impact of input parameter uncertainty and population variability was assessed using global sensitivity analysis. The Extended Clearance Classification System (ECCS) (Varma *et al*. 2015) was used to determine the likely dominate clearance route. For all the chemicals the main clearance route was predicted to be metabolic. This informed the choice of renal clearance rate which was set to zero as this is a conservative assumption in the context of a risk assessment.

D. Model characterisation (modelling workflow)

Step 1 – Scope and purpose of the model

The need is to support risk assessment of novel ingredients for cosmetics products. For novel ingredients without clinical data, PBK predictions may be required to support first-in-man use in the absence of *in vivo* data. An example application would be through comparison of predicted plasma concentrations to points of departure derived from *in vitro* toxicity tests to determine a margin of safety.

Step 2 – Model Conceptualisation

The PBK models were built in Gastroplus 9.6. This software is a specialist software for building PBK models and is used widely in the pharmaceutical and other industries. It includes several dosing options including dermal absorption.

Assumptions

It was assumed that active transport of chemicals had a negligible impact on plasma concentration and the distribution of chemicals within the body was assumed to be entirely perfusion limited.

It was assumed that highly permeable chemicals undergo limited renal excretion due to passive reabsorption.

It was assumed that liver is the only tissue where significant metabolism takes place.

Dermal exposure was assumed to be the only route of exposure for simplicity.

Step 3 – Model parameterisation

The building of the models was staged following a framework with multiple levels. In level 1 only *in silico* parameter estimates were used for all parameters. Sensitivity analysis was then performed to determine the key parameters. In level 2 the key parameters were determined using *in vitro* data.

Applied dose

A deterministic approach was taken for determining the consumer applied. The applied dose for each product was taken from the 90th percentile from European consumer exposure studies (Hall et al., 2007), and the frequency of use from guidance by the SCCS (Scientific committee on consumer safety) (Bernauer et al., 2018), except the kitchen cleaner which was taken from an EPHECT (emissions, exposure patterns, and health effects of consumer products in the EU) survey (Johnson and Lucica, 2012). For these case studies, dermal exposure was assumed to be the only significant route of exposure. For some product types, particularly kitchen cleaner, there may be other important exposure routes that should be considered in the risk assessment.

Dermal Absorption

Skin penetration studies were available for caffeine and coumarin, using the following vehicles: ethanol: Diethylphthalate (with different concentrations), lotion, and laundry hand wash for coumarin and ethanol:water, ethanol:propylene glycol for caffeine. More information can be found in the supplementary materials and methods of Moxon et al. 2019. Partitioning and diffusivity values for the different skin layers were estimated using *in silico* predictions as initial values, and then parameters were fitted against the experimental

data for concentration in each of the skin layers (stratum corneum, viable epidermis, and dermis) as well as the flux into the receptor fluid.

Distribution

The distribution within all tissues was assumed to be perfusion limited. Tissue partition coefficients were calculated using the Lukacova method in Gastroplus.

Both *in silico* and experimentally measured values for unbound plasma fraction were used. *In silico* estimates were made using ADMET Predictor 9.0. Experimental measurements were performed using rapid equilibirum dialysis. Blood to plasma ratio was parameterised similarly through the use of the in-built estimator in Gastroplus and at level 2, experimental data was used.

Metabolism

Liver was assumed to be the only tissue where metabolism took place. At level 1, hepatic metabolism was predicted by ADMET predictor 9.0. At level 2, *in vivo* clearance rate was scaled from an *in vitro* clearance rate. *In vitro* intrinsic clearance came from studies using primary hepatocytes in suspension.

Excretion

For all three compounds the ECCS prediction was for the compound to be primarily cleared through hepatic metabolism. Renal clearance rate was set to zero.

Physicochemical parameters

Measured lipophilicity (log P) value were taken from the literature where available as were acid or base dissociation constants (pKa and pKb). Where either were not available in the literature values were predicted using ADMET predictor 9.0.

Step 4 – Computer implementation (Solving the equations)

The PBK models were built in Gastroplus 9.6. This software is a specialist software for building PBK models and is used widely in the pharmaceutical and other industries.

Step 5 – Model Performance

Local sensitivity analysis

A finite difference method is used to approximate the partial derivative of the C_{max} or AUC with respect to an increase of 5% of each parameter value and used to calculate a sensitivity index to rank the importance of the parameters.

Global sensitivity analysis

The inbuilt population simulator in Gastroplus was used to perform global sensitivity analysis. Parameter distributions are defined either from the experimental/QSAR errors/variance or using GastroPlus' default values around the given parameters, mostly following log-normal distributions, with physiological parameters following GastroPlus' PEAR distribution (Population Estimates for Age-Related).

The simulation times in the population simulator were chosen to ensure that the plasma concentrations reached steady state. The convergence of the output was checked by plotting the running mean, 5th and 95th quantile against the number of iterations. Iterations were carried out until percentile values converged to a steady value.

Predictive capacity - Comparison to clinical data

In order to examine the validity of the model and the reliability of subsequent predictions (not to calibrate the built models), the performance of the model using *in silico* predicted parameters or *in vitro* derived parameters was evaluated by comparing the predictions made to clinical kinetic data for coumarin and caffeine from intravenous dosing sourced from the literature (such human *in vivo* data is not available for sulforaphane). This assesses the accuracy of the systemic model but not the absorption from product use. Skin absorption is determined using *ex vivo* skin penetration studies which typically correlates with *in vivo* absorption. Accuracy is improved if the relevant formulation is used in the skin penetration studies.

Step 6 – Model documentation

The models have been published (Moxon *et al*. 2019).

E. Identification of uncertainties

Model structure

The model used was an established PBK structure run in Gastroplus. Given the large number of tissues included in the model it is not expected that additional tissues would reduce uncertainty. There is the usual uncertainty in PBK modelling from assuming single compartment homogeneous tissues.

Input parameters

Both *in silico* and experimental inputs were used with the experimental inputs forming the basis of higher level models. The prediction/measurement errors were used to inform the parameter distributions for the global sensitivity analysis. There is uncertainty in the scaling methods used for some parameters such as intrinsic clearance. For intrinsic clearance this typically leads to an under prediction of *in vivo* clearance which is conservative for use in a risk assessment.

Model output

The impact of parameter uncertainties and population variability were estimated using Monte Carlo simulations and mean and 95th percentile estimates for the maximum concentration are provided.

F. Model implementation details

Software (version no) Gastroplus 9.6.

G. Peer engagement (input/review)

The model has undergone peer review for publication (Moxon *et al*. 2019).

H. Parameter tables

Full parameter tables are published in Moxon *et al*. 2019 and its supplementary material.

I. References and background information

Moxon, T.E., Li, H., Lee, M.-Y., Piechota, P., Nicol, B., Pickles, J., Pendlington, R., Sorrell, I., Baltazar, M.T. Application of physiologically based kinetic (PBK) modelling in the next generation risk assessment of dermally applied consumer products (2020) Toxicology in Vitro, 63, art. no. 104746.

Baltazar MT. In Preparation. Ab initio systemic safety assessment of coumarin using new approach methodologies applied to hypothetical cosmetic products.

Bernauer, U., Bodin, L., Chaudry, Q., Coenraads, P.J., Dusinka, M., Ezendam, J., Gaffet, E., Lodovico Galli, C., Granum, B., Panderi, I., et al., 2018. "The sccs note of guidance for the testing of cosmetic ingredients and their safety evaluation – 10th revision" sccs/1602/18 - final version.

Hall, B., Tozer, S., Safford, B., Coroama, M., Steiling, W., Leneveu-Duchemin, M.C., McNamara, C., Gibney, M., 2007. European consumer exposure to cosmetic products, a framework for conducting population exposure assessments. Food Chem. Toxicol. 45 (11), 2097–2108.

Johnson, A., Lucica, E., 2012. Survey on Indoor Use and Use Patterns of Consumer Products in Eu Member States. Ipsos. SURVEY REPORT.

Varma, M.V., Steyn, S.J., Allerton, C., El-Kattan, A.F., 2015. Predicting clearance mechanism in drug discovery: extended clearance classification system (eccs). Pharm. Res. 32 (12), 3785–3802.

Part II Checklist for model evaluation

PBK Model Evaluation Checklist	Checklist assessment	Comments
Name of the PBK model (as in the reporting template)	Application of physiologically based kinetic (PBK) modelling in the next generation risk assessment of dermally applied consumer products	
Model developer and contact details	**Authors**: Thomas E. Moxon, Hequn Li, Mi-Young Lee, Przemyslaw Piechota, Beate Nicol, Juliette Pickles, Ruth Pendlington, Ian Sorrell, Maria Teresa Baltazar **Affiliation:** Unilever Safety and Environmental Assurance Centre, Colworth Science Park, Sharnbrook, Bedfordshire MK44 1LQ, UK **Email:** tom.moxon@unilever.com	
Name of person reviewing and contact details	**A. Paini**	
Date of checklist assessment	**June 2020**	
A. Context/Implementation		
A.1. Regulatory Purpose		
1. What is the acceptable degree of confidence/uncertainty (e.g. high, medium or low) for the envisaged application (e.g. priority setting, screening, full assessment?)	**Medium**	PBK modelling in this context is to support first in man without *in vivo* data and risk assessment for market. If a model based on *in vitro* data is not of sufficient confidence, a clinical kinetic study would be used to inform the model.
2. Is the degree of confidence/uncertainty in application of the PBK model for the envisaged purpose greater or less than that for other assessment options (e.g. reliance on PBK model and *in vitro* data vs. no experimental data)?		Uncertainty in PBK model greater than for clinical human study.
A.2. Documentation		
3. Is the model documentation adequate, i.e. does it address the essential content of model reporting template, including the following:		
• Clear indication of the chemical, or chemicals, to which the model is applicable?	**Yes**	

• Is the model being applied for the same scientific purpose as it was developed, or has it been repurposed somehow?	**Yes**	
• Model assumptions?	**Yes**	
• Graphical representation of the proposed mode of action, if known?	**NA**	
• Graphical representation of the conceptual model?	**No**	Commercial software. Representation available elsewhere.
• Supporting tabulation for parameters (names, meanings, values, mean and standard deviations, units and sources)?	**Yes**	
• Relevance and reliability of model parameters?	**Yes**	
• Uncertainty and sensitivity analysis?	**Yes**	
• Mathematical equations available?	**No**	Commercial software used
• PBK model code available?	**No**	Commercial software used
• Software algorithm to run the PBK model code?	**No**	
• Qualification of PBK software platform?	**No**	Evaluated elsewhere
A.3 Software Implementation and Verification		
4. Does the model code express the mathematical model?	**NA**	
5. Is the model code devoid of syntactic and mathematical errors?	**NA**	
6. Are the units of input and output parameters correct?	**Yes**	
7. Is the chemical mass balance respected at all times?	**Yes**	
8. Is the cardiac output equal to the sum of blood flow rates to the tissue compartments?	**Yes**	
9. Is the sum total of tissue volumes equal to total body volume?	**Yes**	
10. Is the mathematical solver a well-established algorithm?	**Yes**	
11. Does the mathematical solver converge on a solution without numerical error?	**Yes**	
12. Has the PBK modelling platform been subjected to a verification process (for a different use, for instance, in the pharmaceutical domain)?	**Yes**	
A.4 Peer engagement (input/review)		
13. Has the model been used previously for a regulatory purpose?		See CS 11 simulations plus
• Is prior peer engagement in the development and review of the model sufficient to support the envisaged application?	**Yes**	

• Is additional review required? Peer engagement includes input/review by experts on specific aspects of model development, individual reviews of the model by experts, or collective reviews by peer review panels. Availability of the comments and tracking of revisions to the model in response to peer input contributes to increased confidence in the model for potential application.	**NA**	
B. Assessment of Model Validity		
B.1 Biological Basis (Model Structure and Parameters)		
14. Is the model consistent with known biology?	**Yes**	
• Is the biological basis for the model structure provided?	**No**	Not in this publication
• Is the complexity of the model structure appropriate to address the regulatory application?	**Yes**	
• Are assumptions concerning the model structure and parameters clearly stated and justified?	**Yes**	
• Is the choice of values for physiological parameters justified?	**Yes**	
• Is the choice of methods used to estimate chemical-specific ADME parameters justified?	**Yes**	
• Saturable kinetics	**No**	
B.2 Theoretical Basis of Model Equations		
15. Are the underlying equations based on established theories, .e.g. Michaelis-Menten kinetics, Fick's laws of diffusion?	**Yes**	
• In the case of PBK models for particles, does the model take into consideration the properties of particles, e.g. particle size ranges, (poor) solubility, aggregation, partitioning and diffusion/sedimentation behaviour?	**NA**	
B.3. Reliability of input parameters		
16. Has the uncertainty (individual variability, experimental reproducibility and reliability) in the input parameters been characterised?	**Yes**	
B.4. Uncertainty and Sensitivity Analysis		
17. Has the impact of uncertainty (individual variability, experimental reproducibility and reliability) in the parameters on the chosen dose metric been estimated?	**Yes**	The uncertainty analysis carried out here does not take into account the uncertainty from the QSAR or experimental system but uses the default GastroPlus distribution.
• Local sensitivity analysis?	**Yes**	

• Global sensitivity analysis?	**Yes**	
18. Is confidence in influential input parameter estimates (i.e., based on comparison of uncertainty and sensitivity) reasonable (within expected values; similar to those of analogues) in view of the intended application?	**Yes**	
B.5. Goodness-of-Fit and Predictivity		
19. For PBK models for which there are sufficient *in vivo* data for the chemical of interest:		
• Suitability as analogue (chemical and biological similarity) been assessed?	**No**	
• Reliable estimation of chosen dose metric for analogue?	**NA**	
• In general is the biological Variability of *in vivo* reference data (from analogue) established?	**NA**	

Part III Overall Evaluation

Overall Conclusion on mode evaluation for the intended application see chapter 3 of the GD.

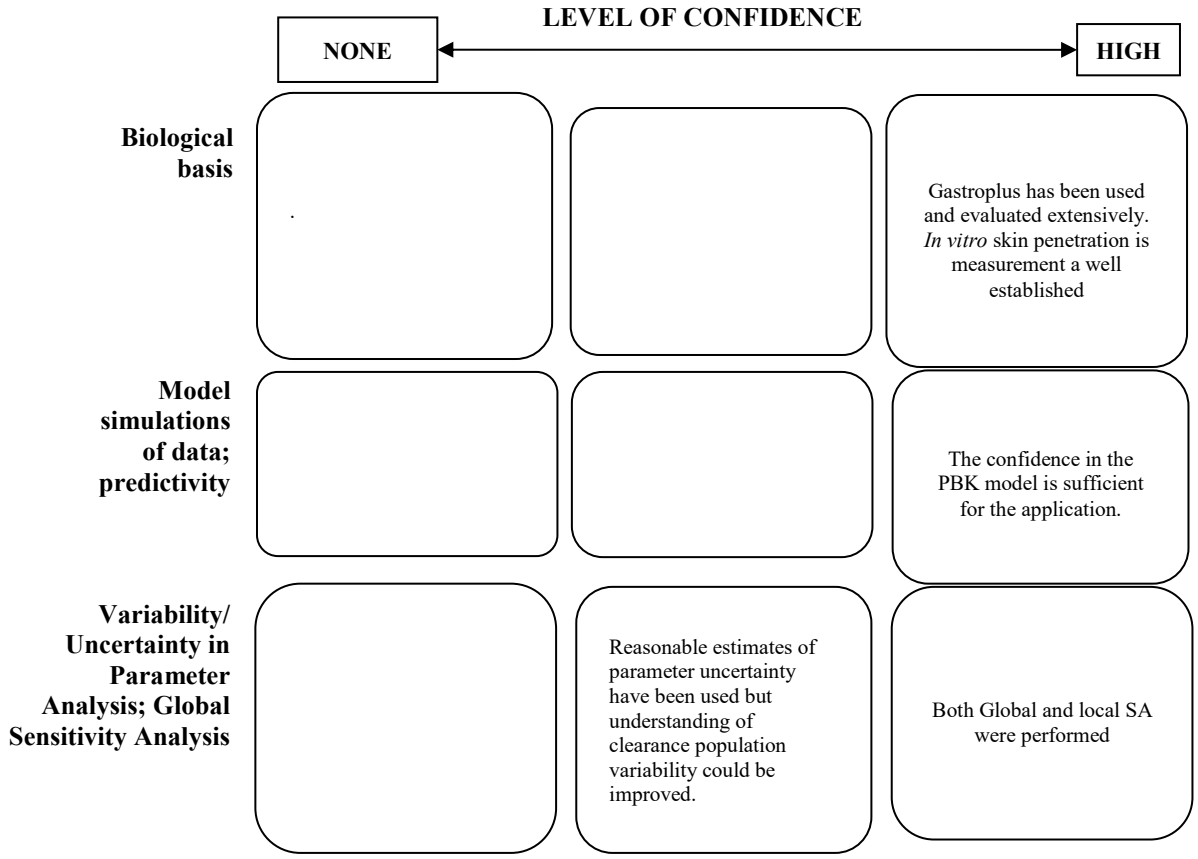

Based on the information reported in the template and the evaluation done with the checklist the commercial software (Gastroplus) can be applied in a risk assessment context with high confidence. In the current context the model was parametrized using *in silico* and *in vitro* data but was also evaluated using historical *in vivo* data, providing proof of concept and evaluation of model performance and potential use of the data in Risk Assessment.

Case Study XIII

Generic Human one compartment and QIVIVE PB-K models

Part I. PBK model reporting template

A. Name of model

Generic human one compartment and QIVIVE PB-K models integrating *in vitro* data, physiological and pathway-related variability to predict kinetics of chemicals in the food safety area

B. Model developer and contact details

Authors: [1]Witold Wiecek, [2]Kevin Darney, [2]Leonie Lautz, [1]Nadia Quignot, [1]Billy Amzal; [2]Camille Bechaux; [3]Jose Cortinhas-Abrahantes and [3]Jean Lou CM Dorne

Affiliation: [1]Certara limited, Paris, France; [2]ANSES, Paris, France; [3]European Food Safety Authority, Parma, Italy

C. Summary of model characterisation, development, validation, and regulatory applicability

For hazard characterisation of chemicals in humans, the prediction of TK parameters can be useful to provide quantitative metrics on elimination patterns with reference to markers of acute exposure (Cmax) and markers of chronic exposure (AUC, clearance). These can 1. support the basis for integrating internal dose in the derivation of reference points/points of departure using human *in vitro* data, 2. provide quantitative data for the derivation of chemical specific adjustment factors in humans for the TK dimension 3. Provide a sound basis for extrapolation between humans and animal test species. 4. Provide alternatives to animal-based testing (EFSA, 2014).

Here, generic human one compartment and PB-K models have been developed to predict chemical kinetics for compounds metabolised by specific pathways (i.e. isoforms) using a step wise approach (Dorne et al., 2005): 1. Development of one compartment and PB-K models and global sensitivity analysis to identify variables influencing model output. 2. scaling of *in vitro* data for the metabolism of the compound to the whole human liver. 3. Integrating human variability in physiology and metabolism (pathway-related variability) in the generic human one compartment and PB-K models. 4. Prediction of kinetic parameters for chemicals relevant to food safety. Uncertainties include for 1. Data availability of *in vitro* and human data on compound-specific metabolism. 2. assumptions for quantitative metabolism data on specific pathways (isoforms) in humans, 3. QIVIVE for metabolism, 4. Availability of distributions for pathway-related variability on specific isoforms. 5. Sensitivity of the generic model and applicability domain.

D. Model characterisation

Step 1 – Scope and purpose of the model (problem formulation)

Development and validation of a human one compartment and QIVIVE PB-K model integrating *in vitro* data, physiological and pathway-related variability to predict chemical kinetics in the food safety area.

Step 2 –Model conceptualisation (model structure, mathematical representation)

The structure of the human generic one compartment and PBK models are presented in figure 1 and 2. The model is a modification of the generic one compartment and PBK multi-compartmental model developed at US-EPA in the httk package and available in Pearce et al (2017). These modifications allow to integrate variability in specific metabolic pathways (e.g. CYP, UGT etc.). Equations are not presented here for the sake of conciseness.

Figure XIII1: Scheme of the one-compartment model and human PBK multi-compartmental model

One compartment model

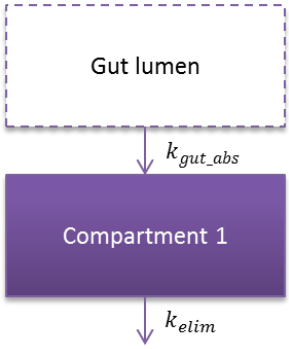

Human PBK multi-compartment model

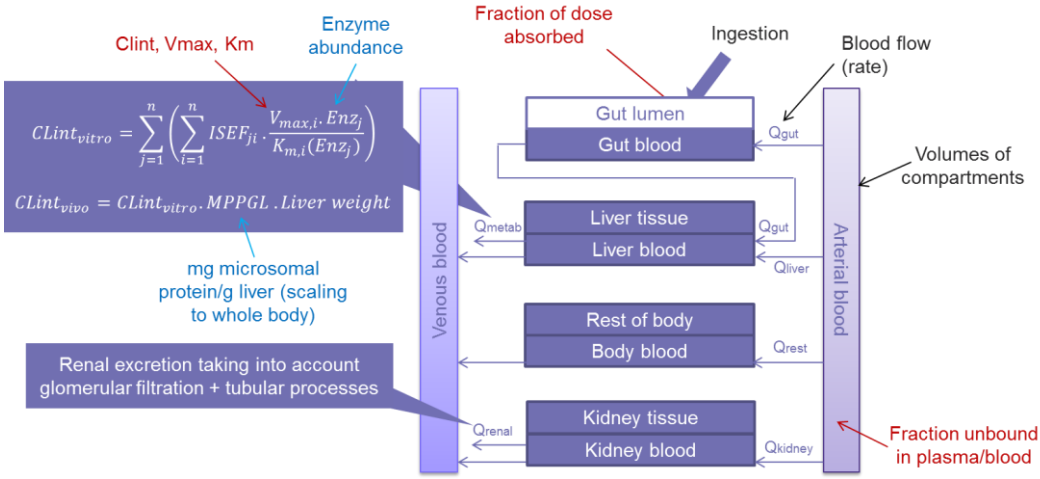

CLint: Intrinsic clearance; V_{max}: Enzyme maximum velocity; K_m: Michaelis-Menten constant; ISEF: Intersystem extrapolation factor.

Step 3 – Model parameterisation (parameter estimation and analysis)

Data collection for model parameterisation was performed for human physiological variables (e.g. body weight, organ weight, age, ventilation rate, hepatic blood flow, body surface) focusing on key organs and systems (plasma, blood, gastro-intestinal system, liver). Since the oral route is of primary relevance for food safety, components of the gastro-intestinal system were included. Table 1 summarises below the data sources used to inform the model parameters.

Table XIII1: High-level overview of the data summary and sources used to inform the model inputs

	Mean values	Population variability	Ranges set for sensitivity analyses
Physiological parameters	Published reviews	Published reviews	Set to default 10% CV
Biological parameters	dedicated meta-analysis of collected data	Published reviews + dedicated meta-analysis of collected data	Set to default 10% CV
Pathway specific TK parameters	Dedicated meta-analyses of collected data	Dedicated meta-analyses of collected data	Set to 0 to 3-fold mean values
Compound-specific physico-chemical, *in vitro* and *in vivo* parameters	Published databases + Dedicated meta-analyses of collected data	NA	NA

Distribution types were assigned to the parameters as follows:

- 'Whole body' physiological parameters such as bodyweight and cardiac output were described by a normal distribution, under the condition that the mean should be larger than three times the standard deviation. Otherwise, a lognormal distribution was used to prevent from simulating negative values.
- •Fractions were assigned a Beta distribution so that it is restricted to the 0-1 interval. These are characterised with shape parameters α and β, which can be derived from the mean and variance. Since $\mu=\alpha/((\alpha+\beta))$ and $\sigma^2=(\alpha\cdot\beta)/((\alpha+\beta)^2\cdot(\alpha+\beta+1))$, this means that $\alpha=((1-\mu)/\sigma^2 -1/\mu)\cdot\mu^2$ and $\beta=\alpha\cdot(1/\mu-1)$.
- Rates (e.g. ingestion or excretion rate) were described with a lognormal distribution characterised by the mean and standard deviation evaluated from the collected data.
- As described in the section below, the sensitivity of the PBK model (see section 5) to the physiological parameters was assessed using three hypothetical chemicals: one chemical that is rapidly absorbed, metabolised and excreted, a second chemical that is slowly absorbed and excreted, but rapidly metabolised, and a third chemical that is slowly absorbed, metabolized and excreted.

Table XIII2 describes the mean parameter values used for this analysis. Mean values of physiological parameters were based on the mean httk values as specified in (Wambaugh et al., 2015). The distribution set for the variations of physiological parameters was uniform ranging +/- 10% around the means: U(min=0.9*mean; max=1.1*mean).

Table XIII2. Parameter mean estimates in the PBK model for three hypothetical chemicals (values are rounded to 2 significant decimals). The physiological parameters being varied for the senstivity analysis (See section 5) are highlighted in bold.

Parameters (variable acronym, unit)	Rapidly absorbed metabolised and excreted	Slowly absorbed and excreted, but rapidly metabolised	Slowly absorbed, metabolised and excreted
Body Weight (BW, kg)		**70**	
Hepatic Clearance (Clmetabolismc, L/h/kg BW)	7	7	0.07
Fraction of red blood cells in the blood (hematocrit, -)		**0.44**	
Rate that chemical enters the gut from gutlumen (kgutabs, 1/h)	2	0.2	0.2
Ratio of concentration of chemical in kidney tissue to unbound concentration in plasma (Kkidney2plasma, -)		1000	
Ratio of concentration of chemical in liver tissue to unbound concentration in plasma (Kliver2plasma, -)		1000	
Ratio of concentration of chemical in rest of body tissue to unbound concentration in plasma (Krest2plasma, -)		1000	
Ratio of concentration of chemical in lung tissue to unbound concentration in plasma (Kgut2plasma, -)		1000	
Ratio of concentration of chemical in lung tissue to unbound concentration in plasma (Klung2plasma, -)		1000	
Cardiac Output (Qcardiacc, L/h/kg BW^3/4)		**13.88**	
Glomerular Filtration Rate (Qgfrc, L/h/kg BW^3/4),	0.31	0.03	0.03
Fraction of cardiac output flowing to the gut (Qgutf, -)		**0.21**	
Fraction of cardiac output flowing to the kidneys (Qkidneyf, -)		**0.22**	
Fraction of cardiac output flowing to the liver (Qliverf, -)		**0.054**	
Volume of arteries per kg body weight (Vartc, L/kg BW)		**0.038**	
Volume of gut per kg body weight (Vgutc, L/kg BW)		**0.016**	
Volume of kidneys per kg body weight (Vkidneyc, L/kg BW)		**0.0042**	
Volume of liver per kg body weight (Vliverc, L/kg BW)		**0.025**	

Volume of lungs per kg body weight (Vlungc, L/kg BW)	**0.0072**
Volume of rest of the body per kg body weight (Vrestc, L/kg BW)	**0.78**
Volume of the veins per kg body weight (Vvenc, L/kg BW)	**0.038**
Plasma Fraction of plasma that is not bound (Funbound, -)	0.1
Ratio blood/plasma concentrations of a chemical to the plasma concentration (Rblood2plasma, -)	1

Distributions for human variability in metabolism were also integrated in the model to generate pathway-related variability. The data collections to generate such distributions were performed through a number of hierarchical Bayesian meta-analysis and meta-regressions for a range of phase I (CYP3A4, PON-1), phase II enzymes (UGT) and some transporters generate pathway-related variability distributions for markers of acute (Cmax) and chronic exposure (clearance, AUC) in healthy adults and these are available in the peer-reviewed literature (Darney et al., 2019; Wiecek et al., 2019b; Darney et al., 2020a,b; Kasteel et al., 2020).

Step 4 – Computer implementation (solving the equations)

The model is a modification of the generic one compartment and PBTK multi-compartmental from the httk application developed at US-EPA by Pearce et al (2017) and has been implemented in a pilot open source R-based platform available at https://zenodo.org/record/2548850#.XqlGZagzZeU with a Creative Common Attribution 4.0 license.

Step 5 – Model Performance

The performance of the model was tested on a number of food relevant compounds as a comparison of predictions and with measured data from the literature.

One compartment model

1 2 3

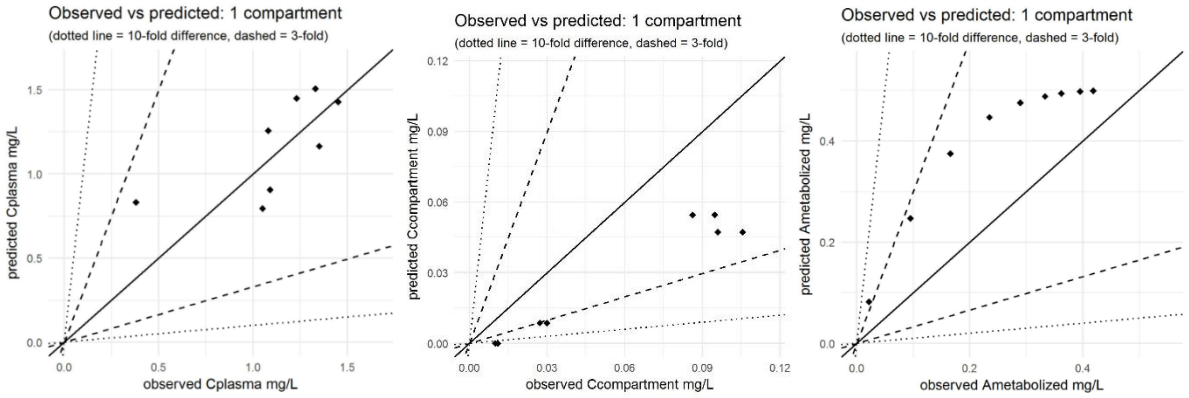

Figure XIII2: Predicted plasma concentrations oxytetracycline and menthol with one compartment TK model vs. measured plasma concentrations (1,2) and predicted fraction metabolised versus measured of diazinon (3). Scatterplot tolerability bounds for 3 (resp.10)-fold difference in dashed (resp. dotted) lines.

PB-K Model

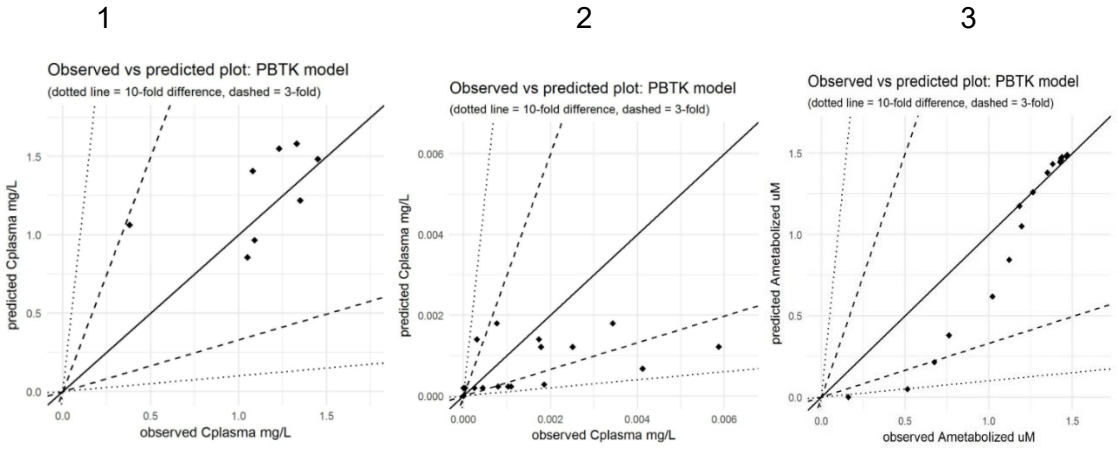

Figure XIII3. Predicted plasma concentrations oxytetracycline, THC with the PB-K model vs. measured plasma concentrations (1,2) and predicted fraction metabolised versus measured of chlorpyrifos (3). Scatterplot tolerability bounds for 3 (resp.10)- fold difference in dashed (resp. dotted) lines.

Sensitivity analysis was performed for 3 theoretical chemicals and 2 different models:

- A model simulation with fixed TK parameters with distributions for physiological and biological parameters representing inter-individual variability
- A model simulation with both sources of uncertainty/variability.

Such an approach allowed for disentangling the various sources of variability/uncertainty from each other according to their physiological natures, and for gauging the impact of ethnicity, age group or polymorphism (depending on the pathway) on the total population variability.

The two following exposure scenarios were simulated, and the results are reported on Figure XIII4 and 5:

- Single bolus dose of 1 mg/kg
- Continuous exposure of 0.1 mg/kg/day

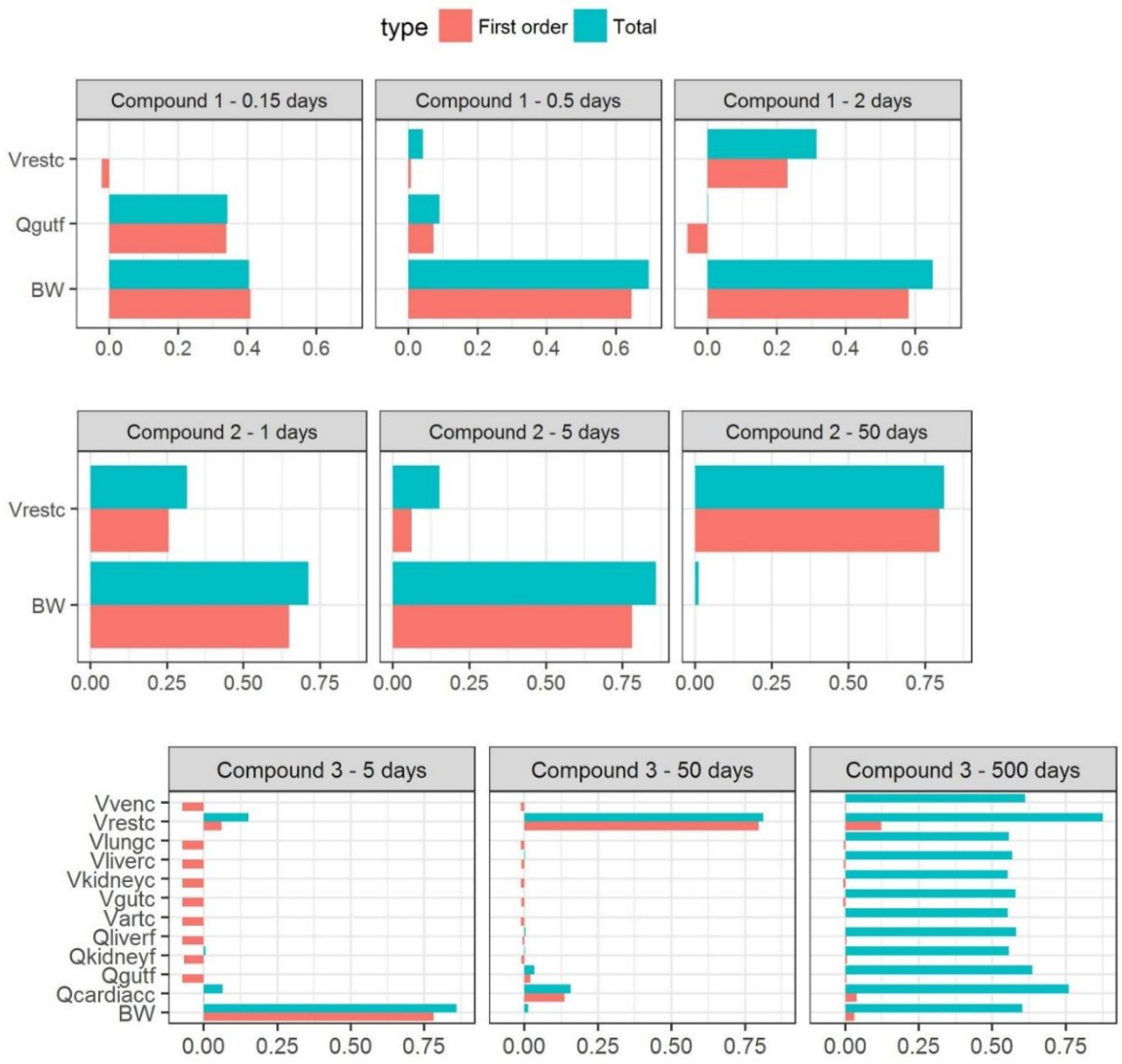

Figure XIII4. Sobol sensitivity analysis of the PBK model or physiological parameters for the 3 hypothetical chemicals – Single dose exposure scenario based on serum concentration measured with on 3 time points.

For the three hypothetical chemicals, body weight (BW) was the most influencing parameter on the PB model output during the absorption phase. BW remained influential during the first elimination phase for the 2 first compounds, while the volume of the rest of the body (Vrestc) has the most important influence for compound 3 slowly absorbed, metabolized and excreted. This parameter has also strong impact with the 2 first compounds, but during the terminal elimination phase. The blood flow to the gut (Qgutf) has also a strong influence during the absorption phase for Compound 1 rapidly absorbed, metabolized and excreted.

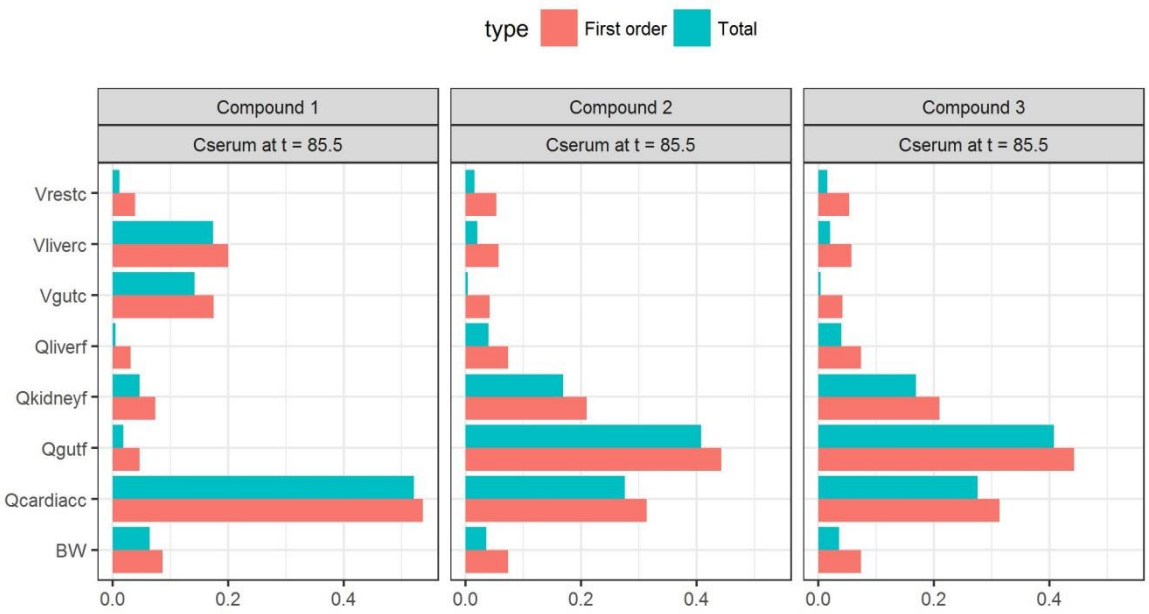

Figure XIII5. Sobol sensitivity analysis of the impact of physiological parameters for the 3 hypothetical chemicals –Repeated exposure scenario with 1 time point. To facilitate the reading, parameters with Sobol indices = 0 were not represented.

The steady-state concentration of compound 1 rapidly absorbed, metabolized and excreted is mostly influenced by the cardiac blood flow (Qcardiacc). For the 2 other compounds, this parameter remains important but the parameter having the strongest influence is the blood flow flowing to the gut (Qgutf). The blood flow flowing to the kidney (Qkidneyf) has also important impact on the steady-state concentrations of the 2 last compounds.

The sensitivity of the PB-K model to changes in **physico-chemical and toxicokinetic parameters** was assessed by varying chemical characteristics via uniform distributions that should represent the whole chemical spectrum, while physiological model parameters were fixed.

The two same exposure scenarios were simulated (Single oral dose of 1 mg/kg and repeated exposure of 0.1 mg/kg/day), the results are reported on figure XIII6 and 7:

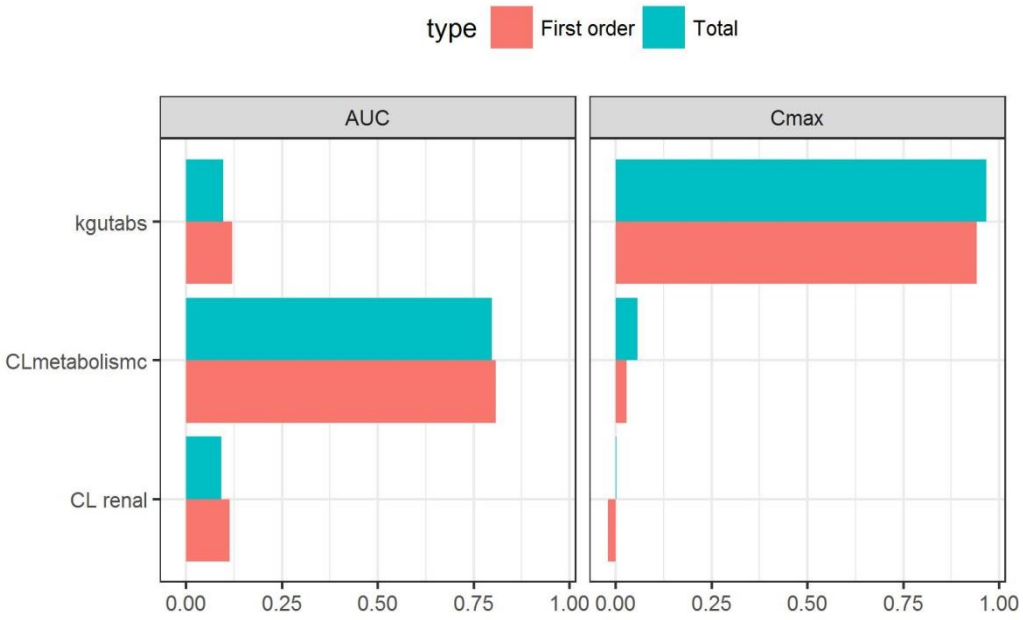

Figure XIII6. Sobol sensitivity analysis for the prediction of human toxicokinetic parameters for a wide range of chemicals – Single exposure scenario.

For single exposure, Cmax was strongly affected by the absorption rate (kgutabs). AUC was mostly impacted by metabolic clearance (CLmetabolismc), whereas renal clearance (CLrenal) and absorption rate (kgutabs) had moderate impact on the outcome.

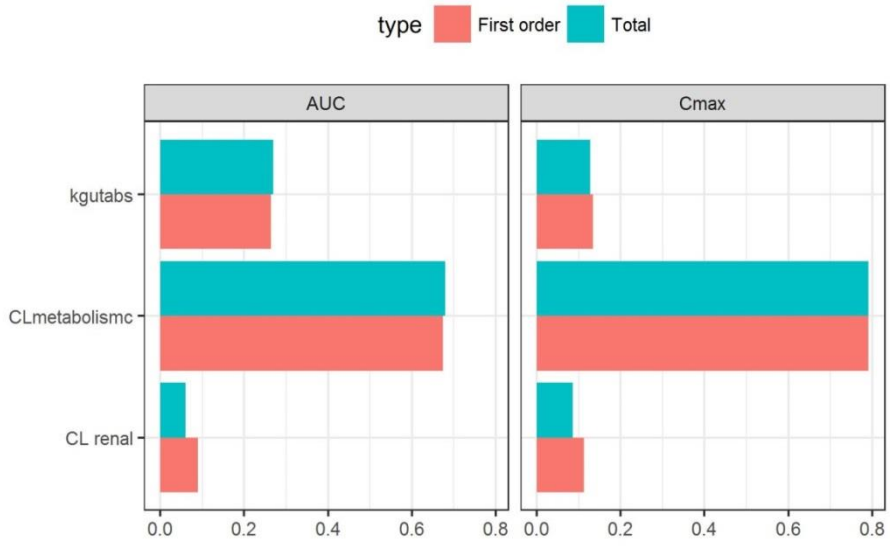

Figure XIII7. Sobol sensitivity analysis for toxicokinetic parameters for a wide range of chemicals – Single exposure scenario.

For repeated exposure, both the Cmax and AUC were mostly influenced by the metabolic clearance (CLmetabolismc).

Step 6 – Model Documentation

The following PBK model was previously published is available in the pilot open source R-based platform available at "TKPlate: R package prototype for TK models graphical interface" under https://zenodo.org/record/2548850#.XqlGZagzZeU with a Creative Common Attribution 4.0 license. It is currently being incorporated in the upcoming EFSA Open source TKplate platform (Dec 2020).

E. Identification of uncertainties

Model structure

Availability of chemical-specific data on ADME in general and specific metabolism, excretion and transporters and inter-individual differences in humans for phase I, phase II, transporters are the main sources of uncertainty in model structure.

Input parameters

Availability on basic human physiological data provides a good basis for this PBK model. The global sensitivity analysis highlighted that gut absorption strongly influence Cmax whereas metabolic clearance may critically affect model outputs for AUC and clearance. Depending on availability of metabolism and excretion data, assumptions can be refined for specific compounds and the sensitivity analysis should be run specifically on a case by case basis.

Model output

Predictions of PK parameters with the one compartment and the PBK model provided good predictions for the 6 compounds of relevance to food safety presented here and were mostly within a 3-fold factor. A Strategy for reducing overall uncertainty will include further data collection on human inter-individual differences for phase I and phase II enzymes and transporters as well as case studies to extend the applicability of the model in a regulatory context.

Overall evaluation of uncertainties: As discussed above

F. Model implementation details

- software (version no): The code was written and executed in in R. 3.3.3 and is available on EFSA knowledge junction (Wiecek et al., 2019b)
- availability of code: Yes, code is accessible via the EFSA knowledge junction https://zenodo.org/record/2548850#.XqmQp6gzZeU.
- software verification / qualification: performed using case studies, internal and external peer review.

G. Peer engagement (input/review)

The input data and model were publsihed in peer reviewed journals and on EFSA website, see references.

H. Parameter tables

Physiological data are available on the EFSA knowledge junction as well as inter-individual variability for a number of metabolic pathways namely CYP3A4, PON-1, UGT and some transporters (Darney et al., 2019; Wiecek et al., 2019b; Darney et al., 2020a,b; Kasteel et al., 2020).

I. References and background information

EFSA (European Food Safety Authority), 2014. Modern methodologies and tools for human hazard assessment of chemicals. EFSA Journal 2014;12(4):3638, 87 pp. doi: 10.2903/j.efsa.2014.3638.

Dorne, J.L.C.M., Walton, K., Renwick, A.G., 2005. Human variability in xenobiotic metabolism and pathway-related uncertainty factors for chemical risk assessment:a review. Food Chem. Toxicol. 43, 203–216.

Pearce, R., Woodrow Setzer, C. Strope, N. Sipes, AND J. Wambaugh. HTTK: R Package for High-Throughput Toxicokinetics. Journal of Statistical Software. American Statistical Association, Alexandria, VA, 79(4):1-26, (2017).

Wiecek W, Dorne JL, Quignot N, Bechaux C, Amzal B (2019a) A generic Bayesian hierarchical model for the meta-analysis of human population variability in kinetics and its applications in chemical risk assessment. Computational Toxicology 12, 100106.

Wiecek, W; Quignot, N; Amzal B; Dorne, JL (2019b) TKPlate: R package prototype for TK models graphical interface. https://zenodo.org/record/2548850#.XqmQp6gzZeU.

Darney K, Testai E, Buratti FM, Di Consiglio E, Kasteel EEJ, Kramer N, Turco L, Vichi S, Roudot AC, Dorne JL, Bechaux C (2019) Inter-ethnic differences in CYP3A4 metabolism: A Bayesian meta-analysis for the refinement of uncertainty factors in chemical risk assessment. Computational Toxicology 12, https://doi.org/10.1016/j.comtox.2019.100092.

Darney K, Turco L, Buratti FM, Di Consiglio E, Vichi S, Roudot AC, Béchaux C, Testai E, Dorne JLCM, Lautz LS. (2020a) Human variability in influx and efflux transporters in relation to uncertainty factors for chemical risk assessment. Food Chem Toxicol. 28; 140:111305. doi: 10.1016/j.fct.2020.111305.

Darney K, Kasteel EEJ, Buratti FM, Turco L, Vichi S, Béchaux C, Roudot AC, Kramer NI, Testai E, Dorne JLCM, Di Consiglio E, Lautz LS. (2020b) Bayesian meta-analysis of inter-phenotypic differences in human serum paraoxonase-1 activity for chemical risk assessment. Environ Int.;138:105609. doi: 10.1016/j.envint.2020.105609.

Kasteel EEJ, Darney K, Kramer NI, Dorne JLCM, L.S Lautz LS (2020) Human variability in isoform-specific UDP-glucuronosyltransferases: markers of acute and chronic exposure, polymorphisms and uncertainty factors. Archives in Toxicology. *In press.*

Part II Checklist for model evaluation

PBK Model Evaluation Checklist	Checklist assessment	Comments
Name of the PBK model (as in the reporting template)	A generic human QIVIVE PB-K model integrating *in vitro* data, physiological and pathway-related variability to predict kinetics of chemicals in the food safety area	
Model developer and contact details	**JL Dorne, EFSA, Parma Italy**	
Name of person reviewing and contact details	**A.Paini**	
Date of checklist assessment	**04/04/2020**	
A. Context/Implementation		
A.1. Regulatory Purpose		
1. What is the acceptable degree of confidence/uncertainty (e.g. high, medium or low) for the envisaged application (e.g. priority setting, screening, full assessment?)	High, priority setting, full assessment	
2. Is the degree of confidence/uncertainty in application of the PBK model for the envisaged purpose greater or less than that for other assessment options (e.g. reliance on PBK model and *in vitro* data vs. no experimental data)?	**yes**	
A.2. Documentation		
3. Is the model documentation adequate, i.e. does it address the essential content of model reporting template, including the following:	**yes**	
• Clear indication of the chemical, or chemicals, to which the model is applicable?	**yes**	
• Is the model being applied for the same scientific purpose as it was developed, or has it been repurposed somehow?	**yes**	
• Model assumptions?	**yes**	
• Graphical representation of the proposed mode of action, if known?	**No**	
• Graphical representation of the conceptual model?	**yes**	
• Supporting tabulation for parameters (names, meanings, values, mean and standard deviations, units and sources)?	**yes**	
• Relevance and reliability of model parameters?	**yes**	
• Uncertainty and sensitivity analysis?	**yes**	
• Mathematical equations?	**yes**	**In publications**
• PBK model code?	**yes**	**In publications**
• Software algorithm to run the PBK model code?	**yes**	**In publications**
• Qualification of PBK software platform?		
A.3 Software Implementation and Verification		
4. Does the model code express the mathematical model?	**yes**	

5. Is the model code devoid of syntactic and mathematical errors?	**yes**	
6. Are the units of input and output parameters correct?	**yes**	
7. Is the chemical mass balance respected at all times?	**yes**	
8. Is the cardiac output equal to the sum of blood flow rates to the tissue compartments?	**yes**	
9. Is the sum total of tissue volumes equal to total body volume?	**yes**	
10. Is the mathematical solver a well-established algorithm?	**yes**	
11. Does the mathematical solver converge on a solution without numerical error?	**yes**	
12. Has the PBK modelling platform been subjected to a verification process (for a different use, for instance, in the pharmaceutical domain)?	**yes**	
A.4 Peer engagement (input/review)		
13. Has the model been used previously for a regulatory purpose?	**No**	
• Is prior peer engagement in the development and review of the model sufficient to support the envisaged application?	**Yes**	
• Is additional review required? Peer engagement includes input/review by experts on specific aspects of model development, individual reviews of the model by experts, or collective reviews by peer review panels. Availability of the comments and tracking of revisions to the model in response to peer input contributes to increased confidence in the model for potential application.	**yes**	
B. Assessment of Model Validity		
B.1 Biological Basis (Model Structure and Parameters)		
14. Is the model consistent with known biology?	**yes**	
• Is the biological basis for the model structure provided?	**yes**	
• Is the complexity of the model structure appropriate to address the regulatory application?	**yes**	
• Are assumptions concerning the model structure and parameters clearly stated and justified?	**yes**	
• Is the choice of values for physiological parameters justified?	**yes**	
• Is the choice of methods used to estimate chemical-specific ADME parameters justified?	**yes**	
• Saturable kinetics	**yes**	
B.2 Theoretical Basis of Model Equations		
15. Are the underlying equations based on established theories, .e.g. Michaelis-Menten kinetics, Fick's laws of diffusion?	**yes**	
• In the case of PBK models for particles, does the model take into consideration the properties of particles, e.g. particle size ranges,	**NA**	

(poor) solubility, aggregation, partitioning and diffusion/sedimentation behaviour?		
B.3. Reliability of input parameters		
16. Has the uncertainty (individual variability, experimental reproducibility and reliability) in the input parameters been characterised?	**yes**	
B.4. Uncertainty and Sensitivity Analysis		
17. Has the impact of uncertainty (individual variability, experimental reproducibility and reliability) in the parameters on the chosen dose metric been estimated?	**yes**	
• Local sensitivity analysis?		
• Global sensitivity analysis?	**yes**	
• Example: ratio of 95th percentile of sample distribution to median of dose metric		
18. Is confidence in influential input parameter estimates (i.e., based on comparison of uncertainty and sensitivity) reasonable (within expected values; similar to those of analogues) in view of the intended application?	**yes**	
B.5. Goodness-of-Fit and Predictivity		
19. For PBK models for which there are sufficient *in vivo* data for the chemical of interest:		
• Suitability as analogue (chemical and biological similarity) been assessed?	**No**	
• Reliable estimation of chosen dose metric for analogue?		
• Variability of *in vivo* reference data well characterised?	**yes**	

NA= Not applicable; NR = Not Reported

Part III Overall Evaluation